DEPARTMENT OF BIOTECHNOLOGY, CHEMISTRY AND PHARMACY

DOCTORATE PROGRAM IN CHEMICAL AND PHARMACEUTICAL SCIENCES

- XXXIV CYCLE-

DOCTORATE COORDINATOR: PROF. MAURIZIO TADDEI

SYNTHESIS OF ANTIFUNGAL COMPOUNDS

SCIENTIFIC-DISCIPLINARY FIELD: **CHIM/08**

SUPERVISOR: **PROF. MAURIZIO TADDEI**

CANDIDATE: **LORENZO JACOPO ILIC BALESTRI**

ACADEMIC YEAR: 2020-2021

"O frati", dissi "che per cento milia
perigli siete giunti a l'occidente,
a questa tanto picciola vigilia

d'i nostri sensi ch'è del rimanente,
non vogliate negar l'esperienza,
di retro al sol, del mondo sanza gente.

Considerate la vostra semenza:
fatti non foste a viver come bruti,
ma per seguir virtute e canoscenza".

Dante Alighieri *La Divina Commedia*
Inferno: C. XXVI, v 112-120.

ABSTRACT

Systemic fungal infections represent a threat to public health, and annually more than 150 million people suffer from fungal diseases. This worrisome data reflects the growing group of patients with immunocompromised conditions: due to cancer chemotherapy, organ transplanting or affected by AIDS, and the outbreaks of azoles resistant strains. Moreover, the global emergency caused by SARS-CoV-2, leading to long term hospitalizations, and intubation increased the susceptibility to develop fungal infections. Therefore, now more than ever, the challenge of developing new antifungal drugs is dramatically urgent.

Our research group has been interested in the great potential of guanylated compounds as new antifungal agents since 2007. During these 15 years, three series of derivatives, characterized by an amidinoureas scaffold, have been developed. The structure of these compounds is new and not shared with other antifungal drugs present on the market. Consequently, they show remarkably antifungal activity, especially among Candida strains resistant to azole drugs. The first chapter of my thesis deals with synthesizing new antifungal compounds with a macrocyclic amidinourea scaffold. Firstly, a novel compound **BM37** was synthesized through a convergent approach using as a key step the ring-closing metathesis (RCM). Secondly, we decided to conduct advanced biological investigations of our lead compound, **BM1**. Consequently, we face the need to prepare this compound on a gram scale. To achieve this result, we changed the synthetic route and took inspiration from Fukuyama's work designing a new strategy to obtain 1 gram of **BM1**.

The second chapter of my thesis explores the design and synthesis of novel inhibitors targeting human chitinases. This project started when we investigated a putative target for the amidinoureas compounds endowed with antifungal activity. This research led us to the Chitinase family. In particular, our interest fell on human chitinases due to their involvement in chronic inflammatory lung diseases. The development of new human chitinase inhibitors, characterized by two different chemical scaffolds, is the aim of this second chapter. The former was the macrocyclic amidinoureas scaffold. Here three derivatives: **BM56, BM57** and **BM58**, were synthesized and evaluated on human chitinases. The latter explored the chemical space related to the 6-piperazine-1-ylpyrazine-2-carboxamide, a new scaffold that emerged from a structure-based virtual screening. In this case, we synthesized a small, focused library of derivatives.

The third chapter of my thesis describes my work as visiting PhD student at Uppsala University. During this period, I have been involved in the alkylation of the N position of 3-methyl indole with several cyclic ketones using a green and efficient amide coupling reagent, the TP3®.

Finally, the last chapter containes chemical and biological data of all the compounds presented in the thesis.

CONTENTS

LIST OF FIGURES

LIST OF SCHEMES

LIST OF TABLES

ABBREVIATIONS

AMCase - Acidic mammalian chitinase

BSI - Bloodstream infection

Boc - Tertbutoxy carbamate

Cbz - Benzyl carbamate

CDR - Candida drug resistance

CHIT1 - Chitotriosidase

CLSI - Clinical and Laboratory Standards Institute

CNS - Central nervous system

COPD - Chronic obstructive pulmonary disease

EDC - 1-ethyl-3-(3-dimethylaminopropyl) carbodiimide

DCE - 1,2-dichloro ethane

DCM – Dichloromethane

DIBAL-H - Diisobutylaluminium hydride

DIAD - Diisopropyl azodicarboxylate

DIPEA - Diisopropyl Ethyl Amine

DMAP - 4-dimethylaminopyridine

DMSO - Dimethyl sulfoxide

HOBt – Hydroxybenzotriazole

HPLC - High Performance Liquid Chromatography

IC - Invasive candidiasis

ICU - Intensive care unit

IFI - invasive fungal infections

MDR - Multidrug resistance

MIC - Minimum inhibitory concentration

MoA – Mode of action

NMR - Nuclear Magnetic Resonance

RCM - Ring closing metathesis; gen, generation

rt - Room Temperature

SAR - Structure-Activity Relationship

TEA - Triethyl amine

TFA - Trifluoroacetic acid

THF – Tetrahydrofuran

VS - Virtual Screening

Chapter 1

Macrocyclic Amidinourea: A Promising Scaffold For The Development Of Novel Antifungal Agents.

1.1 INTRODUCTION

1.1.1 <u>Fungi: cell structure and organization.</u>

Fungi are one of the most interesting and ancient organisms in the world and can exist as single cells or complex multicellular organisms with widespread distribution around the world. They play different roles in the ecosystem; some good, like decomposers of soil and dead specimens, others undoubtedly bad, as parasites of plants and animals, humans included. Defining which species can be considered as Fungi is not straightforward, and it has taken more than 200 years of debate among mycologists. Only recently, thanks to the application of molecular methods, have mycologists been able to positively identify 10 different phyla and estimate that there are 5.1 million species within the fungi kingdom.

The sizes of fungal cells are somewhere between those of bacteria and plant or animal cells. Their cellular organization is like other eukaryotic cells. They possess a cytoplasm full of organelles (mitochondria, endoplasmic reticulum (ER), ribosomes and vacuoles) bounded by a plasma membrane (plasmalemma) and nuclei contain all cellular DNA. Fungal membranes are typical bilayer membranes, but in contrast to mammalian cells, they have ergosterol as their free-flowing agent. Another essential structure present in fungi is the cell wall (

Figure 1-1). It covers important roles, such as protecting fungal cells from osmotic and mechanical stress and controlling cellular permeability. Moreover, it represents a dynamic interface between the fungal cell and the environment and a virulence factor since a lot of toxic molecules are released by this structure. Cell walls consist of several rigid layers. The innermost is more consistent, whereas the outermost changes depending on fungal species. Even though the cell wall composition can change between species of fungi, at least four components are fixed and can be found in all fungi:[1–3]

1. glucans are polysaccharides, made up of monomers of glucose linked together mostly by β 1-3 or β 1-4 bonds. These polysaccharides represent 50-60% of the dry weight of this structure and they are synthesized by a complex of enzymes, namely glucan synthases. Their function is to increase the structural resistance of the wall;

2. chitin is a β -(1,4)-*N*-acetylglucosamine polymer. Its presence can vary greatly depending on the phase of the fungi. For instance, the chitin content in the hyphae of *C. Albicans* is three times higher than in yeasts. Chitin is synthesized by an enzyme called chitin synthase and provides structural rigidity and resistance;

3. glycoproteins are associated with the carbohydrates of the cell wall by O or N linkages. They are involved in signal transmission and the reorganization of the wall components as well as interaction with the host cells and tissues;

4. melanin is a high molecular weight pigment, hydrophobic and with a negative charge. It plays an important role in the defence and survival of fungi from stressor factors such as extreme temperature, UV light and toxins.
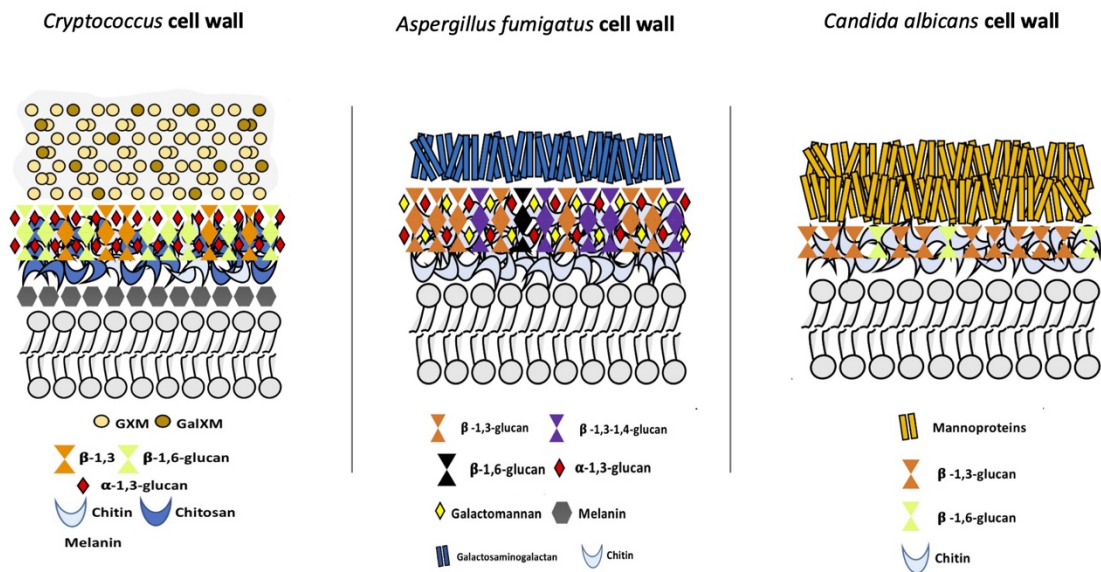
Figure 1-1: Structural organization and composition of the cell wall in different fungi. The innermost layer is a consistent structure composed of the β-glucan-chitin skeleton, whereas the outermost layer has a variable composition depending on the species.

In this thesis, I will focus on pathogenic fungi which represent only 0,0001% of the 5.1 million fungi.[4] Among them, three main types of cells can be identified: hyphae, yeast cells and spores (
Figure 1-2).
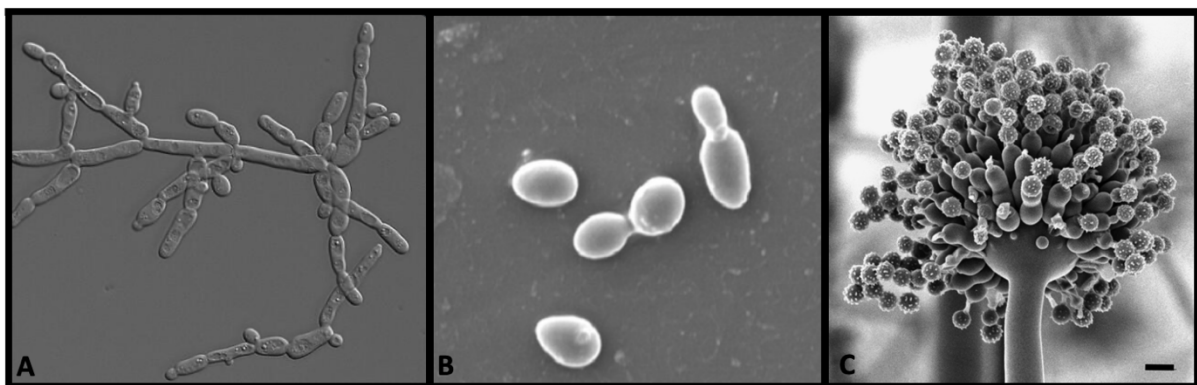
Figure 1-2: Types of fungal cells. From the left to the right: A) Hyphae of *Candida albicans*. B) Yeast of *Candida albicans.* C) Spores of *Aspergillus fumigatus.*

Hyphae are the structural units of moulds, which represent most of the fungi. They are composed of a thin, transparent tubular wall enclosing the protoplasm. Hyphae can be unicellular and multicellular. In multicellular hyphae, the protoplasm is distributed in sections by septa. Septa possess central pores, different in dimension, allowing cytoplasmic and organelle transport between adjacent hyphal compartments. In many types of hyphae, this cytoplasmatic continuity leads to a wide region of prolific cell fusion. Hyphae tend to aggregate and form a weft or tissue, namely *mycelium*. The type of mycelia varies according to its function. Principally, mycelia are involved in the exploration and invasion of the nearby environment, nutrient uptake and mobilization, defence, and reproduction. The most important and studied part of a hypha is the growing cellular element present at the colony periphery,

which is responsible for its elongation. This process involves a small region (a few micrometres), at the apices of the hypha cell, called Spitzenkörper (
Figure 1-3) characterized by a large presence of vesicles and complex organelles. The vesicles are mostly secretory and contain various cell wall synthesizing enzymes. The direction of the hypha growth reflects the environmental signals in a process called thigmotropism, which also plays a fundamental role in the invasion of tissues.[2,3]
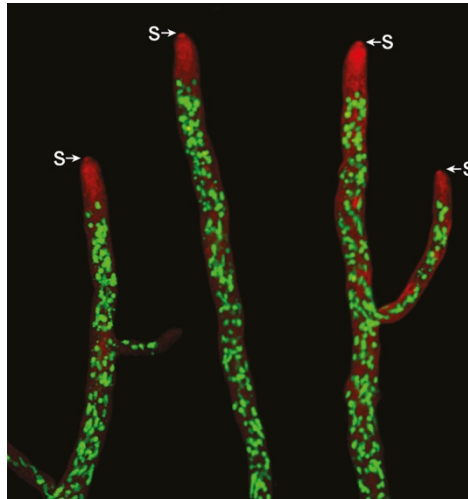
Figure 1-3: Multinucleate hyphae in a colony of *Neurospora crassa:* Nuclei were labelled with a green fluorescent protein. Note the wide region behind the hyphal apex characterised by cytoplasmatic continuity. The Spitzenkörper regions are indicated with arrows, they are tiny regions at the tips of the growing hypha. Membranes were stained with red (FM4-64) showing that the growing hypha is full of organelles and vesicles but without nuclei.

Yeast cells are uninucleated single cells that reproduce by budding or binary fission. Yeasts are characterized by a high metabolic rate and rapid dissemination in aqueous environments, which gives them preference as a growth form during the early stage of infections. For instance, *Candida, Cryptococcus, Histoplasma, Blastomyces,* and *Paracoccidioides* used this form to propagate themselves during infections. Moreover, most of these pathogens are dimorphic fungi. Therefore, they can switch between yeast and hyphal growth form depending on the stage of disease development and the surrounding environment. Dimorphism is a key feature of virulence in human fungal pathogen which will be discussed later in this thesis.[3]

Spores are produced by all fungi and are discrete monocellular or multicellular structures. Spores are usually termed mitospores if they are produced by mitosis or mesopores if derived from a sexual process. Their functions are reproduction and spreading. Chlamydospores are the best-known types of spores since they are produced by a wide range of pathogenic fungi; they are usually large, spherical and thick-walled and they can resist harsh environmental conditions.[3]

In fungi, there is a peculiar growth state, called biofilm, in which all the previous fungal cells exist as a community. Biofilms can grow on liquid and solid surfaces. However, the most important from a clinical point of view are the ones that can grow on medical devices such as urinary and central venous catheters, pacemakers, and mechanical heart valves. The increase in the number of patients with these devices in recent years has prompted an exponential growth in biofilm infections. Although many species of fungi can form biofilms, those of *Candida* are the ones most commonly found. The species of *Candida* capable of forming biofilms are *C. albicans C. krusei, C. tropicalis, C. parapsilosis*.

Among them, *C. albicans* biofilms are the most extensively studied and present a specific architecture: an innermost layer of round yeast cell hyphae and pseudohyphae embedded in the extracellular matrix extending throughout the biofilm. The polymeric matrix is mainly composed of protein and glycoprotein (55%) carbohydrates, such as mannan-glucan complex, lipid (15%) and nucleic acids (5%). The development of *C. albicans* consists of four stages (
Figure 1-4). In the first step, spherical yeast cells reach a solid surface and adhere to it. Then, yeasts proliferate and form a base layer of anchoring cells. This layer evolves when hyphae or pseudohyphae grow and produce the extracellular matrix. In the final step, yeast cells are dispersed from the biofilm to another site, which usually is the bloodstream, leading to invasive systemic infections of tissues or organs.

Biofilms are characterized by an inherent resistance to antifungal drugs which makes them a serious health concern. It has been reported that *C. albicans* biofilms are responsible for 100,000 deaths annually in the United States. Resistance to antifungal drugs depends on two factors. The former is the upregulation of CDR1, CDR2, and MDR1 genes, encoding for efflux pumps, which reduces the concentration of drugs in the biofilms. The latter is the presence of an extracellular matrix that acts as an impenetrable barrier drug. Nowadays, no antifungal drugs specific for *C. albicans* (or any other *Candida* species) exist, making treatment of biofilm-based infections particularly problematic. For this reason, it is important to understand the molecular mechanisms underlying biofilm formation to develop new antifungals that specifically target the biofilm state.[5–7]
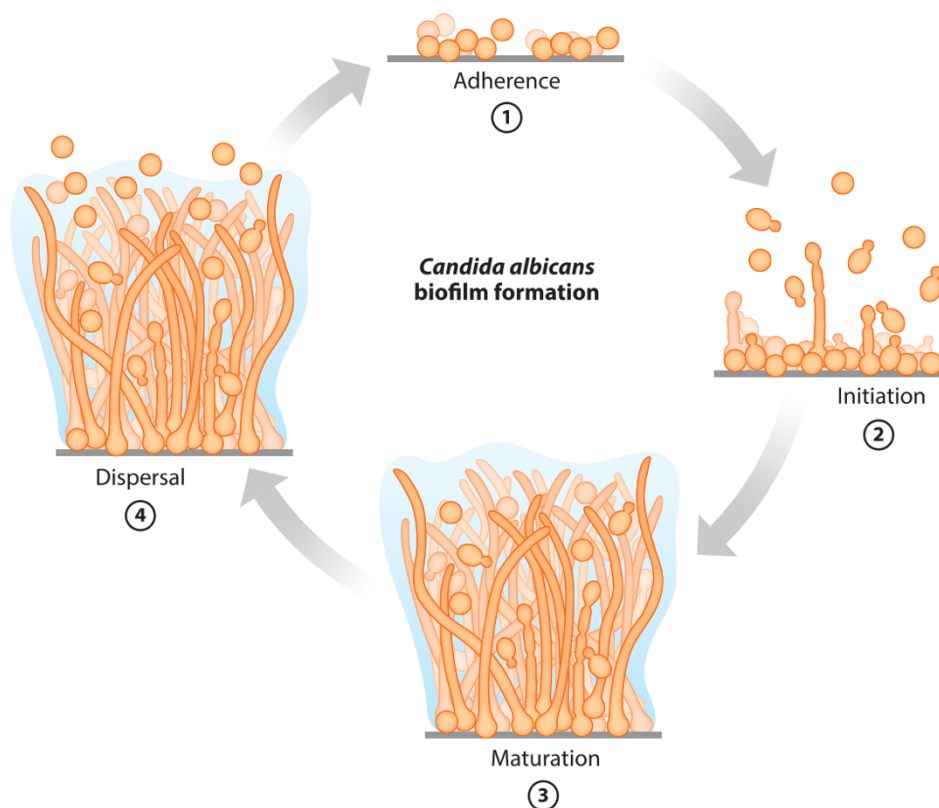
Figure 1-4: Stages of Candida albicans biofilm formation.

1.1.2 <u>Pathogenic fungi.</u>

The ''relationship" between animals and fungi is very ancient, and it has influenced the evolutionary process of both kingdoms. One of the consequences is that animal immune systems have been shaped by this coevolution, as demonstrated by Perovic-Ottstadt et al.[8] They found that a cell surface recognizing of (1,3)-β-D- glucan was present in sponges, which are among the earliest species of metazoa. This acts as a fungal pathogen-associated molecular pattern, showing that also a long time ago, defence from fungal attacks was essential.[8] The tools for fighting the fungal infection increased during animal evolution: insects have the Toll pathway, which releases antimicrobial peptides, while vertebrates added the innate and adaptive immune system. Mammals possess a stable and elevated temperature keeping fungal infections in check, as demonstrated by Casadevall and colleagues.[9] Only a small minority of fungi, for this reason, meet the criteria, suggested by Kohler et al.,[4] necessary to cause human infection:

- grows at a stable elevated temperature (37 ℃ or above);
- reaches internal tissues by sticking into the host barrier;
- uses human organs and tissues to obtain their components;
- eludes the human immune system.

Human Pathogenic fungi can be divided into primary and opportunistic. The former is the species of fungi that are cable of infecting healthy humans, their behaviour comes from the ability to infect and invade other hosts like amoebae or insects. *Cryptococcus neoformans* and *gattii* belong to primary pathogenic fungi[10] and have attracted considerable attention, especially due to the high rates of death caused (625,000 in 2009)[11] in immunocompetent patients. *Cryptococcus* enters humans as small airborne cells (<5 μM in size). It can be latent in the lungs for years until it finds a good opportunity for growth. Once it is reactivated, it reaches the bloodstream where it can disseminate to all the organs as yeast forms*. C. neoformans* has a strong preference for the central nervous system (NCS), where it causes meningitis and, if not treated appropriately, can be lethal. *Cryptococcus* can rely on several virulence factors: a thick capsule composed of glucuronic and galactoxylomannan which prevent the phagocytosis from the immunity cells, a cell wall melanin which protects from oxidative and chemical stressors, and a unique ability to promote its extrusion from phagocytic cells in a process called vomocytosis.[12] Opportunistic fungi are, under healthy and normal immune conditions, humans' harmless commensals. However, once the host loses his immunity shield, these species of fungi shift from innocent commensals to ruthless killers capable of causing 1.7 million deaths per year worldwide.[13] The diseases caused by opportunistic fungi were very uncommon until the 1950s when the first cases of candidiasis associated with antibiotics were reported. Afterwards, the introduction of iatrogenic immunosuppression, HIV widespread, and long-term hospitalization led to an exponential increase in these infections. Three genera of opportunistic fungi are responsible for most fungal infections: *Candida, Aspergillus* and *Pneumocystis*.[4]

1.1.3 <u>Invasive candidiasis.</u>

From a medical point of view, significant fungal infections can be classified into two types according to the site of infection:

- superficial mycoses: localized on skin, skin structure and mucosa. The most relevant are thrush, dermatophytes, and oropharyngeal candidiasis. These diseases are common in immunocompetent subjects and represent annoyances rather than life-threatening diseases;
- invasive fungal infections (IFIs) involve sterile body sites (bloodstream, lung, liver, kidneys, and central nervous system). They are the most serious diseases related to fungal infection and, if left untreated or worsened by other clinical events, can lead to death.

Annually, over 150 million people have a serious fungal disease. IFIs are most often caused by *Candida* spp. (70% of the cases), namely invasive candidiasis (IC),[14] and this is because 60% of healthy people have *Candida* spp. either as a commensal yeast on their skin or in their gut. Furthermore, fungal diseases are associated with higher mortality rates (10-20% among patients with candidaemia) and come at an exorbitant cost for the health care system (US $40.000 per patient).[15,16] Among the 150 species of *Candida*, five species can be accountable for most of the candidiasis. *C. albicans* is the most extensively studied species and is associated with half of the overall candidiasis. The other four names non-albicans *Candida* species (NAC) are *C. parapsilosis, C. tropicalis, C. glabrata*, and *C. krusei,* which only recently have attracted considerable attention due to a worrisome increase in their cases.[17] As described above, *Candida* spp. are normal residents on or in our bodies, in particular, the skin and the gut. However, under specific conditions, such as long-term exposition to antibiotics (which turns into a selective advantage of *Candida* over bacteria), through the breach of the gastrointestinal and cutaneous barriers by cytotoxic chemotherapy or surgery (which enable *Candida*. spp to translocate from the gut into the bloodstream) or impairment of the immune system (which facilitates the dissemination of the *C. albicans*. in the bloodstream), they can shift from commensalism to opportunism. This transition is associated with the induction of virulent traits of *Candida* spp such as:

- morphogenesis in response to environmental factors. In candidiasis, it is well-known that yeasts and hyphae forms are present and cooperate each in its way. Yeasts participate in the early stage of infection since they can readily disseminate in the bloodstream and are resistant to mechanical stress. Once fungal cells have reached a favourable location they shift to hyphae or pseudohyphae (chains of unicellular cells caused by an incomplete budding of mother-daughter separation) which are the preferred form of invading and damaging tissue. Moreover, the morphogenic interchange is also a way to evade the immune system. *C. albican*s yeasts ingested by macrophages respond with hyphal growth because hyphae induce pyroptosis, a form of apoptosis, in immune cells;
- secretion of digestive enzymes such as aspartyl proteases, phospholipases that promote tissue invasion, and proteins that mediate adherence and invasion in endothelial and epithelial cells.[15,16,18]

Another factor that plays a significant role in IC is the health condition of patients. Humans are naturally resistant to most invasive fungal diseases, but if their immune system is knocked out or invasive interventions are required, they become at-risk patients for invasive fungal diseases. For this reason, many studies have focused on which patients should be considered vulnerable.[15,19,20] These include patients with an indwelling central venous catheter, long exposure to broad-spectrum antibiotics, those undergoing organ transplant or major surgery, as well as people with lower immune

defences due to immunosuppressive therapy or diseases (AIDS, neoplasms). Furthermore, the latest global health emergency (caused by SARS-CoV-2) enhances the possibility of patients being susceptible to developing fungal infections. It can lead to lower respiratory disease and severe acute respiratory syndrome, which require mechanical ventilation and longer hospital stays.[21–23]

Finally, timely diagnosis of invasive fungal infections has a major influence on the outcome of the patients, as was well highlighted by Garey et al., who reported that a 1- to 2-day delay in the introduction of antifungal drugs in the therapy has been associated with a doubling of mortality.[24] Nowadays, no clinical signal or symptoms are specific to invasive candidiasis. Thus, one of the most important tools used in clinics is to add an antifungal drug to therapy in the presence of persistent fever in at-risk patients who are non-responsive to bacterial treatments. Although antigen and antibody tests, as well as DNA-bases tests, have been developed and seem to improve the timeliness and accuracy of diagnoses, the gold standard remains a blood culture with all its inherent limitations.[25] The request for sensitivity and specificity tests, able to detect fungal infections, along with the unmet clinical needs for new antifungal agents, represent the next challenge to reduce the burden of death related to fungal infections.

1.1.4   Current antifungal therapies.

The classes of drugs currently available as therapeutic options for invasive fungal infections are only three: polyenes, azoles, and echinocandins.

Polyenes are the oldest family class of antifungal compounds. They act by binding the ergosterol (the equivalent of cholesterol in the animal membrane) and thus disrupting the compactness of the double layer membrane, which is not able to address the normal function, thus leading to fungal death. For this reason, amphotericin B (Figure 1-5), the most representative member of this class, has a fungicidal effect and it is one of the most broad-spectrum antifungal available. However, its major drawback is related to its interaction with cholesterol which leads to significant toxicity for this compound, although the development of formulations of amphotericin B with lipids has reduced this problem. Nowadays, amphotericin in combination with 5 flucytosine remains the treatment of choice for cryptococcal meningitis, whereas for many common invasive fungal infections the better-tolerate azole and echinocandins have replaced it.[15,26–28]
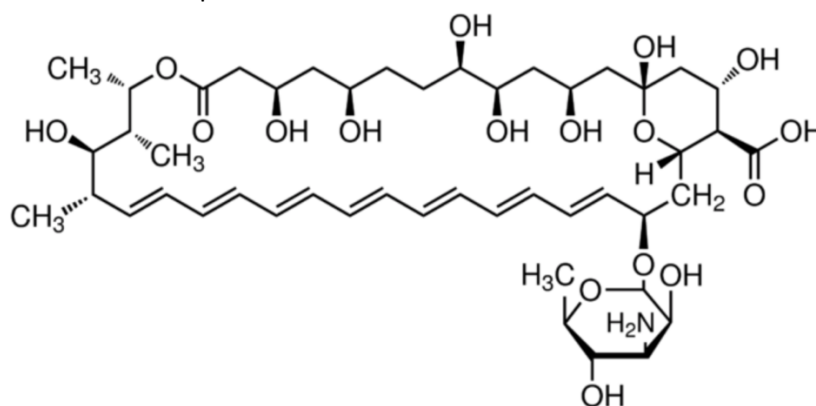
Figure 1-5: Chemical structure of amphotericin B.

Azoles appeared on the market about twenty years later than amphotericin B and immediately became the family of drugs of choice for candidemia and other fungal infections. Their mechanism of

action is the inhibition of lanosterol 14 α -demethylase, an enzyme member of the CYP450 family involved in the synthesis of ergosterol, resulting in an accumulation of 14α- methyl sterols which alters the membrane stability and permeability. The most common azoles used in therapy are fluconazole, voriconazole, and posaconazole (Figure 1-6): they are in general fungistatic (except for voriconazole which is fungicidal towards *A. fumigatus*), well-tolerated and with low toxicity related to the possibility of interfering with other drugs metabolised by CYP450. (Only the first generation of azoles, which bear the imidazole moiety instead of triazole, suffered from significant toxicity.) Moreover, they are the only class of antifungal compounds that can be administrated either intravenously or orally. In general, fluconazole has a wide spectrum against *Candida* and *Cryptococcus*. However, *C. glabrata* and *C. krusei* are intrinsically less susceptible to it and it is used to treat cryptococcal meningitis only in the research-limited region when the quite expensive formulation of amphotericin in combination with 5 flucytosine is not available. Voriconazole is the treatment of choice for *Aspergiulls,* whereas posaconazole acts against mould infections. [15,26,27]
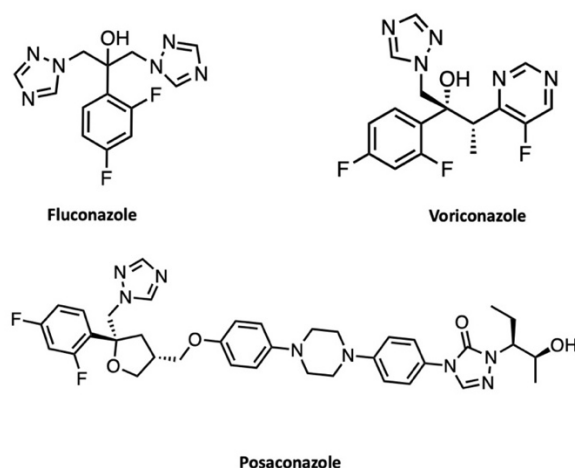
Figure 1-6: Common azoles used in therapy.

Echinocandins are the youngest family members of the antifungal class, even if caspofungin was introduced to the market in the early 2000s. They inhibit the 1,3-b-glucan synthase (GS), a key component for the formation of the cell wall, have broad fungicidal activity against Candida spp (but are fungistatic against *Aspergillus* and have not shown clinically useful activity on *Cryptococcus*), low toxicity (since the target is specific for the fungal cell and not shared with mammalian cells), and a very limited drug-drug interaction. The only drawback is the large molecular weight of this class of molecule that requires an intravenous administration. Nowadays, caspofungin, micafungin and anidulafungin (Figure 1-7) are used clinically for candidemia where represent the first-line therapy for adult patients[15,26,27,29].
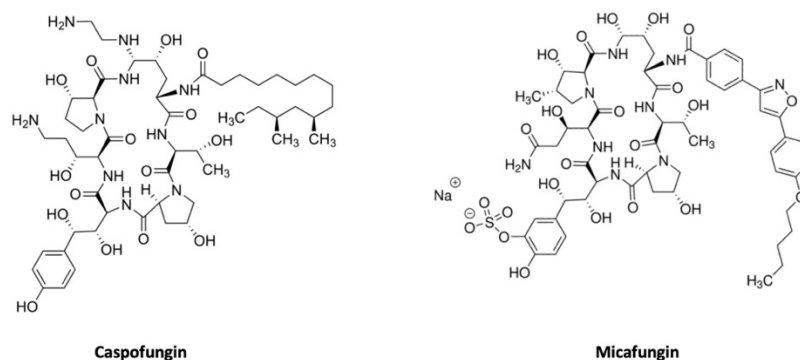
Figure 1-7: Chemical structures of caspofungin and micafungin.

1.1.5   The emergence of antifungal resistance.

The therapeutical options for invasive fungal diseases are quite limited and not able to satisfy the outcomes of fungal infections. Making the situation even worse is the drug resistance among common pathogenic fungi and the lack of a new chemical class in the clinical arsenal of antifungal drugs, unchanged since the discovery of echinocandins in the 1970s. Antifungal drug resistance is not as famous as its counterpart, the antibacterial one, but that does not mean is less worrisome. Drug resistance to one or multi-drug classes can eliminate treatment options, which are few, leading to a devastating effect on patients' outcomes.

At least three factors account for the outbreak of resistant strains. First, there is the careless use of antifungal drugs in agriculture. These drugs have the same targets as most of the compounds used in therapy, which have prompted an environmental reservoir of drug-resistant pathogens. Second, the long-term exposure to antifungal drugs in patients with compromised immune systems, which contributes to reducing the susceptibility of pathogenic fungi to antifungal drugs. Lastly, the capability of formation of drug-impermeable biofilm on implant devices and indwelling catheters contributes to suboptimal drug exposure and enhances the possibility of resistance developing.[30]

Microbiological drug resistance can be classified as primary (intrinsic) or secondary (acquired). In the first case, a strain is naturally not sensitive to a specific drug without previous exposure due to an intrinsic behaviour of the fungi. Examples include *C. glabrata* and *C. krusei* which are both intrinsically resistant to azoles. On the other hand, acquired resistance involves genomic modifications and specific mechanisms which trigger a susceptible strain to become resistant after drug exposure. For instance, *Aspergillus* spp. and *Candida* spp. have acquired azole resistance, and many studies have correlated this resistance to prophylactic and long-term treatment regimens.[31,32] There are many different mechanisms by which fungi can acquire resistance. For better clarity, I have divided them depending on the drug family they belong to.

Azole resistance is common in *Aspergillus* and *Candida* spp., whereas azole resistance among *Cryptococcus* spp. remains low. There are four mechanisms involved in azole resistance:

- *mutation on ERG 11 or Cyp51A.* Erg 11 (in yeast) and Cyp51A (in moulds) are the genes responsible for the synthesis of the Cytochrome P450 enzyme sterol 14α- demethylase, the target enzyme of azoles. Point mutations in these genes inhibit the binding of triazole moiety of the azole to the ferric iron of the heme-binding site and provide the azole resistance. In *Aspergillus* species, mutation on Cyp51A represents the most important mechanism of resistance.[32]

- *overexpression of Erg11 or Cyp51.* The increased expression of these genes is the result of a mutation in the transcription factor UPC2, which is the genetic regulator of ERG. Overexpression of Erg11 results in an abundance of the target enzyme, requiring more drugs to obtain the same inhibition and leading to azole susceptibility;[32]

- *drug effluxes* represent the most significant mechanism of azole-resistance in *Candida spp.* Briefly, the drug efflux consists of the overexpression of membrane-associated efflux pumps which can recognise various chemical substances and facilitate their efflux from the fungal cell. Since they can recognise several drugs, this can lead to phenomes of multidrug resistance. The genes encoding for the efflux pumps belong to two superfamily types: ATP-binding cassette (ABC) or major facilitator superfamily (MFS). The main difference among them is the former encodes for proteins that used ATP-dependent transport, whereas the latter uses the electrochemical proton-motive force to power drug efflux. In *C. Albicans*, CDR1, CDR2 are the genes encoded for efflux pumps of ABC, while the MDR1 belongs to MFS;[32,33]

- *biofilm formation.* Mature biofilms display a complex disposition of yeast and hyphae forms embedded in an exopolymer matrix rich in β-1,3 glucans. This complex architecture can promote drug resistance both by trapping drugs in this polymeric matrix and by induction of drug efflux transports up-regulating the CDR and MDR genes.[7]

Polyenes which acquire resistance among *Candida* and *Cryptococcus* spp. are rare while intrinsical resistance concerns only species of *Aspergillus*. The mechanism of resistance is based on the reduction of ergosterol content in the cell membrane by down-regulation of genes involved such as ERG1, ERG2, ERG3, and ERG4. However, cross-resistance in *Candida* spp. is common in polyene, especially when administrated after an initial treatment with azoles. The reason is that previous treatment with azole can lower the cellular sterol concentrations in antifungal compounds and confer polyene resistance.[31,32]

Echinocandins' resistance is low (in large-scale observational studies, resistance is less than 1% in *C. albicans* and can reach 2% in *C. glabrata*). The mechanism of resistance consists of a mutation of the gene FKS, which encodes the catalytic subunits of glucan synthase. Fortunately, no cross-resistance nor multidrug resistance is reported for this class of compound, which is highly active against *Candida* spp. and the first line of therapy for ICs.[26,31,32]

Finally, an alarm has been caused recently by outbreaks of a candida species, namely *C. auris.* This strain was described for the first time in Japan in 2009 and immediately climbed the negative charts of dangerous pathogens because of its reduced susceptibility to the major antifungal drugs (fluconazole-resistant in 93% of patients; amphotericin B-resistant in 35%, echinocandins in 7%), its ability to spread rapidly and its high mortality rate.[15]

1.1.6   New antifungal drugs.

The development of new antifungal drugs represents our best weapon to address the burden of fungal infection, but it must face up to two fundamental challenges. Firstly, fungi resemble eukaryotic cells, so specific structures to target are fewer in number than with bacteria and, if a compound is toxic to yeast, it is likely to be toxic to humans. Secondly, the regulatory and economic challenges, which are so tough that 80% of new potential antifungal compounds are not able to reach the market. The antifungal drugs that are currently undergoing clinical evaluation are (Figure 1-8) orotomides, ibrexafungerp, rezafungin, and isavuconazole.

Olorofim is the first representative of a family of antifungal drugs (ortomides) with a new mechanism of action, which targets the dihydroorotate dehydrogenase (DHODH), an enzyme that evolved in the pyrimidine biosynthesis as an important molecule in DNA and RNA. Due to this peculiarity, it does not show cross-resistance with other antifungal drugs and possesses a broad spectrum against *Candida* and *Aspergillus*. Moreover, it can be administrated orally.

Ibrexafungerp is a new compound in phase 3 which shares the mechanism of action with echinocandins even if its chemical structure is completely different. It can be administered both orally and intravenously, it is characterized by low drug-to-drug interaction, and it has an increased efficacy among azole- and echinocandin-resistant *Candida* species.

Rezafungin is structurally analogous to anidulafungin. Its peculiarities are represented by increased metabolic stability and a long-acting effect compared to other echinocandins. The activity profile resulted in an ameliorated effect, especially against *C. auris* and biofilms formed by *Candida* species.

Finally, isavuconazole is a new derivative of the family of azoles in phase 4 testing as an antifungal agent. It displays an improved safety profile and reduction of drug-drug interaction compared to other members of the family. It has shown high efficacy against a broad spectrum of fungal infections, and it is available in oral formulation, a desirable feature for new antifungal drugs.[26,34,35]
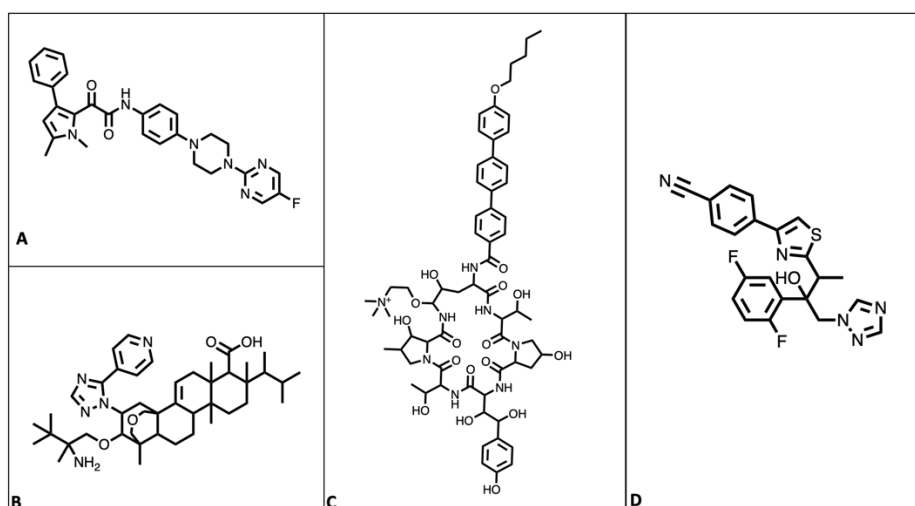
Figure 1-8: Chemical structures of new antifungal drugs. A) Olorofim, the representative of the orotomides, a new antifungal family of compounds. B) Ibrexafungerp the first member of a new glucan synthase inhibitor C) Rezafungin a structurally analogous to anidulafungin. D) Isavuconazole is a new derivative of the family of azoles.

1.2   STATE OF THE ART

1.2.1   In the beginning, there was guazatine.

Guazatine is a broad-spectrum, water-soluble fungicide. Its mechanism of action is based on the alteration of fungi membranes, and it is widely used to control the seed-borne diseases of cereal in agricultures. Guazatine has been classified by the WHO as moderately hazardous for humans and is commercially available in the form of guazatine acetate. It is a complex mixture (Figure 1-9) in which the main components are represented by fully guanidated triamine (**GGG**) 30.6% and diamine (**GG**) 29.5% followed by monoguanidated diamine (**GN**) 9.8% and diguanidined triamines (**GGN**) 8.1% and (**GNG**) 4.5%.[36,37]
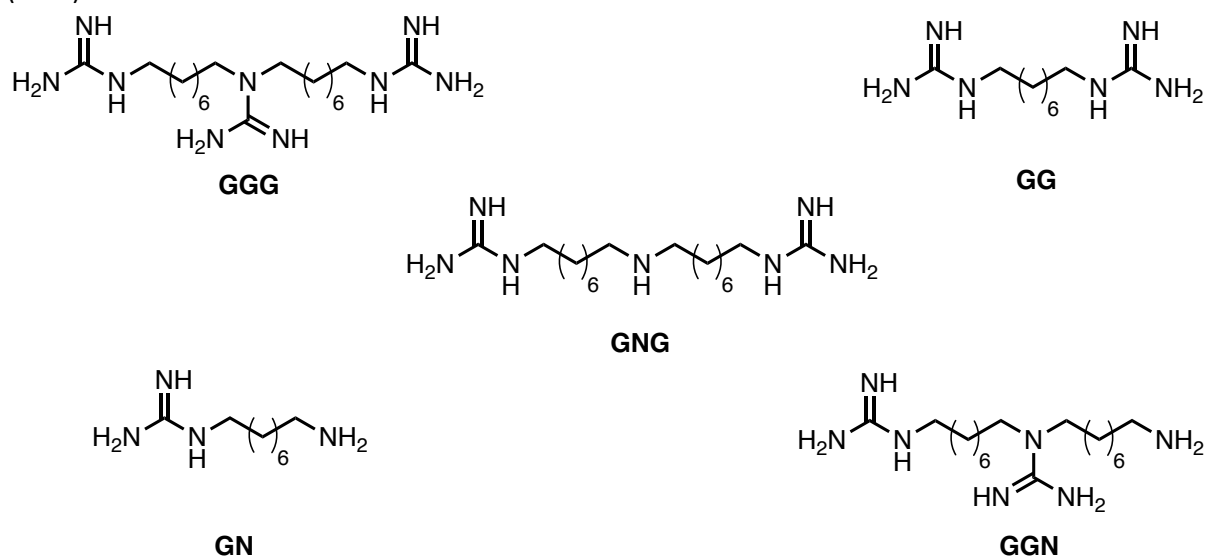
Figure 1-9: Main components of guazatine: GGG 30.6%; GG 29.5%; GN 9.8%; GGN 8.1 %; GNG 4.5%.

In 2007, our research group began to take the first step in the development of antifungal compounds showing a great interest in the antifungal properties of this agricultural fungicide[36]. Therefore, firstly an LC-MS method for identification of the different components of guazatine was set up. Secondly, the purified single components were tested against *Candida* spp. (resistant and wild type) and compared with the activity of the guazatine mixture (Pestanal®) and fluconazole (Table 1-1).

Table 1-1: Antimycotic activity of purified guazatine components, guazatine and fluconazole on 11 *Candida* spp.

Candida strains	MIC$_{50}$(μM)						
	GNN	**GGG**	**GG**	**GNG**	**GN**	**G^a**	**F^b**
Candida albicans ATCC60193	>80	5	>80	80	>80	40	0.8
C. albicans 4T	80	5	>80	80	>80	20	209.0
C. albicans 53T	80	20		40	>80	40	418.0
C. albicans 15T	80	10	>80	80	>80	80	209.0
C. krusei ATCC14243	40	10	>80	20	>80	20	209.0
C. krusei 193T	40	40	>80	20	>80	20	418.0
C.parapsilosis ATCC34136	>80	>80	>80	>80	>80	>80	6.5
C. parapsilosis 64E	40	>80	>80	40	>80	20	3.2
C. parapsilosis 81E	20	>80	>80	20	>80	20	13.0
C. glabrata 70E	80	>80	>80	40	>80	40	209.0
C. tropicalis 86E	20	1.25	40	1.25	>80	10	52.2

^{a} Guazatine, ^{b} fluconazole.

From the result of this test, compounds **GNG** and **GGG** showed good activity overall, with MIC$_{50}$ values lower than the guazatine mixture and fluconazole. In particular, the potent activity on *Candida* fluconazole-resistant strains such as *C. glabrata, C. krusei* and *C. tropicalis* was worthy of mention.[36] Based on such results, our group decided to use one of the most active components, **GNG**, as a model compound for the synthesis of new derivatives with potent antifungal activity. The next step was to study the effect of modification on the terminal guanidine, using the synthetic pathway presented in Scheme 1-1, intending to synthesize asymmetrical guanidine.[38]
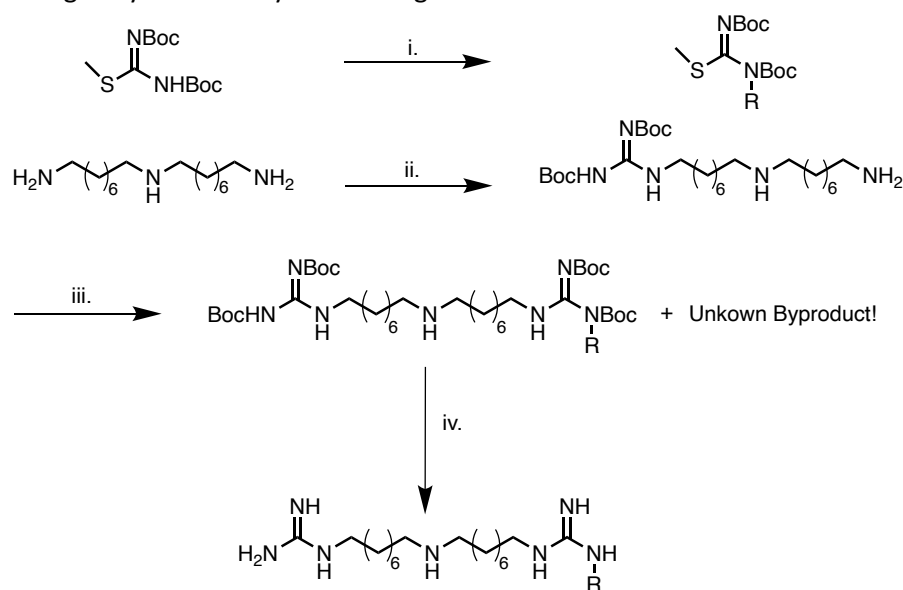
Scheme 1-1: First linear derivatives. (i.) ROH, DIAD, PPh3, THF; (ii.) *N,N'*-di-Boc-S-methylisoyhiourea,THF / MeOH 5:3, 50°C; (iii.) *N,N'*-di-Boc--alkyl-S-methylisoyhiourea, THF, 70°C; (iv.) 10% TFA in dry DCM, r.t.

However, during the synthesis of these news asymmetrical derivatives, an unexpected compound was obtained. This unknown side-product was formed when the aminoguanidine was refluxed with the 1,3-bis(tert-butoxycarbonyl)-2-methylisothiurea in THF at 80 ℃, whereas if the same reaction was conducted at a temperature below 50 ℃ in THF the desired product was obtained. After careful investigation using NMR and mass spectroscopy studies, a macrocyclic structure was proposed (Figure 1-10) which was later confirmed by X-ray analysis.[39]

The proposed mechanism for this macrocyclization (Scheme 1-2) was the initial deprotonation of unsubstituted di-Boc guanidine by the E1cB mechanism. In this case, the base is the terminal amine of the aminoguanidine, leading to the isocyanate. The lost *tert*-butoxide contributes to the deprotonation of the previous amine, which becomes a free nucleophilic and can attack the isocyanate forming the macrocyclic amidinourea with an intramolecular reaction.[40]
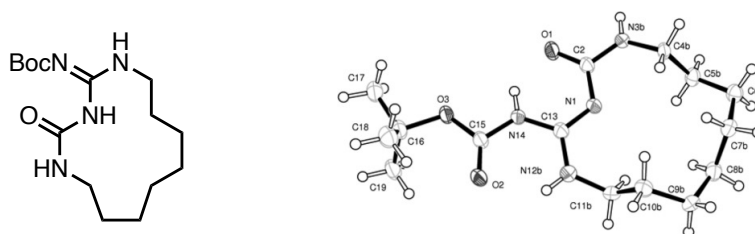
Figure 1-10: X-ray structure of the unexpected side compound.
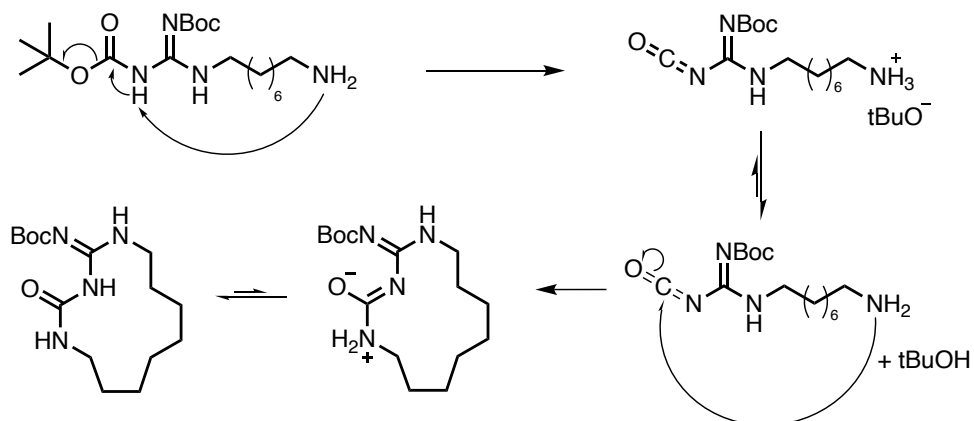
Scheme 1-2: Macrocyclization mechanism.

Once the structure of this unknown compound was identified, a first family of macrocyclic compounds were intentionally synthesized and tested against *Candida* spp. The results of the antifungal assays were surprising, since they showed a good inhibitory profile against the tested strains, in many cases better than their linear analogues.[38] One distinguished itself from the others: **BM1** (Figure 1-11), becoming the representative compound of the amidinoureidic macrocycles. The reference compound is characterized by a macrocyclic core, an alkyl chain linker and a terminal guanidine moiety. In the years that followed, three series of macrocyclic compounds were synthesized and tested. The results of this data gave us more knowledge about the structure-activity relationship of this class of

compounds, which also involved the filing of two patents.[41,42] Moreover, the lead compound **BM1** (Figure 1-11) was studied extensively and, in terms of its in vitro activity and in vivo safety, showed low toxicity and proved its high potential as an antifungal agent.[43]

BM1
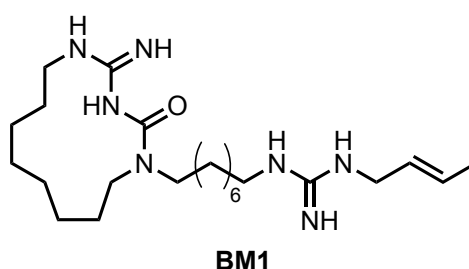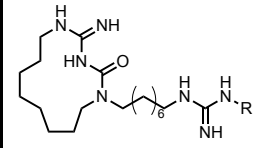
Figure 1-11: Structure of **BM1** the lead compound of the amidinoureidic macrocycles.

1.2.2   The first series of compounds: modifications of the linker moiety.

The first series of compounds were characterized by the presence of different substituents on terminal guanidine to study the effect of this portion on antifungal activity. The different guanylating agents were prepared to start from *N, N'*-di-Boc-*S*-methylisothiourea via Mitsunobu reaction with the opportune alcohol.[38] Once the specific guanylating agents were obtained, macrocyclic derivatives were synthesized following Scheme 1-1 and they were tested against eight clinical isolates of five different *Candida* spp. The results are reported in the table below (Table 1-2).

Table 1-2: Antifungal activity MIC (μM) [a] of the first series

	Antifungal activity MIC (μM)					
	Benzyl	**Prenyl**	**But-2-enly**	**Isobute-nyl**	**Proparg-yl**	**Flucona-zole**
C. albicans ATCC 60193	2.5	40	2.5	20	2.5	0.8
C. albicans 4T	2.5	20	1.25	40	80	209
C. albicans 53T	2,5	20	2.5	40	5	418
C. albicans 15T	5	20	1.25	20	2.5	209
C. krusei ATCC 14243	20	10	5	40	80	209
C. krusei 193T	10	20	5	80	40	418
C. parapsilosis ATCC 34136	80	>80	5	>80	40	6.5
C. parapsilosis 64E	20	>80	5	>80	40	32
C. parapsilosis 81E	20	40	5	>80	40	13
C. glabrata 70E	40	80	20	80	80	209
C. tropicalis 86E	2.5	20	1.25	40	5	52

[a]MIC values are determined at 24h both visually and spectrophotometrically.

Derivatives bearing benzyl or butenyl moieties showed interesting activity toward all the strains tested, with their best activity among cyclic derivatives, followed by the propargyl analogues. Moreover, from the biological data, it seems that linear terminal chains are better for activity compared to a branched moiety. It is worth mentioning that the benzyl and but-2-enyl derivatives

showed a better biological activity profile than fluconazole against *C. albicans*, *C. krusei*, *C. glabrata*, *C. tropicalis.* Among this first series of derivatives, **BM1** resulted in the most active and was selected and used as a reference compound for further development.[38]

1.2.3   The second series of compounds: macrocyclic exploration.

The second series of compounds was designed to explore the chemical space of the amidinoureidic scaffold. The first modifications were performed on the alkyl linker, which was reduced from 8 to 6 terms, resulting in decreased activity. Afterwards, the macrocyclic core was the object of exploration, with the insertion of two functional groups: an ester moiety and an aromatic ring (Figure 1-12). In particular, the corresponding macrolactam **BM17** was characterized by a general decrease in activity, whereas the insertion of benzene fused with the macrocyclic core**, BM19** turned out to be well tolerated, with values of activity comparable to **BM1**. Moreover, this phenyl could be functionalized easier, improving the exploration of chemical space. The size of the macrocyclic was also studied and the two derivatives **BM20** and **BM21**, with 14 and 15 members respectively, were synthesized to evaluate the effects of the macrocycle on the biological activity. These modifications forced us to set up a new synthetic pathway, a convergent approach in which the macrocyclic core was achieved by ring-closing metathesis (RCM). **BM20** and **BM21** emerged as the best compounds of the series showing good activity against wild-type and resistant *Candida* species (Table 1-3).[44]
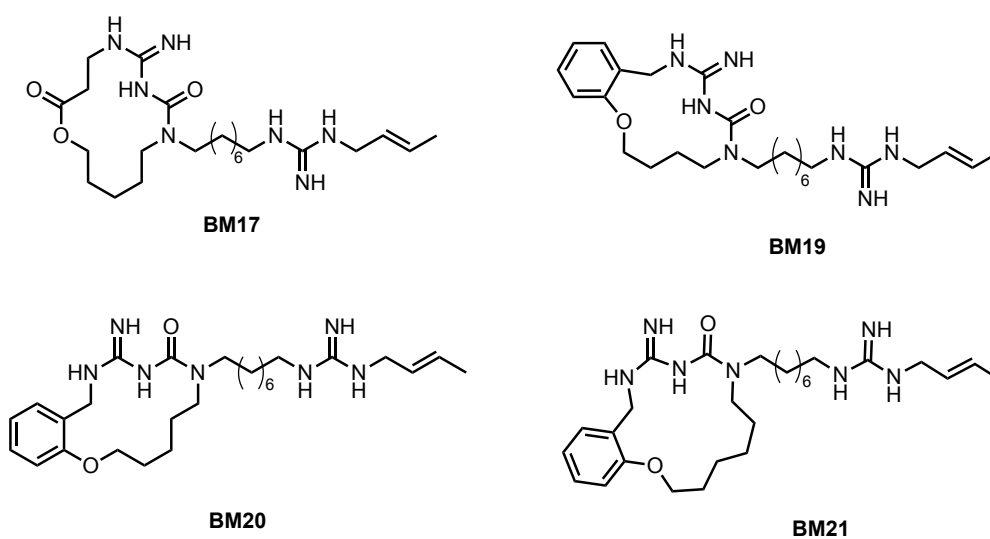
Figure 1-12: The second series of derivatives.

Table 1-3:Antifungal activity MIC_{90} ($\mu g/mL$)[a] of the second series.

Candida strains (n. of strains)	Antifungal activity MIC_{90} ($\mu g/mL$)			
	BM17	**BM19**	**BM20**	**BM21**
C. albicans (22)	32	16	4	4
C. guilliermondii (10)	32	16	2	2
C. krusei (13)	64	32	8	4
C. parapsilosis (24)	32	8	2	2
C. tropicalis (11)	32	8	2	1
C. kefyr (10)	32	4	4	2
C. glabrata (26)	64	64	8	16

[a]MIC_{90} values are determined at 24h both visually and spectrophotometrically.

1.2.4   The third series of compounds: phenyl functionalization.

The third series of compounds were characterized by the presence of a second aromatic ring in the macrocyclic scaffold (Figure 1-13). Firstly, two derivatives were prepared, namely, **BM24**, characterized by a 15-membered macrocycle in which the additional benzyl group is fused with the macrocycle in *ortho*-position, and **BM25,** in which it is in *meta*-position, generating a 16-membered ring. These compounds were tested against several *Candida* spp. Interestingly, **BM24** was found to be more efficient than the correspondent mono-phenyl derivative **BM21** against *C. albicans, C. kefyr, C. parapsilosis,* and *C. guilliermondii*, whereas **BM25**, even though its chemical structure is quite similar to **BM24,** showed a dramatic loss of activity. This again suggests that the size of macrocyclic and its functionalization are important features for the activity of these molecules. Afterwards, functionalization of the phenyl rings with some representative electron-withdrawing and donating groups to gain an understanding of how they could affect antifungal activity was done, starting from derivatives with halogen atoms on this second aromatic ring. Therefore, **BM29** and **BM30**, respectively bearing chlorine and a fluorine atom in position C4 were prepared. As we can see from the report in Table 1-4, the halogenated derivatives exerted a strong antifungal activity against *C. glabrata* with *C. krusei* and *C. kefyr* which are strains not susceptible to fluconazole.
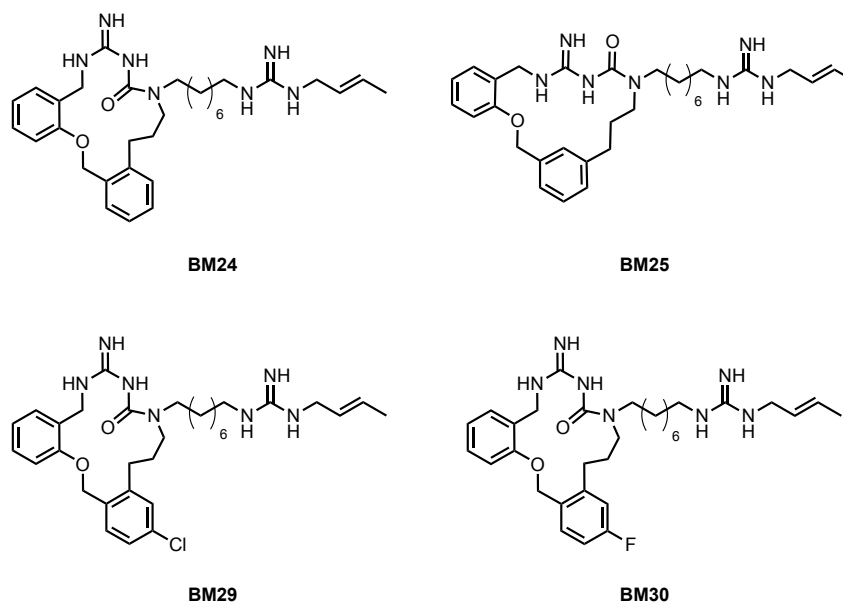
Figure 1-13: Structure of the third series of compounds.

Table 1-4: Third series MIC$_{90}$ analysis in µg/mL [a].

Candida strains (*n. of strains*)	Antifungal activity MIC$_{90}$ (µg/mL)			
	BM24	**BM25**	**BM29**	**BM30**
C. albicans (22)	1	64	3.12	3.12
C. guilliermondii (10)	4	128	1.56	3.12
C. krusei (13)	8	64	1.56	3.12
C. parapsilosis (24)	1	64	3.12	3.12
C. tropicalis (11)	8	64	1.56	1.56
C. kefyr (10)	2	32	1.56	3.12
C. glabrata (26)	16	512	6.25	12.5
C. lipolytica (10)	256	n.a.	12.5	6.25

[a]MIC$_{90}$ values are determined at 24h both visually and spectrophotometrically.

1.3   AIM OF THE WORK.

For the antifungal project, my work concerned two different aspects (Figure 1-14).

The former was the synthesis of **BM37** bearing a methyl group on one of the phenyl groups. This was in line with what had been done previously, focusing attention on designing and synthesizing novel derivatives in which the macrocycle core is modified using an additional aromatic ring bearing some representative electron-withdrawing and donating groups, with the purpose of enlarging our knowledge and understanding of the structure-activity relationship with this new family of macrocyclic amidinoureas. In this case, the introduction of an apolar substituent with an electron-donating effect, quite different from the halogen substituents which were used before to functionalize this aromatic ring, allowed us to evaluate how the activity might react to the presence of this group as well as collect more information about the role of this fragment of the scaffold on the antifungal activity.

The latter was the development of a new synthetic strategy for scaling up the synthesis of **BM1** to produce grams of this compound and perform many biological assays. These data could help us to gain deep knowledge about our reference compound **BM1**.

PART A: Synthesis of **BM37.**

PART B: Gram-scale synthesis of **BM1.**

Synthesis of a novel derivative bearing a lipophilic and electron donating group.

Scale-up synthesis of **BM1** to perform advanced biological investigations.
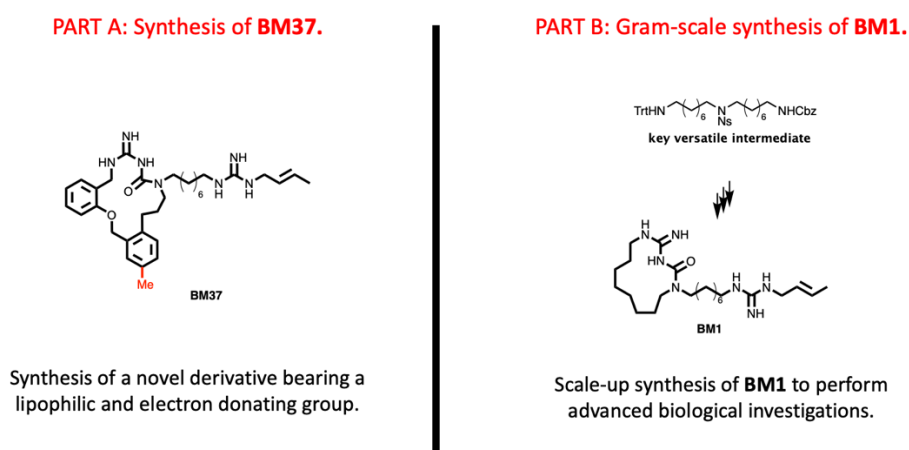
Figure 1-14: Purposes of the antifungal project.

1.4   PART A: SYNTHESIS OF BM37.

1.4.1   Synthetic route for the macrocyclic scaffold.

Since compound **BM37** bears two aromatic rings in the macrocycle, the synthetic route used in our previous works had to be adapted. Therefore, we set up a new synthetic pathway. The synthesis of **BM37** started from hydrolysis of the commercially available methyl 2-iodo-5-methyl benzoate using lithium hydroxide monohydrate (Scheme 1-3). The corresponding benzoic acid **1** was reduced with a borane dimethyl sulfide complex furnishing the benzylic alcohol in quantitative yield, without further purification.[45] Afterwards, the hydroxyl group was converted into a better living group, the chloride **3**, using Tosyl chloride, DMAP, and TEA in dry DCM in an unusual manner.
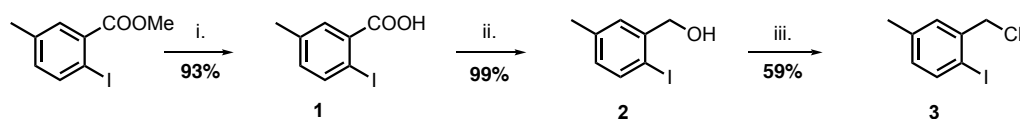
Scheme 1-3: Synthesis of **BM37**. Reagent and condition. (i.) LiOH*H$_2$O, THF/MeOH/H$_2$O 3:1:1, r.t., 5h; (ii.) BH$_3$-Me$_2$S, dry THF, 0 °C-r.t., 12 h, N$_2$; (iii.) Tosyl chloride, DMAP, dry TEA, dry CH$_2$Cl$_2$, 0 °C-r.t., 16 h, N$_2$.

This functional group interconversion led to the corresponding chloride instead of the expected tosylate. (Scheme 1-4).[46] This elegant way to form the chloride could be explained by the presence of an electron-withdrawing group (EWG) attached to the aromatic ring, the iodine atom in this case, which made the benzyl tosylate initially formed more reactive and capable of being substituted by the nucleophilic Chlorine, leading to the chloride derivative.
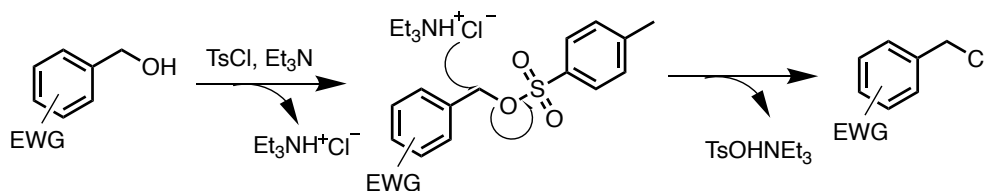
Scheme 1-4: Proposed mechanism for the formation of the chloride.

Chloride **3** was then used for the following O-alkylation (Scheme 1-5). The salicylic aldehyde was deprotonated using potassium carbonate as a base, leading to *in situ* formation of the aryloxide, the active species, capable of substituting the benzyl chloride **3**. The reaction was promoted by a catalytic amount of sodium iodide. The introduction of the vinyl group on benzylic ether **4** was made using the Stille reaction.[47] In this palladium catalysed coupling reaction the 14-electron Pd(0) complex, the active species, was generated by reduction of the palladium acetate using triphenylphosphine, while Tri-n-butyl(vinyl)tin is the source of the vinyl group. Once I got the aldehydic compound **5,** it was transformed into the amine **7** in two steps. Firstly, it was converted to aldoxime by condensation of the aldehydic function present on compound **5** with hydroxylamine hydrochloride in ethanol at reflux. Afterwards, the resulting aldoxime was directly reduced to the corresponding primary amine **7** thanks to the Clemmensen reduction, using Zn° in acid conditions.
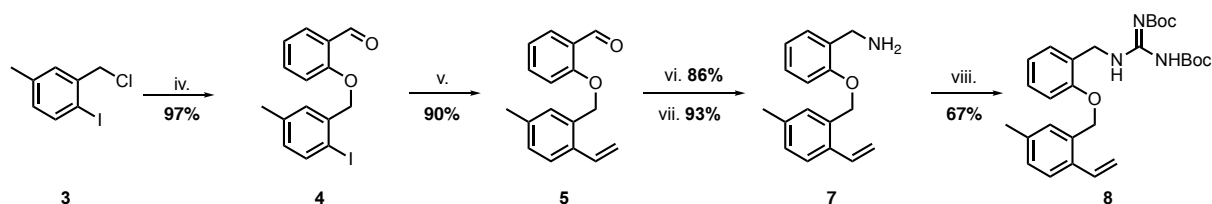
Scheme 1-5: Synthesis of **BM37**. Reagents and conditions. (iv.) Salicylaldehyde, K$_2$CO$_3$, NaI, CH$_3$CN, reflux, 16 h; (v.) tributyl(vinyl)tin, Pd (OAc)$_2$, PPh$_3$, dry THF, reflux, 16 h, N$_2$; (vi.) NH$_2$OH*HCl, pyridine, EtOH, reflux, 3 h; (vii.) Zn dust, 2N HCl, THF, reflux, 4 h; (viii.) *N,N'*-Di-Boc-1H-pyrazole-1-carboxamidine, DIPEA, THF, r. t., 16 h.

The guanidine introduction was achieved by reacting the intermediates **7** with *N,N'*-Di-Boc-1H-pyrazole-1-carboxamidine and DIPEA in THF (Scheme 1-6).[48,49] At this point, the guanidine-protected derivative **8** was coupled with the amine linker **9** through an amdinourea-forming reaction which took place in THF at reflux in presence of a base such as DIPEA or TEA. This reaction was the intermolecular version of the intramolecular macrocyclization already described above in Scheme 1-1.[38,40] Compound **10,** due to the presence of the double bond, was ready to undergo the ring-closing metathesis (RCM).[50,51] This reaction is air-sensitive and required strict conditions, such as a freshly degassed solvent, a 2nd generation Grubb's catalyst, and a very diluted condition. The efficacy of the method of degassed solvent is one of the most important factors accounting for a good outcome of RCM. We used the Freeze-Pump-Thaw technique to achieve a better result in the reaction. Briefly, this process consists of three steps: the solvent in a sealed round-bottomed flask is completely frozen using liquid N$_2$, afterwards, the flask, still immersed in the N$_2$, is opened up to a vacuum for 2-3 minutes to evacuate the headspace of the flask. Finally, the vacuum is closed, and the flask is removed from the liquid nitrogen and thawed at room temperature, which allows gas bubbles present in the solvent to escape from it. This procedure is repeated two times before the catalyst is added, and then a final cycle is performed to remove oxygen introduced during the addition of the catalyst. The concentration of the reaction mixture also influences the good outcome of this reaction because it avoids intermolecular reactions. For this reason, I used 2 mM concentration in the reaction mixture. The RCM reaction provided compound **11** as a mixture of **E** and **Z**. Analysis of the integrations and peaks presented around the double bond region (δ 6-7 ppm) of the NMR spectra, showed that the Z isomer was predominant. The next step was hydrogenation, which reduced the double-bond leading to compound **12**. During this step, the Cbz protecting group was removed as well, using an H$_2$ atmosphere on Pd/C 10% and a few drops of HCl concentrated, which promoted the elimination of the carbamate provided the free ammine **12** as chloride salt.
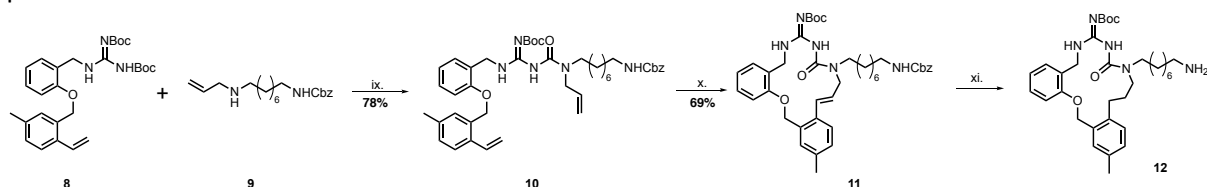
Scheme 1-6: Synthesis of **BM37**. Reagents and conditions. (ix.) dry TEA, dry THF, reflux, 16 h, N$_2$; (x.) 2nd gen. Grubb's catalyst, degassed dry CH$_2$Cl$_2$, reflux, 16 h, N$_2$; (xi.) H$_2$, 1 atm, Pd/C 10%, cat. HCl 36%, i-PrOH, r. t., 4 h.

The final two steps (Scheme 1-7) were a second guanylating with the *N,N'*-Di-Boc-N-crotyl-1*H*-pyrazole-1-carboxamidine, a pre-synthesized guanylating agent bearing the crotyl moiety, with excess DIPEA to desalt the free amine formed before. Once we obtained compound **13,** this was deprotected from Boc groups with trifluoroacetic acid, furnishing the final compound as trifluoroacetic salts **BM37.**
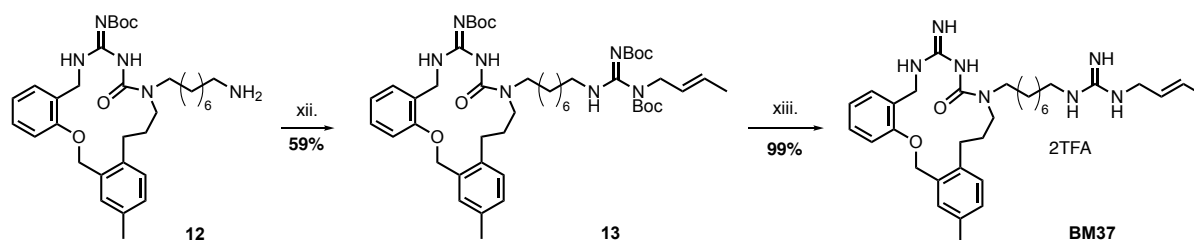
Scheme 1-7: Synthesis of **BM37**. Reagents and conditions. (xii.) *N,N'*-Di-Boc-N-crotyl-1*H*-pyrazole-1-carboxamidine, dry DIPEA, dry THF, reflux, 12 h; (xiii.) TFA, CH₂Cl₂, r. t., 12 h.

1.4.2   Synthesis of the linker and the guanylating agent.

The linker moiety (Scheme 1-8) was prepared starting from the available amino octanoic acid. Firstly, the amino group of the linker was protected with benzyl chloroformate. Then, the Cbz protected compound **14** was coupled with allylamine using EDC and HOBt in dry DMF to afford the amide **15**, in which the amide functional group needed to be reduced to amine **9**, the linker of the derivative **BM37.** This reaction was carried out to exploit the mild capacity of DIBAL-H to act as a reducing agent of the amide group, while at the same time not acting so strongly as to affect the double bond of the allylamine or the elimination of the Cbz group. However, the yield of this reaction was generally low (35-55 %) since problems occurred during the work-up, including a massive aluminium emulsion which was hard to work with, and the purification process, since the amine **9** tended to smear out leaving a long tail behind it which required the use of an additive in the eluent, the NH₃(aq) in my case, to elute this product. The recovery of SM which has not reacted by column could be considered a positive side of this reaction since it can undergo the reduction again.
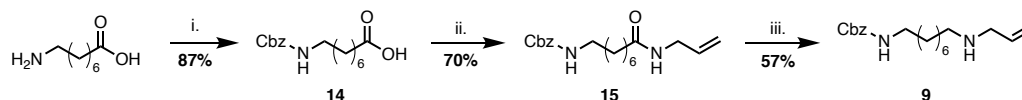
Scheme 1-8: Synthesis of the linker **9**. Reagents and conditions. (i.) Benzyl Chloroformiate, K₂CO₃, THF/H₂O DCM, 0°C to r.t., 12 h; (ii.) Allylamine, EDC, HOBt, DIPEA, dry DMF, r.t., 16 h; (iii.) DIBAL-H, dry DCM, 0°C to r.t., 16h.

Regarding the synthesis of the guanylating agent **16** (Scheme 1-9)**,** this took place through a smooth and high yield Mitsunobu reaction starting from di-boc- pyrazole-carboxamidine and crotyl alcohol.[38,52]
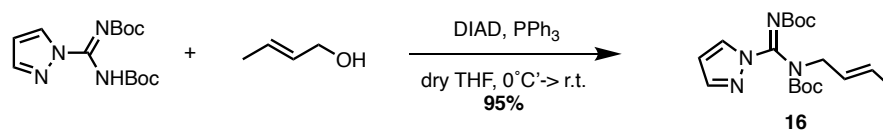
Scheme 1-9: Synthesis of the guanylating agent **16**.

1.4.3   Biological evaluation of BM37.

Once synthesized, the compound **BM37** was tested for its antifungal activity and compared to other derivatives of these series. For the antifungal activity, **BM37** was evaluated by determining the MIC₉₀ against more than 100 strains belonging to 8 different Candida species (*C. albicans, C. guilliermondii, C. crusei, C. parapsilosis, C. tropicalis, C. kefyr, C. glabrata,* and *C. lipolytica*) plus 15 strains of *C. neoformans*, with each strain isolated from a patient in oral, vaginal, anorectal, urine, stool, blood, central venous catheter, and respiratory tract infections. MICs were determined following liquid growth inhibition trials conducted according to Clinical and Laboratory Standards Institute (CLSI)

guidelines, using serial dilutions of the compounds dissolved in an appropriate buffer with two different final concentrations in a 96-well flat-bottom Microtiter plate.[53–56] The first one ranged from 256 to 0.125 µg/mL for **BM24**, **BM37** and Fluconazole, whereas compounds **BM29** and **BM30** were tested using a final concentration ranging from 200 to 1.56 µg/mL. The antifungal assays were performed at the Institute of Microbiology of "University Cattolica del Sacro Cuore" by the group of Professor Maurizio Sanguinetti and Dr Francesca Bugli.

Table 1-5: Valuation of the antifungal activity of **BM37.**

Fungal strains	Antifungal activity MIC90 [μg/mL] [a]				
	BM24	**BM29**	**BM30**	**BM37**	**F**[b]
C. albicans (22)	1	3.12	3.12	4	2
C. guilliermondii (10)	4	3.12	1.56	2	4
C. krusei (13)	8	3.12	1.56	2	256
C. parapsilosis (24)	1	3.12	3.12	16	0.5
C. tropicalis (11)	8	1.56	1.56	4	2
C. kefyr (10)	2	3.12	1.56	4	1
C. glabrata (26)	16	12.5	6.25	16	16
C. lipolytica (10)	256	6.25	12.5	4	n.t.[c]
C. neoformans (15)	n.t. [c]	3.12	3.12	4	2

[a] MIC_{90} values were determined at 24h both visually and spectrophotometrically. [b] Fluconazole. [c] not tested.

From the results of the antifungal trials (Table 1-5), we can assert that the introduction of a methyl group on the phenyl ring was beneficial and well-tolerated. **BM37,** indeed, showed an enhancement of activity, with MIC values, 2- to 4-fold lower than **BM24,** against *C. guilliermondii*, *C. tropicalis*, and *C. krusei,* a species resistant to common azole drugs. The activity of **BM37** was comparable in many cases to the halogen derivatives **BM29** and **BM30**, the most active compounds of this third series. It is also important to underline the strong antifungal activity exerted by **BM37**, comparable with halogen derivatives and fluconazole, against *C. neoformans*, the pathogenic fungi responsible for fatal meningitis.

In summary, the introduction of an apolar group on the aromatic ring resulted in a general increase of activities, with the slightly loose toward *C. albicans* and *C. parapsilosis*. This information could be useful to know because, in the future, apolar substituents could be introduced to increase the lipophilicity of these compounds, ameliorating their permeability and pharmacokinetics profile but retaining their antifungal activity. Moreover, biological data showed that small point modifications in the structure lead to strong active (**BM37**, **BM29**, **BM30**) or inactive compounds (**BM25**), providing us with a clear idea that these compounds could interact with a precise cellular target, yet to be defined.

1.5 PART B: BM1 Gram-scale synthesis.

BM1 is the lead compound of this series of macrocyclic amidinourea derivatives. It shows good antifungal activity against *Candida* wild types as well as resistant strains. Moreover, its structure is new and not shared with other antifungal compounds which made it reasonable to hypothesize a mechanism of action different from other antifungal compounds. Having these desirable characteristics that a novel antifungal should have, we decided to thoroughly investigate its ADMET profile with in vitro and in vivo pharmacokinetic and acute toxicology studies.[43] For these reasons, we faced the challenge of preparing greater amounts of compound **BM1** than what we usually managed. This triggered us to set up a convenient strategy to prepare, easily and affordably, grams of **BM1**.

1.5.1 Previous synthesis of BM1.

The first described synthesis of **BM1** used the commercially available bis(8-aminooctyl) amine.[38] Two subsequent guanylations of the primary amino groups, by using *N, N'*- di-Boc-S-methylisothiourea and *N, N'*-di-Boc-N-[(E)-but-2-en]-S-methylisothiourea respectively, followed by cyclization in refluxing THF in presence of TEA and a final Boc deprotection, led to the desired compound. This synthetic route was pretty good with only 4 steps with a total yield of 14%. However, since the withdrawal from the market of the commercial starting material, new synthetic pathways had to be explored and tried. Two routes were explored. The first one was the homemade synthesis of bis(8-aminooctyl) amine itself in four steps starting from 1,8- dibromooctane, as described in Scheme 1-10.[57] Nevertheless, using this synthetic route on large scale meant using a large quantity of hazardous sodium azide and involved an overload of work and time, since the purification of these derivatives required long and tricky column chromatography even on a small scale, making this procedure unsuitable for scaling up.
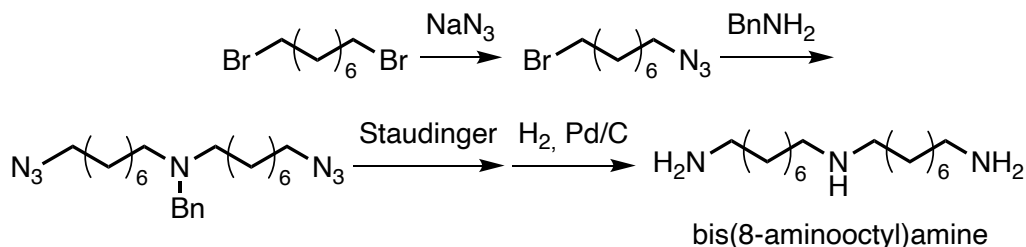
Scheme 1-10: Synthesis of bis(8-aminooctyl) amine.

In a second approach (Scheme 1-11), the macrocyclic scaffold was obtained by using DIBAL-H to reduce the amide obtained by coupling the mono-guanylated-1,8-diaminooctane and the Cbz-protected 8-aminooctanoic acid.[44] One of the drawbacks of this method is the use of DIBAL-H as a reducing agent for the amide. This choice was dictated due to the presence of other carbonyl groups in the molecule, but it led to moderate to low yields, difficult purification and handling (during the work-up a massive aluminium emulsion is formed) and so was not consistently reproducible in a large-scale procedure.
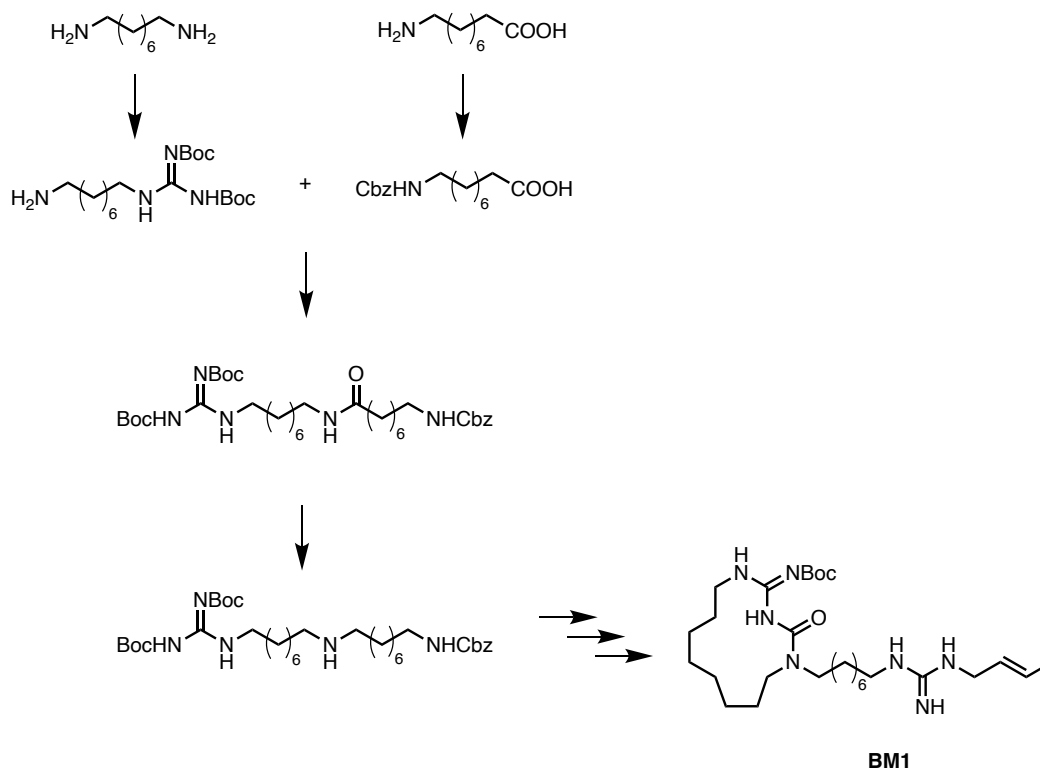
Scheme 1-11: Synthesis of **BM1** using the second approach.

1.5.2   A new synthetic approach for BM1.

The previous synthetic routes resulted unsuitable for providing **BM1** on a gram scale. Therefore, a new synthetic approach was developed. The first step was to jump into the chemical literature regarding the methodology for the preparation of different types of amines and polyamine.[58,59] Since these chemical species play an interesting and key role in the biological activity of compounds. The chemistry focused on this topic is massive and it was not easy to find an effective synthetic method without getting lost. Therefore, we decided to focus our attention on the work of Fukuyama and his co-workers.[60–62] They developed strategies for the selection of protective groups for nitrogenous atoms to use during amine synthesis. In our case, after a careful evaluation of the possible options, we decided that the cornerstone of the synthesis would be the intermediate **20,** the bis(8-aminooctyl) amine in the tri-protected form, with trityl, Cbz and nosyl as the protecting groups of choice. This intermediate offers many advantages, such as lowering both the time and costs of production (because protecting groups make it less polar and easier to handle and purify) and versatility, since the three different groups are orthogonal to each other, meaning they can be selectively removed in different conditions, allowing us to deprotect only the chosen amine.[63]
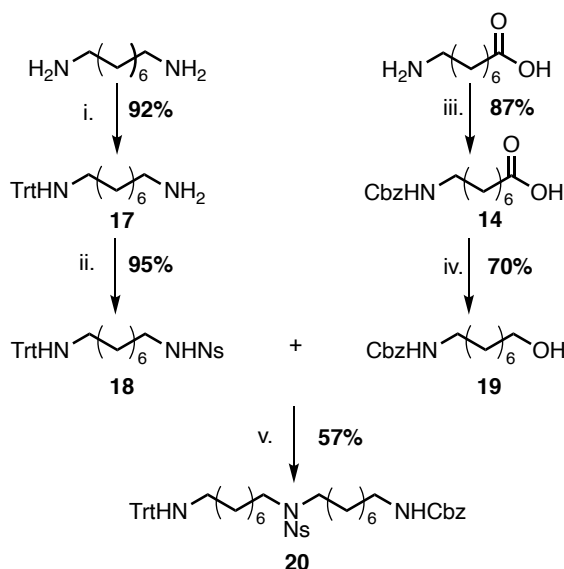
Scheme 1-12: Synthesis of intermediate **20**. (i.) Trityl chloride, DCM, 0 °C to r. t., 2 h; (ii.) Nosyl chloride, DIPEA, DCM, r. t., 1 h, (iii.) CbzCl, NaHCO₃, H₂O/THF, -10 °C to r. t., 16 h; (iv.) Me₂SBH₃, dry THF, r. t., 16 h; (v.) DIAD, PPh₃, dry THF, r.t, 3 h.

The synthesis started (Scheme 1-12) with the commercially available diamino octane which was coupled with trityl chloride in DCM at 0 °C. Column purification afforded compound **17**, in which the other free amine was protected with the nosyl group using DIPEA as a base. These reactions occurred with good yields and without difficulties. The synthesis of fragment **19** of the molecule was the same as described before. Briefly, the amino group of 8-aminooctanoic acid was first protected using Cbz and then the acidic function of the molecule was reduced using BH₃-dimethyl sulfoxide. Once we obtained the two fragments **18** and **19**, they were coupled together using the Mitsunobu reaction in presence of DIAD (diisopropyl azodicarboxylate), Ph₃P and THF dry. The reaction took place with the initial combination of triphenylphosphine with DIAD leading to a neutral species containing two separate charges intermediate, namely betaine. Thereafter, the amine protected with nosyl group was the only one able to protonate (since acidic for its behaviour as sulphanilamide) this betaine provides the phosphonium intermediate. This intermediate bound the alcohol oxygen and activated it as a leaving group. The final substitution of deprotonated sulphanilamide on this activated alcohol led to compound **20** and triphenylphosphine as the by-product.[64] Once we got compound **20**, the three subsequent reactions had the advantage of being one-pot-two-steps. First, there was the trityl deprotection which was carried out in TFA and using triethylsilane.[65] Trityl cleavage was a reduction process of the initially formed trityl cation, with its characteristic yellow colour, to the corresponding triphenylmethane by triethylsilane. The deprotection could be simply monitored by observation of the disappearance of the yellow colour and it was very quick. Once the reaction was finished, the excess of TFA and triethylsilane were easily removed *in vacuo* leaving the corresponding amine as trifluoracetic salt and the inert triphenylmethane. The following guanylation with *N, N'*-Di-Boc-1H-pyrazole-1-carboxamidine and DIPEA gave compound **21**. Afterwards, the nosyl group was removed from compound **21** using thiophenol and K₂CO₃ in dry DMF.[66] The cleavage of the nosyl group occurred with an aromatic nucleophilic substitution with the nucleophilic thiol. This reaction involved (Scheme 1-13) the initial addition of a thiolate to the aromatic ring of the nosyl amides forming the Meisenheimer complex, followed by the elimination of sulfur dioxide and the free amine. The excess of thiophenol and K₂CO₃ was eliminated during the work-up by washing with water and 5% NaHCO₃,

whereas the byproduct 1-nitro-4-(phenyl sulfonyl)benzene was left in place since it did not interfere with the next step.
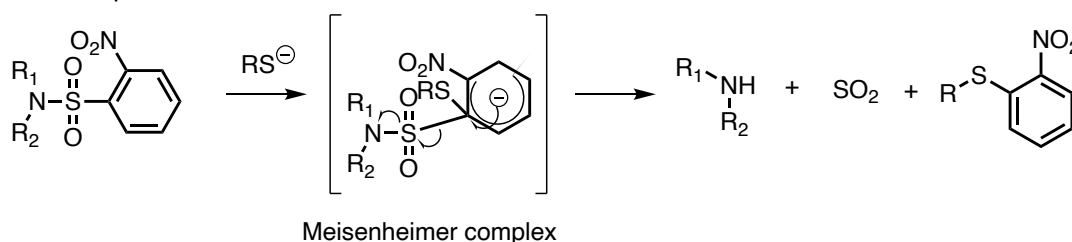
Scheme 1-13: Deprotection mechanism for the nosyl amide.

At this point, the solvent was removed (Scheme 1-14), and the crude product was heated at reflux with TEA in THF giving compound **22**.[40] The following reactions were a Cbz deprotection by hydrogenation leaving the primary amine, which was guanylated with compound **16** giving compound **23**. The final step was the deprotection from the Boc groups using HCl 4M in dioxane, furnishing **BM1** as a chloride salt.[63]
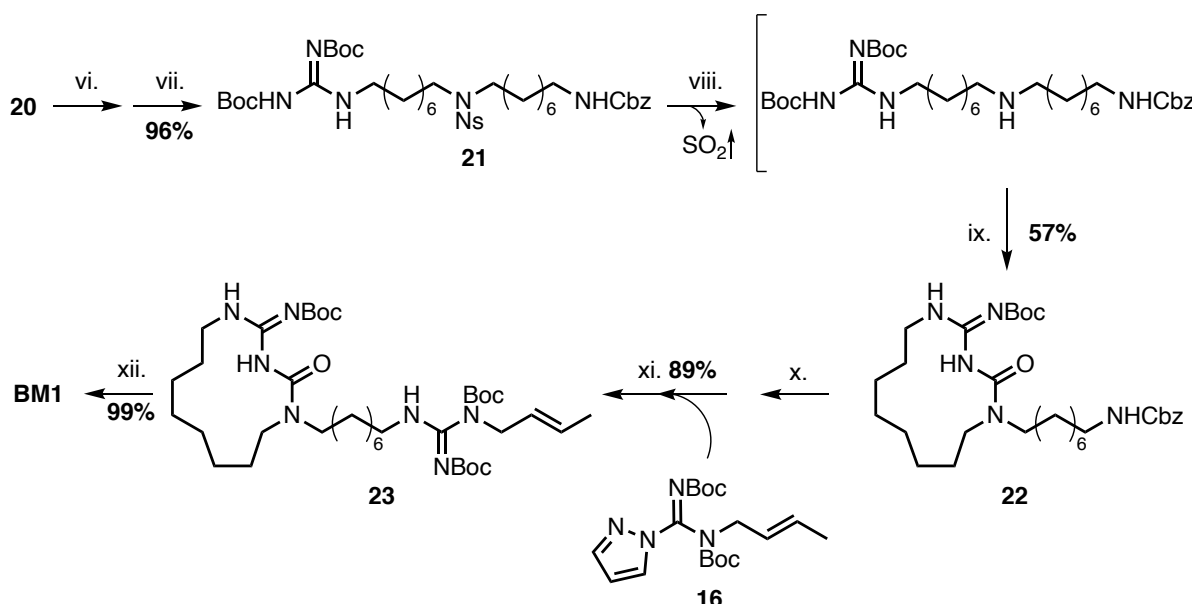
Scheme 1-14: Last steps of the synthesis of **BM1**. (vi.) TFA, Et₃SiH, DCM, 0 °C to r. t., 1 h; (vii.) *N*, *N'*-Di-Boc-1H- pyrazole-1-carboxamidine, DIPEA, THF, r. t., 16 h; (viii.) Thiophenol, K₂CO₃, dry DMF, r. t., 7 h; (ix.) TEA, THF, reflux, 16 h; (x.) H₂, 10% Pd/C, cat. 37% HCl, *i*-PrOH, r. t., 3 h; (xi.) **16**, TEA, THF, r. t., 16 h; (xii.) HCl 4M in Dioxane, 23 h.

1.5.3 *In vitro* and *in vivo* ADME analysis of BM1

Once synthesized, the pharmacokinetic profile of **BM1** was evaluated.[67] In vitro, ADME experiments on **BM1** displayed (Table 1-6) a high-water solubility of 1mg/mL and a high affinity for the plasmatic protein AGP, a predictable result given that this plasmatic protein can bind cationic molecules like **BM1**. Moreover, its hydrophilic behaviour was in line with the low value of passive permeability found in the PAMPA experiment. The metabolic stability of this compound was determined in presence of human liver microsomal protein. The result showed that **BM1** was not susceptible to metabolism since 95% of the unmodified compound was detected. Because of its high metabolic stability, no reactive intermediates are formed. The possibility to inhibit CYP3A4 was also evaluated, Figure 1-15, and **BM1** resulted in being a non-inhibitor of this enzyme. Since fungal infections are common among patients

in therapy with immunosuppressor or anti-HIV drugs, the knowledge derived from these data valorised **BM1** as an antifungal agent, allowing its potential coadministration with other drugs.

Table 1-6: In vitro pharmacokinetic properties of **BM1**.

LogS [a] (log mol/L)	Membrane permeation [b] Papp [c] × 10 [−6] (cm/s)	Metabolic stability [d] (%)	Major metabolites [e] (%)	Binding human serum proteins Kd (μM)[f]	
				AGP	HSA
- 2.61	< 0.1	95	M + OH (5)	12.2	212.1

[a]Aqueous solubility was determined using LC-MS method 1 reported in supporting data (log mol/L). [b] Membrane permeation was determined with a PAMPA technique. [c] Apparent Permeability. [d] The human liver microsome stability is expressed as a percentage of unmodified parent drugs. [e] M = mass of the parent drug; the percentage of metabolite experimentally determined via LC-MS is reported in parentheses. [f] Dissociation constant (Kd) values are measured using the indirect fluorescence method.
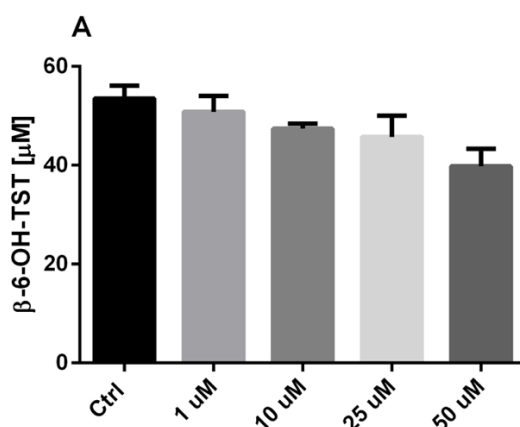
Figure 1-15: Inhibition of CYP3A4 isoform activity on **BM1**, measured as the concentration of β6-hydroxytestosterone (β6-OH-TST), compared to the control (Ctrl) mix in absence of compounds.

In vivo pharmacokinetic studies were conducted on rats using two different administration routes: IV injection and PO administration (Table 1-7). However, in the latter, the level of **BM1** was less than the limit of quantification so no data could be obtained. From the pharmacokinetic data, we can assert that **BM1** tends to be distributed in extracellular liquid (Vd >15), as expected from its hydrophilicity which routes it to renal excretion. This hypothesis was confirmed by the presence of the unmodified compound in high concertation in kidneys and urine samples. No accumulation in the brain or liver was detected. Moreover, **BM1** is compatible with daily administration, as supported by C_{max}, AUC $t_{1/2}$ data. In vivo toxicology experiments were performed, and the data displayed neither clinical signs of toxicology effect nor alteration in cellular morphology, supporting the safety of **BM1** in clinical use.

Table 1-7: Pharmacokinetic profile of **BM1.**

PK Parameter	Unit	10 mg/kg IV value	2 mg/kg IV value
$t_{1/2}$	h	13.01	15.68
T_{max}	h	0.08	0.08
C_{max}	µg/mL	2.78	0.87
C_0	µg/mL	3.15	1.14
$AUC_{0\rightarrow 24h}$	µg/mL*h	6.11	1.11
$AUC_{0\rightarrow\infty}$	µg/mL*h	7.83	1.44
$AUMC_{0\rightarrow\infty}$	µg/mL*h^2	108.27	20.82
$MRT_{0\rightarrow\infty}$	H	13.82	14.45
V_z	(mg/kg)/(µg/mL)	23.95	31.40
Cl	(mg/kg)/(µg/mL)/h	1.28	1.39

Data calculated with PKSolver.[68] C_{max}: maximum concentration observed. C_0: concentration at time 0 (estimated). Tmax: time of maximum concentration observed. MRT: mean residence time. AUC: area under the curve. AUMC: area under the first moment curve. Vz: volume of distribution. Cl: clearance. $t_{1/2}$: half-life. n.d.: not detected. IV: intravenous.

1.6   CONCLUSION

The currently available antifungal drugs cannot satisfy the burden of fungal infection. Now more than ever, the ambitious challenge of developing new antifungal drugs is mandatory if we want to reduce the dramatic number of deaths related to fungi. The peculiarities sought out in a new potential antifungal are low toxicity, no CYP450-interactions, a novel model of action and the availability of an oral administration.

For these reasons, we investigated the family of compounds characterized by the macrocyclic amidinoureas scaffolds that seem to have all the right characteristics to become a potential new therapeutical class of antifungal agents. The impressive work made to develop a gram-scale synthesis of **BM1**, from an economic and workload point of view, permitted an extensive and accurate study of its pharmacokinetic profile. Its ADME profile results were excellent, with high solubility and microsome stability. Moreover, it did not inhibit the CYP450 cytochrome and in vivo toxicology studies supported the safety of **BM1** in clinical trials. All of this information supports its potential as an antifungal agent with a new mechanism of action, low toxicity and no potential harmful drug-drug interaction through the CYP450 enzyme system. On the downside, there is the limited oral bioavailability found, linked with the low value of permeability found, that does not allow, to date, oral administration. Future perspectives on increasing its permeability could result from the promising activity of **BM37**. The biological data displayed that an apolar substituent (in this case, the methyl group) was well-tolerated and gave more room for improvements with the introduction of lipophilic substituents to ameliorate the permeability and allowed oral alternatives, a desirable feature in antifungal drugs. Another step forward could disclose the mechanism of action of these classes of compounds. From the amount of data in our possession on **BM1**, we know that it showed good antifungal activity, especially for *Candida* strains resistant to azole and amphotericin. Its structure is new and not shared with other drugs, so it is plausible to think that its molecular target is different to other antifungal agents. Besides, from the structure-activity relationship data derived from three series of macrocycles, we can suppose that the molecular target is a cellular structure, an enzyme, or a protein, since small modifications in their chemical structure can enhance (**BM37**, **BM29**, **BM30**) or annihilate its biological activity (**BM25**). The research of the mode of action of amidinoureas not only has given us further knowledge about these classes of compounds but also a completely different research project was pursued. The considerations and the work described in the next chapter of this thesis regarding a new therapeutic application of the macrocyclic amidinoureas scaffold.

Chapter 2

Targeting Human Chitinases: Design, Synthesis And Biological Evaluation Of Novel Inhibitors

2.1   INTRODUCTION

2.1.1   Chitin and chitinase.

Chitin is a polymer formed by units of N-acetyl-D-glucosamine (GlcNAc) linked with β 1-4 glycosidic bonds. It is the second most abundant polymer and the major structural component of the exoskeletons of crustaceans and insects, house dust mites (HDM), and fungal cell walls.[69] The different biological functions provided by the chitin are related to the different crystalline forms in which it can exist, namely, α- chitin, β-chitin and γ-chitin. The main difference between these three forms is represented by how the chitin chains are disposed of. In the α- chitin, chains are arranged in an antiparallel manner which ensures strong hydrogen bonds resulting in mechanical strength and stability. For this reason, α- chitin is the major structural component of the exoskeleton of a fungal cell. In β-chitin, the chains are disposed in a parallel manner, resulting in a less compact form due to weak intramolecular forces. It is commonly found in cocoons and squid pens. Finally, γ-chitin is a mixture of the α- chitin β-chitin chains and is found mostly in mushrooms.[70,71]

Chitin synthase is the enzyme responsible for producing chitin in chitin-containing organisms. This enzyme belongs to the GT2 family of polymerizing glycosyltransferases. The chitin chains are formed by the addition of GluNAc units from the non-reducing end of the chitin chains and, once they are produced as linear polymers, they are assembled into microfibrils of various lengths and diameters extruding from the cell wall.[72]

Conversely, Chitinases are the enzymes that hydrolyse the β 1-4 glycosidic bond presented in the GlcNAc of chitin chains. Chitinases are widely distributed enzymes present in plants, insects, fungi, and bacteria. In these organisms, chitinases play different biological functions such as the acquisition of food, defence against pathogens and regulation of innate immune defence against pathogens. Chitinases belong to the Glycosyl Hydrolase (GH) family and are classified based on their sequence identity and structural homology to GH18, GH19 and GH20. The family of GH19 are constituted mainly by plants and nematodes chitinase, whereas the GH18 family includes a large group of chitinolytic enzymes from bacteria, fungi viruses and animals. GH18 can be further divided into true chitinase, which can hydrolyse chitin into shorter $(GluNAc)_2$ or $(GluNAc)_3$ oligosaccharides and enzymatically inactive chitinase namely, chitinase-like proteins, which can bind but not hydrolyse the chitin. The catalytic domain of GH18 is a structural feature that is highly conserved and consists of a catalytic domain connected with a hinge. As regards the scope of this thesis will be focused only on human chitinase and, in particular, on the role of these chitinases in human diseases.[73]

2.1.2   Human Chitinase.

Although humans do not use nor produce chitinase, their genomes are encoded for several chitinases, all belonging to the GH18 family: Two endochitinases namely, acidic mammalian chitinase (AMCase) and chitotriosidase 1 (CHIT1), which possess chitin hydrolysing activity and some enzymatically inactive chitinase-like-lectins, also known as Chitinase-Like Proteins (CLPs)[74], which are catalytically inactive due to the modifications of the critical aminoacidic presented in the active site.

CHIT1 is the first chitinase discovered in humans and it is mainly present in tissue such as the lungs, spleen, liver, thymus and specific cells of the immune system (activated macrophages and neutrophils) in response to different pro-inflammatory signals.[75]

AMCase is the other enzymatically active chitinase found in humans and is mainly present in gastrointestinal tracts and in the lungs, where it is released into the airway lumen by epithelial cells.

The location of this protein in specific parts of the body underlines its role in the digestion of chitinous food and defence against chitin-containing pathogens.[76]

CLPs, such as CHID1 YKL-40, and YKL-39, are a set of proteins that are structurally related to the GH18 chitinase but lack catalytic activity. They are expressed mainly by neutrophils, macrophages, epithelial cells, and dendritic cells.[77]

2.1.3   Implications of Human Chitinase in Diseases.

Recently, several studies have shown that human chitinases are a crucial player in type II inflammation diseases.[78] Therefore, AMCase and CHIT1 have attracted considerable attention as potential targets in chronic respiratory diseases, including asthma, and chronic obstructive pulmonary disease (COPD) and fibrosis.

Asthma is a type 2 inflammatory disease caused by a dysregulation of the T-helper 2(Th2) response in the induction and maintenance of the inflammatory state. In a study conducted by Zhu et al., AMCase was found highly expressed in lung tissue of asthmatic patients and animal models of asthma and correlated with the Th2 inflammatory response through an IL-13-dependent mechanism, suggesting its involvement in the disease. Moreover, AMCase inhibition using AMCase antisera or allosamidin (a potent chitinase inhibitor) resulted in a reduction of the inflammatory cells in mice challenged with ovalbumin as well as amelioration of the asthma symptoms.[79,80]

Other studies have shown the role of CHIT1 in other chronic inflammatory respiratory diseases such as idiopathic pulmonary fibrosis (IPF), sarcoidosis, chronic obstructive pulmonary disease (COPD). In these studies, high levels and activity of CHIT1 were correlated to the high level of pro-inflammatory factors suggesting its key role in the inflammatory response development.[81,82]

Conversely, it was worth mentioning that there are also studies demonstrating that AMCase and CHIT1 play only a protective role in type II inflammation and no may not be a good target in chronic respiratory diseases.[83–85]

As described above, various studies tried to elucidate the role of chitinase in type II inflammatory diseases. However, to date, there is evidence that suggests the hypothesis that chitinase plays an adverse role in these diseases, whereas other proofs contradict it. To shed more light on the role of AMCase and CHIT1 in these diseases, we need inhibitors with high selectivity and potency for both enzymes and with satisfactory profiles allowing the administration study in the animal model. The search for inhibitors having these desirable features has prompted the research in this field and in recent years, a growing number of compounds have been described. In the next section, I will discuss the most relevant compounds inhibitors of chitinase reported in the literature.

2.1.4   Chitinase inhibitors.

To date, several classes of natural or rational design chitinase inhibitors have been reported, demonstrating that human chitinases are one of the hot topics in pharmaceutical chemistry.

The first class of chitinases inhibitor is allosamidin (Figure 2-1), a metabolite found in the mycelium of *Streptomyces* species. This compound displays a potent inhibitory activity against all family GH18 chitinases. The efficacy in vivo of allosamidin was used by Zhu et al. as a chemical probe to demonstrate the association between AMCase and asthma. Even if allosamidin is the widely used and studied inhibitor, another seven natural derivatives have been identified so far, including methylallosamidin and demethylallosamidin.[86,87]

Other natural product chitinase inhibitors are represented by the cyclic pentapeptides argifin and argadin (Figure 2-1). These compounds are characterized by a potent low micromolar inhibition activity against AMCase and CHIT1 and a distinctive mechanism of action since these peptide-like compounds can mimic the protein-carbohydrate interactions among chitin and chitinase.[88–90]

The next family of compounds are Xanthine derivatives representing the first drug-like inhibitors specifically tailored for human chitinase (Figure 2-1). These compounds were identified by a screening of a commercial library of molecules. From this first attempt, the 1,3-dimethylxanthine emerged as a promising scaffold but was characterised by low inhibitory activity and lack of selectivity. Further modification led to bisdionin C, a potent inhibitor with low micromolar activity on both enzymes and bisdionin F, the first rational design inhibitor characterized by great potency and selectivity for AMCase. The latter displayed the same activity values as in vivo experiments and its administration showed an ameliorative effect on the principal hallmark of allergic inflammation.[91–93]
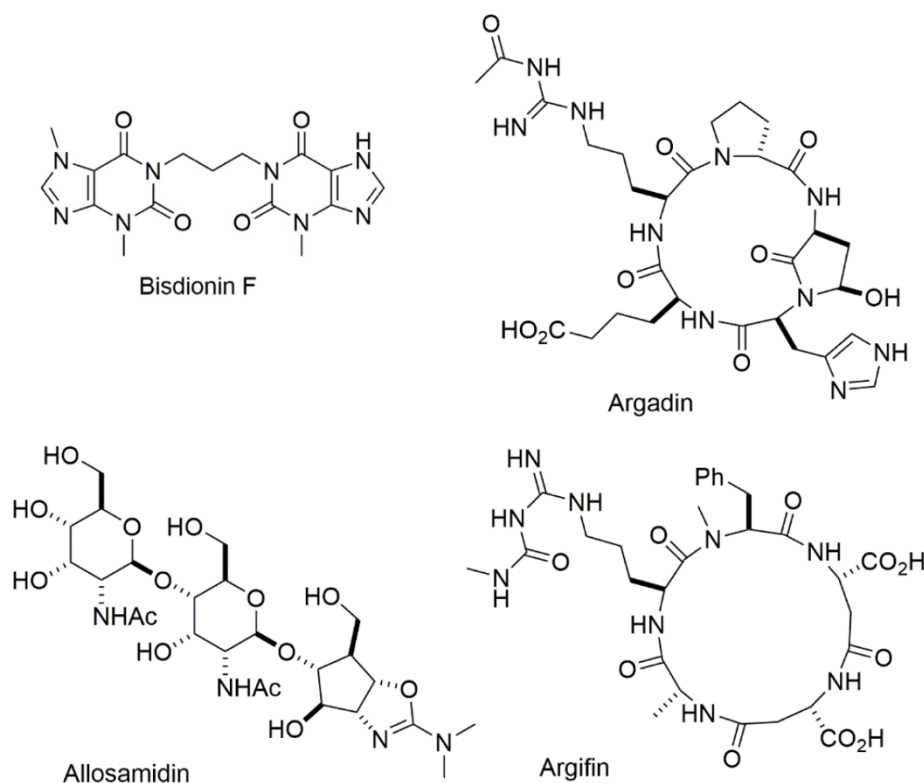
Figure 2-1: Examples of natural chitinase inhibitors.

Another study conducted by Wyeth and his research group using a combination of high-throughput screening, fragment-based drug design and in silico screening could identify two compounds with a drug-like profile and high potency, namely Wyeth 1 and Wyeth 2 (Figure 2-2). These compounds were orally active and reduced the chitinase activity in bronchoalveolar lavage (BAL) fluid of mice challenged with house dust mite (HDM) allergen but had a low selectivity between AMCase and CHIT1.[94]

OncoArendi Therapeutics used the positive drug-like features of Wyeth 1 as a starting point and to improve its potency and selectivity. Thanks to the impressive and complete work made by Mazur et al., they achieved a new series of derivatives characterized (Figure 2-2) by an IC50 in the low nanomolar range and with a great selectivity against AMCase or CHIT1 enzyme. The most promising compounds of their series are OAT-177 mice AMCase inhibitor (IC50 =19 nM), OAT-1441 great potency and selectivity against human AMCAse (IC50= 7 nM), OAT-2068 a mice CHIT1 selective inhibitor (mCHIT1 IC50= 29 nM), and finally OAT-870 a dual inhibitor of chitinases. These compounds can be

used as tools in future studies involving the role of human chitinases, AMCase and CHIT1, in vivo animal models of their excellent PK profile. However, further developments of some of these molecules (OAT-177, OAT-870) are hampered by the significant toxicity due to their high affinity for the hERG ion channel and dopamine transported (DAT). Investigation on the enhancement of the toxicity effects led to compound OATD-01, a clinical candidate with anti-fibrotic efficacy which currently is completing phase 1b of its clinical trials.[95–98]
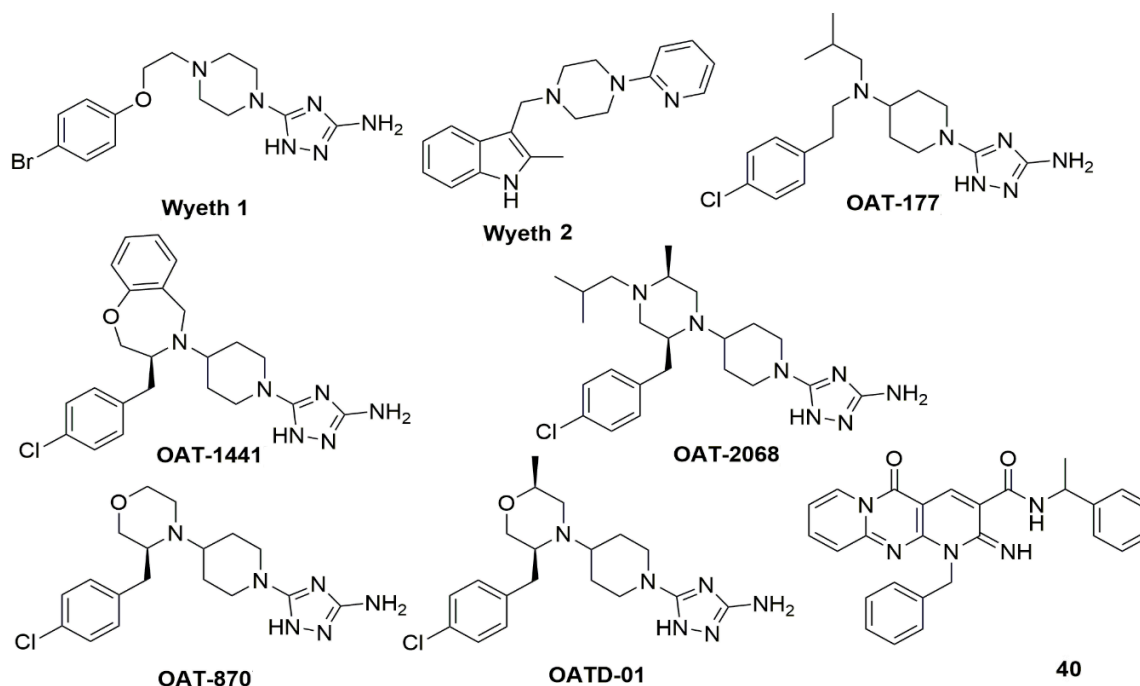
Figure 2-2: Drug-like chitinase inhibitors.

Finally, Jiang et al. using a structure-based virtual screening have identified a series of chitinase inhibitors characterized by dipyrido-pyrimidine scaffold where their best inhibitor compound 40 showed a selectivity 80-fold for hCHIT1 and a Ki value of 49nM.[99]

2.2   STATE OF THE ART

2.2.1   In search of the target.

As mentioned before macrocyclic amidinoureas represent an interesting family of compounds with strong antifungal activity against various *Candida* species, including drug-resistant species. However, many details concerning their mechanism of action (MOA) are still unknown. Since the identification of the biological target of these compounds could significantly improve the rational design of future derivatives as well as give us a better understanding of their structure-activity relationship, it was decided to thoroughly investigate it. An early clue about their mechanism of action emerged from the data of the transcription analysis of *C. albicans* exposed to **BM1**, which showed an up-regulation of several genes including the two which encoded for efflux pump, namely CDR1 and CDR2. From the literature, we know that the species of fungi which express these efflux pumps are less susceptible to antifungal drugs since these pumps drastically reduce the drug's concentration in the cell. Moreover, in many cases, it is the antifungal agent that serves as an inducer for these genes and, at the same time, as a substrate for the transporter. To test the hypothesis that **BM1** could be a substrate for these transporters, it was incubated with *C. albicans* wild-type control (CAF2-1) and mutants, lacking both

these genes, and to great surprise, the latter resulted in more resistance than the wild-type. This indicates a unique feature of this compound, requiring the presence of an ABC transporter to be taken up. Besides, its mechanism of action involved an intracellular target since when the compound **BM1** was not able to enter, as in the case of mutant species, no activity was measured. To test if an intracellular accumulation of **BM1** effectively happened in its mechanism of action a fluorescent derivative of **BM1** was prepared. The fluorescent microscopy experiments in Figure 2-3 confirmed the intracellular loading of the compound because fluorescence was mostly associated with the cytoplasm.[43] Unfortunately, no precise cell structures could be accurately identified from this analysis, so other solutions were considered.
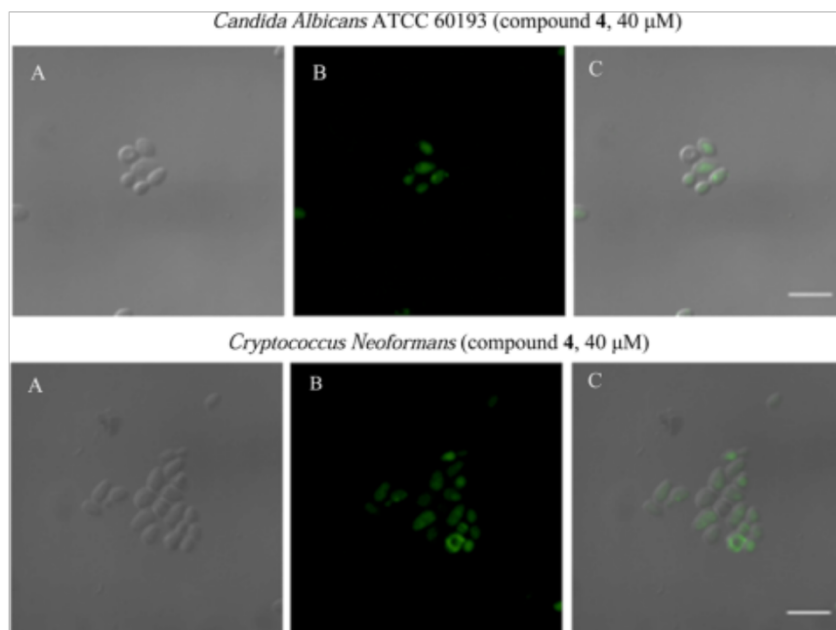
Figure 2-3: Confocal microscope images of C. albicans ATCC 60193 and C. neoformans cells treated with a fluorescent compound at 40 µM concentration. Panels A, B, and C show the visible, fluorescent, and merged images, respectively. Scale bar = 10 µm.

2.2.2   <u>Target fishing protocol.</u>

In silico target fishing is a computational approach analogous to the experimental target finding that makes it possible to identify the biological target of an active compound using its structural information and data from the biological database. The advantages of this procedure are several, starting from the low cost compared to experimental ones and a relatively rapid prediction of the primary target along with the off-target effects of specific compounds. Since this computational procedure represents a reliable method of identification of the mechanism of action, it was decided to pursue this method. The protocol was set up using the protein available on the Protein Data Bank. A first attempt was made focusing on the crystal structure of a protein from the genus *Candida* co-crystallized with at least one compound but, since it resulted in a selection of only 95 crystal structures, it was decided to enlarge this set of references by including the whole phylum of *Ascomycota*, leading to an initial database of 3,636 structures. Afterwards, as reported in the article of Maccari et al.[100], a specific protocol for the target fishing was set up, which resulted in the final ranking list of Table 2-1.

Table 2-1: Final ranking list of the proteins resulting from the target fishing procedure. Chitinase and xylanase are the most represented.

Entry	PDB ID	Protein name	EC	Rocs Score	Bind Score	Consensus Rank
1	3CHE	CHITINASE	3.2.1.14	0.74	-81.47	1
2	1DGP	ARISTOLOCHENE SYNTHASE	4.1.99.7	0.59	-77.59	2
3	2Z8G	ISOPULLULANASE	3.2.1.57	0.65	-66.73	3
4	1B3Z	XYLANASE	3.2.1.8	0.60	-68.85	4.5
5	3CHF	CHITINASE	3.2.1.14	0.66	-65.98	4.5
6	1LLF	LIPASE 3	3.1.1.3	0.67	-63.85	6
7	1B3X	XYLANASE	3.2.1.8	0.60	-67.49	7.5
8	3G7N	LIPASE	3.1.1.3	0.61	-66.40	7.5
9	4IIH	BETA-GLUCOSIDASE 1	3.2.1.21	0.69	-62.12	9
10	1B3Y	XYLANASE	3.2.1.8	0.60	-67.41	10
11	1W9V	CHITINASE	3.2.1.14	0.65	-62.66	11

Among the top eleven ranked structures, it can be noted that chitinase and xylanase are the two most representative proteins of this final list. Both enzymes owing to the family of glycosidase. Xylanases are enzymes that degrade the b-1,4-xylan. Chitinases, instead, hydrolyse chitin, the main component of the fungal cell wall, and thus are involved in its remodelling. Moreover, the three crystal structures of chitinase B from *Aspergillus fumigatus* (highlighted in blue in Table 2-1) were resolved in complex with the natural compound argifin and two oligopeptides synthesized during a molecular simplification study which resembles our compounds (Figure 2-4). Indeed, they present a macrocyclic portion and a terminal moiety (capable of being positively charged due to its basicity) linked by a carbon-atom linker. For these reasons, chitinases were supposed to be a putative target and investigated deeper**.**
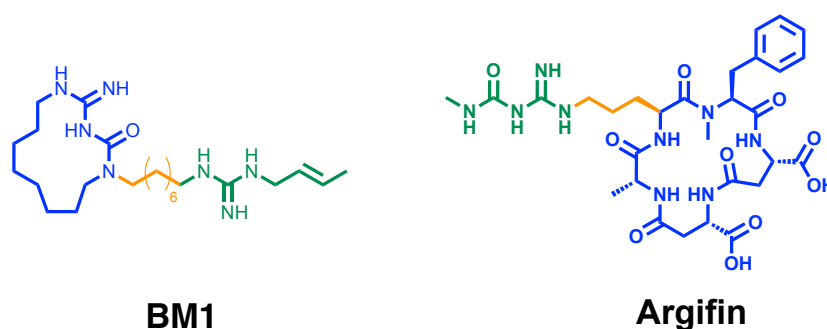
BM1   **Argifin**

Figure 2-4: Comparison between **BM1** and argifin. Both compounds presented a macrocyclic portion (shown in blue), a spacer linker (in orange) and a terminal moiety (in green), capable of being positively charged.

2.2.3   Validation of the Chitinase hypothesis.

To support the result of the target fishing protocol, an inhibition activity test was performed. No commercially available kits of Candida chitinase were present on the market at that time, and efforts to produce Candida chitinase in our laboratory were unsuccessful. For this reason, our choice fell on the homologue protein extracted from *Trichoderma viride*, since it was the best commercial solution with a high degree of similarity to the *Candida* one. The most representative compounds from our three series of antifungal compounds were tested to obtain reliable information on the inhibition activity of these compounds. The results in terms of K_i and IC$_{50}$ are reported in Table 2-2.

Table 2-2: First assays against T. viride chitinase.

Compound	Scaffold	R	IC$_{50}$[μM]	K_i [μM]
BM1	A		157.0	50.8
BM3	A		130.0	42.0
BM7	A		111.0	35.8
BM8	A		140.0	45.3
BM9	A		97.0	31.3
BM13	A		108.0	34.8
BM20	B (m=2)		55.0	17.8
BM21	B (m=3)		35.5	14.1
BM24	C		54.9	17.7

From the data, all the tested derivatives showed good inhibition of the enzyme with K_i values below 50 μM, which confirmed the chitinase hypothesis. The lead compound **BM1** is a good chitinase inhibitor, yet the best activity profiles were found for compounds **BM21** and **BM24** with a K_i= 14-18 μM.

The knowledge from these computational studies stimulated us to design novel compounds with high affinity and potency for the chitinase enzyme. This ambitious target was achieved by comparing the binding modes of **BM1** and **argifin** and noticing that they were much the same. Indeed, in both compounds, the macrocyclic portion and the linear chain assumed the same orientation, and this allowed them to interact with the Glu 177 residues. However, if closely observed (Figure 2-5), the

amidinoureas moiety of argifin was cable of doing two additional key interactions with Asp175 and Tyr 245 of the target enzymes.[100]
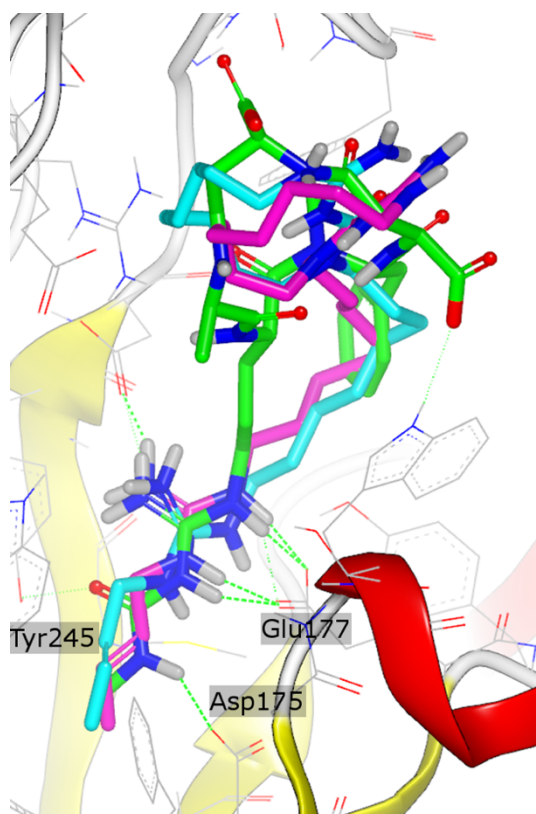
Figure 2-5: Binding mode of BM1 in the active site of chitinase (PDBID: 1W9V). The protein is represented in lines and cartoons. Argifin is represented as green sticks, while the shape comparison pose and the docked pose are represented as cyan and magenta sticks, respectively. Hydrogen bonds are represented as green dashes.

Based on these observations, it was assumed that merging (Figure 2-6) our best chitinase inhibitor (**BM21**), with the amidinoureas moiety of **argifin** could provide a new compound, **BM22**, in which the inhibitory activity might be improved thanks to these two additional interactions with active chitinase sites.
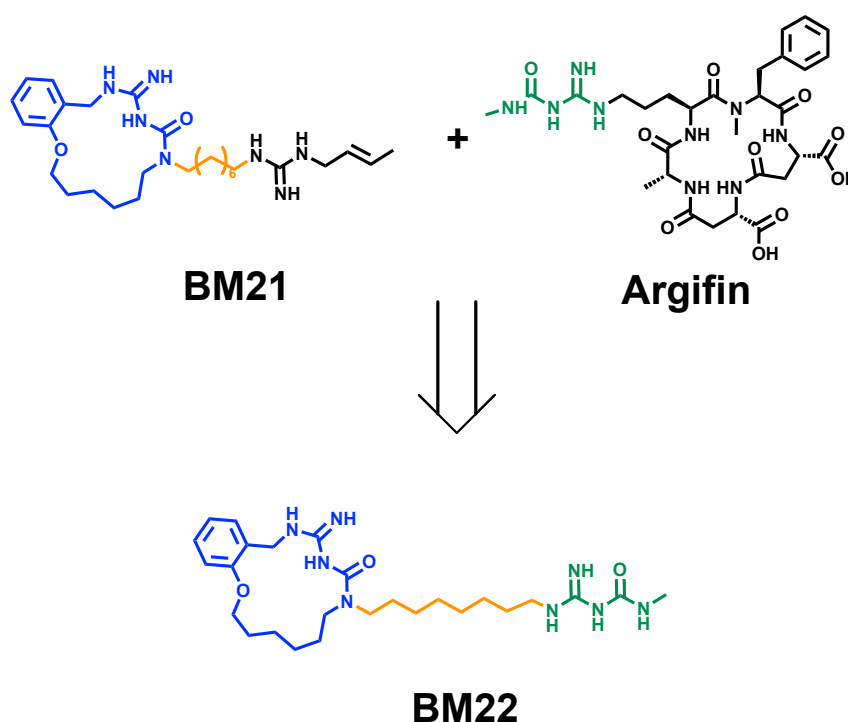
Figure 2-6: Merging of the chemical structure of **BM21** and Argifin to obtain **BM22**.

2.2.4   BM22: a new potent inhibitor of *T. viride* chitinases.

The new derivative was synthesized straightforwardly, as described in the article of Maccari et al. The optimized derivatives were tested against *T. viride* chitinase (Table 2-3) and found to be a potent inhibitor with K_i values of 0.22 µM, over 50-fold lower than its parent compound (**BM21**), confirming the initial hypothesis. Conversely to this data, when **BM22** was tested against *Candida* strains, a reduction of its antifungal activity was shown with respect to **BM21**. This behaviour was explained by the structural change of **BM22** from the positive-charged terminal guanidine of **BM21** (pK$_a$≈12) to the neutral amidinoureas moiety of argifin (pK$_a$≈6) and the use of a cationic polyamine transporter to cross the fungal membrane. Therefore, the likely lesser affinity of **BM22** for this cation transporter could be related to its reduced antifungal activity.[100]

Table 2-3: Inhibitor activity of the new derivative **BM22** and comparison between other deviates of the first and second series.
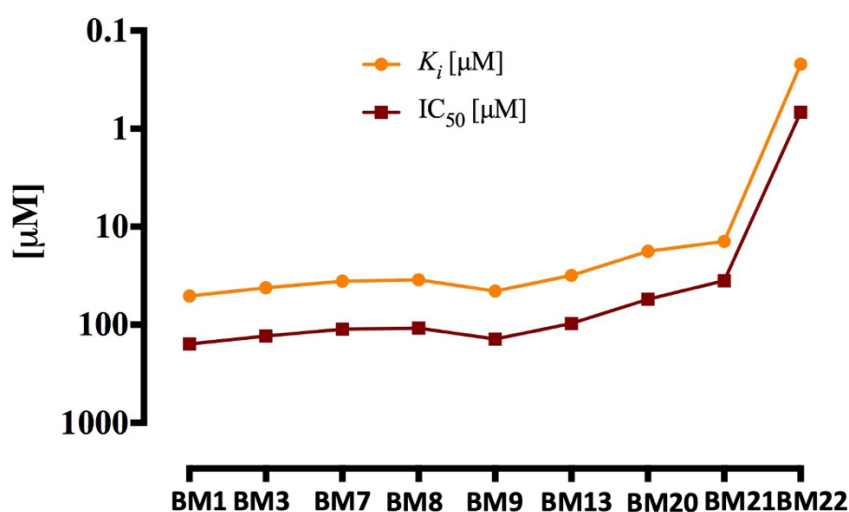
2.2.5   Activity on Human Chitinases

The two human chitinases, hAMCase and hCHIT1, have recently attracted considerable attention for their critical roles in the modulation of the immune response in asthma and other chronic inflammatory lung diseases. Since our best inhibitor of *T. viride* chitinase, **BM22**, has been rationally designed and has shown quite remarkable inhibitory activity, it was tested against the two human chitinases in order to understand, if these proteins could be targeted by our amidinoureas compound. Therefore, compound **BM22** and its precursor **BM21** were biologically evaluated, using a fluorometric assay, against hAMCase and hCHIT1.

Table 2-4: Biologically evaluation of **BM21** and **BM22** against AMCase and CHIT1.

Inhibitors	hAMCase		hCHIT1	
	% Inhibition[a]	K_i (μM)	% Inhibition[a]	K_i (μM)
Bisdionin F	52.7 ± 3.7^b	0.14 ± 0.11	98.5 ± 0.1^a	0.17 ± 0.1
BM22	58.8 ± 1.2	13.2 ± 0.2	26.0 ± 1.5	n.d.[c]
BM21	$<5\%$	n.d.[c]	n.d.[c]	n.d.[c]

[a][Inh] = 50 μM; [b][Inh] = 1 μM; [c] not determined.

As we can see from the data in Table 2-4, **BM22** showed good inhibitory activity on AMCase (K_i of 13.1 μM), whereas the data on the other enzymatically active chitinase (CHIT1) were very low, suggesting a possible selectivity for this compound respect to AMCase.

Moreover, the data derived from compound **BM21**, bearing the guanidine moiety instead of the amidinourea, showed a complete loss of activity, again suggesting that the amidinoureas moiety was fundamental for the inhibitor activity. It is worth mentioning that switching from chitinase of *T.viride* to human (AMCase or CHIT1) led to a strong decrease in activity suggesting that even if they belong to the same family GH18 there are the structural difference among fungi and human chitinase in accordance with the work of Huang et al.[101]

2.2.6   The first series of AMCase inhibitors.

The promising inhibitory activity data of **BM22** against AMCase encouraged us to move forward with the design and synthesis of the first series of derivatives. In this series (Scheme 2-1) the attention was focused on the modification of three main strategic structural features of **BM22**: the terminal amidinoureas moiety, the macrocyclic core, and the length of the linker, in order to evaluate the role of structural features of the lead compound **BM22** in the inhibition of human chitinases.
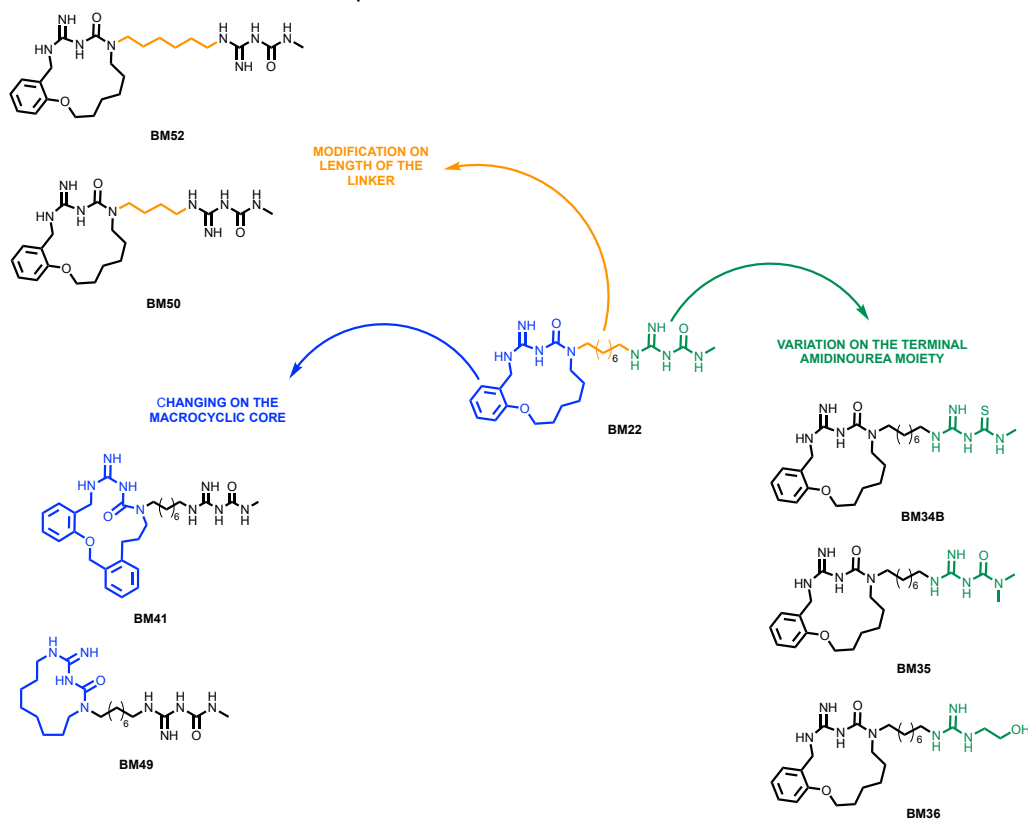
Scheme 2-1: First series of macrocyclic amidinoureas as inhibitors of AMCase.

The first series of derivatives were tested on both enzymes, and the data were reported in Table 2-5

Table 2-5:Evaluation of the first series of derivatives inhibitor of AMCase.

Compounds	hAMCase		hCHIT1	
	% Inhibition[a]	$K_i(\mu M)$	% Inhibition[a]	$K_i(\mu M)$
BM22	58.8 ± 1.2	13.2 ± 0.1	26.0 ± 1.5	n.d.[b]
BM52	51.9 ± 1.7	12.9 ± 0.5	19.5 ± 3.1	n.d.[b]
BM50	41.1 ± 2.4	n.d.[b]	21.9 ± 3.3	n.d.[b]
BM36	7.7 ± 2.1	n.d.[b]	NT	n.d.[b]
BM35	12.7 ± 5.6	n.d.[b]	18.4 ± 7.4	n.d.[b]
BM34B	13.6 ± 6.3	n.d.[b]	<5	n.d.[b]
BM49	50.3 ± 3.2	n.d.[b]	n.t.	n.d.[b]
BM41	83.7 ± 2.1	3.5 ± 0.2	32.3 ± 1.7	n.d.[b]

[a][Inh] = 50 µM; [b] not determined.

The results of the enzymatical tests showed that the terminal amidinoureas moiety is crucial for activity. Indeed, all modifications (**BM34B**, **BM35**, **BM36**) led to a dramatic loss of activity highlighting the key role of the interaction of terminal moiety with the aminoacidic present in the catalytic pocket. The linker moiety also seemed to be important to the activity of compounds, since shortening the length from 8 terms to 4 caused a decrease in activity, whereas a 6 terms length was well tolerated and resulted in good inhibitory activity. However, the most interesting consideration derived from the modification of the macrocyclic core, since removing the aromatic ring led to compound **BM49** with a slight decrease in activity, whereas the introduction of a second phenyl (**BM41**) allowed a significant enhancement of activity with an increase of 1.5-fold of percentage inhibition and lowering the K_i at 3.5 µM. It is worth mentioning that these derivatives showed promising selectivity against hAMCase with respect to hCHIT1.

2.2.7   <u>Structural based virtual screening on human AMCase.</u>

The recent interest in the inhibition of AMCase for the development of therapeutics against allergic airway inflammatory diseases has prompted the pursuit of, alongside the ongoing development of derivatives with macrocyclic amidinoureas scaffold, a new and different project with the goal of identifying inhibitors of AMCase proteins with new chemical structures. To achieve this goal, a structure-based virtual screening was set up. This computational procedure can identify new scaffolds of molecules active towards an interesting target, in our case the hAMCase. The first step was the selection of crystallographic data in the compound Wyeth 1[94] co-crystallized with the human AMCase (PDB:3RM4). This crystal structure allowed the generation of an early pharmacophoric model that was optimized through compounds reported in a recent patent from OncoArendi.[102] The database of commercially available compounds used for the virtual screening was the ZINC Purchasable Now. After

an initial filtration step based on structural factors (only compounds presenting a positive nitrogen atom bonded with three aliphatic carbon atoms were selected because this group was present in all the most active compounds reported in the OncoArendi patent[102]) and pharmacophoric model filtration, the initial huge number of compounds (12.8 million) present in the ZINC database was reduced to 15,828 molecules. Afterwards, a docking analysis was performed, and the first 150 compounds were selected. A final visual inspection and a FAF-Drug3 PAINS analysis led to 10 compounds that were purchased and underwent biological evaluation in a fluorescent enzymatic assay as AMCase inhibitors.

Table 2-6: Biological evaluation of the purchased compounds on hAMCase after the SBVS procedure.

Compounds	% Inhibition[a]
DF01	<5
DF02	10.9 ± 7.7
DF03	8.4 ± 6.8
DF04	29.4 ± 3.4
DF05	<5
DF06	<5
DF07	<5
DF08	<5
DF09	8.9 ± 1.4
DF10	8.9 ± 1.3

[a][Inh] = 50 μM

Among this first series of derivatives (Table 2-6), some of them resulted to be inactive or with a low percentage of inhibition (8-11%). The most interesting compound of this first series was represented by **DF04,** which showed a percentage of inhibition of 29.4±3.4 and a K_i value of 25.6 ± 3.3 μM.
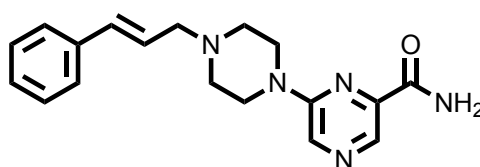
DF04

Figure 2-7: Structure of DF04.

Investigating the binding mode of the best compound, **DF04,** highlighted a predictable pose comparable with the crystallographic derivative (Figure 2-8). The pyrazine-2-carboxamide group was able to form H Bond interactions with the catalytic residues Asp138 and Glu140 and with OH groups of Tyr212 and Tyr27 inside the active site; it also formed interaction with Trp360 and Met210. Its tail, instead, occupied the hydrophobic pocket constituted by Tyr267, Ala295, Ile300, and Leu364 side chains.
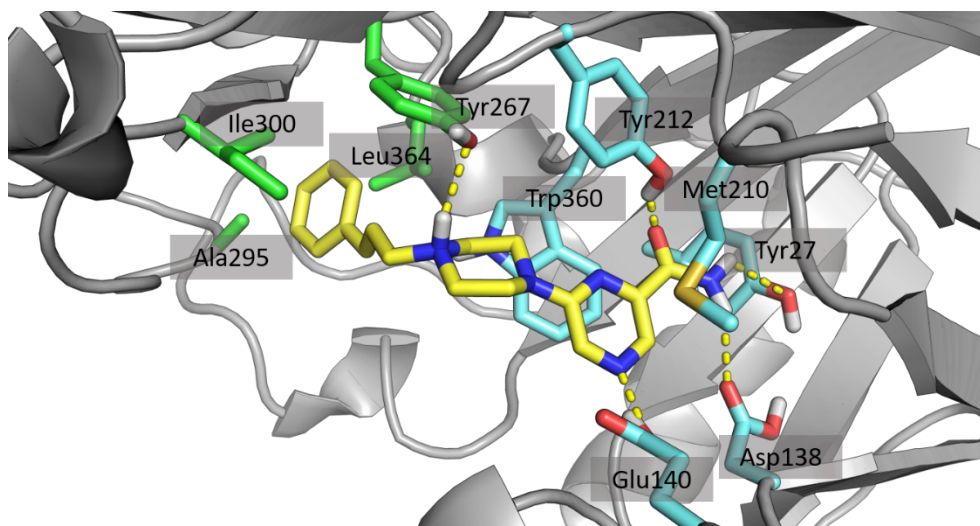
Figure 2-8: **DF04** (Yellow) binding mode inside the binding pocket. Green residues represent the hydrophobic pocket; Cyan residues represent the active site.

2.3   AIM OF THE PROJECT.

My project regarding the development of human chitinase inhibitors embraced the design and synthesis of molecules belonging to two different scaffolds.

The first was the macrocyclic amidinoureas scaffold. Following what has been done previously and with the aim of enriching our knowledge about this family of compounds as inhibitors of human chitinase, three compounds were synthesized: **BM56**, **BM57**, and **BM58**. The data from the first series told us that the introduction of a second phenyl ring in the macrocyclic scaffold caused a dramatic increase in the activity. The introduction of a phenyl ring as a functional group in the macrocycle had the additional advantage of being easily functionalized with several chemical groups. The compounds that I synthesized were characterized by the presence of two different halogen atoms, fluorine, and chlorine, on one the phenyl rings. The aim of this project was the exploration of the chemical space related to the macrocycle core and the evaluation of its effect on the inhibitory activity in human chitinases. These results would merge with the data of other previously synthesized derivatives, and help us gain a better understanding of the structure-activity relationship of these series of compounds. The second scaffold is the 6-piperazine-1-ylpyrazine-2-carboxamide scaffold which characterized compound **DF04** and emerged from a structure-based virtual screening. This scaffold is innovative and quite different from the other chitinase inhibitors described to date. Although the inhibitory values of these derivatives were still not competitive with other known inhbitors they represented a weak-but-novel chemotypes drug-like compounds, with low molecular weight and easy availability from a synthetic point of view. For these reasons, we considered the 6-piperazine-1-ylpyrazine-2-carboxamide an interesting scaffold and we decided to synthesize a focused library of compounds. Specifically, I focused my attention on the exploration of the aromatic ring portion, which interacts with the hydrophobic pocket of the active site of the enzyme. Therefore, a series of compounds bearing different lipophilic substituents on the phenyl ring, such as halogen atoms and various carboxamide groups, were synthesized and biologically evaluated to see if any additional interactions could be formed between this portion of the molecule and the aminoacidic residues presented in this pocket, which could lead to an optimization of the activity data of this class of compounds.

PART A: Synthesis of **BM56**, **BM57**, **BM58**.
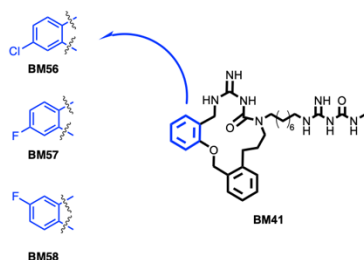
Exploration of the chemical space by the synthesis of a small library of derivatives bearing halogen atoms on one of the phenyl groups.

PART B: First series of **DF04** derivates.
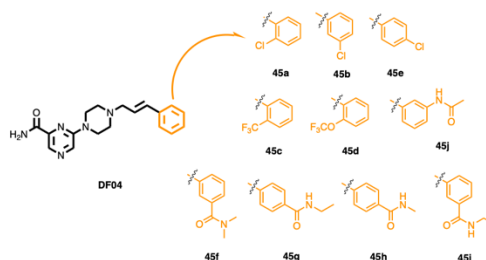
Introduction of several lipophilic substituents on the phenyl group to enhance the possibility to make new interactions with the hydrophobic pocket of AMCase.

2.4　PART A: The second series of AMCase inhibitors.

2.4.1　Synthesis of compound BM56, BM57, BM58.

The synthetic route used for these compounds is the same described for compound **BM37** and reported as an overview in the scheme below (Scheme 2-2). However, some modifications were introduced in the previous synthesis to obtain the terminal amidinoureas moiety and avoid the poor resistance of the benzyl phenyl ether group in the hydrogenation step that in some cases led to a byproduct characterized by the opening of the macrocycle. In the next part, I will describe these issues and the efforts made to overcome them.
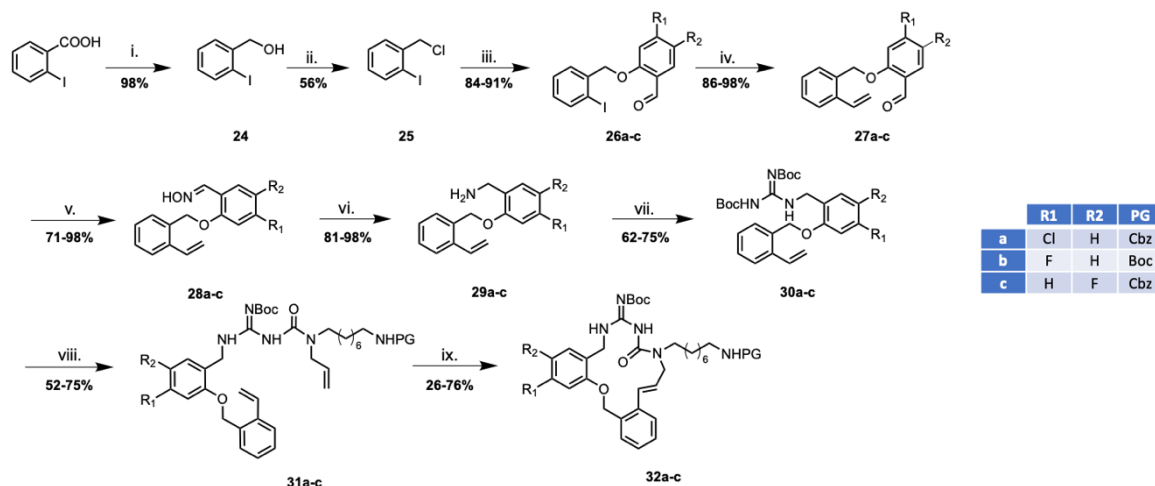
Scheme 2-2: Synthesis of intermediates **32a-c**. Reagents and conditions. (i.) BH_3-Me_2S, dry THF, 0 °C-r.t., 12 h, N_2; (ii.) tosyl chloride, DMAP, dry TEA, dry CH_2Cl_2, 0 °C-r.t., 16 h, N_2. (iii.) 2-Hydroxy-4-R_1-5-R_2-benzaldehyde, K_2CO_3, NaI, CH_3CN, reflux, 16 h; (iv.) tributyl(vinyl)tin, Pd $(OAc)_2$, PPh_3, dry THF, reflux, 16 h, N_2; (v.) $NH_2OH*HCl$, pyridine, EtOH, reflux, 3 h; (vi.) Zn dust, 2N HCl, THF, reflux, 4 h; (vii.) *N,N'*-Di-Boc-1H-pyrazole-1-carboxamidine, DIPEA, THF, r. t., 16 h. (viii) **9** or **40**, dry TEA, dry THF, reflux, 16 h, N_2; (ix.) 2nd gen. Grubb's catalyst, degassed dry CH_2Cl_2, reflux, 16 h, N_2.

In our first synthetic route Scheme 1-6, the cleavage of the Cbz group and the hydrogenation of the double bond of the macrocyclic core were achieved in one step using Pd/C 10% and a few drops of HCl 36% in isopropanol at r.t. under H_2 atmosphere. In this step, the catalytic amount of HCl served to avoid the poisoning of the Pd/C by the amines trapping them as hydrochloride salt and promoting the deprotection.[103,104] Although this procedure usually worked well in the macrocyclic amidinoureas synthetic routes, sometimes depending on reaction conditions and structural effects, the hydrogenolysis of the benzyl phenyl ether group was observed, and a by-product characterised by the opening of the macrocycle was detached. This hypothesis was supported by a mass spectrometry analysis, with a new signal corresponding to a molecular weight greater than two units greater to the desired product as well as NMR spectra, in which the benzylic methylene signal disappeared, replaced by a new signal related to the methyl group (Figure 2-9).
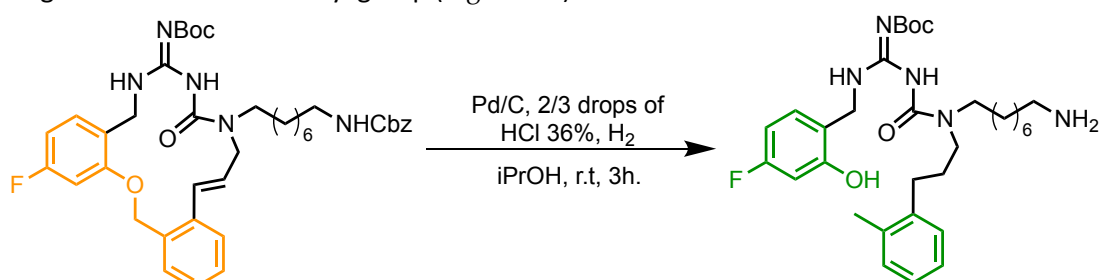
Figure 2-9: The benzyl phenyl ether (BPE) group was highlighted in orange, instead of the structure of the opening macrocycle, characterised by a phenol and a tolyl group, in green.

To avoid the formation of this by-product, we made several attempts (Scheme 2-3). Firstly, as suggested by the literature,[104] we changed the strength of the acid from the strong HCl to the weaker Acetic acid, as illustrated in the synthetic route (x.) presented in Scheme 2-3. This attempt worked well for compounds **33a** and **33c**, although the reaction time was increased (eight hours instead of the four usually required).

On the other hand, for compound **34b**, the situation did not change at all, and the main product obtained using this procedure was the macrocycle opening.

Therefore, other attempts were made. Secondly, we removed the acid or replaced it with ammonium acetate or ammonium chloride, as reported in the work of Sajiki on selective hydrogenolysis.[105] However, in these cases, only the hydrogenation of the double bond occurred, whereas we found that the hydrogenolysis of the Cbz group was inhibited. Finally, since these attempts were unsuccessful, we decided to change the protecting group on the linker moiety in order to bypass the formation of this tedious by-product (Scheme 2-3). The choice fell on another well-known carbamate protecting group, namely Boc. The main difference between these protecting groups is in how they are cleaved: Cbz using hydrogenolysis on Pd/C, while Boc in an acid environment. A new linker moiety **40**, bearing the Boc group was synthesised and used to afford the derivative **32b**. Subsequently, the double bound was removed mildly by hydrogenation in the absence of acid. The hydrogenation occurred smoothly for 4 hours, the reaction was monitored by mass spectrometry until the signal of the starting material had disappeared completely, and then the reaction mixture was filtrated over Celite to remove the palladium catalyst and directly used in the next step without any further purification. The cleavage of the Boc group was carried out with TFA at 10% v/v solution in DCM, furnishing compound **35b** in quantitative yield. This new synthetic strategy had the advantage of affording the free amine **35b** as trifluoracetic acid without any traces of the opened macrocycle byproduct. As a drawback, the cleavage of Boc guanidine moiety at this stage resulted in a more polar compound with a more demanding purification, as free guanidines can form a long streak behind them during column chromatography. However, in both cases, we obtained the amines, in the form of acetate (**33a,c**) or trifluoroacetic salt (**35b**), which were coupled with *N*, *N'*-Di-Boc-1*H*-pyrazole-1-carboxamidine at room temperature using DIPEA in excess as a base to afford the guanidine derivatives **36a-c.**
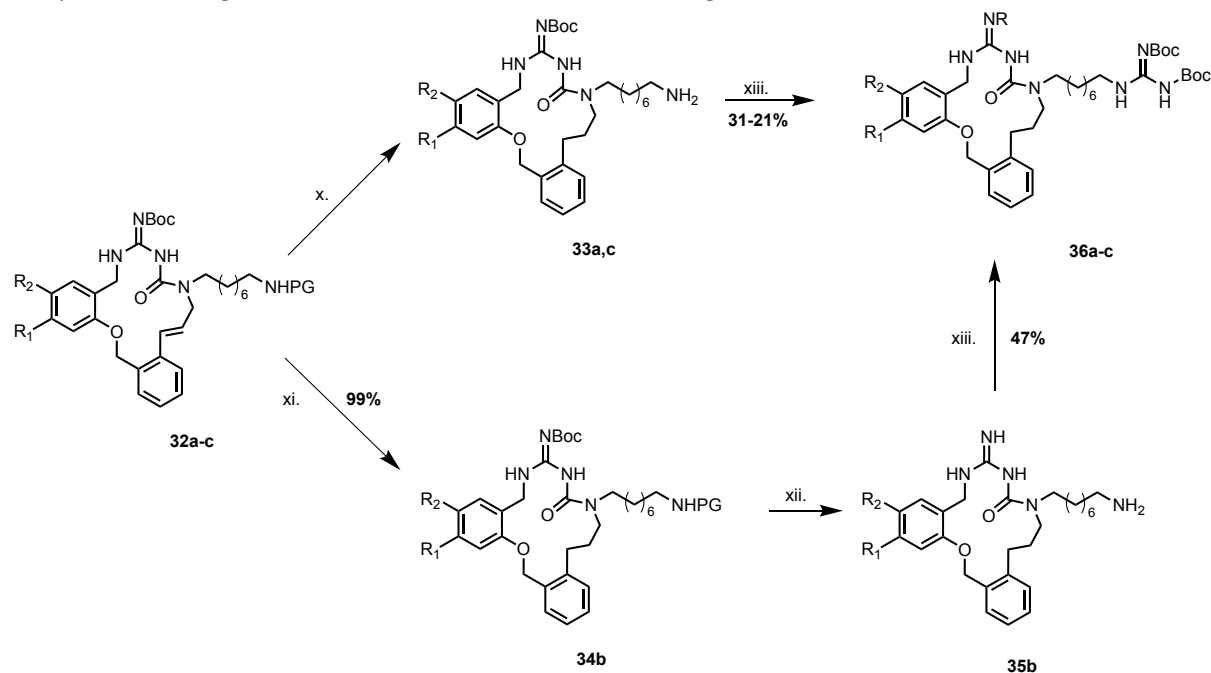
Scheme 2-3: The problematic step of hydrogenation. (x.) H₂, 1 atm, Pd/C 10%, cat. AcOH, i-PrOH, r. t., 8 h.; (xi.) H₂, 1 atm, Pd/C 5%, cat, i -PrOH, r. t., 4 h;(xii.) 10% CF₃COOH in DCM, r. t., 3 h; (xiii.) *N,N'*-Di-Boc-1*H*-pyrazole-1-carboxamidine, DIPEA, THF, r. t., 16 h.

These guanylated compounds, presenting an unsubstituted di-Boc guanidine, were able to react with methylamine in a sealed tube under reflux overnight giving the amidinoureas terminal moiety of compounds **37a-c**. Final deprotection of the Boc groups using TFA gave compounds **BM56**, **BM57**, and **BM58** as trifluoroacetic acid salts (Scheme 2-4).

	R.	R$_1$	R$_2$
BM56	Boc	Cl	H
BM57	H	F	H
BM58	Boc	H	F
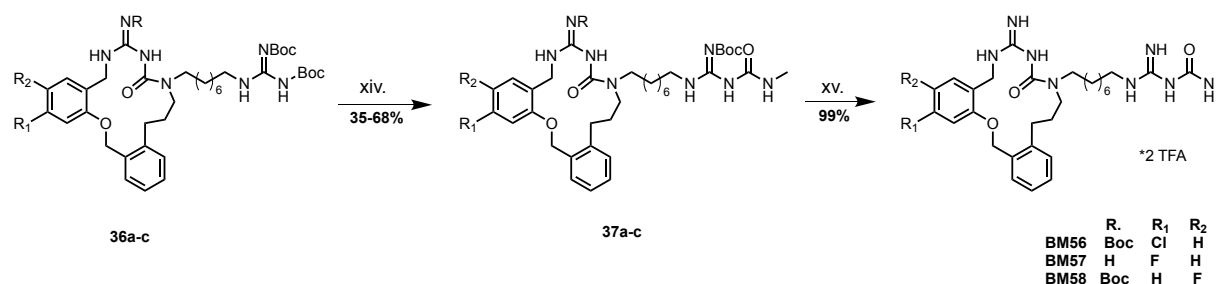
Scheme 2-4: Final step of synthesis of **BM56**, **BM57** and **BM58**: (xiv)Methylamine sol. In H$_2$O, DIPEA, THF, 80 °C, sealed tube, 16h; (xv.) TFA 10% in DCM, rt, 8h.

2.4.2 Synthesis of the Boc protected linker moiety.
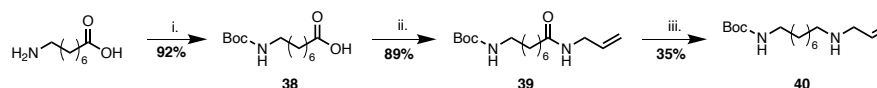
Scheme 2-5: Synthesis of the linker 40. Reagents and conditions. (i.) (Boc)$_2$O, NaOH, Dioxane/H$_2$O, 0°C to r.t., 12 h; (ii.) Allylamine, EDC, HOBt, DIPEA, dry DMF, r.t., 16 h, (iii.) DIBAL-H, dry DCM, 0°C to r.t.,16h.

The new linker bearing a terminal Boc protecting group was synthesized (Scheme 2-5) using the same conditions described previously in Scheme 1-8 but, during the first step, Boc anhydride was replaced by chlorobenzyl formate.

2.4.3 Biological evaluation of compounds BM56, BM57, BM58.

The prepared compounds were then tested against the human chitinases (AMCase e CHIT1) by means of a direct fluorimetric assay using the following procedure. Mixtures of the enzyme (AMCase e CHIT1) and 50 µM of the inhibitors were incubated for 20 minutes on the reading plate. At the end of the incubation, the substrate (4-methylumbelliferyl β-D-*N*, *N'*, *N''*-triacetylchitotrioside) was added, and the reading was conducted by monitoring the time dependence of substrate hydrolysis followed by fluorescence (excitation wavelength, 400 nm: emission wavelength, 440-460 nm). The rationale behind this test is that the measured fluorescence is directly related to the activity of the enzymes. Therefore, the more the inhibitory activity of our compounds, the lesser the activity of the enzyme and the lesser the fluorescent moiety that was freed and detached. The results of the screening compounds are reported in Table 2-7. The K_i was determined only for compounds showing an inhibition ≥50%, using a competitive model of inhibition in triplicate. As a control, bisdionin F, a known Chitinase inhibitor was used.[106] Inhibition tests were performed at the Department of Medical Biotechnologies of "Policlinico Santa Maria alle Scotte" by Professor Jean-Denis Docquier and Dr Filomena Sannio, whom I thank profusely for their precious help.

Table 2-7: Evaluation of the inhibitory activities of **BM56**, **BM57**, **BM58** against hAMCase and hCHIT1.

Compound	AMCase		CHIT1	
	% Inh [a]	$K_i(\mu M)$	% Inh [a]	$K_i(\mu M)$
Bisdionin F	52.7 ± 3.7^b	0.14 ± 0.1	98.45 ± 0.1^a	0.17 ± 0.05
BM22	58.8 ± 1.2	13.2 ± 0.1	26.0 ± 1.5	n.d.[b]
BM41	83.7 ± 2.1	3.5 ± 0.2	32.3 ± 1.7	n.d.[b]
BM56	60.9 ± 0.6	21.0 ± 2.2	<5	n.d.[b]
BM57	81.9 ± 0.8	2.9 ± 0.2	10 ± 0.7	n.d.[b]
BM58	66.0 ± 2.1	17.9 ± 2.0	<5	n.d.[b]

[a][Inh] = 50 μM; [b][Inh] = 1 μM; [c] not determined.

All the new synthesized compounds showed a good percentage of inhibitory activity (Table 2-7) in some cases (**BM56** and **BM58**) comparable to the lead compound **BM22** or better as in the case of **BM57**. In contrast, a decrease in the activity value was measured for compounds **BM56** and **BM58** with respect to **BM41**, the most active compound of the entire series.

These data confirmed that the introduction of phenyl rings in the macrocyclic structure had a strong influence on the inhibitory activity of these compounds because their functionalization led to a valuable change in the activity value of this family of compounds. Presumably, the occurrence of aromatic rings in the macrocyclic core made new favourable interactions (stacking interactions) between these compounds and the target enzyme that improved the binding and stabilized the formed complex. Consequently, modifying the electron density and the chemical properties of the phenyl ring through the introduction of halogen substituents resulted in a modulation of the stacking interactions with the target protein along with the inhibitory activity.

As we can see in the case of **BM56** and **BM58**, the introduction of the chlorine and fluorine atoms in the C5 and C4 positions respectively, led to a drastic increase in the K_i value (7 and 5 folders higher than **BM41**), whereas for **BM57**, the introduction of a fluorine atom in position C5 seemed to be beneficial for the activity and *Ki* value compared to **BM41** was measured.

It is interesting to notice that the introduction of halogen substituents on the first phenyl ring plays a significant role also in the selectivity properties of these compounds. Indeed, all the halogenated derivatives showed a remarkable decrease in their activity value on the CHIT1 enzyme compared to **BM41** or **BM22**. This observation is worth mentioning since gave us more knowledge on how to obtain selective derivatives, desirable properties, and search for new chitinase inhibitors.

Further studies evaluating the effect of substitution on the second aromatic ring and the introduction of different electron-withdrawing or donating groups on the activity values of these derivatives are currently underway in our laboratories. From the results of these data, we will gain more knowledge about the structure-activity relationship, helping us understand which direction to go for the next generation of more potent AMCase inhibitors.

2.5   PART B: FIRST SERIES OF DF04 DERIVATIVES.

The new derivatives of **DF04** were characterized by the presence of two different lipophilic functional groups on the aromatic ring; compounds **45a-e**, bearing halogen atoms at different positions on the phenyl ring, whereas derivatives **45f-j** possess a carboxamide group as a substituent.

For the synthesis of this first series of **DF04** deviates, a convergent synthesis was set up (Scheme 2-6) that involved compound **43** as a common intermediate. The general procedure for all derivatives is depicted in Scheme 2-6. The synthesis was started by a Wittig reaction between the opportune aldehydic derivatives and the phosphonium ylide, the commercial triphenylphosphoranylidene acetaldehyde in this case.[107,108] Given the presence of the aldehydic functions as an electron-withdrawing group, the resulting ylide is stabilized by this group and tends to give only the *E*-alkenes.[109] This result was confirmed by the NMR signal presented in the alkenyl field of the spectra which showed a coupling constant of 14-16 Hz typical of trans protons for all the derivatives. One problem related to this synthetic strategy is the fact that the product can compete with the starting material for the commercial Wittig reagent to form a byproduct derived from a second Wittig reaction. The high similarity in terms of polarity that the product and the side-product presented make their isolation and purification difficult. To avoid the formation of this by-product, an excess of aldehydic starting material was used. The α,β-unsaturated aldehydes **42a-j** were transformed into the corresponding amines through a direct reductive amination.[110] This reaction proceeded in one pot, using STAB as a reducing agent. STAB is a mild reducing agent, selective for the imine, which allowed the presence of the ester moiety on the compounds. Finally, the esters **44a-j** were directly transformed in the primary amides **45a-j** using an excess of ammonia (NH_3 7N in methanol) under microwave irradiation.[111]
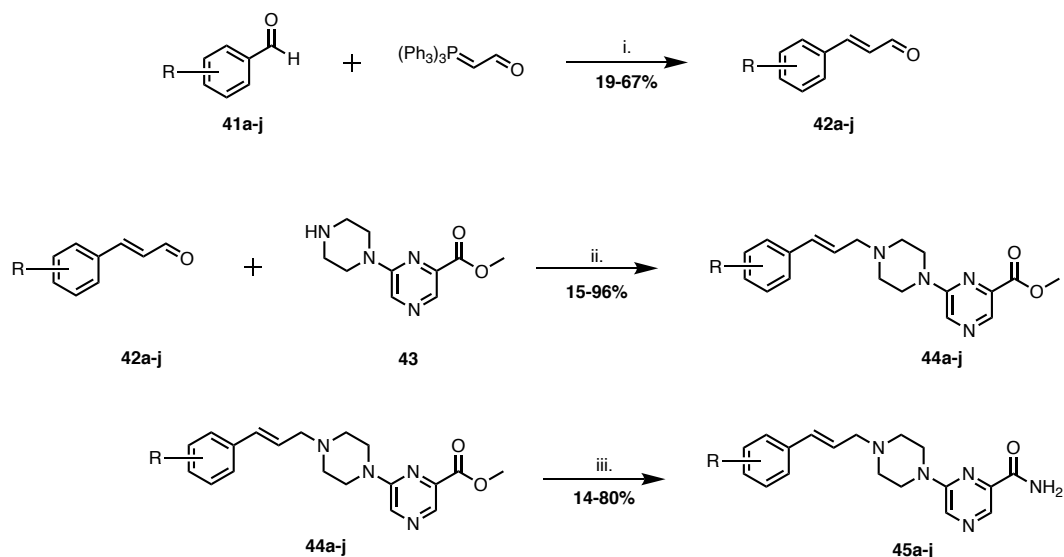
Scheme 2-6: General procedure for the synthesis of the derivatives **45 a-j**. i.) Dry toluene, reflux overnight; ii.) STAB, DCE, r.t, overnight; iii.) NH_3 in MeOH 7N, MW, 45 °C, 5minutes.

The intermediate **43** was prepared starting from the commercially available pyrazinoic acid. This compound was transformed into the methyl ester **46** through the Fisher esterification.[112] Then, the *N*-oxide intermediate **47** was prepared, obtained thanks to m-chloroperbenzoic acid, which directed the subsequent chlorination in thionyl chloride in position 6 (**48**).[113] During this step, both the 2,6 and the 2,4-disubstituted pyrazinoic acids were obtained, with the former in higher yield. The compounds were discerned via ^{1}H-NMR spectroscopy.[114] Finally, the replacement of the chlorine atom with the piperazine using microwave irradiation gave the desired intermediated **43** (Scheme 2-7).
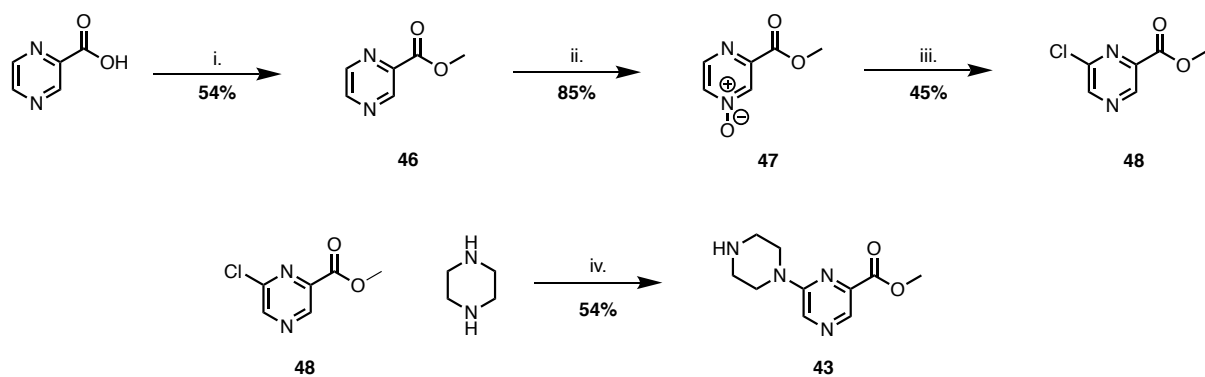
Scheme 2-7: Synthesis of the common intermediate **43**. i.) H_2SO_4 conc., MeOH, r.t overnight; ii.) mCPBA 77%, DCE, 60°C, 16 h; iii.) SOCl2, reflux, 7h; iv.) Piperazine, DIPEA, DMF, MW, 60°C, 15 minutes, sealed tube.

Conversely to the halogen derivatives which were synthesized starting from the commercially available aldehydic precursor, compounds bearing an amidic portion as a substituent (Scheme 2-8). As commercially available starting compounds, we selected the opportune formyl benzoic acids. These starting compounds were converted to their respective acyl chlorides using thionyl chloride and DMF/DCM as the solvent of the reaction. Then, this reaction mixture was directly added to a solution of the specific amine in order to obtain the appropriate amide **41f-i**. Once obtained, the compounds followed the general synthetic route (Scheme 2-6).[115]
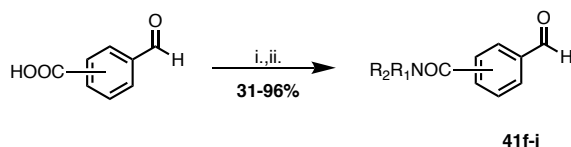
Scheme 2-8: General procedure for the amidic derivatives **41f-i**. i.) $SOCl_2$, DMF dry, DCM dry, reflux, 2h; ii.) NR'R' 'in H_2O at 0°C, r.t for 2 h.

For compound **41j** which contained the acetanilide as the substituent, the synthesis was slightly different (Scheme 2-9). We prepared it by coupling the commercial 3-Aminobenzyl alcohol and the Acetic anhydride. The compound **49j** was then oxidated using MnO_2, an inorganic oxidating agent specific for benzyl alcohol, to provide the compound **41j**.[116]
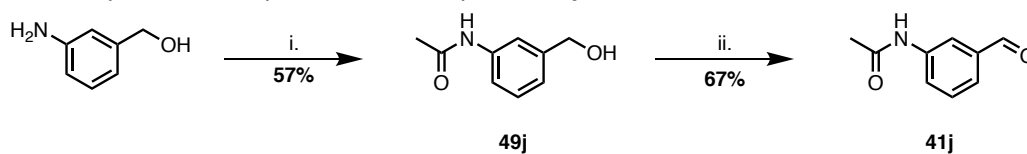
Scheme 2-9: Synthesis of the acetanilide derivatives **41j**. i.) Acetic anhydride, O°C, THF dry, r.t, 15 minutes; NaOH 2,5 M, $NaHCO_3$(ss), MeOH, r.t, 5 minutes; ii.) MnO_2, MEK, r.t, 2 days.

2.5.1 Biological evaluation of new DF04 derivatives.

The activity of this series of derivatives was evaluated against the hAMCase (Table 2-8) using the same fluorometric assay used for the macrocyclic compounds and described in paragraph 2.4.3.

Table 2-8: Evaluation of the inhibitory activities of new derivatives of **DF04** against hAMCAse.

Compound	% Inh [a] on AMCase
Bisdionin F	52.7±5.2[b]
DF04	29.4±3.4
45a	25.6±5.4
45b	37.9±5.9
45c	15.6±6.6
45d	20.8±4.8
45e	15.9±7.3
45f	19.4±1.5
45g	16.6±4.4
45h	27.4±1.3
45i	22.8±1.2
45h	n.t.

[a][Inh] = 50 μM; [b][Inh] = 1 μM; [c] not determined.

All the tested compounds showed low percentages of inhibitory activities. However, some preliminary considerations can be made on this small library of compounds.

Compounds bearing a mildly electron-withdrawing group (EWD), such as amide, in the meta position of the aromatic ring (**45f** and **45i**) resulted in less activity than the preliminary lead compound **DF04**.

The introduction of CF_3(**45c**) or OCF_3(**45d**), two strong EWDs in the ortho position, led to a decrease in the activity of these derivatives.

Compounds containing a chlorine atom (a weak electron-withdrawing group) increased the activity value in compound **45b** or a percentage of inhibition like the **DF04,** as in **45a**.

It is noteworthy that compound **45g**, bearing an amide in the para position, with an ethyl substituent instead of a methyl group, has a percentage of inhibition of halved if compared to **DF04** and **45h**. This decrease might be due to the steric hindrance of the substitution on the amide, not well tolerated in the hydrophobic pocket.

Finally, in contrast to what we expected, the introduction of lipophilic substituents on the phenyl rings seemed to have a limited influence on the inhibitor activity of these derivatives.

Nevertheless, it is worth noticing that the 6-piperazine-1-ylpyrazine-2-carboxamide scaffold of these derivatives is new and quite different from other chitinase inhibitors. Moreover, they have a drug-like profile and are easily produced.

From here on, there is still much that needs to be done to develop an inhibitor with low micromolar activity. A step forward, from a medicinal chemistry perspective, could be to synthesize new derivatives, in which other parts of the preliminary lead compound **DF04**, such as the central piperazine ring or the terminal pyrazine moiety, will be replaced or substituted with other structural analogues. The aim would be to obtain more active compounds and further knowledge regarding their structural activity relationship.

2.6   CONCLUSION

Human chitinases have garnered considerable attention since several studies have shown their involvement in the modulation of the immune response and their implication in chronic inflammatory lung diseases.

On the other hand, other studies have recently cast a shadow on their actual roles and, in contrast, proposed a protective effect of these enzymes. For this reason, the role of chitinase in chronic inflammatory lung diseases remains controversial, and more experiments are required to disclose their function. Medicinal chemistry can promote the design of new inhibitors with high potency, improved selectivity and a suitable drug-like which could help to shed more light on the role of human chitinases in Th2-mediated lung diseases.

We recently reported the discovery of a new potent and rational design compound specified tailored for *T. viride* chitinase, namely **BM22**. Its good activity prompted us to test this molecule against both human chitinases (hAMCase and hCHIT1), displaying a promising activity and AMCase/CHIT1 selectivity, features that triggered us to move forward by developing two series of derivatives with structural modifications.

From the biological activity data of these series, the best modification resulted in compound **BM41** occurring in two aromatic rings in the structure. Besides, the aromatic ring is a functional group easily functionalized with different groups, and this allowed us to explore its chemical space with the synthesis of a focused library of compounds bearing two different halogen atoms on one of the phenyl rings. All the compounds showed good activity profiles, but one derivative, **BM57,** distinguished itself from others by displaying a high potency (K_i = 2.9 μM) and a better AMCase/CHIT1 selectivity than **BM41**. Although we have only a limited amount of data, it seems that the functionalization of the phenyl ring, in this case with halogen atoms, could be related to a sort of selectivity for the hAMCase, since all the three halogenated derivatives showed a pronounced selectivity for this enzyme. This result is interesting because the high structural homology of AMCase and CHIT1 enzymes makes the search for selective inhibitors a challenge and one of the most desired features in human chitinase inhibitors. However, further derivatives need to synthesize to support this preliminary hypothesis. Moreover, It would be interesting to evaluate the ADME profiles of the most active compound of this series through in vitro studies. Indeed an excellent pharmacokinetic profile could make these compounds appealing as potential pharmacological tools in an animal model with chronic inflammatory diseases for studying the controversial role of human chitinase in these diseases.

For the **DF04** scaffold, a series of derivatives were synthesized to evaluate the effect of lipophilic substituents on the phenyl ring of this compound since it interacted with a hydrophobic pocket. Unfortunately, all the compounds showed retention or decrease of activity and the most interesting resulted in compound **45b** with a percentage of inhibition of 38%. Looking ahead, the 6-piperazine-1-ylpyrazine-2-carboxamide represents a novel and drug-like scaffold, yet its values of the activity are still not competitive with other known inhibitors. From here on, extensive work from a synthetic and computational point of view is required to obtain a micromolar inhibitor bearing this scaffold.

Chapter 3

Indole N-alkylation

3.1   OVERVIEW

During my period as a guest PhD student at the Uppsala University Biomedical Centre, Department of Medicinal Chemistry, I was involved in two projects: the IRAP project and the N-indole alkylation project.

The first project regards the insulin-regulated aminopeptidase (IRAP), a class of zinc-metallopeptidase enzymes belonging to the M1 family of aminopeptidase. They are present in high density in brain areas associated with cognitive, sensory, and motor functions. Their function is exploited by cleaving the N-terminal amino acid residue of several bioactive peptide regulators of cognition in vitro, such as vasopressin and oxytocin. Several studies demonstrated that inhibition of IRAP leads to an extension of the half-life of these neuropeptide substrates. In addition, this enzyme plays a crucial role in the process of physiological cognition. For these reasons, the IRAP receptor is a considerable and attractive potential macromolecular target to treat Alzheimer's disease or other cognitive disorders. During my period at the Uppsala University Biomedical Centre, Department of Medicinal Chemistry, I was involved in the development and synthesis of small molecules as inhibitors of the IRAP protein. My work was focused mainly on aryl sulfonamides derivatives identified through a high-throughput screen as IRAP inhibitors. The synthesized analogues will be evaluated in the IRAP enzymatic inhibition assays. The result of these data will give us more knowledge about the structure-activity relationship and help us understand in which direction to go for the next generation of IRAP inhibitors. However, this project is strictly confidential and protected by several patents, therefore, I cannot describe or show the synthesis, the structure of the molecules or the biological activity for the derivatives that I synthesized.[117–120]

On the other hand, I can describe the other project in which I was involved, the N-indole alkylation project.

3.2   INTRODUCTION

The indole ring system represents a structural element recurring in several compounds present in nature. For example, plants produce the growth hormone heteroauxin, a derivative of the indole, along with several alkaloid natural compounds containing the indole ring in their structure.[121] Fungi produce many substances containing the indole ring: one example is psilocybin which has psychedelic effects on humans.[122] Mammalians use the indole scaffold to produce two hormones: serotonin and melatonin. The former is a neurotransmitter that plays a fundamental role in the central nervous system, and cardiovascular and gastrointestinal systems.[123] The latter is a hormone involved in timing the circadian rhythms and regulation of the immune system.[124] Besides, the indole structure is part of the tryptophan which is one of the nine essential amino acids. Accordingly, in addition to its widespread function in nature, an impressive number of drugs approved in the market contain this "privileged structure", to the extent that the indole scaffold is the ninth-most frequently occurring heterocycle in FDA- approved drugs.[125–127] Indomethacin (a non-steroidal anti-inflammatory drug used for pain, fever, stiffness) and vincristine (one of the earliest anti-tumour agents appearing on the market) are two well-known examples of drugs approved containing these indole rings.[128] The broad spectrum of biological activities of indole derivatives has attracted considerable attention in organic and medicinal chemistry. Consequently, the chemistry literature is full of synthetic methodologies

with the aim of the construction of this ring or the introduction of different types of substituents into it.[129–131]

However, some indole derivatives still remain difficult to synthesize since only a few methods to obtain them are described in the literature.[132] Thus, this is the case of the N-indole alkylation, a reaction providing indole derivatives with a wide range of substitutions on their nitrogen atom. Substitutions on this atom can be simple such as benzyl or alkyl chains or more challenging such as alkyl branched chains, sterically hindered groups, and chiral alkyl substituents. Examples of compounds with these specific fragments in their structures are shown in Figure 3-1, pointing out that N- alkylated indoles are an attractive scaffold in medicinal chemistry.
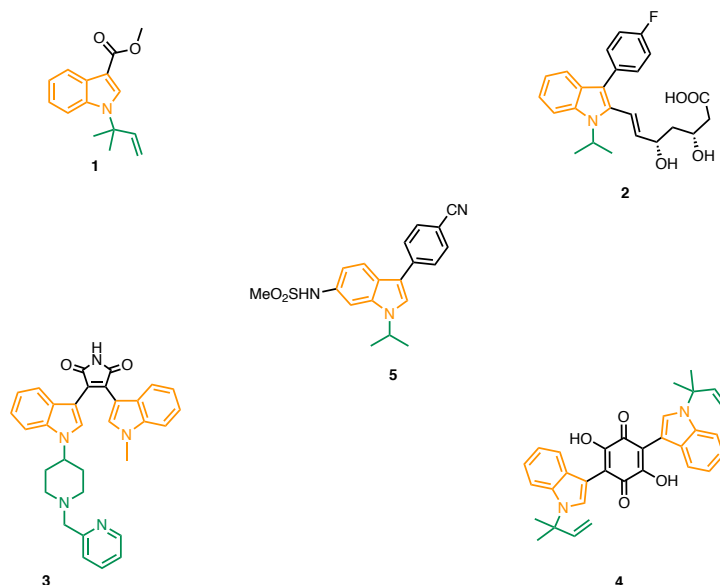
Figure 3-1: Examples of drugs currently used, presenting the N-alkylated fragment in their structures. 1, 4) **Derivatives 1** and **4** containing the 1,1-dimethyl-2-propenyl fragment have antifungal and anticancer activity respectively; 2) Fluvastatin (**Compound 2**) is a hypocholesterolaemia agent; 3) **Compound 3** (Enzastaurin) possess antitumor activity; 5) **Compound 5** is an antagonist of progesterone receptors used for the treatment of leiomyoma.

The methods used for the N-alkylation currently reported in the literature can be divided into four types.

The first method involves the enhancement of the inertness of the nitrogen atom to act as a nucleophile using a strong base able to deprotonate it. Therefore, the indolyl anion formed is able to attack the electrophilic reagents providing the N-alkylation. Although this approach has been used successfully in the N-alkylation of heterocyclic systems containing an N-alkyl substituent, problems arise when substrates are base-sensitive. Moreover, hazardous and toxic matters derived from a strong base and alkylated agents make this procedure unappealing for an industrial application.[133,134]

Another approach consists of a Mitsunobu-reaction exploiting the acidic behaviour of the nitrogen atom occurring in the indole ring and the opportune alcohol. However, this reaction works well as long as the indole derivatives possess electron-withdrawing groups on their rings, increasing the acidity of the indole nitrogen, otherwise, the low NH acidity hampers the alkylation. Besides, challenging purifications and the poor atom economy are two other problems related to the Mitsunobu reaction that limit the use of this strategy.[135]

The third approach is related to organic metallic chemistry. Traditional methods in this field such as palladium catalysed N-alkylation, exploiting the π allyl chemistry, or copper catalysed reaction of indoles, as well as the recently reported methods using chiral transition metal catalysts, have garnered attention as a reliable method to perform this reaction with a grade of selectivity and control otherwise unachievable using the previous methods.[132,136] However, pharmaceutical applications based on transition metal catalysts remain limited because of their high cost and the necessity of catalyst being removed at the end of the process.

Finally, a new strategy to achieve the N-indole alkylation using the cheap Et₃SiH and TFA has been described by Clanton et al. This procedure represents a simple and metal-free method to develop N-alkylation and works well with many substrates. On the downside, the lack of reactivity among ketone is a limiting factor since no branched chain on the carbon adjacent to the nitrogen can be obtained.[132,136]

3.3   STATE OF THE ART

Propyl phosphonic acid cyclic anhydride (T3P®) is an efficient and widely used water scavenger and coupling reagent for amide synthesis. The most interesting properties of this acid include its low toxicity, broad functional group tolerance and easy work-up procedure.[137,138] Consequently, it has recently garnered the attention of organic and medicinal chemists, and a variety of new applications have been described, including the direct conversion of carboxylic acid and amides into nitriles,[139] the synthesis of alkenes from alcohols,[140] the formation of Weinreb amides,[141] the conversion of carboxylic acids into acid azides, and in the synthesis of several substituted heterocyclic rings.[142,143]

In 2011, Odell et al. described a rapid, mild and efficient one-pot synthesis of indole using T3P® and microwave irradiation. This method represents a valid alternative to the procedures found in the literature employing strong acids or toxic reagents. During the investigation of the indole synthesis outlined in this paper, a side reaction involving the N-alkylation was observed.[144] In continuation of this observation, further studies investigating the employment of T3P® in the N-alkylation of indole compounds were conducted. The model reaction selected was between the 3-methyl indole (1 equiv) and cyclohexanone (3 equiv) in the presence of T3P® (50% solution in AcOEt). The reaction conditions were optimized by fine-tuning experiments, in which different times and temperatures were tested for the reaction. The best condition resulted at 120 ℃ under microwave irradiation (MW) for 20 min, furnishing the full conversion of the 3-methyl indole into 1-(cyclohex-1-en-1-yl)-3-methyl-1H-indole) with an excellent yield (94%) and easy purification (only a filtration through a plug of silica).
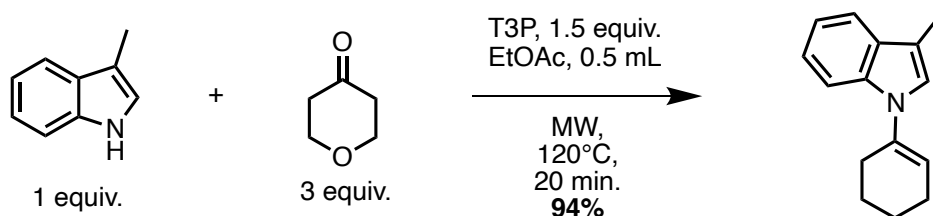
Scheme 3-1: Prototype reaction for the N-alkylation using T3P®.

Once these parameters were optimized, the substrate scope of this reaction was examined with two aims: investigation of the heterocyclic portion and the ketone/aldehyde portion. In the former, the influence of a variety of heterocyclic ring compounds was investigated using the cyclohexanone as the reference ketone, whereas in the latter a variety of ketones linear and branched, cyclic and acyclic were studied using the 3-methyl indole as the reference compound.

3.4   AIM OF THE PROJECT

My work concerning this project consisted of a further extension of the ketone/aldehyde scope of this reaction using different 6-membered ring ketones. The results of this work are reported in Table 3-1.
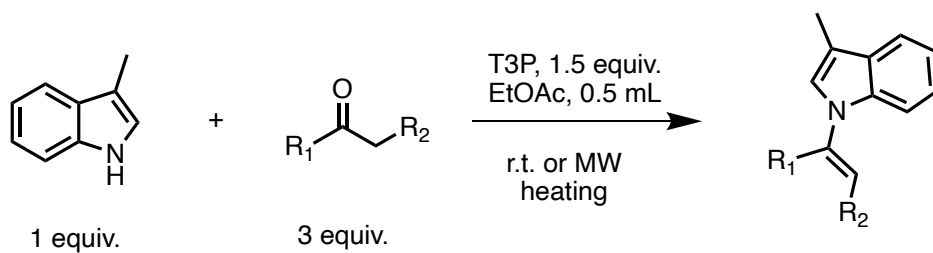
Table 3-1: N-alkylation in the presence of T3P®: ketones scope.

ENTRY	KETONE	PRODUCT	EQUIV. KETONE	TEMP.	TIME (min)	YIELD
1			3	120	20	94%
2			3	r.t.[a]	180	44%
3			3	160°C	60	no reaction
4			3	r.t. [a]	240	55%
5			5	160 °C	60	no reaction
6			3	120 °C	20	40%

[a] room temperature.

The first ketone used was the oxan-4-one (Table 3-1, entry 2). The reaction was carried out using the optimized condition of 120 °C for 20 minutes, and a black solution was obtained (the initial reaction mixture before heating had been a pale-yellow solution). TLC and HPLC-UV/MS analysis showed that the starting material, 3-methyl indole, had been consumed, however no trace of the product was observed. Presumably, under this reaction condition, the reaction might have been so violent that the desired product decomposed after formation Therefore, we decided to set up again the reaction at room temperature instead. This attempt worked well, and TLC analysis (30 minutes later) showed that part of the starting material transformed to another spot, which HPLC-UV/MS confirmed as the desired product. The reaction was monitored using TLC and HPLC-UV/MS every 30 minutes, and 3 hours after, the reaction was stopped with a good yield and rate of conversion (44%). It is interesting to notice a tiny difference in the structure of the six-member ring ketone, the presence of methylene (entry-1) or oxygen (entry-2) in position 4, led to a remarkable difference in the yield of the reaction, indicating that the nature of the substituent had a considerable effect on the rate of conversion.

Next, we made an attempt using pinacolone (3,3-dimethyl-2-butanone). Although it is an acyclic ketone, it represents a fascinating substrate for the reaction study since it is branched and sterically encumbered and could help study the steric effects of this reaction. The attempts with pinacolone were carried out using three different conditions: 120 °C for 20 minutes, and 160 °C for 20 minutes, 160 °C for 1 hour with five equivalents of pinacolone. Although we increased the temperature, the reaction time and the equivalents for these reactions, these attempts did not provide the desired product. The TLC and HPLC-UV/MS analysis no trace of the product and the starting materials were recovered unchanged after silica gel. This result suggested that sterically hindered groups nearby the reactive position hampered the conversion of the starting material into the desired product.

We subsequently examined the piperidone scaffold (Table 3-1, Entries-4 and 5). The difference between these two reactants was the protecting group used for the amine. In the former, the amino group was protected using the Boc group, whereas in the latter a benzylamine was used.

For the *N*-Boc-4-piperidone, the first attempt was conducted at 120 °C for 20 minutes and led to a fully recovered starting material, the 3-methyl indole, and a partially recovered *N*-Boc-4-piperidone. The presence of a very viscous and sticky solution after heating could point to a polymer derived from the polymerization of the deprotected 4-piperidone. Presumably, the acidic media formed by the use of T3P® in addition to the high temperature led to the deprotection of the Boc group and the subsequent release of the 4-piperidones, which started to polymerize, corroborating the viscous solution found.[145] Consequently, an attempt with *N*-Boc-4-piperidone was carried out under mild conditions: room temperature and without the use of microwaves heating. After four hours, a good conversion to the product was achieved (55% isolated yield). Notably, the product obtained from this entry could be a good building block for pharmaceutical relevant derivatives since the Boc group is easily cleaved, and the resulting amine could further be functionalized.

On the other hand, the attempts with *N*-benzyl protected 4-piperidone did not work, although strong conditions were employed: 160 °C for 20 minutes, and 160 °C for 1 hour with five equivalents of *N*-benzyl-piperidone. In this case, we hypothesized that the reaction issues might be related to a solubility problem (1 benzylpiperidin-4-one is a dense brown liquid that once added to the reaction mixture, did not entirely solubilize).

Finally, a substituted cyclohexanone, the ethyl 4-oxocyclohexane-1-carboxylate (Entry-6), was used. The reaction with this substrate worked well, and after 20 minutes at 120 °C, the SM was partially transformed into the product (40% the percentage of conversion). On the downside, a challenging purification, a long isocratic hexane flash chromatography due to the high similarity in terms of the

polarity of the product and the starting material present, was required to afford the product. It would be interesting to run the reaction again at elevated temperature, for instance, 160 ℃ for 20 minutes, to see if a better conversion could be achieved which also would ease product purification.

3.5   CONCLUSION

The indole structural fragment is a recurring heterocyclic system with a broad spectrum of biological activities. Consequently, the chemical literature focused on this "privileged heterocyclic ring" is massive. Although there is a large number of procedures presented in the literature, the same cannot be said for the N-alkylation of indole. This reaction remains a poorly accessible procedure, which works well and with a wide range of substrates only in the presence of metal transition catalysts.

Herein, we reported a procedure to obtain N-alkylated indoles with the employment of the green reagent T3P and microwave irradiations. This procedure presented many features which made it a worthy alternative for providing this structural fragment. The reaction is one-pot synthesis, using mild conditions, mostly ketones work at room temperature without the needing of microwave heating, and has an easy purification using a rapid filtration over a plug of silica. Moreover, it works well with a variety of substituted cyclic ketones (40-60% yield). For these reasons, this represents a valid metal-free alternative that can give facile access to several building blocks and novel biologically active compounds.

Chapter 4

Materials and methods

4.1 GENERAL INFORMATION

All commercially available chemicals were used as purchased (Aldrich, Alfa-Aesar). Thin-layer chromatography (TLC) was carried out using Merck TLC plates silica gel 60 F254. TLCs were visualized under UV light and stained with ninhydrin, bromocresol green, or basic permanganate stains. Chromatographic separations were performed on columns packed with silica gel (230-400 mesh, for flash technique).

^{1}H-NMR and **^{13}C-NMR** were recorded on a Bruker Avance 400 spectrometer at 400 MHz and 100 MHz, respectively. Spectra are reported in parts per million (δ scale) and internally referenced to the CDCl$_3$ at δ 7.26 ppm, CD$_3$OD at δ 3.31 ppm, DMSO-d$_6$ at δ 2.50 ppm, Acetone at δ 2.05 ppm, and CD$_2$Cl$_2$ at δ 5.32 ppm. Chemical shifts for carbon are reported in parts per million (δ scale) and referenced to the carbon resonances of the solvent (CDCl$_3$ at δ 77.0, CD$_3$OD at δ 49.0 ppm, DMSO-d$_6$ at δ 39.5 ppm, Acetone at δ 29.8 ppm, and CD$_2$Cl$_2$ at δ 53.8 ppm). Data are shown as following: chemical shift, multiplicity (s = singlet, d = doublet, t = triplet, q = quartet, qi = quintet, m = multiplet and/or multiplet resonances, bs = broad singlet), coupling constants (J) in Hertz (Hz), and integration. Mass spectra (LCMS (ESI)) were acquired using an Agilent 1100 LC-MSD VL system (G1946C) by direct injection with a 0.4 mL/min flow rate using a binary solvent system of 95/5 MeOH/H$_2$O. UV detection was monitored at 221 or 254 nm. Mass spectra were acquired in positive or negative mode scanning over the mass range 100-1500 *m/z*, using a variable fragmentor voltage of 0-70 V.

The purity of compounds was assessed by reverse-phase liquid chromatography and a mass spectrometer with a UV detector at λ= 254 nm and an electrospray ionization source (ESI). All the solvents were HPLC grade. Mass spectral (MS) data were obtained using a LC/MSD VL system with a 0.4 mL/min flow rate using a binary solvent system of 95:5 (v/v) methyl alcohol/water. UV detection was monitored at 254 nm. Mass spectra were acquired in positive mode scanning over the mass range of 50-1500. The following ion source parameters were used: drying gas flow, 9 mL/min; nebulize pressure, 40 psig; drying gas temperature, 350°C. Chromatographic separation of final products were conducted using a Polaris C18 column (150 - 4.6 mm, 5 µm particle size) at a flow rate of 0.8 mL min-1 with a mobile phase composed of 50% CH$_3$CN/50% H$_2$O-formic acid 0.1%.

Anhydrous reactions were performed into flame-dried glassware after three cycles of vacuum/ dry nitrogen and were run under a positive pressure of dry nitrogen.
Anhydrous solvents were prepared by distillation over the appropriate agent: dichloromethane and acetonitrile were dried over calcium hydride; tetrahydrofurane was dried over sodium/benzophenone. Anhydrous dimethylformamide and toluene were used as purchased. Degassed dichloromethane and toluene were prepared by using the freeze-pump-thaw method. Dry DIPEA was purchased from Merck. Dry TEA was dried over KOH and distilled under nitrogen atmosphere

Microwave reactions were conducted using a CEM Discover Synthesis Unit (CEM Corp., Matthews, NC). The machine consists of a continuous focused microwave power delivery system with operator-selectable power output from 0 to 300 W. The temperature of the contents of the vessel was monitored using a calibrated infrared temperature control mounted under the reaction vessel. All experiments were performed using a stirring option whereby the contents of the vessel are stirred by

means of a rotating magnetic plate located below the microwave cavity and a Teflon-coated magnetic stir bar in the vessel.

4.2 BIOLOGY

4.2.1 <u>MIC Evaluation</u>

The synthesized compounds were assayed against more than 100 strains belonging to 8 Candida spp. (C. albicans, C. guilliermondii, C. krusei, C. parapsilosis, C. tropicalis, C. kefyr, C. glabrata, and C. lipolytica) and 15 strains of Cryptococcus neoformans isolated from oral, vaginal, anorectal, urine, stool, blood, central venous catheter, and respiratory tract specimen with each strain representing a single isolate from a patient. Yeast cells were grown in Yeast-Peptone-Dextrose (YPD) medium at 37 °C for 16 h and 150 rpm orbital shaker. Cells were then sub-inoculated in fresh YPD medium and grown to an optical density of 0.3. The turbidity of the inoculum was adjusted to 0.5 McFarland and diluted 1:500 in RPMI 1640 broth, corresponding to around 2.5×10^5 CFU/mL. MICs were determined by liquid growth inhibition assays by Clinical and Laboratory Standards Institute (CLSI) guidelines, using two serial dilutions of the compounds dissolved in an appropriate buffer. The first one from 256 to 0.125 µg/mL for **BM24**, **BM37** and Fluconazole, whereas compound **BM29** and **BM30** were tested using a final concentration ranging from 200 to 1.56 µg/mL. Plates were incubated at 35 °C, and MICs were visualized after 24 hours as the lowest concentration of the tested compound that completely inhibited cell

The minimal inhibitory concentrations (MICs) were determined at 24 h both visually and spectrophotometrically. By visual endpoint determination, MICs were determined according to a S-I-R scale, with S (susceptible) indicating an optical clear culture, I (intermediate susceptibility) indicating a slightly hazy culture, and R (resistant) indicating no reduction in turbidity. The MIC_{90} was defined as the lowest concentration of a drug which corresponds to an S culture. Microtitration plates were stirred using a microtitration plate shaker before reading to ensure uniform turbidity. MICs were obtained by measuring the S10 absorbance at 450 nm with a microtitration plate reader. The value of the blank was subtracted from the reading of the rest of the wells. Two endpoints were defined for each antifungal agent tested, with MIC_{80} indicating the lowest drug concentration resulting in a reduction of growth of 80% or more (determined spectrophotometrically) compared with the growth of the control, and MIC_{90} indicating the lowest drug concentration resulting in a reduction in growth of 90% (determined spectrophotometrically) compared with the growth of the control. The MIC90 was also defined as the spectrophotometric endpoint.

4.2.2 <u>Chitinase Enzymatic Assays</u>

Inhibition assays were performed using commercially available human Acidic Mammalian chitinase or human Chitotriosidase (both bought from CycLex Co. Ltd., Japan) at 25 °C in 40 mM Na_3PO_4, 20 mM citric acid, 20 µg/ml BSA buffer (pH 4.2). Mixtures containing the AMCase enzyme at 0.4 ng/mL or hCHIT1 at 0.05 µg/mL and 50 µM of inhibitors were incubated for 20 min on a multi-well plate (Perkin Elmer Spectra plate). The substrate (4-methylumbelliferyl β-D-*N*,*N'*,*N''*-triacetylchitotrioside, Sigma-Aldrich, St Louis, USA) was then added at a final concentration of 20 µM. The chitinase activity was determined by monitoring the time dependence of substrate hydrolysis followed by fluorescence (excitation wavelength, 400 nm; emission wavelength, 440-460 nm). The rate of substrate hydrolysis in the absence and presence of inhibitor were determined in triplicate and allowed to calculate the percentage of enzyme inhibition according to the following equation:

$$\% \: Inh = 100 - \left(\frac{v_i}{v_0} \times 100 \right)$$

where v_i and v_0 are the rate of hydrolysis in presence and absence of inhibitor. Assays containing no inhibitor, no enzyme or Bisdionin F, a known chitinase inhibitor, were run in parallel as controls. Inhibition constants (K_i values) were determined using the above-described assay and the rate of substrate hydrolysis of 20 µM 4-methylumbelliferyl β-D-*N*,*N'*,*N''*-triacetylchitotrioside was measured in the presence of variable concentrations of inhibitors (0 to 100 µM). The analysis of the plot of the ratio v_o/v_i as a function of [I], allowed to compute the K_i value, as previously described, considering a competitive model of inhibition:[106]
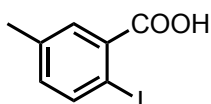
$$K_i = \frac{K_m}{(K_m + [S]) \times slope}$$

where K_m is the Michaelis-Menten constant (determined as 12 µM for AMCase and 1.48 µM for CHIT1), [S] is the concentration of the substrate.

4.3   CHEMISTRY

4.3.1   Synthesis of BM37

*Synthesis of 2-iodo-5-methylbenzoic acid.*

1

To a stirred solution of methyl 2-iodo-5-methylbenzoate (975 µL, 5.92 mmol) in THF/MeOH/H$_2$O 3:1:1 (130 mL), lithium hydroxide monohydrate (734.0 mg, 17.75 mmol) was added and the mixture stirred at r. t. for 4 h. Then more lithium hydroxide monohydrate (245.0 mg, 5.92 mmol) was added and the reaction stirred at r. t. for another 1 h. HCl 1N was added dropwise until pH 2. The aqueous phase was extracted with EtOAc three times, and the collected organic layers were dried over anhydrous Na$_2$SO$_4$, filtered, and evaporated ur *in vacuum*. The crude was purified by flash chromatography on silica gel (Hex/EtOAc 1:0; Hex/EtOAc 0:1). to give 2-iodo-5-methylbenzoic acid **1**. **Yield**: 93%. **^{1}H-NMR** (400 MHz, CDCl$_3$) δ ppm 12.39 (s, 1H), 7.86 (d, *J* = 7.6 Hz, 1H), 7.81 (s, 1H), 6.98 (d, *J* = 7.2 Hz, 1H), 2.32 (s, 3H). **^{13}C-NMR** (100 MHz, CDCl$_3$) δ ppm 168.9, 139.6, 136.6, 134.5, 134.2, 131.5, 98.7, 21.2. **MS (ESI)** *m/z* = 260.9 [M - H]$^-$.

*Synthesis of (2-iodo-5-methylphenyl) methanol.*
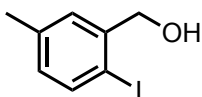
2

To a stirred suspension of 2-iodo-5-methylbenzoic acid **1** (1443.0 mg, 5.51 mmol) in dry THF (26.0 mL), borane dimethyl sulfide complex (1.6 mL, 16.52 mmol) was added dropwise under N$_2$ atmosphere at 0 °C. Then, the reaction mixture was allowed to gently warm at r.t. and stirred for 12 h. Water and K$_2$CO$_3$ were carefully added, and the mixture was stirred for additional 30 min. Then, the mixture was extracted with EtOAc and washed twice with 1N NaOH and then, with brine. The organic layer was dried over anhydrous Na$_2$SO$_4$, filtered, and evaporated to dryness under vacuum to give **2** as a white solid. **Yield**: 99%. **^{1}H-NMR** (400 MHz, CDCl$_3$) δ ppm 7.65 (d, *J* = 8.0 Hz, 1H), 7.24 (s, 1H), 6.80 (d, *J* = 8.0 Hz, 1H), 4.60 (s, 2H), 2.29 (s, 3H), 2.10 (bs, 1H). **^{13}C-NMR** (100 MHz, CDCl$_3$) δ ppm 145.9, 140.1, 134.6, 129.4, 126.3, 91.8, 59.8, 21.2.

Synthesis of 2-(chloromethyl)-1-iodo-4-methylbenzene.

3
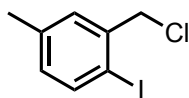
To a stirred solution of **2** (1419.0 mg, 5.72 mmol) in dry CH_2Cl_2 (52.0 mL), freshly distilled dry TEA (796 µL, 5.72 mmol), and DMAP (838.0 mg, 14.26 mmol) were added under N_2 atmosphere at 0 °C. Then, *p*-toluenesulfonyl chloride (4070.0 mg, 21.38 mmol) was added portionwise and the reaction mixture was stirred for additional 30 min at 0 °C, then at r.t. for 16 h. The solvent was removed by evaporation *in vacuum* and the crude was purified by flash chromatography on silica gel, eluting with Hex/EtOAc 1:0; Hex/EtOAc 9:1 to give compound **3**. **Yield**: 59%. **^{1}H-NMR** (400 MHz, $CDCl_3$) δ ppm 7.70 (d, *J* = 7.6 Hz, 1H), 7.28 (s, 1H), 6.81 (d, *J* = 8.0 Hz, 1H), 4.62 (s, 2H), 2.29 (s, 3H). **^{13}C-NMR** (100 MHz, $CDCl_3$) δ ppm 141.2, 140.3, 134.9, 130.8, 130.2, 106.5, 45.4, 21.2.

### Synthesis of 2-((2-iodo-5-methylbenzyl)oxy)benzaldehyde.

4
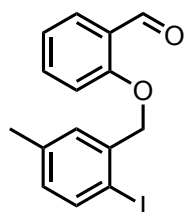
To a stirred solution of salicylaldehyde (394 µL, 3.70 mmol)) in CH_3CN (21.0 mL), K_2CO_3 (511.0 mg, 3.70 mmol), NaI (126.0 mg, 0.84 mmol), and **3** (896.0 mg, 3.37 mmol) were added and the reaction mixture was stirred at reflux for 16 h. After evaporation *in vacuum*, the residue was dissolved in EtOAc, 1N NaOH was added, and the mixture was stirred at r.t. for additional 10 min. Then, the mixture was extracted with EtOAc three times, and the combined organic layers were washed with brine, dried over anhydrous Na_2SO_4, filtered, and evaporated to dryness under vacuum to give **4**. **Yield**: 97%. **^{1}H-NMR** (400 MHz, $CDCl_3$) δ ppm 10.57 (s, 1H), 7.86 (d, *J* = 8.0 Hz, 1H), 7.72 (d, *J* = 8.0 Hz, 1H), 7.54 (t, *J* = 8.4 Hz, 1H), 7.30 (s, 1H), 7.05 (m, 2H), 6.86 (d, *J* = 7.6 Hz, 1H), 5.11 (s, 2H), 2.30 (s, 3H). **^{13}C-NMR** (100 MHz, $CDCl_3$) δ ppm 187.5, 161.4, 141.4, 140.2, 135.2, 134.1, 131.6, 129.9, 128.1, 125.6, 121.1, 115.7, 85.8, 70.1, 21.2. **MS (ESI)** *m/z* = 374.9 [M + Na]⁺.

Synthesis of 2-((5-methyl-2-vinylbenzyl)oxy)benzaldehyde.

5
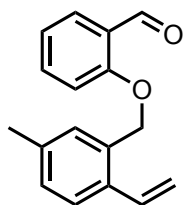
To a stirred solution of **4** (1153.0 mg, 3.28 mmol) in dry THF (46 mL), palladium acetate (73.0 mg, 0.33 mmol) and triphenylphosphine (172.0 mg, 0.66 mmol) were added under N_2 atmosphere. Then, tributyl(vinyl)tin (1134 µL, 3.93 mmol) was added dropwise and the reaction mixture was stirred at reflux for 16 h. After cooling, the mixture was filtered through a plug of celite, and the filtrate was evaporated to dryness under vacuum. The residue was diluted with EtOAc, washed with $NaHCO_3$ss and brine. Then, it was dried over anhydrous Na_2SO_4, filtered, and evaporated to dryness under vacuum. The crude was purified by flash chromatography on silica gel (Hex/EtOAc 1:0; Hex/EtOAc 9:1)

to compound **5**. **Yield**: 90%. **¹H-NMR** (400 MHz, CDCl₃) δ ppm 10.47 (s, 1H), 7.84 (d, *J* = 7.6 Hz, 1H), 7.56 (t, *J* = 1.6 Hz, 1H), 7.52 (d, *J* = 1.6 Hz, 1H), 7.22 (s, 1H), 7.16 (d, *J* =7.6 Hz, 1H), 7.05 (m, 2H), 6.93 (m, 1H), 5.64 (d, *J* = 17.2 Hz, 1H), 5.28 (d, *J* = 10.8 Hz, 1H), 5.17 (s, 2H), 2.35 (s, 3H). **¹³C-NMR** (100 MHz, CDCl₃) δ ppm 187.5, 161.4, 138.3, 137.4, 137.3, 136.2, 135.2, 131.6, 128.2, 127.5, 127.4, 125.6, 121.1, 115.7, 113.0, 70.1, 21.2.

Synthesis of 2-((5-methyl-2-vinylbenzyl)oxy)benzaldehyde oxime .

6
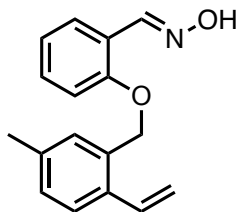
To a stirred solution of benzaldehyde **5** (746.0 mg, 2.96 mmol) in EtOH (45.0 mL), pyridine (287 µL, 3.55 mmol) and hydroxylamine hydrochloride (511.0 mg, 7.40 mmol) were added. The mixture was stirred at reflux for 3 h. After cooling, the mixture was evaporated to dryness under vacuum and the residue was dissolved in EtOAc, washed with brine twice, dried over anhydrous Na₂SO₄, filtered, and evaporated to dryness under vacuum to afford compound **6**. **Yield**: 86%. **¹H-NMR** (400 MHz, CDCl₃) δ ppm 8.50 (s, 1H), 7.74 (d, *J* = 7.2 Hz, 1H), 7.45 (d, *J* = 8.0 Hz, 1H), 7.34 (t, *J* = 7.2 Hz, 1H), 7.19 (s, 1H), 7.15 (d, *J* = 8.0 Hz, 1H), 6.94 (m, 3H), 5.64 (d, *J* =17.2 Hz, 1H), 5.28 (d, *J* = 11.2 Hz, 1H). 5.09 (s, 2H), 2.34 (s, 3H). **¹³C-NMR** (100 MHz, CDCl₃) δ ppm 163.9, 159.5, 138.3, 137.4, 137.3, 136.2, 130.8, 129.8, 128.2, 127.5, 127.4, 122.4, 120.8, 115.4, 113.0, 70.1, 21.2.

Synthesis of (2-((5-methyl-2-vinylbenzyl)oxy)phenyl)methanamine.


7

To a stirred solution of aldoxime **6** (678.0 mg, 2.54 mmol) in THF (36.0 mL), zinc dust (1651.0 mg, 25.39 mmol) and 2N HCl (13.0 mL, 25.39 mmol) were added, and the reaction mixture was stirred at reflux for 4 h. After cooling, the solvent was evaporated *in vacuo*, the residue was basified with NaOH 2N and extracted with EtOAc. The collected organic layers were dried over anhydrous Na₂SO₄, filtered and the solvent was evaporated to dryness *under vacuum* to afford product **7**. **Yield**: 93%. **¹H-NMR** (400 MHz, CDCl₃) δ ppm 7.46 (d, *J* = 7.6 Hz, 1H), 7.17 (m, 4H), 6.94 (m, 3H), 5.65 (d, *J* = 17.6 Hz, 1H), 5.26 (d, *J* = 10.8 Hz, 1H), 5.07 (s, 2H), 3.80 (s, 2H), 2.35 (s, 3H), 1.61 (bs, 2H). **¹³C-NMR** (100 MHz, CDCl₃) δ ppm 158.6, 138.3, 137.4, 137.3, 136.2, 128.3, 128.2, 127.9, 127.7, 127.6, 127.5, 122.1, 113.2, 113.0, 70.1, 42.8, 21.2.

*Synthesis of the protected guanidine 8.*

8
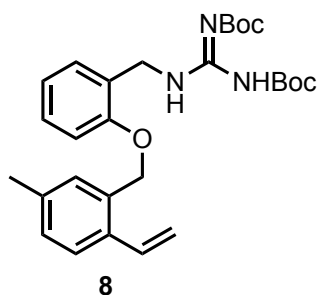
To a stirred solution of primary amine **7** (596.0 mg, 2.36 mmol) in THF (26 mL), *N,N'*-Di-Boc-1H-pyrazole-1- carboxamidine (950.0 mg, 3.06 mmol) and DIPEA (411 µL, 2.36 mmol) were added. The reaction mixture was stirred at r.t. for 16 h. After cooling, EtOAc was added, and the mixture was washed with water and brine. After drying over anhydrous Na_2SO_4, the mixture was filtered and evaporated to dryness under vacuum. The crude residue was purified by flash chromatography on silica gel (Hex/EtOAc 1:0; Hex/EtOAc 8:2). to give the pure compound **8**. **Yield**: 67%. **^{1}H-NMR** (400 MHz, $CDCl_3$) δ ppm 11.22 (bs, 1H), 8.66 (bs, 1H), 7.41 (d, *J* = 8.0 Hz, 1H), 7.31 (d, *J* = 7.6 Hz, 1H), 7.25 (m, 2H), 7.11 (d, *J* = 8.0 Hz, 1H), 6.92 (m, 3H), 5.61 (d, *J* = 17.6 Hz, 1H), 5.26 (d, *J* = 11.6 Hz, 1H), 5.10 (s, 2H), 4.64 (d, *J* = 5.2 Hz, 2H), 2.32 (s, 3H), 1.48 (s, 9H), 1.42 (s, 9H). **^{13}C-NMR** (100 MHz, $CDCl_3$) δ ppm 163.6, 156.8, 156.0, 152.9, 138.0, 137.5, 134.0, 133.6, 133.3, 129.8, 129.3, 129.0, 128.9, 125.9, 120.8, 115.7, 111.6, 111.4, 82.6, 79.0, 68.2, 40.6, 28.9, 28.3, 28.0, 21.1 .

### *Synthesis of the amidinourea 10.*

10
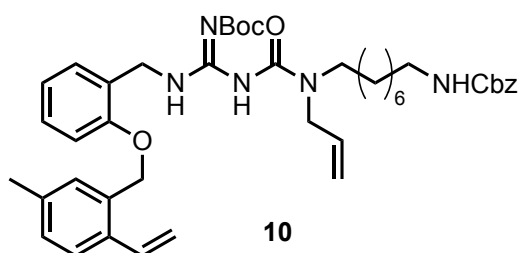
To a stirred solution of **8** (780.0 mg, 1.58 mmol) in dry THF (48.0 mL), a solution of linker **9** (*N*-(8-(allylamino) octyl)-2-phenylacetamide (651.0 mg, 2.05 mmol) in dry THF (48.0 mL) and freshly distilled dry TEA (219 µL, 1.58 mmol) were added dropwise under N_2 atmosphere. The reaction mixture was stirred at reflux for 16 h. After cooling, EtOAc was added, and the mixture was washed with water and brine. After drying over anhydrous Na_2SO_4, the mixture was filtered and evaporated to dryness under vacuum. The crude residue was purified by flash chromatography on silica gel (Hex/EtOAc 1:0; Hex/EtOAc 8:2) to give pure compound **10**. **Yield**: 78%. **^{1}H-NMR** (400 MHz, $CDCl_3$) δ ppm 12.31 (d, *J* = 10.0 Hz, 1H), 8.40 (bs, 1H), 7.43 (d, *J* = 7.6 Hz, 1H), 7.33 (m, 5H), 7.25 (m, 3H), 7.11 (d, *J* = 7.6 Hz, 1H), 6.93 (m, 3H), 5.76 (m, 1H), 5.61 (d, *J* = 17.6 Hz, 1H), 5.25 (d, *J* = 10.8, 1H), 5.10 (m, 5H), 4.98 (d, *J* = 10.4 Hz, 1H), 4.55 (dd, *J* = 5.6 Hz, 15.2 Hz, 2H), 4.05 (d, *J* = 4.8 Hz, 1H), 3.90 (d, *J* = 4.8 Hz, 1H), 3.36 (t, *J* = 7.2 Hz, 1H),3.21 (t, *J* = 7.6 Hz, 1H), 3.14-3.10 (m, 2H), 2.32 (s, 3H), 1.41 (s, 9H), 1.26-1.18 (m, 12H). **^{13}C-NMR** (100 MHz, $CDCl_3$) δ ppm 163.8, 163.7, 156.5, 156.3, 154.0, 153.9, 153.2, 137.5, 136.7, 135.3, 134.7, 134.1, 133.6, 133.4, 129.4, 129.3, 129.0, 128.9, 128.4, 126.8, 125.9, 120.7, 115.6, 115.4, 111.5, 81.8, 68.2, 66.4, 50.4, 48.4, 47.5, 45.6, 41.0, 40.0, 29.8, 29.3, 29.2, 28.5, 28.1, 26.9, 26.8, 26.6, 20.9. **MS (ESI)** *m/z* = 370.7 $[M + 2H]^{2+}$.

### *Synthesis of the macrocycle 11.*

11
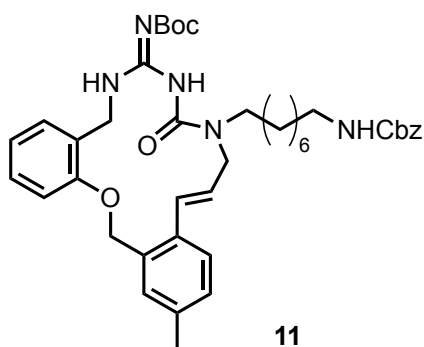
To a stirred solution of amidinourea derivative **10** (208.0 mg, 0.28 mmol) in freshly degassed dry CH_2Cl_2 (138.0 mL, 2.00 mM solution), a solution of 2nd generation Grubb's catalyst (48.0 mg, 0.06 mmol) in freshly degassed dry CH_2Cl_2 (1.0 mL) was added dropwise under N_2 atmosphere. The reaction mixture was stirred at reflux for 16 h. After cooling, the mixture was evaporated to dryness under vacuum. The crude residue was purified by flash chromatography on silica gel (Hex/EtOAc 1:0; Hex/EtOAc 8:2) to give macrocycle **11**. **Yield**: 69%. **^{1}H-NMR** (400 MHz, CDCl$_3$) δ ppm 12.29 (s, 1H), 8.38 (t, *J* = 6.3 Hz, 1H), 7.30 (m, 5H), 7.95 (m, 7H), 6.52 (d, *J* = 15.6 Hz, 1H), 6.10 (dt, *J* = 15.6 Hz, 5.8 Hz, 1H), 5.07 (d, *J* = 7.0 Hz, 4H), 4.70 (bs, 1H), 4.59 (d, *J* = 6.3 Hz, 2H), 3.88 (d, *J* = 5.8 Hz, 2H), 3.34 (m, 2H), 3.14 (q, *J* = 6.8 Hz, 2H), 2.32 (s, 3H), 1.55 (m, 4H) 1.46 (s, 9H), 1.27 (m, 8 H). **^{13}C-NMR** (100 MHz, CDCl$_3$) δ ppm 171.0, 164.1, 156.4, 155.7, 154.0, 153.5, 136.7, 136.6, 134.1, 133.6, 131.0, 130.6, 129.5, 128.9, 128.4, 127.9, 127.8, 127.5, 127.1, 126.5, 125.5, 125.2, 124.9, 121.2, 82.1, 70.6, 66.6, 66.4, 52.0, 49.5, 48.0, 41.0, 39.3, 29.8, 29.6, 29.3, 29.2, 28.8, 28.7, 28.2, 27.9, 27.7, 26.9, 26.6, 26.3, 25.5, 21.0, 20.9. **MS (ESI)** *m/z* = 711.9 [M + H]$^+$.

Synthesis of the amine 12.

12
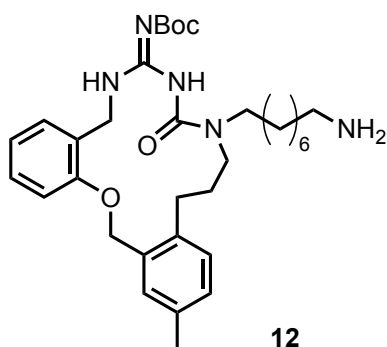
To a stirred solution of **11** (122.0 mg, 0.17 mmol) in isopropanol (19.0 mL), Pd/C 10% (36.0 mg, 0.03 mmol) and a few drops of HCl 36% were added. The reaction mixture was subject to three cycles of vacuum followed by a flush of H_2 before being stirred under H_2 (1 atm) for 4 h. Then, the mixture was filtered through a plug of Celite, and the filtrate was evaporated to dryness under vacuum. The crude product was used directly in the next step without any further purification. **LCMS (ESI)** *m/z* =580.4 [M + H]$^+$.

Synthesis of the protected guanidine 13.

13
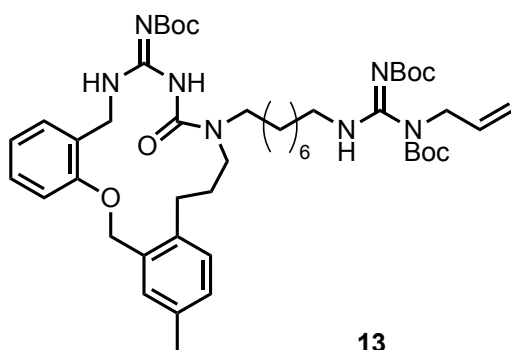
To a stirred solution of the crude in dry THF (5.0 mL), a solution of the crotyl guanylating agent (*N,N'-*Di-Boc- (E)-*N*-crotyl-1*H*-pyrazole-1-carboximidamide, 60.0 mg, 0.17 mmol) in dry THF (2.8 mL) and dry DIPEA (89 µL, 0.51 mmol) were subsequently added under N_2 atmosphere. The reaction mixture was stirred at reflux for 12 h. After cooling, the mixture was evaporated to dryness under vacuum and the residue was dissolved in EtOAc, washed with water twice and brine. After drying over anhydrous Na_2SO_4, the mixture was filtered, and evaporated to dryness under vacuum. The crude residue was purified by flash chromatography on silica gel, eluting with Hexane/EtOAc 8:2 to give pure compound **13**. **Yield**: 59% over two steps. **^{1}H-NMR** (400 MHz, CDCl$_3$) δ ppm 12.19 (s, 1H), 12.08 (s, 1H), 8.52 (s, 1H), 8.50 (s, 1H), 7.24 (m, 1H), 7.17 (m, 2H), 7.13 (m, 2H), 6.94 (m, 1H), 5.62 (m, 1H), 5.49 (m, 1H), 5.00 (s, 2H), 4.55 (d, *J* = 6.4 Hz, 2H), 4.14 (m, 2H), 3.19 (m, 4H), 3.11 (t, *J* = 8.0 Hz, 2H), 2.47 (t, *J* = 8.0 Hz, 2H), 2.33 (s, 3H), 1.94 (m, 2H), 1.63 (d, *J* = 6.8 Hz, 7H), 1.47 (s, 9H), 1.46 (s, 9H), 1.44 (s, 9H), 1.27 (s, 8H). **^{13}C-NMR** (100 MHz, CDCl$_3$) δ ppm 163.5, 155.6, 153.6, 139.5, 135.3, 133.8, 131.4, 129.8, 129.6, 127.4, 126.5, 126.1, 124.9, 120.5, 116.5, 113.7, 82.1, 76.6, 69.5, 49.9, 49.5, 49.4, 47.8, 47.3, 47.3, 43.8, 38.1, 37.0, 32.7, 31.8, 26.9, 26.8, 22.6, 20.8, 19.6, 17.6, 14.0. **LCMS (ESI)** *m/z* = 876.5 [M + H]$^+$.

Synthesis of compound BM37.

BM37
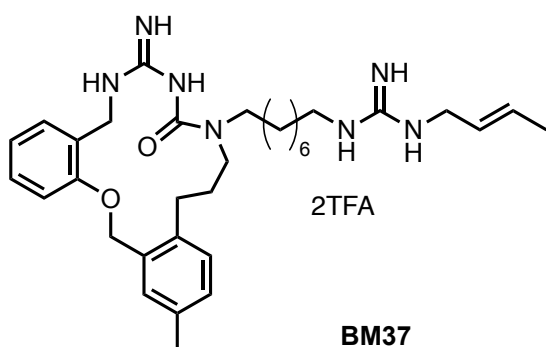
To a stirred solution of **13** (10.0 mg, 0.014 mmol) in dry CH$_2$Cl$_2$ (1.7 mL), freshly distilled TFA (300 µL, final concentration 10% v/v) was added dropwise. The reaction mixture was stirred at r.t. for 12 h. The mixture was evaporated to dryness under vacuum. Then, it was treated with toluene and methanol and evaporated to dryness under vacuum to remove TFA residue. The crude was treated with Et$_2$O and Hexane, then decanted and the solvents were pipetted off. This procedure was repeated several times to yield compound **BM37**. **Yield:** 99%. **^{1}H-NMR** (300 MHz, CD$_3$OD) δ ppm 7.23 (m, 5H), 6.96 (m, 2H), 5.72 (m, 1H), 5.50 (m, 1H), 5.04 (m, 2H), 4.42 (m, 2H), 3.73 (d, *J* = 5.1 Hz, 2H), 3.53 (m, 2H), 3.30 (s, 2H), 3.16 (t, *J* = 6.9 Hz, 2H), 2.72 (m, 2H), 2.34 (m, 3H), 2.04 (m, 2H), 1.73 (m, 3H), 1.56 (m, 4H), 1.34 (m, 9H). **^{13}C-NMR** (75 MHz, CD$_3$OD): δ ppm 159.7, 156.73, 155.2, 137.6, 137.0, 134.4, 128.9, 128.8,

128.0, 127.1, 126.8, 125.3, 121.6, 114.1, 69.3, 45.5, 45.0, 42.5, 41.7, 31.5, 28.8, 28.6, 28.6, 28.2, 27.2, 26.9, 26.8, 26.6, 21.0, 16.5. **LCMS (ESI)** *m/z* = 576.4 [M + H]⁺.

4.3.2   Synthesis of the linker and guanylating agent
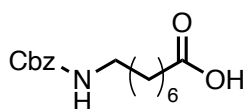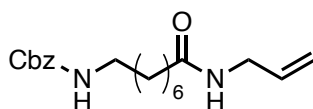
Synthesis of N-(Cbz)-Aminooctanoic acid 14.

14

8-Aminooctanoic acid (500.0 mg, 3.14 mmol) and K_2CO_3 (867.0 mg, 6.28 mmol) were suspended in dry THF/H_2O 1:1(15 ml). Then, CbzCl (0,7 mL, 4,71 mmol) was added and the resulting mixture was stirred at r.t. 16h. The reaction was quenched with EtOAc and H_2O. Aqueous phase was separated, and the pH of aqueous phase was adjusted to 2 by addition of HCl 4N and extracted twice with EtOAc. Combined organic phases were then dried over Na_2SO_4, filtered, and evaporated under reduced pressure. The crude product was used in the next step without any further purification 87%. **¹H-NMR** (400 MHz CDCl₃) δ ppm 10.70 (s, 1H), 7.35-7.29 (m, 5H), 5.07 (s, 2H), 4.71 (bs, 1H), 3.16 (m, 2H,), 2.32 (t, 2H, *J* = 7.6 Hz), 1.61 (t, 2H, *J* = 6.8 Hz), 1.48 (m, 2H), 1.30 (m, 6H). **¹³C-NMR** (100 MHz CDCl₃) δ ppm 178.7, 156.4,136.5, 128.4, 128.0, 128.0, 66.5, 41.4, 33.8, 29.7, 28.6, 26.4, 24.7. **LRMS (**ESI) *m/z* 609.0 [2M+Na] ⁺, 316.0 [M+Na] ⁺, 294.1 [M+H] ⁺.

Synthesis of N-Allylamide 15.

15

N-(Cbz)aminooctanoic acid 1 (1500.0 mg, 5.12 mmol), HOBt (691.0 mg, 5.12 mmol), EDC (660 mg, 5,12 mmol), DIPEA (1.1 ml, 6.14 mmol) and allylamine (0.4 ml, 5.12 mmol) were mixed in dry DMF (8.0 ml) at 0 ˚C. The resulting mixture was stirred 15' at 0 ˚C and then overnight at room temperature. The reaction was quenched with NaHCO₃, and then the aqueous phase was separated and extracted with EtOAc. The organic layers were collected, and the solvent was evaporated under reduce pressure. The crude residue was purified with flash chromatography on silica gel, eluting with 50% EtOAc/Hex to give compound **15**. **Yield:** 70%. **¹H-NMR** (400 MHz CDCl₃) δ ppm 7.34-7.24 (m, 5H), 5.81 (m, 1H), 5.53 (s, 1H), 5.18 (s, 2H), 5.13(t, *J* = 4.8Hz, 1H), 5.09(d , *J* = 9.2 Hz, 1H), 4.74(bs, 1H), 3.86 (t, 2H, *J* = 5.6 Hz), 3.16 (q, *J* = 12.8 Hz, 2H), 2.16 (t, *J*=7.6Hz, 2H), 1.61(m, 2H), 1.47 (m, 2H), 1,30(m, 2H). **¹³C-NMR** (CDCl₃) δ ppm 172.8, 156.3,136.5, 134.2, 128.4, 127.9, 127.6, 116.9, 66.4, 41.7, 40.8, 36.4, 29.7, 28.9, 28.7, 26.3,25.4. **LRMS** (ESI) *m/z* = 687.0 [2M+Na] ⁺, 355.0 [M+Na] ⁺, 333.1 [M+H]⁺.

Synthesis of the secondary amine 9.
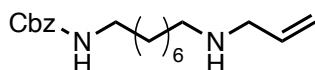
9

A stirred solution of **15** (400.0 mg, 1.20 mmol) in dry CH_2Cl_2 (8.0 mL) under N_2 atmosphere was cooled to 0 ˚C and a solution of DIBAL-H 1N in DCM (3.0 mL, 3.00 mmol) was added dropwise. The mixture was stirred at 0 ˚C for 2 h and then further DIBAL-H (3.0 mL, 3.00 mmol) was added. The mixture was stirred at 0 ˚C for 30 min and then at room temperature for 2 h. The reaction was quenched with EtOAc and by addition of a saturated solution of the Rochelle salt. Organic layers were separated and washed with NaOH 1N and brine. The combined organic phases were dried over Na_2SO_4, filtered and concentrated under reduce pressure. The crude residue was purified with flashchromatography on silica gel, eluting with a 5/4/0,5/0,5 mixture of Hex/EtOAc/MeOH/NH_3 to give compound **9**. **Yield**: 57%.**^{1}H-NMR** (400MHz $CDCl_3$) δ ppm 7.34-7.24 (m, 5H), 5.89 (m, 1H), 5.17 (d, 1H) 5.13 (s, 2H), 3.22 (d, *J* = 6Hz, 2H), 3.16 (q, *J* = 13.2Hz, 2H), 2.58 (t, *J* = 6.8Hz, 2H),1.46 (m, 2H). **^{13}C-NMR** (100 MHz $CDCl_3$) δ ppm 156.3, 141.2, 134.2, 129.0, 128.1, 127.9,116.0, 65.0, 52.1, 49.8, 41.9, 31.0, 29.9, 29.4, 27.0, 26.8. **LRMS** (ESI) *m/z* = 659.0 [2M+Na]+, 341.0 [M+Na]+, 319.0 [M+H]+.

<div align="center">

*Synthesis of compound 16.*

</div>
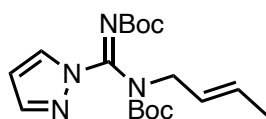
16

To a stirred solution of *N,N'*-diBoc-pyrazologuanidine (1000.0 mg, 3.22 mmol) in dry THF (20.0 mL) under N_2 atmosphere, triphenylphosphine (1270.0 mg, 4.19 mmol) and crotyl alcohol (0.4 mL, 4.19 mmol) were added. The mixture was cooled to 0 °C and DIAD (0.9 mL, 4.84 mmol) was added dropwise. The mixture was stirred at 0°C for 15 min then at room temperature for 2 h. The mixture was diluted with EtOAc and washed with water. The aqueous phase was backextracted with EtOAc. The combined organic phases were washed with brine, dried over Na_2SO_4, filtered, and evaporated under reduce pressure. The crude residue was purified with flash chromatography on silica gel, eluting with 10% EtOAc/Hex to give pure compound **16**. **Yield**: 95%.**^{1}H-NMR** (400 MHz $CDCl_3$) δ ppm 7.89 (s, 1H), 7.66 (s, 1H), 6.37 (s, 1H), 5.60 (m, 2H), 4.18 (m, 2H), 1.62 (s, 3H), 1.44 (s, 9H), 1.22 (s, 9H). **LCMS (ESI)** *m/z* = 387.1 [M+Na]+, 365.1 [M+H]+.

4.3.3   New synthesis of BM1.

<div align="center">

Synthesis of (8-aminooctyl) (triphenylmethyl)amine 17.

</div>
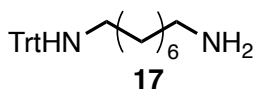
17

To an ice-cold solution of 1,8-Diaminoctane (14.5 g, 100.4 mmol) in DCM (85 mL), trityl chloride (8 g, 28.0 mmol) was added portion wise. The resulting solution was stirred at room temperature for 2 h. Then, the reaction mixture was partitioned between DCM/5% $NaHCO_3$ aq; the organic phase was washed with brine, dried over Na_2SO_4, filtered, and evaporated in vacuo. The crude mixture was purified by chromatography on silica gel (DCM/MeOH 8:2) yielding compound **17** as a yellow oil. **Rf** = 0.30 (DCM/MeOH 9:1). **Yield**: 96% (10.6 g, using trityl chloride as reference). **^{1}H-NMR** (400 MHz $CDCl_3$):

δ ppm 7.47 (d, *J* = 6.8 Hz, 6H), 7.26 (t, *J* = 7.9 Hz, 6H), 7.17 (t, *J* = 7.0 Hz, 3H), 2.74 (t, *J* = 6.6 Hz, 2H), 2.11 (t, *J* = 8.0 Hz, 2H), 1.47 (m, 3H), 1.27 (m, 7H), 0.88 (m, 2H). **^{13}C-NMR** (100 MHz CDCl$_3$): δ ppm 146.4, 128.7, 127.6, 126.2, 70.9, 43.6, 41.7, 30.4, 30.1, 29.3, 27.8, 27.5, 27.3. **LCMS(ESI)** *m/z*: 386.9 [M+H]$^+$.

### *Synthesis of 4-nitro-N-(8-(tritylamino) octyl) benzenesulfonamide 18.*

18
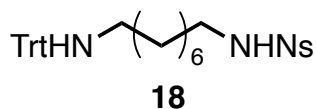
To a solution of (8-aminooctyl) (triphenylmethyl)amine (9.85 g, 25.49 mmol) and DIPEA (11.1 mL, 63.73 mmol) in DCM nosyl chloride (5.65 g, 25.49 mmol) was added portionwise. The reaction mixture was stirred at room temperature for 1 h. The mixture was diluted with DCM and extracted with water. The organic layer was washed with brine, dried over Na$_2$SO$_4$, filtered, and evaporated. The crude mixture was purified by chromatography on silica gel (PE/EtOAc 7:3) yielding compound **18** as a pale-yellow solid. **Rf** = 0.42 (PE/EtOAc 8:2). **Yield**: 95% (13.8 g). **^{1}H-NMR** (400 MHz CDCl$_3$): δ ppm 8.35 (d, *J* = 8.2 Hz, 2H), 8.05 (d, *J* = 8.4 Hz, 2H), 7.47 (d, *J* = 8.4 Hz, 6H), 7.27 (t, *J* = 7.4 Hz, 6H), 7.19 (m, 3H), 4.63 (bs, 1H), 3.00 (q, *J* = 7.2Hz, 2H), 2.13 (m, 2H), 1.58 (m, 2H), 1.45 (m, 3H), 1.21 (m, 7H). **^{13}C-NMR** (100 MHz CDCl$_3$): δ ppm 150.0, 146.2, 128.7, 128.3, 128.2, 127.8, 126.3, 124.4, 48.3, 43.7, 43.4, 29.6, 29.3, 28.9, 27.2, 26.7, 26.4. **LCMS(ESI)** *m/z*: 571.9 [M+H]$^+$.

Synthesis of benzyl (8-hydroxyoctyl) carbamate 19.

19
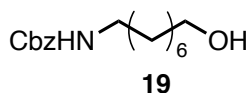
To a solution of **14** (13 g, 44.30 mmol) in dry THF (150.0 mL), Me$_2$SBH$_3$ (12.6 mL, 132.90 mmol) was added dropwise. The reaction mixture was stirred overnight under N$_2$ atmosphere. Once starting material disappeared (monitored by TLC), H2O was added dropwise. Then, K$_2$CO$_3$ was added, and the mixture was stirred for 30'. Subsequently, EtOAc was added, and the organic layer was washed with 1N NaOH and brine, dried over Na$_2$SO$_4$, filtered, and evaporated. The crude mixture was purified by flash chromatography on silica gel (PE/EtOAc 6:4) yielding compound **19** as a white solid. **Rf** = 0.18 (PE/EtOAc 6:4). **Yield**: 93% (12.4 g) **^{1}H-NMR** (400 MHz CDCl$_3$): δ ppm 7.33 (m, 5H), 5.09 (s, 2H), 4.72 (bs, 1H), 3.63 (t, *J* = 6.4 Hz, 2H), 3.18 (q, J 6.4 Hz, 2H), 1.57-1.49 (m, 6H), 1.31 (m, 6H). **^{13}C-NMR** (100 MHz CDCl$_3$): δ ppm 156.8, 136.9, 128.7, 128.2, 128.0, 66.7, 62.9, 41.3, 32.9, 30.1, 29.5, 29.4, 26.9, 25.9. **LCMS (ES)** *m/z*: 279.9 [M+H]$^+$.

### *Synthesis of the tri-protected amine 20.*

20
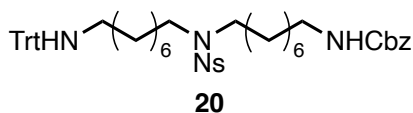
18 (5 g, 8.74 mmol) was dissolved in dry THF (50.0 mL) and treated sequentially with PPh3 (2.12 g, 10.49 mmol), **19** (2.93 g, 10.49 mmol). Afterwards, DIAD (2.7 mL, 10.49 mmol) was added dropwise slowly, and the reaction mixture was stirred for 3 h, under N$_2$, at room temperature. Then, the solvent was removed, and the residue was partitioned between H$_2$O/DCM, washed with brine, dried over Na$_2$SO$_4$, filtered, and evaporated in vacuo. The crude was purified by column chromatography on silica gel (PE/EtOAc 9:1 to 8:2) giving compound **20** as a colourless oil. **Rf** = 0.26 (PE/EtOAc 8:2). **Yield:** 76% (5.54 g). **^{1}H-NMR** (400 MHz CDCl$_3$): δ ppm 8.33 (d, *J* = 8.6 Hz, 2H), 7.96 (d, *J* = 8.0 Hz, 2H), 7.47 (d, *J* = 7.4 Hz, 7H), 7.26 (m, 10H), 7.18 (t, *J* = 7.6 Hz, 3H), 5.09 (s, 2H), 4.72 (bs, 1H), 3.15 (m, 6H), 2.11 (t, *J* = 7.0 Hz, 2H), 1.57 (m, 4H), 1.49 (m, 6H), 1.26 (m, 14H).**^{13}C-NMR** (100 MHz CDCl$_3$): δ ppm 156.2, 150.0,

146.3, 136.2, 129.1, 128.9, 128.7, 128.3, 127.6, 127.5,127.1, 126.9, 67.4, 50.2, 45.3, 40.1, 29.6, 29.4, 29.1, 28.5, 28.3, 27.9, 27.6, 27.4, 26.9, 26.8, 26.6, 26.3. **LCMS (ES)** *m/z*: 833.8 [M+H]$^+$.

Synthesis of the protected guanidine 21.

21
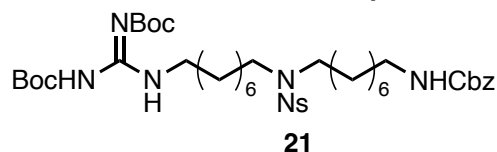
To a solution of **20** (3.5 g, 4.20 mmol) in DCM (38 mL), cooled at 0 °C, Et$_3$SiH (2.02 mL, 12.60 mmol) and TFA (1.9 mL, 5%) were added. The reaction mixture was allowed to reach room temperature and stirred under N$_2$ for 1 h. After that time, the mixture was concentrated in vacuo and co-evaporated several times with DCM until a white solid formed. The crude mixture was dissolved in dry THF (70 mL) and to this solution, dry DIPEA (1.1 mL, 6.30 mmol) was added dropwise at room temperature. Then, *N,N'*-Di-Boc-1H-pyrazole-1-carboxamidine (1.70 g, 5.46 mmol) was added in one pot. The reaction mixture was stirred at room temperature for 16 h, under nitrogen atmosphere. The mixture was partitioned between H$_2$O/EtOAc, the organic layer was washed with brine, dried over Na$_2$SO$_4$ and evaporated to dryness. Purification by silica gel chromatography (PE/EtOAc 8:2) afforded compound **21** as a viscous oil. **Rf** = 0.11 (PE/EtOAc 9:1). **Yield**: 96% over two steps (3.36 g). **^{1}H-NMR** (400 MHz CDCl$_3$): δ ppm 11.50 (s, 1H), 8.35 (d, *J* = 8.2 Hz, 2H), 7.98 (d, *J* = 8.8 Hz, 2H), 7.35 (m, 5H), 5.10 (s, 2H), 4.76 (bs, 1H), 3.41 (q, *J* = 5.8 Hz, 2H), 3.15 (m, 6H), 1.50 (m, 28H), 1.27 (m, 14H). **^{13}C-NMR** (100 MHz CDCl$_3$): δ ppm 166.1, 157.1, 154.1, 150.1, 146.2, 136.4, 129.1, 128.7, 128.3, 127.2, 124.5, 82.1, 48.2, 43.7, 29.7, 29.2, 28.5, 28.4, 27.8, 27.4, 26.9, 26.7, 26.5, 26.3. **LCMS (ESI)** *m/z*: 834.0 [M+H]$^+$.

Synthesis of macrocyclic derivate 22.

22
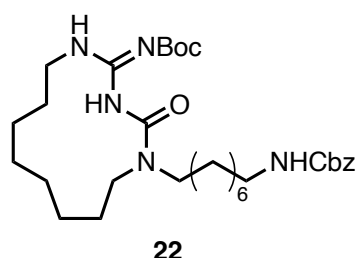
To a stirred solution of **21** (3.30 g, 3.96 mmol) in dry DMF (17 mL), K$_2$CO$_3$ (2.19 g, 15.84 mmol) and Thiophenol (0.8 mL, 7.92 mmol) were added, and the reaction mixture was stirred at room temperature for 7 h. The reaction mixture was partitioned between H$_2$O/EtOAc, the water layer was extracted with EtOAc twice and the organic layers were washed with brine, dried over Na$_2$SO$_4$, filtered, and evaporated in vacuo. The crude mixture was solubilized in dry THF (600 mL) and to this, dry TEA (0.55 mL, 3.96 mmol) was added. The resulting solution was heated at reflux for 16 h, under N$_2$. The solvent was evaporated, and the crude purified by flash chromatography (PE/EtOAc 85:15), affording compound **22** as a colourless oil. **Rf** = 0.56 (PE/EtOAc 8:2). **Yield**: 57% yield over two steps (1.3 g). **^{1}H-NMR** (400 MHz CDCl$_3$): δ ppm 12.10 (s, 1H), 8.10 (bs, 2H), 7.35 (m, 5H), 5.09 (s, 2H), 4.71 (bs, 1H), 3.45 (m, 2H), 3.38 (q, *J* =7.5 Hz, 2H), 3.26-3.15 (m, 4H), 1.65 (m, 6H), 1.54 (m, 6H), 1.46 (m, 12H), 1.27 (m, 12H). **^{13}C-NMR** (100 MHz CDCl3): δ ppm 163.6, 156.0, 153.8, 153.2, 136.4, 127.7, 127.6, 81.6, 66.1, 46.7, 46.0, 40.7, 39.3, 29.5, 29.1, 28.9, 28.1, 27.5, 26.7, 26.3, 25.9, 25.5, 24.9, 23.4 ppm. **LCMS (ESI)** *m/z*: 574.0 [M+H]$^+$, 595.9

Synthesis of the protected guanidine 23.

23
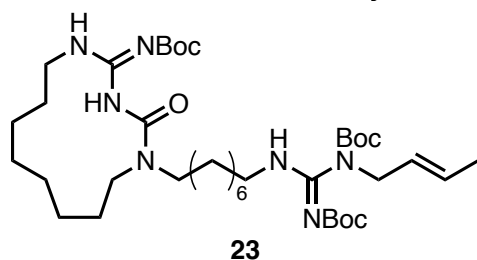
To a solution of **22** (1.30 g, 2.26 mmol) in i-PrOH (125 mL), Pd/C 10 wt.% (96 mg, 0.90 mmol) and 14 drops of 37% HCl were added. The reaction mixture was stirred for 48 h under H_2 atmosphere. Once starting material disappeared (monitored by TLC), the reaction mixture was filtered through a pad of Celite using 85:15 DCM:MeOH as solvent. The filtrate was evaporated in vacuo to dryness and resolubilized in dry THF (38 mL). To this solution, dry TEA (0.47 mL, 3.40 mmol) was added dropwise and then, **16** (1.07 g, 2.94 mmol) was added in one pot. The reaction mixture was stirred at room temperature overnight, under N_2. The reaction mixture was partitioned between H_2O/EtOAc, washed with brine, dried over Na_2SO_4, and evaporated in vacuo. The crude mixture was purified by flash chromatography on silica gel (PE/EtOAc 85:15) affording compound **23** as a sticky colourless oil. **Rf** = 0.63 (PE/EtOAc 8:2). **Yield**: 89% yield over two steps (1.5 g). **¹H-NMR** (400 MHz CDCl₃): δ ppm 12.10 (s, 1H), 8.08 (bs, 1H), 5.65 (dq, *J* = 15.0, 6.2 Hz, 1H), 5.50 (m, 1H), 4.17 (s, 2H), 3.45 (t, *J* = 8.0 Hz, 2H), 3.36 (q, *J* = 7.0 Hz, 2H), 3.24 (m, 4H), 1.66 (m, 7H), 1.56 (m, 6H), 1.49 (s, 11H), 1.46 (s, 19H), 1.31 (m, 13H). **¹³C-NMR** (100 MHz CDCl₃): δ ppm 164.0, 154.1, 153.6, 82.0, 47.1, 46.3, 39.6, 29.4, 29.2, 28.5, 28.2, 28.1, 27.9, 27.1, 26.8, 26.2, 25.9, 25.3, 25.3, 23.7, 23.6, 17.7. **LCMS (ESI)** *m/z*: 736.1 [M+H]⁺.

Synthesis of BM1.

BM1
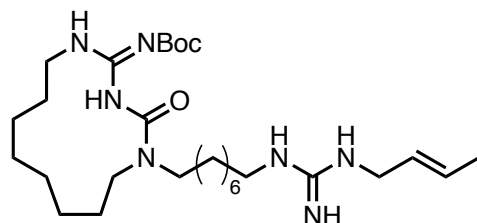
To **23** (1.5 g, 2.04 mmol), 4N HCl in Dioxane (30 mL) was added and the resulting solution was stirred for 23 h at room temperature. Then, the solvent was evaporated in vacuo and co-evaporated several times with DCM until a white solid was obtained. **Yield**: 99% (1.01 g). **MP**: 96-99°C. **¹HNMR** (400 MHz CD₃OD): δ ppm 5.75 (dq, *J* = 15.0, 8.0 Hz, 1H), 5.49 (m, 1H), 3.75 (m, 2H), 3.52 (m, 2H), 3.41-3.34 (m, 4H), 3.18 (t, *J* = 8.0 Hz, 2H), 1.71 (m, 7H), 1.60 (m, 4H), 1.38 (m, 18H). **¹³C-NMR** (100 MHz CD₃OD): δ ppm 156.0, 155.4, 153.4, 128.7, 125.1, 46.9, 46.3, 42.7, 41.3, 41.0, 28.9, 28.8, 28.6, 27.2, 26.3, 26.2, 26.1, 25.7, 23.0, 22.7, 16.6. **LCMS (ESI)** *m/z*: 436.3 [M+H]⁺.

4.3.4   Synthesis of BM56, BM57 and BM58.

Synthesis of (2-iodophenyl) methanol 24.
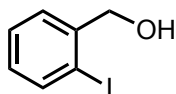
24

To a stirred solution of 2-iodobenzoic acid (3 g, 12.09 mmol) in dry THF (40 mL) under N_2 atmosphere cooled to 0 °C, borane dimethyl sulfide complex (3.44 mL, 36.29 mmol) was added dropwise. The mixture was allowed to gently warm at room temperature and stirred for 12h. Water and K_2CO_3 were carefully added, then the mixture was stirred for 30 min. The mixture was extracted with EtOAc (50 mL) and washed twice with NaOH 1N (30 mL) and with brine (30 mL). The organic phase was dried over Na_2SO_4, filtered, and concentrated under reduced pressure, to give pure 2-iodobenzyl alcohol **24** as a white solid. **Yield:** 98%. **^{1}H-NMR** (400 MHz, CDCl$_3$): δ ppm 7.80 (d, J = 8.0 Hz, 1H), 7.44 (d, J = 7.2 Hz, 1H), 7.35 (t, J = 7.6 Hz, 1H), 6.98 (t, J = 8.0 Hz, 1H), 4.66 (s, 2H). **^{13}C-NMR** (100 MHz, CDCl$_3$): δ ppm 139.0, 136.7, 128.9, 128.3, 126.5, 95.4, 64.5.

Synthesis of 1-(chloromethyl)-2-iodobenzene 25.
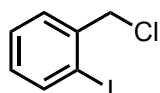
25

To a stirred solution of 2-iodobenzyl alcohol **1a** (2.78 g, 11.88 mmol) in DCM (80 mL) at 0°C, triethylamine (1.66 mL, 11.88 mmol) and 4-dimethylaminopyridine (1.74 g, 14.26 mmol) were added. Then *p*-toluenesulfonyl chloride (4,07 g, 21,38 mmol) was added portionwise, and the solution was stirred for 30 min at 0°C. Then it was left at room temperature and stirred overnight. The solvent was evaporated, and the crude residue was purified with flash chromatography on silica gel, eluting with hexane to give compound **25**. **Yield:** 56%. **^{1}H-NMR** (400 MHz, CDCl$_3$): δ ppm 7.85 (d, J = 7.6 Hz, 1H), 7.47 (d, J = 8 Hz, 1H), 7.34 (t, J = 7.2 Hz, 1H), 6.99 (d, J = 8 Hz, 1H), 4.66 (s, 2H). **^{13}C-NMR** (100 MHz, CDCl$_3$): δ ppm 139.8, 135.6, 129.7, 129.3, 126.7, 96.8, 44.2.

*Synthesis of 4-chloro-2-((2-iodobenzyl) oxy)benzaldehyde 26a.*
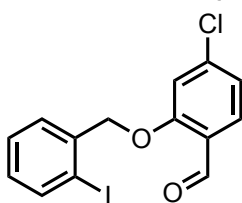
26 a

To a stirred solution of 4-chloro-2-hydrooxybenzaldehyde (475.0 mg, 1.98 mmol) in CH$_3$CN (11 mL), K2CO3 (287.6 mg, 2.07 mmol), NaI (70.5 mg, 0.47 mmol) and 25 (1.30 g, 5,16 mmol) were added. The mixture was stirred at reflux for 12 h. Solvent was then evaporated under reduced pressure and the residue dissolved in EtOAc (5 mL). NaOH 1N (10 mL) was added and the mixture stirred for 10 min at room temperature. Organic phase was then separated, and the aqueous layer was extracted three times with EtOAc . The combined organic phases were washed with brine, dried over Na2SO4, filtered, and concentrated under reduce pressure to give pure compound **26a**. **Yield** 84%. **^{1}H-NMR** (400 MHz, CDCl$_3$): δ ppm 10.46 (s, 1H), 7.88 (d, 1H, J = 7.6 Hz), 7.79 (d, 1H, J = 8.8 Hz), 7.47 (d, 1H, J = 6.4 Hz), 7.39 (t, 1H, J = 7.6 Hz), 7.05 (m, 3H), 5.12 (s, 2H). **^{13}C-NMR** (100 MHz, CDCl$_3$): δ ppm 188.3, 160.9, 142.0,

141.8, 139.6, 139.5, 137.5, 130.1, 129.8, 129.6, 129.0, 123.7, 121.2, 74.6 . **MS (ES)** *m/z* = 426.8 [M+MeOH+Na]$^+$, 394.9 [M+Na]$^+$.

Characterization of 4-fluoro-2-((2-iodobenzyl) oxy)benzaldehyde 26b.
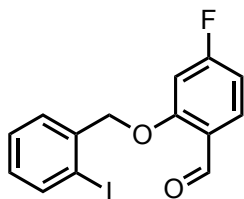
26 b

Yield 91%. **^{1}H-NMR** (400 MHz, CDCl$_3$): δ ppm 10.45 (s, 1H), 7.89 (d, *J* = 4.0 Hz, 1H), 7.87 (d, *J* = 8.0 Hz, 1H), 7.47 (d, *J* = 8.0 Hz, 1H), 7.38 (t, *J* = 7.8 Hz, 1H), 7.06 (t, *J* = 14.0 Hz, 1H), 6.75 (m, 2H), 5.12 (s, 2H), 1.23 (s, 1H). **^{13}C-NMR** (100 MHz, CDCl$_3$): δ ppm 188.0, 168.8, 166.2, 162.3, 139.5, 137.5, 130.8, 128.6, 122.0, 108.7, 101.0, 97.3, 76.9, 74.6. **MS (ES)** *m/z* = 713.0 [2M+H]$^+$, 411.0 [M+MeOH+Na]$^+$, 379.0 [M+Na]$^+$.

Characterization of 5-fluoro-2-((2-iodobenzyl) oxy)benzaldehyde 26c.
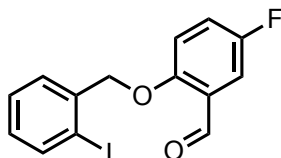

26 c

Yield 86%. **^{1}H-NMR** (400 MHz, CDCl$_3$): δ ppm 10.504 (d, *J* = 3.2 Hz, 1H), 7.88 (d, *J* = 8.0 Hz, 1H), 7.53 (dd, *J* = 4.0 Hz, 1.1 Hz, 1H), 7.46 (d, *J* = 8.0 Hz, 1H), 7.37 (t, *J* = 7.4 Hz, 1H), 7.23 (m, 1H), 7.04 (m, 1H), 5.14 (s, 2H). **^{13}C-NMR** (100 MHz, CDCl$_3$): δ ppm 188.6, 166.8, 166.2, 163.3, 140.6, 137.5, 131.9, 129.1, 121.0, 108.4, 103.0, 96.5, 78.4, 75.4. **MS (ES)** *m/z* = 411.0 [M+MeOH+Na]$^+$, 379.0 [M+Na]$^+$.

### *Synthesis of 4-chloro-2-((2-vinylbenzyl) oxy) benzaldehyde 27a.*
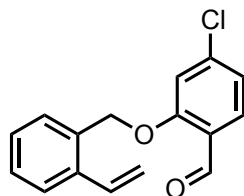
27 a

In a flask with magnetic stirrer, the iodide **26a** (600.0 mg, 1.61 mmol) was dissolved in dry THF (25 mL) under N$_2$ atmosphere. Palladium acetate (36.0 mg, 0.16 mmol) and triphenylphosphine (84.4 mg, 0.32 mmol) were added. Then tributyl(vinyl)tin (557 μL, 1.93 mmol) was added dropwise and the mixture was stirred at reflux for 16 h. After cooling, the mixture was filtered through a plug of Celite and the solvent was evaporated *in vacuo*. The residue was diluted with EtOAc and washed with NaHCO$_3$ss and brine. The organic layers were dried over anhydrous Na$_2$SO$_4$, filtered and the solvent was evaporated *in vacuo*. The residue was purified by flash chromatography (Hex/EtOAc 1:0; Hex/EtOAc 98:2) to give compound **27a**. **Yield** 86%. **^{1}H-NMR** (400 MHz, CDCl$_3$): δ ppm 10.36 (1H, s), 7.78 (d, *J* = 8.3 Hz, 1H), 7.56 (d, *J* = 7.6 Hz, 1H), 7.39 (m, 2H), 7.32 (d, *J* = 7.4 Hz, 1H), 7.09 (s, 1H,), 7.03 (d, *J* = 8.3 Hz, 1H,), 6.94 (dd, *J* = 17.3 Hz 11.0 Hz, 1H,), 5.70 (1H, d, *J* = 17.3 Hz), 5.36 (1H, d, *J* = 11.0 Hz), 5.19 (2H, s). **^{13}C-NMR** (100 MHz, CDCl$_3$): δ ppm 188.4, 161.2, 141.7, 137.3, 133.4, 132.0, 129.5, 129.1, 129.0, 127.9, 126.4, 123.7, 121.6, 117.3, 113.6, 69.2, **MS (ES)** *m/z* = 327.1 [M+MeOH+Na]$^+$, 295.0 [M+Na]$^+$.

Characterization of 4-fluoro-2-((2-vinylbenzyl) oxy)benzaldehyde 27b.
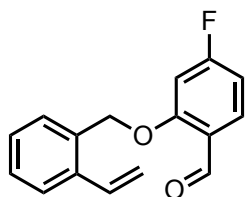
27 b

Yield 98%. **¹H-NMR** (400 MHz, CDCl₃): δ ppm 10.35 (s, 1H), 7.86 (t, *J* = 4.0 Hz, 1H), 7.56 (d, *J* = 7.6, 1H), 7.40 (d, *J* = 7.2 Hz, 1H), 7.36 (d, *J* = 7.6 Hz, 1H), 7.31 (d, *J* = 7.2 Hz, 1H), 7.05 (dd, *J* = 17.2 Hz, 1.7 Hz, 1H) 6.75 (m, 2H), 5.69 (d, *J* = 17.6 Hz, 1H), 5.36 (d, *J* = 10.8 Hz, 1H), 5.19 (s, 2H). **¹³C-NMR** (100 MHz, CDCl₃): δ ppm 189.4, 157.3, 156.6, 154.2, 134.6, 128.1, 127.3, 125.9, 122.4, 122.2, 118.7, 115.6, 114.2, 113.9, 77.9, 70.5. **MS (ES)** *m/z* = 311.1 [M+MeOH+Na]⁺, 279.1 [M+Na]⁺.

Characterization of 5-fluoro-2-((2-vinylbenzyl) oxy)benzaldehyde 27c.
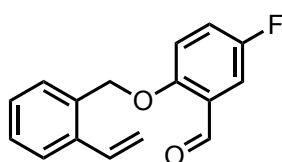
27 c

Yield 91%. **¹H-NMR** (400 MHz, CDCl₃): δ ppm 10.39 (s, 1H), 7.55 (d, *J* = 8 Hz, 1H), 7.50 (dd, *J* = 8.4, 1.3 Hz, 1H), 7.38 (d, *J* = 7.6 Hz, 1H), 7.35 (d, *J* = 7.2 Hz, 1H), 7.25 (m, 1H), 7.04 (dd, *J* = 8.8, 1.4 Hz, 1H), 6.95. (dd, *J* = 17.2, 1.9 Hz, 1H), 5.69 (d, *J* = 17.2 Hz, 1H), 5.35 (d, *J* = 11.2 Hz, 1H), 5.19 (s, 1H). **¹³C-NMR** (100 MHz, CDCl₃): δ ppm 188.6, 158.3, 157.2, 155.9, 133.4, 129.0, 127.9, 126.3, 122.5, 122.2, 117.1, 114.8, 114.8, 114.1, 113.9, 69.6. **MS (ES)** *m/z* = 311.1 [M+MeOH+Na]⁺, 279.1 [M+Na]⁺.

### Synthesis of 4-chloro-2-((2-vinylbenzyl) oxy)benzaldehyde oxime 28a.
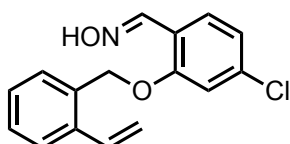
28 a

To a stirred solution of aldehyde **27a** (324 mg, 1,18 mmol) in EtOH (18 mL), pyridine (115 μL, 1.43 mmol) and hydroxylamine hydrochloride (204.9 mg, 2.97 mmol) were added. The mixture was heated at reflux for 3.5 h. After cooling solvent was evaporated. The residue was dissolved in EtOAc, washed with brine, dried over Na₂SO₄, filtered and concentrated under reduce to afford compound **28a**. **Yield** 71%. **¹H-NMR** (400 MHz, CDCl₃): δ ppm 8.43 (s, 1H), 8.01 (br, 1H), 7.66 (d, 1H, *J* = 8.0 Hz), 7.55 (d, 1H, *J* = 7.6 Hz), 7.36 (m, 2H), 7.30 (d, 1H, *J* = 8.0 Hz), 6.99 (d, 1H, *J* = 1.6 Hz), 6.91 (m, 2H), 5.69 (d, *J* = 17.6 Hz, 1H), 5.36 (d, *J* = 10.8 Hz, 1H), 5.10 (s, 2H). **¹³C-NMR** (100 MHz, CDCl₃): δ ppm 157.0, 145.6, 137.3, 136.8, 133.5, 132.4, 129.0, 128.9, 127.9, 127.4, 126.3, 121.5, 119.5, 117.2, 113.1, 69.0 . **MS (ES)** *m/z* = 310.0 [M+Na]⁺, 288.0 [M+H]⁺.

Characterization of 4-fluoro-2-((2-vinylbenzyl) oxy) benzaldehyde oxime 28b.
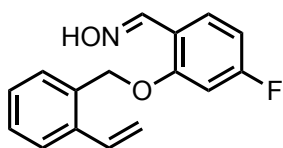
28 b

Yield 91%. **^{1}H-NMR** (400 MHz, CDCl$_3$): δ ppm 8.42 (s, 1H), 7.70 (t, *J* = 8 Hz, 1H), 7.55 (d, *J* = 7.6 Hz, 1H), 7.36 (m, 2H), 7.29 (d, *J* = 7.2 Hz, 1H), 6.92 (q, *J* = 10.8 Hz, 1H), 6.69 (m, 2H), 5.68 (d, *J* = 17.6 Hz, 1H), 5.36 (d, *J* = 10.8 Hz, 1H), 5.09 (s, 2H). **^{13}C-NMR** (100 MHz, CDCl$_3$): δ ppm 203.1, 192.7, 165.9, 163.4, 157.9, 145.6, 137.2, 133.5, 132.4, 128.8, 127.9, 126.3, 117.2, 108.2, 100.5, 68.9. **MS (ES)** *m/z* = 310.1 [M+K]$^+$, 294.1 [M+Na]$^+$, 272.1 [M+H]$^+$.

Characterization of 5-fluoro-2-((2-vinylbenzyl) oxy) benzaldehyde oxime 28c.
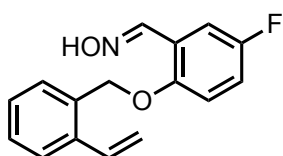
28 c

Yield 98%. **^{1}H-NMR** (400 MHz, CDCl$_3$): δ ppm 8.22 (1H, s), 7.61 (1H, t, *J* = 8.0 Hz), 7.55 (1H, d, *J* = 7.6 Hz), 7.36 (2H, m), 7.33 (1H, d, *J* = 7.2 Hz), 6.84 (q, *J* = 10.8 Hz, 1H), 6.69 (2H, m), 5.51 (1H, d, *J* = 17.6 Hz), 5.43 (1H, d, *J* = 10.8 Hz), 5.23 (2H, s). **^{13}C-NMR** (100 MHz, CDCl$_3$): δ ppm 203.1, 192.7, 165.9, 163.4, 157.8, 145.6, 137.2, 133.5, 132.4, 129.0, 127.9, 126.3, 117.2, 108.2, 101.5, 68.5. **MS (ES)** *m/z* = 294.1 [M+Na]$^+$, 272.1 [M+H]$^+$.

*Synthesis of (4-chloro-2-((2-vinylbenzyl) oxy) phenyl)methanamine 29a.*
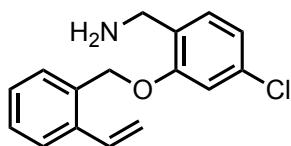
29 a

To a stirred solution of oxime **28a** (400.0 mg, 1.40 mmol) in THF (20 ml), Zn (910.0 mg, 14 mmol) was added. HCl 2N (7.0 ml) was added and the mixture was stirred at reflux for 2 h. The reaction mixture was cooled to room temperature, filtered on a Celite pad to remove the excess of metallic zinc and the filtrate was concentrate under reduced pressure. The residue was dissolved in EtOAc and extracted with HCl 3N for three times. The aqueous phase was basified with solid potassium carbonate and extracted with DCM (3x20mL). The combined organic phases were dried over Na$_2$SO$_4$ and filtered. Solvent was evaporated under reduce pressure to give the primary amine **29a** which was used in the next step without any further purification. **Yield** 81%. **^{1}H-NMR** (400 MHz, CD$_3$OD): δ ppm 7.58 (d, *J* = 7.7 Hz, 1H), 7.40 (d, *J* = 7.4 Hz, 1H), 7.30 (t, *J* = 7.6 Hz, 1H), 7.27 (d, *J* = 7.6 Hz, 1H), 7.18 (d, *J* = 8.0 Hz, 1H), 7.09 (d, *J* = 1.7 Hz, 1H), 7.00 (dd, *J* = 17.4 Hz, 11.0 Hz, 1H), 6.91 (dd, *J* = 8.0 Hz, 1.8 Hz, 1H), 5.72 (d, *J* = 17.4 Hz, 1H), 5.31 (d, *J* = 12.0 Hz, 1H), 5.12 (2H, s), 3.66 (2H, s). **^{13}C-NMR** (100 MHz, CDCl$_3$): δ ppm 158.8, 139.1, 136.6, 133.7, 129.4, 129.2, 128.5, 127.5, 125.6, 120.3, 115.4, 112.0, 68.3, 40.5. **MS (ES)** *m/z* = 296.0 [M+Na]$^+$, 274.1 [M+H]$^+$.

Characterization of (4-fluoro-2-((2-vinylbenzyl) oxy)phenyl)methanamine 29b.
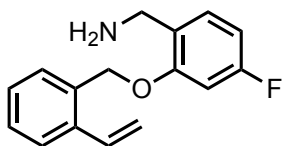

29 b

Yield 98%. **^{1}H-NMR** (400 MHz, CD$_3$OD): δ ppm 7.58 (dd, *J* = 7.7 Hz, 1.3 Hz, 1H), 7.40 (dd, *J* = 7.4 Hz, 1.5 Hz, 1H), 7.33 (d, *J* = 7.6 Hz, 1H), 7.26 (m, 1H), 7.18 (d, *J* = 8.0 Hz, 1H), 7.09 (d, *J* = 1.9 Hz, 1H), 7.00 (dd, *J* = 17.4, 11.0 Hz, 1H), 6.91 (dd, *J* = 8.0, 2.0 Hz, 1H), 5.71 (dd, *J* = 17.4, 1.3 Hz, 1H), 5.31 (dd, *J* = 11.0, 1.3 Hz, 1H), 5.12 (s, 2H), 4.80 (s, 1H), 3.67 (s, 2H). **^{13}C-NMR** (100 MHz, CD$_3$OD): δ ppm 157.4, 138.6, 137.2, 133.7, 129.4, 129.1, 128.5, 127.5, 125.5, 120.3, 115.3, 112.0, 68.2, 40.4. **MS (ES)** *m/z* = 258.1 [M+H]$^+$.

*Characterization of (5-fluoro-2-((2-vinylbenzyl) oxy)phenyl)methanamine 29c.*
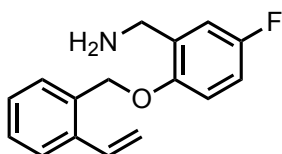
29 c

Yield 89%. **^{1}H-NMR** (400 MHz, CD$_3$OD): δ ppm 7.61 (d, *J* = 7.7 Hz, 1H), 7.41 (dd, *J* = 7.6 Hz, 1.5 Hz, 1H), 7.35 (d, *J* = 7.4 Hz, 1H), 7.26 (m, 1H), 7.15 (d, *J* = 8.2 Hz, 1H), 7.04 (d, *J* = 1.9 Hz, 1H), 7.01 (dd, *J* = 17.4, 11.5 Hz, 1H), 6.89 (dd, *J* = 8.5, 2.4 Hz, 1H), 5.71 (dd, *J* = 17.4, 11.3 Hz, 1H), 5.28 (dd, *J* = 10.8, 1.3 Hz, 1H), 5.12 (s, 2H), 4.84 (s, 1H), 3.67 (s, 2H). **^{13}C-NMR** (100 MH CD$_3$OD): δ ppm 157.4, 138.6, 137.4, 133.9, 129.8, 129.3, 128.6, 127.9, 125.7, 120.6, 115.8, 112.3, 68.6, 40.7. **MS (ES)** *m/z* = 258.1 [M+H]$^+$.

Synthesis of the protected guanidine 30a.
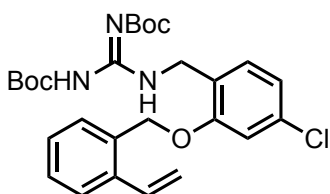
30 a

To a stirred solution of primary amine **29a** (200.0 mg, 0.73 mmol) in THF 8.5 mL), N,N'-Di-Boc-1H-pyrazole-1-carboxamidine (294.0 mg, 0.95 mmol) and DIPEA (0,09 mL, 0.52 mmol) were added. The mixture was stirred at room temperature for 12 h. After cooling EtOAc was added and the organic phase was washed with water and brine. After drying over Na$_2$SO$_4$ the mixture was filtered and concentrated under reduce pressure. The crude residue was purified with flash chromatography on silica gel, eluting with 10% EtOAc/Hex to give pure compound **30a**. **Yield:** 75%. **^{1}H-NMR** (400 MHz, CDCl$_3$): δ ppm 11.45 (s, 1H), 8.64 (s, 1H), 7.52 (d, *J* = 7.5 Hz, 1H), 7.41 (d, *J* = 7.2 Hz, 1H), 7.32 (t, *J* = 7.1 Hz, 1H), 7.26 (m, 2H), 6.96 (d, *J* = 11.1 Hz, 1H), 6.96 (m, 1H), 6.91 (d, *J* = 1.8 Hz, 1H), 5.66 (d, *J* = 17.3 Hz, 1H), 5.34 (d, *J* = 11.0 Hz, 1H), 5.10 (s, 2H), 4.59 (d, *J* = 5.4 Hz, 2H), 1.48 (s, 9H), 1.44 (s, 9H). **^{13}C-NMR** (100 MHz, CDCl$_3$): δ ppm 157.1, 155.9, 152.9, 137.0, 134.2, 133.6, 132.7, 130.5, 128.9, 128.6, 127.8, 126.1, 124.6, 120.8, 117.0, 112.3, 82.9, 79.2, 68.4, 40.0, 28.2, 28.0. **MS (ES)** *m/z* = 538.2 [M + Na]$^+$, 516.2 [M + H]$^+$.

Characterization of the protected guanidine 30b.
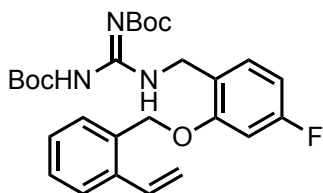
30 b

Yield: 70%. **¹H-NMR** (400 MHz, CDCl₃): δ ppm 11.45 (s, 1H), 8.64 (s, 1H), 7.41 (d, *J* = 7.7 Hz, 1H), 7.38 (d, *J* = 7.5 Hz, 1H), 7.32 (t, *J* = 8.0 Hz, 1H), 7.26 (m, *J* = 2H), 6.64 (m, 1H), 5.66 (dd, *J* = 17.4 Hz, 1.3 Hz, 1H), 5.34 (dd, *J* = 11.0 Hz, 1.3 Hz, 1H), 5.10 (s, 2H), 4.59 (d, *J* = 5.5 Hz, 2H), 1.48 (s, 9H). **¹³C-NMR** (100 MHz, CDCl₃): δ ppm 157.1, 155.9, 152.9, 137.0, 134.2, 133.6, 132.7, 130.5, 128.9, 128.5, 127.8, 126.1, 124.5, 120.8, 117.0, 112.3, 82.9, 68.4, 39.9, 28.2, 27.9. **MS (ES)** *m/z* = 522.3 [M+Na]⁺, 500.3 [M+H]⁺.

Characterization of the protected guanidine 30c.
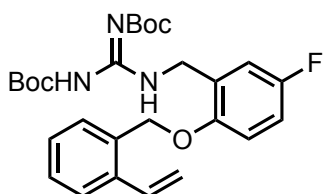
30 c

Yield: 62%. **¹H-NMR** (400 MHz, CDCl₃): δ ppm 11.45 (s, 1H), 8.60 (s, 1H), 7.41 (d, *J* = 7.5 Hz, 1H), 7.32 (d, *J* = 7.5 Hz, 1H), 7.29 (t, *J* = 8.0 Hz, 1H), 7.25 (m, 2H), 6.94 (dd, *J* = 7.4, 1.2 Hz 1H), 6.64 (m, 2H), 5.66 (d, *J* = 17.4 Hz, 1H), 5.34 (d, *J* = 11.0 Hz, 1H), 5.10 (s, 2H), 4.57 (d, *J* = 5.5 Hz, 2H), 1.44 (s, 9H). **¹³C-NMR** (100 MHz, CDCl₃): δ ppm 203.1, 165.9, 162.9, 147.0, 134.2, 133.6, 132.7, 130.5, 129.9, 128.5, 127.8, 126.1, 122.5, 121.8, 117.0, 113.3, 85.9, 69.4, 39.9, 30.2, 28.9. **MS (ES)** *m/z* = 522.3 [M+Na]⁺, 500.3 [M+H]⁺.

Synthesis of the amidinourea 31a.
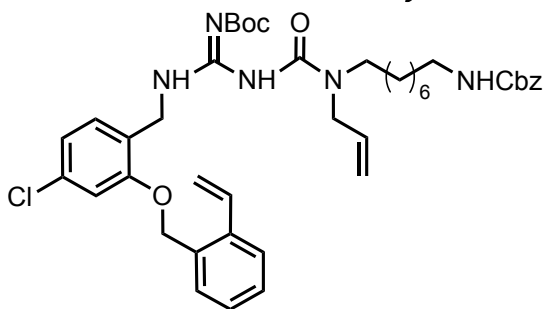
31 a

To a stirred solution of protected guanidine **7a** (256.0 mg, 0.50 mmol) in dry THF (10.0 mL), a solution of linker (206.7 mg, 0.65 mmol) in dry THF (6.0 mL) and triethylamine (0.07 mL, 0.51 mmol) were added dropwise under N₂ atmosphere. The mixture was heated at reflux and stirred for 12 h. After cooling EtOAc was added and the organic phase was washed with water and brine. After drying over Na₂SO₄ the mixture was filtered and concentrated under reduce pressure. The crude residue was purified with flash chromatography on silica gel, eluting with 20% EtOAc/Hex to give pure compound. **Yield** 52%. **¹H-NMR** (400 MHz, CDCl₃): δ ppm 12.29 (d, *J* = 13.0 Hz, 1H), 8.40 (s, 1H), 7.53 (d, *J* = 7.6 Hz, 1H), 7.42 (d, *J* = 7.4 Hz, 1H), 7.33 (m, 5H), 7.29 (m, 2H), 7.17 (dd, *J* = 7.5, 4.0 Hz, 1H), 6.96 (d, *J* = 11.0 Hz, 1H), 6.91 (m, 2H), 5.78 (m, 1H), 5.67 (d, *J* = 17.3 Hz, 1H), 5.34 (d, *J* = 11.0 Hz, 1H), 5.09 (s, 2H), 5.07

(s, 2H), 5.00 (m, 1H), 4.73 (br, 1H), 4.50 (d, *J* = 5.5 Hz, 1H), 4.47 (d, *J* = 5.5 Hz, 1H), 4.02 (d, *J* = 4.7 Hz, 1H), 3.89 (d, *J* = 4.3 Hz, 1H), 3.32 (t, *J* = 7.2 Hz, 1H), 3.20 (t, *J* = 7.2 Hz, 1H), 3.14 (m, 2H), 1.49 (m, 4H), 1.42 (s, 9H), 1.22 (m, 8H). **^{13}C-NMR** (100 MHz, CDCl$_3$): δ ppm 163.6, 156.8, 153.9, 153.3, 137.0, 134.6, 133.6, 132.9, 130.0, 129.4, 128.8, 128.6, 128.4, 128.1, 128.0, 127.8, 126.1, 125.5, 120.7, 116.9, 115.5, 115.4, 112.2, 82.1, 68.4, 66.5, 60.3, 48.4, 41.0, 39.4, 29.3, 29.2, 29.4, 28.0, 26.9, 26.6, 23.8. **MS (ES)** *m/z* = 782.3 [M + Na]$^+$, 760.3 [M + H]$^+$.

*Characterization of the amidinourea 31b.*
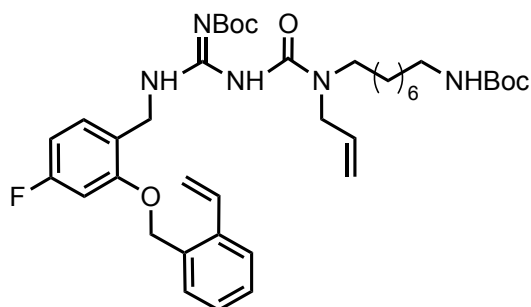
31b

Yield 59%. **^{1}H-NMR** (400 MHz, CDCl$_3$): δ ppm 12.30 (d, *J* = 7.4 Hz, 1H), 8.40 (s, 1H), 7.52 (d, *J* = 8.0 Hz, 1H), 7.41 (d, *J* = 5.4 Hz, 1H), 7.34 (d, *J* = 7.1 Hz, 1H), 7.27 (t, *J* = 10.5 Hz, 1H), 6.93 (m, 4H), 5.66 (d, *J* = 12.2 Hz, 1H), 5.33 (d, *J* = 8.0 Hz, 1H), 5.90 (s, 2H), 5.01 (m, 2H), 4.51 (dd, *J* = 17.4 Hz, 3.2 Hz, 2H), 4.00 (dd, *J* = 13.4 Hz, 1.8 Hz, 2H), 3.2 (dd, *J* = 17.4 Hz, 2.2 Hz, 2H), 3.06 (s, 2 H), 1.50 (s, 9H), 1.48 (s, 9H), 1.36 (m, 8H). **^{13}C-NMR** (100 MHz, CDCl$_3$): δ ppm 164.0, 161.6, 153.8, 153.3, 137.0, 135.2, 134.6, 133.6, 132.9, 130.1, 128.7, 128.5, 127.8, 126.1, 122.5, 120.3, 116.9, 115.4, 106.8, 100.1, 99.8, 82.0, 68.4, 50.4, 48.4, 47.5, 45.7, 40.8, 40.5, 39.4, 30.0, 29.1, 28.4, 28.0, 27.0, 26.7, 23.8 **MS (ES)** *m/z* = 722.4 [M + Na]$^+$, 710.4 [M + H]$^+$.

Characterization of the amidinourea 31c.
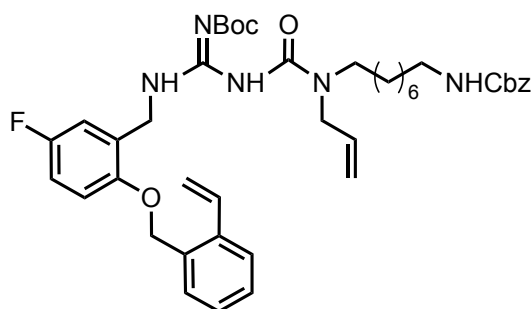
31 c

Yield 75%. **^{1}H-NMR** (400 MHz, CDCl$_3$): δ ppm 12.28 (s, 1Hz), 8.41 (s, 1H), 7.52 (d, *J* = 7.5 Hz, 1H), 7.44 (d, *J* = 7.4 Hz, 1H), 7.35 (m, 5H), 7.32 (d, *J* = 6.9 Hz, 1H), 7.29 (d, *J* = 7.3 Hz, 2H), 7.24 (m, 1H), 7.24 (m, 1H), 6.94 (d, *J* = 9.7 Hz, 2H), 5.76 (m, 1H), 5.66 (d, *J* = 16.4 Hz, 1H), 5.32 (d, *J* = 10.8 Hz, 2H), 5.15 (s, 2H), 5.09 (m, 3H), 5.01 (d, *J* = 9.9 Hz, 1H), 4.55 (dd, *J* = 14.8, 6.0 Hz, 2H), 4.05 (d, *J* = 5.3 Hz, 1H), 3.89 (d, *J* = 5.3 Hz, 1H), 3.36 (t, *J* = 7.6 Hz, 1H), 3.21 (t, *J* = 8.0 Hz, 1H), 3.16-3.11 (m, 2H), 1.51 (m, 4H), 1.42 (s, 9H), 1.21 (m, 8H). **^{13}C-NMR** (100 MHz, CDCl$_3$): δ ppm 163.7, 156.5, 154.1, 153.9, 153.3, 135.3, 134.7, 133.7, 129.3, 129.0, 128.7, 128.6, 128.4, 128.3, 128.0, 127.8, 126.8, 126.0, 120.7, 116.6, 115.5, 111.5, 81.9, 68.1, 66.5, 50.5, 48.4, 47.5, 45.7, 41.0, 40.0, 29.9, 29.4, 29.2, 28.5, 28.0, 27.0, 26.9, 26.6. **MS (ES)** *m/z* = 744.4 [M + H]$^+$.

Synthesis of the macrocycle 32a.
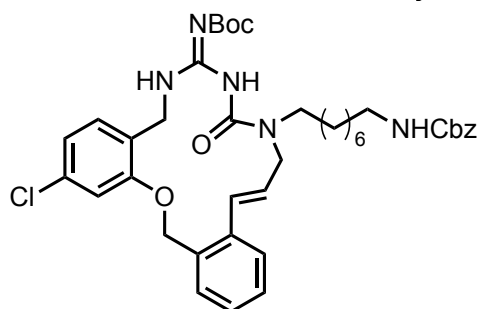
32 a

To a stirred solution of amidinourea derivative **31a** (200.0 mg, 0,27 mmol) in degassed Toluene (145 mL, 2 mM solution), a solution of 2nd generation Grubb's catalyst (45.0 mg, 0.05 mmol) in degassed Toluene (2.0 mL) was added dropwise under N_2 atmosphere. The mixture was heated at reflux and stirred overnight. After cooling solvent was evaporated under reduced pressure. The crude residue was purified with flash chromatography on silica gel, eluting with 15% EtOAc/Hex to give the macrocycle compound as mixture of E/Z isomers. **Yield** 78%. **^{1}H-NMR** (400 MHz, CDCl$_3$): δ ppm 12.27 (s, 1H), 8.39 (s, 1H), 7.56 (d, J = 7.7 Hz, 1H), 7.34 (m, 5H), 7.23 (d, J = 7.5 Hz, 2H), 7.15 (d, J = 7.4 Hz, 1H), 7.10 (d, J = 8.1 Hz, 1H), 6.96 (s, 1H), 6.91 (d, J = 8.1 Hz, 1H), 6.49 (d, J = 15.6 Hz, 1H), 6.15 (dt, J = 15.6, 5.6 Hz, 1H), 5.13 (s, 2H), 5.08 (s, 2H), 4.76 (br, 1H), 4.52 (d, J = 6.2 Hz, 2H), 3.92 (m, 2H), 3.35 (t, J = 8.0 Hz, 2H), 3.16 (q, J = 6.3 Hz, 2H), 1.54 (m, 2H), 1.46 (s, 9H), 1.25 (m, 10H). **^{13}C-NMR** (100 MHz, CDCl$_3$): δ ppm 156.1, 154.1, 137.0, 133.0, 130.4, 129.1, 129.0, 128.4, 128.2, 128.1, 128.0, 127.0, 126.7, 125.6, 125.2, 120.8, 113.0, 70.7, 66.5, 60.3, 51.9, 48.1, 41.0, 29.9, 29.6, 29.3, 29.2, 28.6, 28.0, 26.9, 26.6, 23.8. **MS (ES)** *m/z* = 754.4 [M + Na]+, 732.3 [M + H]$^+$.

Characterization of the macrocycle 32b.
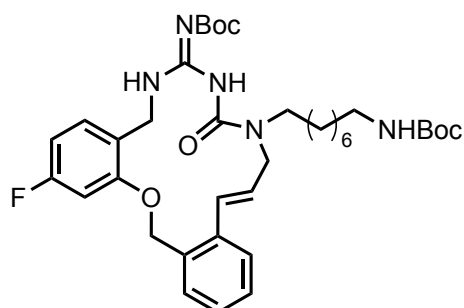
32 b

Yield 28%. **^{1}H-NMR** (400 MHz, CDCl$_3$): δ ppm 12.25 (s, 1H), 8.33 (s, 1H), 7.53 (d, J = 7.8 Hz, 1H), 7.32 (m, 2H), 7.28 (t, J = 8 Hz, 1H), 7.19 (t, J = 10.3 Hz, 1H), 6.69 (d, J = 8.3 Hz, 1H), 6.59 (m, 2H), 6.12 (dd, J = 17.2, 3.1 Hz, 1H), 5.10 (s, 2H), 4.51 (d, J = 10.4 Hz, 2H), 3.93 (d, J = 7.3 Hz, 2H), 3.33 (t, J = 7.6 Hz, 2H), 3.05 (s, 2H), 1.43 (s, 9H), 1.40 (s, 9H), 1.22 (s, 8H). **^{13}C-NMR** (100 MHz, CDCl$_3$): δ ppm 225.3, 183.9, 171.2, 164.1, 163.2, 154.1, 153.6, 137.2, 130.5, 129.1, 128.9, 127.1, 127.0, 126,9, 126.8, 125.7, 123.4, 107.1, 101.1, 100.9, 82.4, 70.6, 60.4, 51.8, 48.1, 39.1, 30.0, 29.4, 29.2, 29.2, 28.7, 28.1, 27.3, 26.7, 23.9, 21.0, 20.8 . **MS (ES)** *m/z* = 704.4 [M + Na]+, 682.4 [M + H]$^+$.

Characterization of the macrocycle 32c.
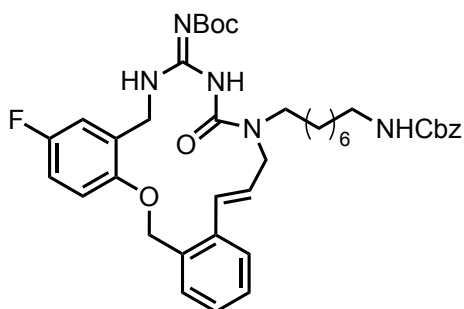
32 c

Yield 26%. **^{1}H-NMR** (400 MHz, CDCl$_3$): δ ppm 12.27 (s, 1H), 8.40 (s, 1H), 7.58 (d, *J* = 8.0 Hz, 1H), 7.34 (m, 5H), 7.30 (d, *J* = 7.1 Hz, 2H), 7.23 (m, 3H), 6.98 (d, *J* = 7.6 Hz, 1H), 6.93 (t, *J* = 7.6 Hz, 1H), 6.58 (d, *J* = 15.6 Hz, 1H), 6.16 (dt, *J* = 15.6 Hz, 5.2 Hz, 1H), 5.15 (s, 2H), 5.08 (s, 2H), 4.69 (s, 1H), 4.61 (d, *J* = 6.4 Hz, 1H), 3.92 (d, *J* = 5.2 Hz, 2H), 3.35 (t, *J* = 7.6 Hz, 2H), 3.16 (q, *J* = 6.4 Hz, 2H), 1.57 (s, 4H), 1.46 (m, 9H), 1.23 (s, 6H). **^{13}C-NMR** (100 MHz, CDCl$_3$): δ ppm 163.7, 155.3, 154.2, 153.6, 138.1, 137.8, 136.9, 129.6, 129.4, 129.1, 128.8, 128.7, 128.3, 126.5, 122.9, 118.6, 99.9, 82.2, 72.2, 66.5, 45.1, 44.1, 43.4, 40.9, 31.1, 29.3, 29.2, 28.5, 27.3. **MS (ES)** *m/z* = 738.4 [M + Na]+, 716.4 [M + H]$^+$.

Synthesis of compound 34b.
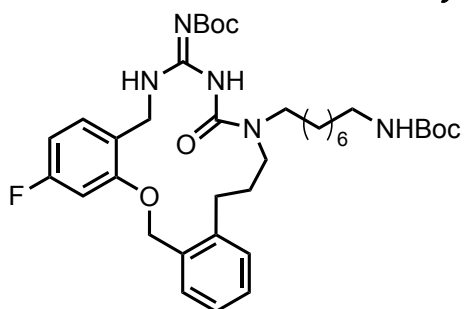
34b

In a flask with magnetic stirrer, macrocycle compound **32b** (53.0 mg, 0.07 mmol) was dissolved in isopropanol (8.5 mL) and 10% Palladium on Carbon (4.1 mg, 0.003 mmol). The flask was subjected to three cycles of vacuum followed by flush of H$_2$ before being stirred under H$_2$ atmosphere for 4h. The mixture was filtered through a plug of Celite, and then solvent was evaporated *in vacuo*. The crude product obtained was used directly in the next step without any further purification. **Yield:** quantitative. **^{1}H-NMR** (400 MHz, CDCl$_3$): δ ppm 12.20 (1H, s), 8.49 (1H, s), 7.30 (1H, d, *J* = 7.2 Hz), 7.25 (1H, d, *J* = 6.8 Hz), 7.20 (1H, d, *J* = 6.8 Hz), 7.11 (1H, d, *J* = 7.6 Hz), 6.80 (1H, s), 6.74 (1H, d, *J* = 7.6 Hz), 5.02 (2H, s), 4.51 (2H, d, *J* = 6 Hz), 3.21 (2H, t, *J* = 6.8 Hz), 3.14 (2H, t, *J* = 8.0 Hz), 3.07 (2H, m), 2.53 (2H, t, *J* = 7.6 Hz), 1.99 (2H, m), 1.57 (4H, m), 1.46 (9H, s), 1.42 (9H, s), 1.26 (8H, m). **^{13}C-NMR** (100 MHz, CDCl$_3$): δ ppm 201.4, 167.3, 165,3, 161.0, 153.6, 134.1, 130.7, 129.9, 128.9, 126.4, 125.8, 121.2, 111.7, 82.1, 78.9, 69.4, 68.5, 53.3, 49.8, 47.3, 40.63, 39.87, 37.9, 30.8, 30.3, 30.0, 29.6, 29.4, 29.2, 28.7, 28.4, 28.1, 27.0, 26.7, 25.3, 21.4.

Synthesis of the protected guanidine 36a.
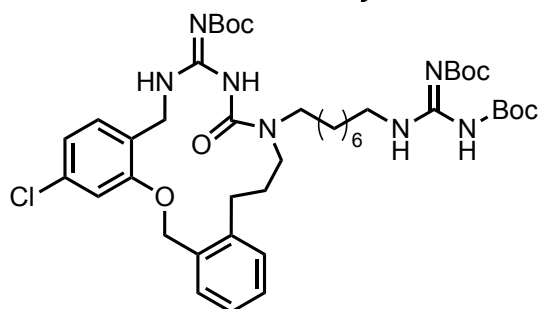
36a

In a flask with magnetic stirrer, protected macrocycle **32a** (43 mg, 0.06 mmol) was dissolved in isopropanol (7.0 mL). Then 10% Palladium on Carbon (12.5 mg, 0.01 mmol) and two drops of Acetic acid were added. The flask was subjected to three cycles of vacuum followed by flush of H_2 before being stirred under H_2 atmosphere for 8h. The mixture was filtered through a plug of Celite, and then solvent was evaporated *in vacuo*. The crude containing compound **33a** was directly used in the next step.
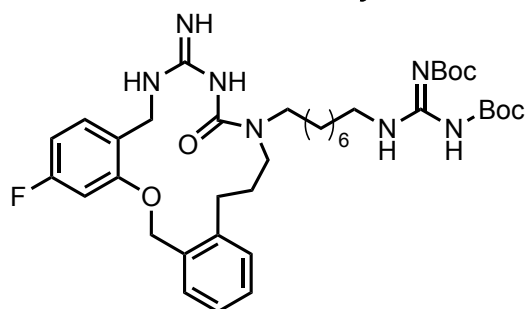
In a flask with magnetic stirrer, the crude amine **33a** (43.0mg, 0.07 mmol) was dissolved in THF (6.0 mL). Then, *N,N'*-Di-Boc-1*H*-pyrazole-1-carboxamidin*e* (30 mg, 0.09 mmol) and DIPEA (37 µL, 0.22 mmol) were added and the mixture was stirred at room temperature for 16 h. The reaction was diluted with EtOAc and washed with H_2O. The organic phase was dried over anhydrous Na_2SO_4, filtered and the solvent was evaporated *in vacuo*. The residue was purified by flash chromatography (Hex/EtOAc 1:0; Hex/EtOAc 8:2). **Yield (over two steps):** 31%. **^{1}H-NMR** (400 MHz, CDCl$_3$): δ ppm 12.13 (s, 1H), 11.45 (s, 1H), 8.50 (s, 1H), 8.39 (s, 1H), 7.33 (m, 2H), 7.25 (m, 1H), 7.21 (d, *J* = 7.1 Hz, 1H), 7.13 (d, *J* = 8.0 Hz, 1H), 6.96 (s, 1H), 6.89 (d, *J* = 7.6 Hz, 1H), 5.01 (s, 2H), 4.46 (d, *J* = 6.0 Hz, 2H), 3.40 (m, 2H), 3.19 (t, *J* = 7.6 Hz, 2H), 3.10 (t, *J* = 8.0 Hz, 2H), 2.46 (m, 2H), 1.94 (m, 2H), 1.51 (m, 4H), 1.46 (m, 27H), 1.17 (s, 8H). **^{13}C-NMR** (100 MHz, CDCl$_3$): δ ppm 163.3, 153.6, 142.7, 133.2, 132.6, 130.7, 130.0, 129.2, 125.9, 120.5, 111.3, 69.7, 49.8, 47.4, 40.8, 37.9, 33.8, 30.8, 30.2, 29.3, 29.2, 28.9, 28.4, 28.2, 28.0, 27.9, 27.0, 26.7. **MS (ES)** *m/z* = 864.4 [M+Na]$^+$.

Characterization of the protected guanidine 36c.
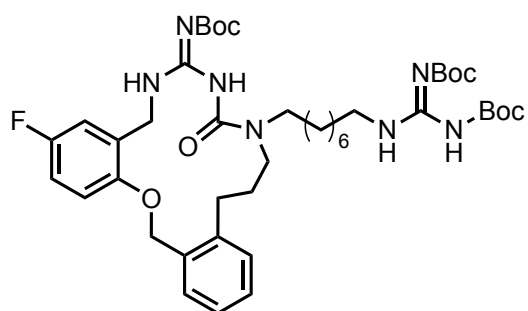
36c

Yield (over two steps): 21%. **^{1}H-NMR** (400 MHz, CDCl$_3$): δ ppm 12.18 (s, 1H), 8.50 (s, 1H), 8.27 (s, 1H), 7.30 (d, *J* = 7.4 Hz, 1H), 7.25 (d, *J* = 7.5 Hz, 1H), 7.21 (d, *J* = 7.1 Hz, 1H), 7.11 (m, 1H), 6.96 (d, *J* = 7.05 Hz, 1H), 6.86 (m, 2H), 5.02 (s, 2H), 4.50 (d, *J* = 8.2 Hz, 2H), 3.37 (d, *J* = 8.6 Hz, 2H), 3.21 (t, *J* = 10.4 Hz, 2H), 3.11 (t, *J* = 10.9 Hz, 2H), 2.49 (t, *J* = 9.8 Hz, 2H), 1.95(m, 2H), 1.49 (m, 4H), 1.29 (s, 9H), 1.23 (s, 9H), 1.21 (s, 9H), 1.19 (s, 8H). **^{13}C-NMR** (100 MHz, CDCl$_3$): δ ppm 167.1, 161.3, 158.8, 154.1, 154.0, 147.5, 144.4, 141.2, 136.8, 129.3, 128.4, 128.3, 128.2, 127.1, 126.2, 116.6, 116.4, 115.5, 114.9, 114.8, 80.4,

68.7, 44.9, 44.4, 41.1, 40.4, 31.7, 29.0, 28.9, 28.4, 28.3, 28.2, 27.5, 27.4, 26.8, 26.6. **MS (ES)** *m/z* = 848.5 [M+Na]$^+$.

Synthesis of the protected guanidine 36b.

36b

In a flask with magnetic stirrer, protected macrocycle **34b** (50 mg, 0.07 mmol) was dissolved in dry CH$_2$Cl$_2$ (1.8 mL) under N$_2$ atmosphere. Then freshly distilled TFA (10% v/v, 200 µL) was added dropwise, and the mixture was stirred at room temperature for 7h. The reaction mixture was concentrated *in vacuo*. The residue was decanted several times with Et$_2$O and Hexane. The crude containing compound **35b** was directly used in the next step, which followed the same procedure that gave compound **36a.Yield (over two steps):** 47%. **^{1}H-NMR** (400 MHz, CDCl$_3$): δ ppm 11.46 (s, 1H), 8.27 (s, 1H), 7.32 (m, 2H), 7.25 (d, *J* = 7.5 Hz, 1H), 7.18 (t, *J* = 10.6 Hz, 1H), 7.10 (t, *J* = 13.4 Hz, 1H), 6.68 (d, *J* = 7.8 Hz, 1H), 6.53 (t, *J* = 10.4 Hz, 1H), 5.03 (s, 2H), 4.37 (s, 2H), 3.35 (m, 2H), 3.21 (t, *J* = 14.5 Hz, 2H), 3.15 (s, 2H), 2.51 (t, *J* = 17.6 Hz, 2H), 1.86 (s, 2H), 1.55 (m, 4H), 1.48 (s, 9H), 1.47 (s, 9H), 1.23 (m, 8H). **^{13}C-NMR** (100 MHz, CDCl$_3$): δ ppm 164.2, 163.1, 162.2, 158.8, 154.0, 147.5, 141.2, 136.8, 130.9, 130.8, 129.3, 128.4, 127.1, 126.2, 124.9, 108.1, 102.2, 79.8, 68.7, 44.9, 44.4, 41.5, 41.1, 31.9, 29.0, 29.0, 28.2, 28.1, 27.5, 27.4, 26.6. **MS (ES)** *m/z* = 748.4 [M+Na]$^+$.

Synthesis of protected amidinoureas 37a.
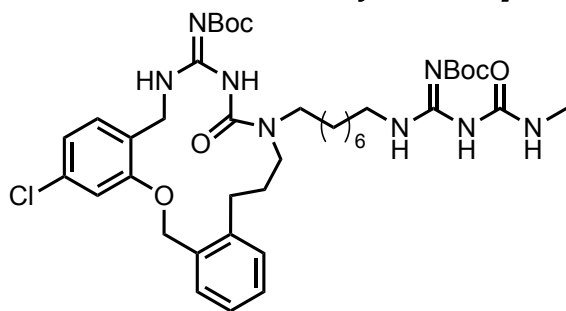
37a

To a solution of di-Boc-protected guanidine **37a** (46.0 mg, 0.06 mmol) in THF (2.8 mL) in a glass tube, DIPEA (0.010 mL, 0.06 mmol) and a 40% solution of methylamine in H$_2$O (0.41 mL, 0.83 mmol) were added. The tube was sealed and warmed to 80 °C overnight. Then the solvent was evaporated, and the crude was purified with flash chromatography on silica gel, eluting with 20% EtOAc in Hexane to give pure compound. **Yield** 68%. **^{1}H-NMR** (400 MHz, CDCl$_3$): δ ppm 12.18 (s, 1H), 8.50 (t, 1H, *J* = 6.4 Hz), 7.35 (d, *J* = 7.4 Hz, 1H), 7.32 (m, 1H), 7.25 (d, *J* = 9.2 Hz, 1H), 7.21 (m, 1H), 7.15 (d, *J* = 8.1 Hz, 1H), 6.97 (d, *J* = 1.9 Hz, 1H), 6.90 (d, *J* = 8.2 Hz, 1H), 5.02 (s, 2H), 4.47 (d, 2H, *J* = 6.0 Hz), 3.21 (m, 4H), 3.11 (t, 2H, *J* = 8.4 Hz), 2.78 (m, 3H), 2.49 (t, 2H, *J* = 8.4 Hz), 1.95 (m, 2H), 1.53 (m, 4H), 1.47 (m, 18H), 1.26 (m, 8H). **^{13}C-NMR** (100 MHz, CDCl$_3$): δ ppm 163.3, 152.8, 149.6, 143.0, 133.8, 130.8, 129.9, 129.2,

127.4, 125.9, 120.5, 111.3, 111.1, 82.0, 69.7, 49.9, 47.4, 40.9, 37.9, 30.9, 30.2, 28.7, 28.1, 28.0, 26.9, 26.5, 23.8, 20.7, 17.2. **MS (ES)** *m/z* = 821.3 [M+Na]$^+$.

Characterization of protected amidinoureas 37b.
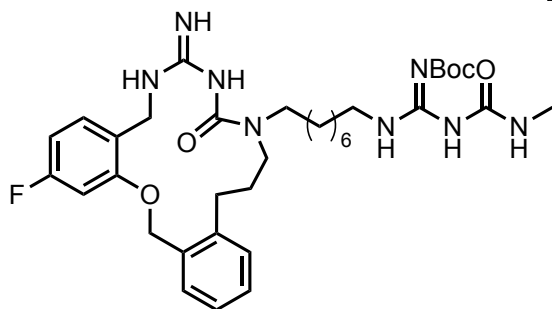
37b

Yield 36%. **¹H-NMR** (400 MHz, CDCl₃): δ ppm 12.09 (s, 1H), 7.95 (s, 1H), 7.25 (q, *J* = 17.5 Hz, 1H), 7.20 (d, *J* = 7.3 Hz, 1H), 7.18 (t, *J* = 10.3 Hz, 1H), 7.11 (t, *J* = 17.8 Hz, 1H), 6.69 (d, *J* = 7.5 Hz, 1H), 6.54 (t, *J* = 10.7 Hz, 1H), 5.18 (s, 1H), 5.06 (s, 2H), 4.38 (s, 2H), 3.22 (s, 4H), 3.15 (s, 2H), 2.75 (d, *J* = 7.1 Hz, 3H), 2.51 (t, *J* = 15.6 Hz, 2H), 1.94, (s, 2H), 1.48 (s, 4H), 1.44 (s, 9H), 1.23 (m, 8H). **¹³C-NMR** (100 MHz, CDCl₃): δ ppm 164.2, 163.1, 162.2, 158.7, 155.9, 154.0, 141.2, 140.6, 136.8, 130.8, 129.3, 128.4, 127.1, 126.2, 124.9, 124.9, 124.9, 107.9, 102.2, 80.3, 68.7, 44.9, 44.4, 41.5, 41.1, 31.9, 29.0, 29.0, 28.2, 27.5, 27.4, 26.8, 26.6, 26.2. ppm. **MS (ES)** *m/z* = 705.3 [M+Na]⁺, 683.3 [M+H]⁺.

Characterization of protected amidinoureas 37c.
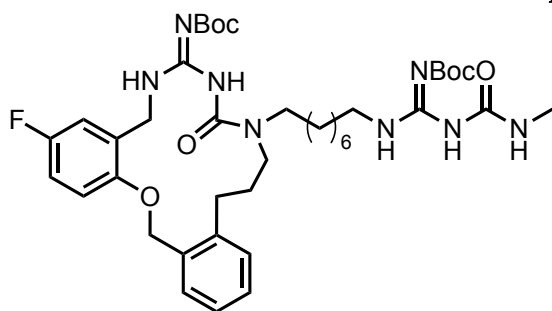
37c

Yield 35%. **¹H-NMR** (400 MHz, CDCl₃): δ ppm 12.15 (s, 1H), 8.50 (s, 1H), 7.95 (s, 1H), 7.31 (d, *J* = 7.6 Hz, 1H), 7.25 (d, *J* = 7.8 Hz, 1H), 7.21 (d, *J* = 7.2 Hz, 1H), 7.18 (m, 1H), 6.96 (dd, *J* = 14.1, 2.05 Hz, 1H), 6.87 (m, 2H), 5.11 (s, 1H), 5.02 (s, 2H), 4.50 (d, *J* = 8.1 Hz, 2H), 3.23 (m, 4H), 3.17 (t, *J* = 15.4 Hz, 2H), 2.75 (t, *J* = 7.9 Hz, 3H), 2.49 (t, *J* = 10.8 Hz, 2H), 1.96 (m, 2H), 1.54 (m, 4H), 1.49 (s, 9H), 1.47 (s, 9H), 1.28 (s, 8H). **¹³C-NMR** (100 MHz, CDCl₃): δ ppm 167.1, 160.3, 155.9, 154.8, 154.1, 154.0, 144.4, 141.2, 140.6, 136.8, 129.3, 128.4, 128.2, 127.1, 126.2, 116.6, 115.5, 114.8, 80.3, 68.7, 44.9, 44.4, 41.1, 40.5, 40.4, 31.9, 29.0, 28.4, 28.2, 27.3, 27.1, 26.8, 26.7, 26.4. ppm. **MS (ES)** *m/z* = 805.4 [M+Na]⁺.

Synthesis of BM56.
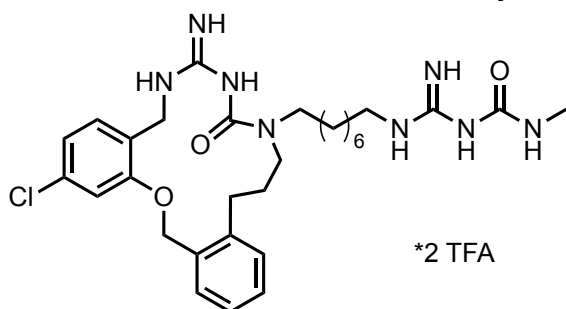
Yield: quantitative. **¹H-NMR** (400 MHz, CD₃OD): δ ppm 7.41 (m, 1H), 7.27 (m, 2H), 7.22 (m, 3H), 6.98 (d, *J* = 8.0 Hz, 1H), 5.07 (s, 2H), 4.37 (m, 2H), 3.52 (m, 2H), 3.29 (m, 4H), 2.78 (m, 2H), 2.74 (s, 3H), 2.07 (m, 2H), 1.59 (m, 2H), 1.53 (m, 2H), 1.31 (m, 8H). **¹³C-NMR** (100 MHz, CD₃OD): δ ppm 163.1, 162.2, 162.1, 158.5, 152.8, 141.2, 136.8, 132.6, 130.1, 129.3, 128.4, 128.1, 127.1, 126.2, 124.7, 115.1, 65.3, 44.8, 42.3, 41.4, 41.1, 32.8, 29.0, 28.9, 27.4, 26.5, 25.6, 25.2, 24.4, 22.2. **MS (ES)** *m/z* = 621.4 [M+Na]⁺, 599.4 [M+H]⁺.

Characterization of BM57.
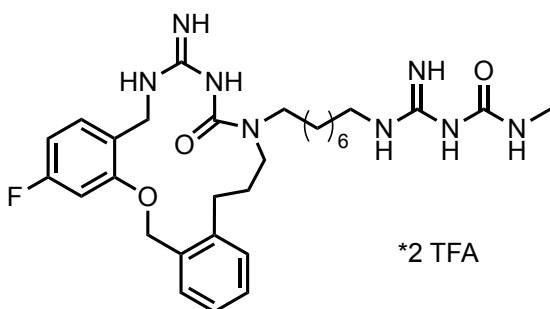
Yield: quantitative. **¹H-NMR** (400 MHz, CDCl₃): δ ppm 7.44 (d, *J* = 7.2 Hz, 1H), 7.35 (m, 2H), 7.29 (t, *J* = 10.4 Hz, 1H), 7.01 (d, *J* = 8.4 Hz, 1H), 6.69 (t, *J* = 15.4 Hz, 1H), 5.06 (s, 2H), 4.37 (s, 2H), 3.49 (s, 2H), 3.29 (s, 2H), 3.23 (t, *J* = 17.4 Hz, 2H), 2.78 (s, 2H), 2.74 (s, 3H), 2.12 (m, 2H), 1.59 (m, 2H), 1.54 (t, *J* = 10.5 Hz, 2H), 1.28 (m, 8H). **¹³C-NMR** (100 MHz, CD₃OD): δ ppm 164.2, 163.1, 162.2, 162.1, 158.7, 152.8, 141.2, 136.8, 130.8, 129.3, 128.4, 127.1, 126.2, 124.9, 107.9, 102.1, 68.8, 45.8, 42.6, 41.5, 41.0, 31.9, 29.1, 29.0, 27.5, 27.4, 26.8, 25.5, 24.2, 23.2. **MS (ES)** *m/z* = 583.4 [M+H]⁺.

Characterization of BM58
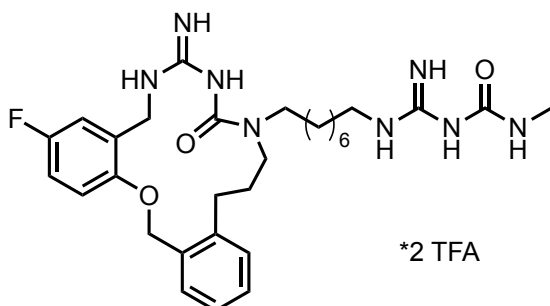
Yield: quantitative. **¹H-NMR** (400 MHz, CD₃OD): δ ppm 7.41 (m, 1H), 7.32 (m, 2H), 7.23 (s, 1H), 7.07 (m, 3H), 5.06 (s, 2H), 4.50 (s, 2H), 3.27 (m, 6H), 2.74 (s, 3H), 2.70 (m, 2H), 1.99 (m, 2H), 1.59 (t, *J* = 10.6 Hz, 2H), 1.53 (t, *J* = 10.3 Hz, 2H), 1.48 (m, 8H). **¹³C-NMR** (100 MHz, CD₃OD): δ ppm 163.1, 162.2, 162.1, 159.8, 154.8, 152.8, 141.2, 136.8, 129.3, 128.4, 128.2, 127.1, 126.2, 116.6, 115.3, 114.8, 65.6, 45.1, 43.4, 41.6, 39.9, 32.9, 29.2, 29.1, 27.5, 27.4, 26.8, 26.2, 25.8, 23.9. **MS (ES)** *m/z* = 583.3 [M+H]⁺.

4.3.5 Synthesis of the Boc linker 40.

Synthesis of 8-((tert-butoxycarbonyl) amino) octanoic acid 38.
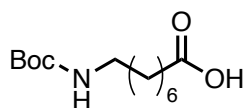
38

In a flask with magnetic stirrer, 8-aminooctanoic acid (1000 mg, 6.29 mmol) was dissolved in dioxane/H_2O 2:1 (24 mL) and NaOH (252 mg, 6.29 mmol) was added. Then di-*tert*-butyl-dicarbonate (1510 mg, 6.92 mmol) was added to the mixture on ice/NaCl bath. The mixture was stirred for 16 h at room temperature. The reaction was concentrated *in vacuo*. The residue was acidified with HCl 1N and extracted with EtOAc. Organic layers were dried over anhydrous Na_2SO_4, filtered and evaporated *in vacuo*. The residue was purified by flash chromatography (Hex/EtOAc 5:5). **Yield:** 92%. **^{1}H-NMR** (400 MHz, CDCl$_3$): δ ppm 4.57(bs, 1H), 3.10-2.98 (m, 2H), 2.29 (t, *J* = 7.2 Hz, 2H), 1.62-1.55 (m, 4H), 1.40 (s, 9H), 1.45-1.32 (m, 6H). **^{13}C-NMR** (100 MHz, CDCl$_3$): δ ppm 179.0, 156.6, 79.0, 40.5, 33.9, 29.8, 28.8, 28.3, 27.73, 26.4, 24.5.

Synthesis of tert-butyl (8-(allylamino)-8-oxooctyl) carbamate 39.
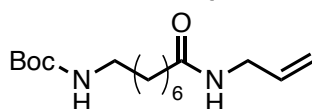
39

Yield: 89%. **^{1}H-NMR** (400 MHz, CDCl$_3$): δ ppm 6.03 (bs, 1H), 5.80-5.71 (m, 1H), 5.12-5.03 (m, 2H), 4.60 (bs, 1H), 3.82-3.75 (m, 2H), 3.07-2.99 (m, 2H), 2.13 (t, *J* = 7.2 Hz, 2H), 1.61-1.50 (m, 4H), 1.37 (s, 9H), 1.30-1.19 (m, 6H) ppm. **^{13}C-NMR** (100 MHz, CDCl$_3$): δ ppm 173.0, 156.0, 134.3, 116.0, 78.9, 41.7, 40.4, 36.4, 29.9, 28.3, 26.4, 25.5.

Synthesis of tert-butyl (8-(allylamino)octyl)carbamate 40.
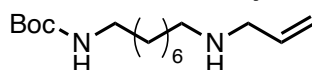
40

Yield: 35%. **^{1}H-NMR** (400 MHz, CDCl$_3$): δ ppm 5.89-5.80 (m, 1H), 5.12-5.00 (m, 2H), 4.60 (bs, 1H), 3.18 (d, *J* = 5.6 Hz, 2H), 3.05-3.00 (m, 2H), 2.53 (t, *J* = 6.8 Hz, 2H), 1.52-1.47 (m, 4H), 1.37 (s, 9H), 1.30-1.19 (m, 8H). **^{13}C-NMR** (100 MHz, CDCl$_3$): δ ppm 155.9, 136.8, 115.6, 78.8, 52.4, 49.3, 40.5, 29.9, 29.3, 29.1, 28.7, 28.3, 27.1, 26.6.

4.3.6 Synthesis of DF04 derivatives.

General procedure for preparation of α,β-unsaturated aldehydes 42a-e.

Synthesis of (E)-3-(2-chlorophenyl) acrylaldehyde 42a.
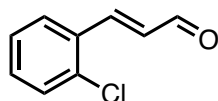
42a

To a solution of (Triphenylphosphoranylidene)acetaldehyde (1190.0 mg, 3.91 mmol) in dry Toluene (10mL), (E)-3-(2-chlorophenyl)acrylaldehyde (500.0 mg, 3.56 mmol) was added under a fllush of nitrogen. The reaction mixture was sttired at 85 °C under a flush of nitrogen for 17 h, then cooled down and concentrated under reduced pressure. The residue was dissolved in EtOAc and washed several times with a ss of $NaHCO_3$ and then with brine. The ogrnaic layer was sperated and dried over Na_2SO_4. Flash chromatography on silica gel, (EP/ EtOAc = 9/1) afford compound **42a**. **Yield:** 54%.**^{1}H-NMR** (400 MHz, $CDCl_3$): δ ppm 9.74 (d, *J* = 7.6 Hz, 1H), 7.91(d, *J* = 16.0 Hz, 1H), 7.64(d, *J* = 7.6 Hz, 1H), 7.44(d, *J* = 8.0 Hz, 1H), 7.33 (m, 2H), 6.68 (dd, *J* = 16.0 Hz, *J* = 7.6, 1H); **^{13}C-NMR** (100 MHz, $CDCl_3$): δ ppm 193.5, 147.9, 135.1, 132.0, 131.9, 130.5, 130.3, 127.8, 127.2.

Characterization of (E)-3-(4-chlorophenyl) acrylaldehyde 42b.
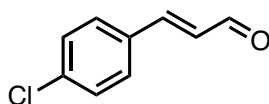
42b

Yield: 20%. **^{1}H-NMR** (400 MHz, $CDCl_3$): δ ppm 9.67(d, *J* = 7.6 Hz, 1H), 7.48 (d, *J* = 8.0 Hz, 2H), 7.45 (d, *J* = 16.0 Hz, 1H), 7.38 (d, *J* = 8.0 Hz, 2H), 6.66 (dd, *J* = 16.0 Hz, 7.6 Hz, 1H); **^{13}C-NMR** (100 MHz, $CDCl_3$): δ ppm 193.3, 150.9, 137.2, 132.4, 129.5, 129.3, 128.8.

Characterization of (E)-3-(2-(trifluoromethyl) phenyl) acrylaldehyde 42c.
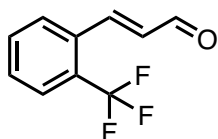
42c

Yield: 30%.**^{1}H-NMR** (400 MHz, $CDCl_3$): δ ppm 9.74 (d, *J* = 7.6 Hz, 1H), 7.86 (d, *J* = 16.0 Hz, 1H), 7.74 (d, *J* = 8.0 Hz, 2H), 7,60 (m, 1H), 7.52 (m, 1H), 6.68 (dd, *J* = 16.0 Hz, 7.6 Hz, 1H); **^{13}C-NMR** (100 MHz, $CDCl_3$): δ ppm 193.2, 147.4, 132.6, 132.2, 131.9, 130.4, 127.9, 126.3, 125.18, 122.5.

Characterization of (E)-3-(2-(trifluoromethoxy) phenyl) acrylaldehyde 42d

42d
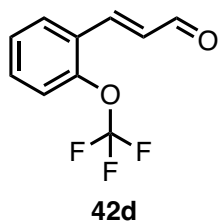
Yield: 67%. **¹H-NMR** (400 MHz, CDCl₃): δ ppm 9.73 (d, *J* = 7.6 Hz, 1H), 7.73 (d, *J* = 16.0 Hz, 1H), 7.69 (m, 1H), 7.47(m, 1H), 7.34(m, 2H), 6.73(dd, *J* = 16.0 Hz, 7.6 Hz, 1H); **¹³C-NMR** (100 MHz, CDCl₃): δ ppm 193.4, 147.4, 144.6, 137.7, 132.3, 130.8, 127.9, 127.2, 121.7, 121.3.

Characterization of (E)-3-(3-chlorophenyl) acrylaldehyde 42e.

42e
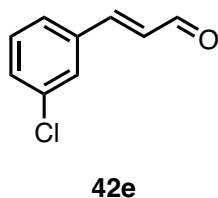
Yield: 64%. **¹H-NMR** (400 MHz, CDCl₃): δ ppm 9.65 (d, *J* = 7.6 Hz, 1H), 7.37 (m, 1H), 7.53 (m, 2H), 7.37 (d, *J* = 8.0 Hz, 1H), 7.04 (d, *J* = 16.0 Hz, 1H), 6.81 (dd, *J* = 16.0 Hz, 7.6 Hz, 1H). **¹³C-NMR** (100 MHz, CDCl₃): δ ppm 193.7, 149.8, 134.8, 134.3, 130.7, 129.6, 128.6, 127.6, 125.6.

General procedure for preparation of α,β-unsaturated aldehydes 42f-j:

Synthesis of 3-formyl-N, N-dimethylbenzamide 41f.

41f
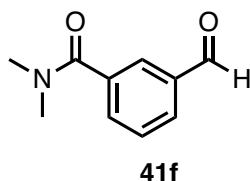
To a suspension of 3-formylbenzoic acid (1500.0 mg, 10.00 mmol) in dry CH₂Cl₂ (3.0 mL), thionyl chloride (870 µL, 12.00 mmol) and DMF (250 µL) were added at room temperature under a flush of nitrogen. The reaction mixture was stirred at refluxed under nitrogen for 2 h. The resulting viscous solution was then cooled down and poured slowly (dropwise over 15 min) into a solution of dimethyl amine 40 wt% in H₂O (4.5 mL, 36.00 mmol) previosuly cooled with an ice-water bath and this mixture stirred for 1 h at 0°C. The reaction mixture was treated with satured acquoes NaHCO₃ and extracted three times with DCM. The combine organic layer was dreid over NaSO₄ and then concentrated to afford compound **41f**. **Yield:** 86%. **¹H-NMR** (400 MHz, CDCl₃): δ ppm 9.99 (s, 1H), 7.89 (m, 2H), 7.66 (m, 1H), 7.56 (m, 1H), 3.09 (s, 3H), 2.96 (s, 3H). **¹³C-NMR** (100 MHz, CDCl₃): δ ppm 194.3, 173.2, 136.2, 135.3, 133.4, 131.3, 129.6, 128.9, 37.5.

Characterization of N-ethyl-4-formylbenzamide 41g.
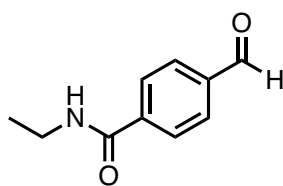
41g

Yield: 91% **¹H-NMR** (400 MHz, CDCl₃): δ ppm 9.93 (s, 1H), 8.01 (m, 2H), 7.89 (m, 2H), 6.16 (bs, 1H), 3.49 (m, 2H), 1.25 (t, *J* = 7.2 Hz, 3H). **¹³C-NMR** (100 MHz, CDCl₃): δ ppm 191.6, 166.7,139.8, 138.5 128.3, 127.3, 35.1, 13.5

Characterization of 4-formyl-N-methylbenzamide 41h.
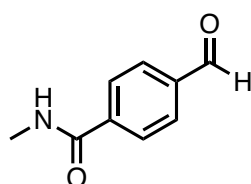
41h

Yield: 96%. **¹H-NMR** (400 MHz, CDCl₃): δ ppm 10.03 (s, 1H), 7.89 (m, 4H), 6.43 (bs, 1H), 3.04 (d, *J* = 4.8 Hz, 3H). **¹³C-NMR** (100 MHz, CDCl₃): δ ppm 191.6, 168.5, 139.7, 133.2, 129.9, 128.2, 26.8

Characterization of N-ethyl-3-formylbenzamide 41i.
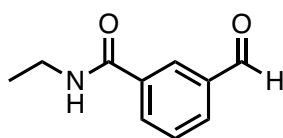
41i

Yield: 31%. **¹H-NMR** (400 MHz, CDCl₃): δ ppm 9.94 (s, 1H), 8.21 (s, 1H), 8.03 (d, *J* = 7.6 Hz, 1H), 7.89 (d, *J* = 7.6 Hz, 1H), 7.50 (t, *J* = 7.6 Hz, 1H), 3.43 (q, *J* = 7.2 Hz, 2H), 1.19 (t, *J* = 7.2 Hz, 3H). **¹³C-NMR** (100 MHz, CDCl₃): δ ppm 196.2, 166.5, 136.3, 133.2, 133.0, 130.6, 129.6, 129.2, 35.1, 14.7.

Synthesis of N-(3-formylphenyl) acetamide 41j.
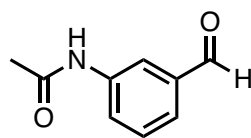
41j

MnO₂ (4884.0 mg, 56.56 mmol) was added To a solution of **49j** (320.0 mg, 1.94 mmol) in butanone (24.0 mL), and the resulting mixture was stirred at room temperature for four days. The resulting balck solution as filtrated through a pad of Celite with MeOH and concentrated under reduced pressure to obtain a black oil. This reisdue oil was dissolved in EtOAc and washed with water and then brine. The combined organic pahese were dried over Na₂SO₄ and concentrated under reduced pressure. Flash chromatography using EP/EtOAc 5:5 as eluent afford compound **41j. Yield:** 67%. **¹H-NMR** (400 MHz, CD₃OD): δ ppm 9.93 (s, 1H), 8.16 (s, 1H), 7.82(d, *J* = 7.8 Hz, 1H), 7.62 (m, 1H), 7.48 (t, *J* = 7.8 Hz, 1H), 2.16 (s, 3H). **¹³C-NMR** (100 MHz, CD₃OD): δ ppm 192.8, 170.1, 138.69, 136.87, 126.8, 126.3, 120.5, 23.9

Synthesis of (E)-N, N-dimethyl-3-(3-oxoprop-1-en-1-yl)benzamide 42f.
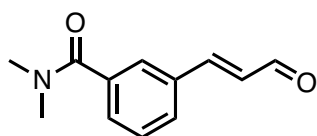
42f

To a solution of (triphenylphosphoranylidene)acetaldehyde (611.0 mg, 2.03 mmol) in dry toluene (23 mL) was added (E)-N,N-dimethyl-3-(3-oxoprop-1-en-1-yl)benzamide (**41f**) (700.0 mg, 4.07 mmol) under a flush of nitrogen. The mixture was stirred at 85 °C under nitrogen for 17 h, cooled down and concentrated under reduced pressure. The residue was dissolved in EtOAc and was washed with a saturated solution of $NaHCO_3$ and then with brine. The organic phaeses were dried with Na_2SO_4, filtered, and evaporated under reduced pressure. The mixture was purified with flash chromatography on silica gel, (EP/ EtOAc 8:2 to EP/ EtOAc 6:4) to afford the corresponding products **42f**. **Yield:** 19%.
^{1}H-NMR (400 MHz, $CDCl_3$): δ ppm 9.66 (d, *J* = 7.6 Hz, 1H), 7.57 (m, 2H), 7.47 (m, 2H) 6.96 (m, 1H), 6.67 (dd, *J* = 16.0 Hz, 7.6 Hz, 1 H), 3.07 (s, 3H), 2.95(s, 3H). **^{13}C-NMR** (100 MHz, $CDCl_3$) δ ppm 193.7, 175.3, 154.8, 137.3, 135.8, 134.2, 131.0, 128.6, 126.8, 126.8, 37.5.

Characterization of (E)-N-ethyl-4-(3-oxoprop-1-en-1-yl) benzamide 42g.
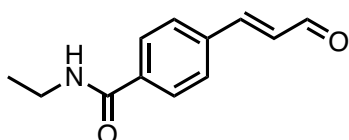
42g

Yield: 54%. **^{1}H-NMR** (400 MHz, $CDCl_3$): δ ppm 9.71 (dd, *J* = 7.6, 1H), 7.94 (m, 2H), 7.68 (m, 2H), 7.32 (dt, *J* = 16.0, 7.6 Hz, 1H), 6.53 (m, 1H), 6.16 (bs, 1H), 3.49 (m, 2H), 1.25 (t, *J* = 7.2 Hz, 3H).**^{13}C-NMR** (100 MHz, $CDCl_3$) δ ppm 193.44, 166.31, 153.36, 137.46, 134.41, 129.68, 127.47, 126.03, 35.07, 14.67.

Characterization of (E)-N-methyl-4-(3-oxoprop-1-en-1-yl) benzamide 42h.
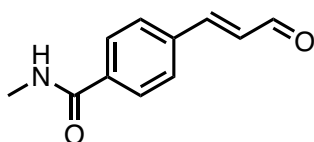
42h

Yield: 48%. **^{1}H-NMR** (400 MHz, $CDCl_3$): δ ppm 9.70 (d, *J* = 7.6 Hz, 1H), 7.83 (d, *J* = 8.0 Hz, 2H), 7.56 (d, *J* = 8.0 Hz, 2H), 7.49 (d, *J* = 16.0 Hz, 1H), 7.24 (bs, 1H), 6.70 (dd, *J* = 16.0 Hz, 7.6 Hz, 1H), 2.98 (s, 3H) **^{13}C-NMR** (100 MHz, $CDCl_3$) δ ppm 193.4, 169.6, 153.4, 137.5, 134.3, 129.7, 127.6, 126.0, 26.8.

Characterization of (E)-N-ethyl-3-(3-oxoprop-1-en-1-yl) benzamide 42i.
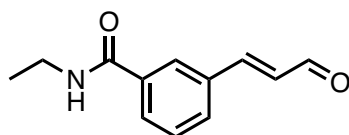
42i

Yield: 19%. **^{1}H-NMR** (400 MHz, CD_3OD): δ ppm 9.65 (d, *J* = 7.6 Hz, 1H), 8.07 (s, 1H), 7,86 (d, *J* = 7.6 Hz, 1H), 7.77 (d, *J* = 7.6 Hz, 1H), 7.66 (d, *J* = 16.0 Hz, 1H), 7.48 (t, *J* = 7.6 Hz, 1H), 6.80 (dd, *J* = 16.0 Hz, 7.6 Hz, 1H), 3.40 (q, *J* = 7.2 Hz, 2H), 1.21 (t, *J* = 7.2 Hz, 3H). **^{13}C-NMR** (100 MHz, CD_3OD): δ ppm 193.7, 163.6, 156.7, 135.2, 134.6, 133.1, 129.3, 128.8, 126.7, 125.2, 35.1, 14.7.

Characterization of (E)-N-(3-(3-oxoprop-1-en-1-yl)phenyl)acetamide 42j.
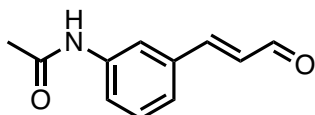
42j

Yield: 33%. **^{1}H-NMR** (400 MHz, CDCl$_3$): δ ppm 9.66 (dd, *J* = 7.6, 1.0 Hz, 1H), 7.91 (s, 1H), 7.83 (t, *J* = 2.0 Hz, 1H), 7.65 (d, *J* =7.8 Hz, 1H), 7.63 (d, *J* = 16.0 Hz, 1H), 7.68 (t, *J* = 7.8 Hz, 1H), 7.69 (d, *J* = 7.8 Hz, 1H), 6.67 (dd, *J* = 16.0, 7.6 Hz, 1H), 2.20 (s, 3H). **^{13}C-NMR** (100 MHz, CDCl$_3$) δ 193.7 168.7, 153.2, 139.5, 134.8, 129.7, 129.2, 124.5, 1228, 120.2, 24.7.

General procedure for the reductive amination 44a-j.

Synthesis of methyl (E)-6-(4-(3-(2-chlorophenyl) allyl) piperazin-1-yl) pyrazine-2-carboxylate 44a.
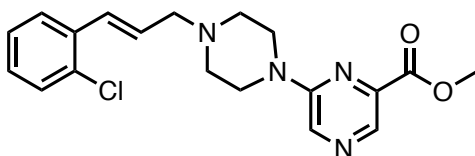
44a

Methyl 6-(piperazine-1-yl) pyrazine-2-carboxylate **43** (61.0 mg, 0.27 mmol) was treated with (E)-3-(2-chlorophenyl) acrylaldehyde **42a** (50.0 mg, 0.30 mmol) in DCE (4 mL). Subsequentially, STAB (81.0 mg, 0,38 mmol) was added and the reaction mixture stirred at room temperature for 2h. Afterwards, the reaction mixture was treated with DCM and washed with a statured solution of NaHCO$_3$ for three times, and then with brine filtered, and evaporated under reduced pressure. The crude residue was purified with flash chromatography on silica gel (EP/EtOAc = 2/8 to EtOAc 100%) to afford compound **44a**. **Yield:** 96%. **^{1}H-NMR** (400 MHz, CDCl$_3$): δ ppm 8.51 (s, 1H), 8.26 (s, 1H), 7.52 (d, *J* = 7.6 Hz, 1H), 7.32 (d, *J* = 8.0 Hz, 1H), 7.20 (m, 2 H), 6.94 (d, *J* = 16.0 Hz, 1H), 6.28 (dt, *J* = 16.0 Hz, 6.8 Hz, 1H), 3.93 (s, 3 H), 3.74 (t, *J* = 4.4 Hz, 4H), 3.28 (d, *J*= 6.8 Hz, 2H), 2.67 (t, *J* = 4.4 Hz, 4H); **^{13}C-NMR** (100 MHz, CDCl$_3$): δ ppm 166.2, 153.8, 140.1, 134.6, 133.9, 133.8, 132.9, 130.2, 129.7, 128.7, 126.9, 126.8, 126.7, 60.7, 52.6, 52.4, 44.0.

Characterization of Methyl (E)-6-(4-(3-(4-chlorophenyl) allyl) piperazin-1-yl) pyrazine-2-carboxylate 44b.
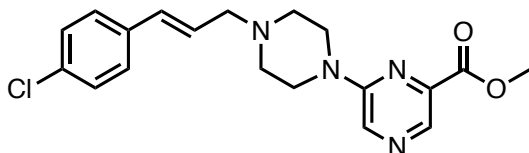
44b

Yield: 48%. **^{1}H-NMR** (400 MHz, CDCl$_3$): δ ppm 8.52 (s, 1H), 8.26 (s, 1H), 7.26(m, 4H), 6.52 (d, *J* = 16.0 Hz, 1H) 6.28 (dt, *J* = 16.0 Hz, *J* = 6.8 Hz, 1H), 3.93 (s, 3H), 3.77 (m, 4H), 3.27 (d, *J* = 6.8 Hz, 2H) 2.70 (m, 4H);**^{13}C-NMR** (100 MHz, CDCl$_3$): δ ppm 165.2, 153.7,140.1, 134.8, 134.0, 133.8, 133.5, 130.6, 128.7, 127.6, 125.4, 60.6, 52.6, 52.3, 43.8.

Characterization of Methyl (E)-6-(4-(3-(2-(trifluoromethyl) phenyl) allyl) piperazin-1-yl) pyrazine-2-carboxylate 44c.
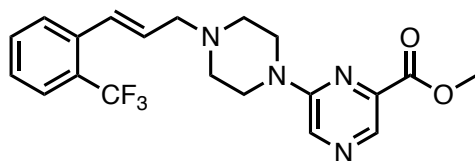
44c

Yield: 65%. **¹H-NMR** (400 MHz, CDCl₃): δ ppm 8.51 (s, 1H), 8.27 (s, 1H), 7.61 (d, = 7.6 Hz, 2H), 7.48 (m, 1H), 7.33 (m, 1H), 6.94 (d , *J* = 16.0 Hz, 1H), 6.27 (dt, *J* = 16.0 Hz, *J* = 6.8 Hz, 1H), 3.93 (s, 3H), 3.77 (m, 4H), 3.30 (d, *J*= 6.8 Hz, 2H), 2.70 (m , 4H); **¹³C-NMR** (100 MHz, CDCl₃): δ ppm 165.2, 153.7, 140.1, 135.6, 133.9, 133.8, 131.8, 130.6, 127.5, 127.4, 125.7, 125.6, 122.8, 60.6, 52.6, 52.3, 43.9.

Characterization of Methyl (E)-6-(4-(3-(2-(trifluoromethoxy) phenyl) allyl) piperazin-1-yl) pyrazine-2-carboxylate 44d.
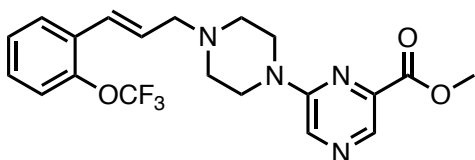
44d

Yield: 63%. **¹H-NMR** (400 MHz, CDCl₃): δ ppm 8.50 (s, 1H), 8.25 (s, 1H), 7.57 (m, 1H), 7.22 (m, 3H), 6.69 (d, *J* = 16.0 Hz, 1H), 6.33 (dt, *J* = 16.0 Hz, 6.8 Hz, 1H), 3.92 (s, 3H), 3.73 (t, *J* = 4.4Hz, , 4H), 3.27 (d, *J* = 6.8 Hz, 2H), 2.66 (t, *J* = 4.4 Hz, 4H); **¹³C-NMR** (100 MHz, CDCl₃): δ ppm 165.2, 153.8, 146.2, 140.1, 133.9, 133.8, 129.9, 128.7, 126.9, 126.9, 126.7,121.8, 121.3, 119.3, 60.8, 52.5, 52.4, 43.9.

Characterization oof methyl (E)-6-(4-(3-(3-chlorophenyl) allyl) piperazin-1-yl) pyrazine-2-carboxylate 44e.
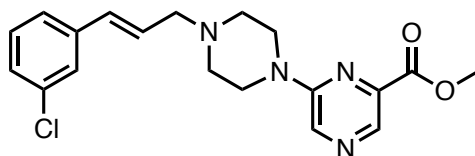
44e

Yield: 60%. **¹H-NMR** (400 MHz, CDCl₃): δ ppm 8.46 (s, 1H), 8.12 (s, 1H), 7.56 (d, *J* = 7.6 Hz, 1H), 7.37 (d, *J* = 8.0 Hz, 1H), 7.29 (m, 2 H), 6.60 (d, *J* = 16.0 Hz, 1H), 6.32 (dt, *J* = 16.0 Hz, 6.8 Hz, 1H), 3.93 (s, 3 H), 3.84 (t, *J* = 4.4 Hz, 4H), 3.37 (d, *J*= 6.8 Hz, 2H), 2.87 (t, *J* = 4.4 Hz, 4H);**¹³C-NMR** (100 MHz, CDCl₃): δ ppm 164.8, 153.6, 142.7, 136.8, 136.4, 134.2, 132.8, 131.7, 129.9, 128.7, 127.2, 126.6, 125.7, 60.2, 52.8, 52.3, 45.3.

Characterization of Methyl (E)-6-(4-(3-(3-(dimethylcarbamoyl) phenyl) allyl) piperazin-1-yl) pyrazine-2-carboxylate 44f .
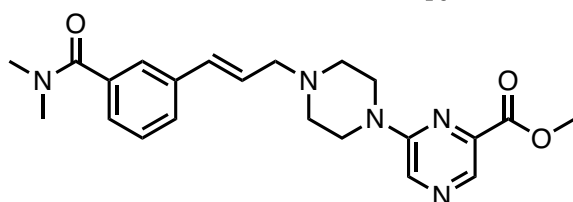
44f

Yield: 47%. **¹H-NMR** (400 MHz, CDCl₃): δ ppm 8.49 (s, 1H), 8.25 (s, 1H), 7.38 (m, 2H), 7.30 (m, 1H), 7.23 (d, *J*= 7.4 Hz, 1H) ,6.53 (d, *J* = 15.6 Hz, 1H), 6.29 (dt, *J* = 15.6 Hz, 6.4 Hz ,1H), 3.91 (s, 3H), 3.73 (m, 4H), 3.23 (d, *J* = 6.4 Hz, 2H), 3.07 (s, 3H), 2.94 (s, 3H), 2.63 (m, 4H); **¹³C-NMR** (100 MHz, CDCl₃): δ ppm 171.2, 165.2, 153.8, 140.1, 136.8, 136.7, 133.8, 128.6, 128.5, 127.4, 127.3, 126.1, 125.0, 124.8, 60.6, 52.5, 52.3, 43.9, 39.4, 35.2.

Characterization of Methyl (E)-6-(4-(3-(4-(ethylcarbamoyl) phenyl) allyl) piperazin-1-yl) pyrazine-2-carboxylate 44g.

44g
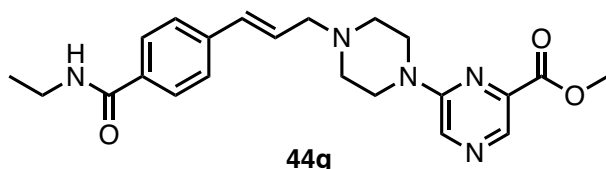
Yield: 15%. **¹H-NMR** (400 MHz, CDCl₃): δ ppm 8.50 (s, 1H), 8.25 (s, 1H), 7.70 (d, *J* = 7.6 Hz, 2H), 7.39 (d, *J* = 7.6 Hz, 2H), 6.56 (d, *J* = 15.6 Hz, 1H), 6.35 (m, 1H), 6.21 (bs,1H), 3.92 (s, 3H), 3.72 (m, 4H), 3.46 (t, *J* = 6.4 Hz, 2H), 3.23 (m, 2H), 2.63 (s, 4H), 1.22 (m, 3H); **¹³C-NMR** (100 MHz, CDCl₃): δ ppm 168.9, 165.2, 153.8, 140.1, 139.5, 133.8, 133.7, 132.8, 127.2, 127.1, 126.4, 126.3, 60.7, 52.6, 52.5, 44.1, 34.8, 14.

Characterization of Methyl (E)-6-(4-(3-(4-(methylcarbamoyl) phenyl) allyl) piperazin-1-yl) pyrazine-2-carboxylate 44h.

44h
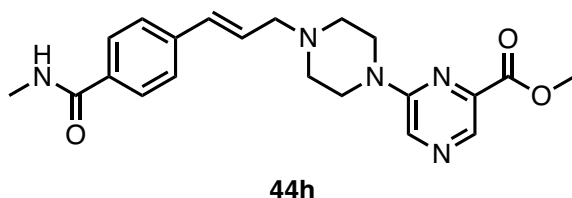
Yield: 29%. **¹H-NMR** (400 MHz, CDCl₃): δ ppm 8.49 (s, 1H), 8.24 (s, 1H), 7.70 (d, *J*= 8.2 Hz, 2 H), 7.38 (d, *J* = 8.2 Hz, 2H), 6.55 (d, *J* = 15.6 Hz, 1H), 6.35 (m, 1H), 3.92 (s, 3H), 3.70 (t, *J* = 4.4 Hz , 4H), 3.21 (d, *J* = 6.4 Hz, 2H), 2.96 (d, *J* = 4.8 Hz, 3H), 2.61 (t, *J* = 4.4 Hz, 4H); **¹³C-NMR** (100 MHz, CDCl₃): δ ppm 168.1, 165.2, 153. 8, 140.1, 139.5, 133.8, 133.5, 132.7, 129.9, 127.7, 127.18, 126.35, 60.7, 52.6, 52.5, 44.1, 26.7.

Characterization of Methyl (E)-6-(4-(3-(3-(ethylcarbamoyl) phenyl) allyl) piperazin-1-yl) pyrazine-2-carboxylate 44i.

44i
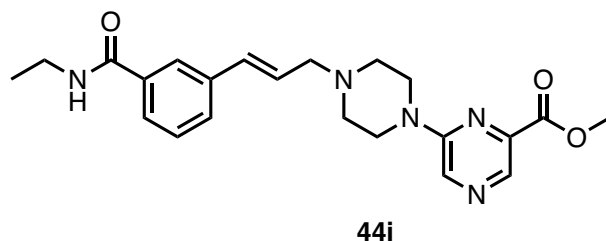
Yield: 21 %. **¹H-NMR** (400 MHz, CDCl₃): δ ppm 8.48 (s, 1H), 8.23 (s, 1H), 7.77 (s, 1H), 7.58 (d, *J* = 7.6 Hz,1H), 7.44 (d, *J* = 8.0 Hz, 1H), 7.32 (m , *J* = 7.6 Hz, 8.0 Hz ,1H), 6.54 (d, *J* = 15.6 Hz, 1H), 6.31 (m, 2H), 3.91 (s, 3H), 3.69 (t, *J* = 4.4 Hz, 4H), 3.45 (q, *J* = 7.2 Hz, 2H), 3.19 (d, *J* = 6.4 Hz, 2H) 2.60 (t, *J* = 4.4 Hz, 4H), 1.20 (t, *J* = 7.2 Hz, 3H); **¹³C-NMR** (100 MHz, CDCl₃): δ ppm 167.2, 165.2, 153.8, 140.0, 137.0, 135.2, 133.8, 132.8, 128.9, 128.6, 126.8, 125.8, 124.9, 60.6, 52.6, 52.3, 44.1, 34.9, 14,8.

Characterization of methyl (E)-6-(4-(3-(3-acetamidophenyl) allyl) piperazin-1-yl) pyrazine-2-carboxylate 44j.


44j
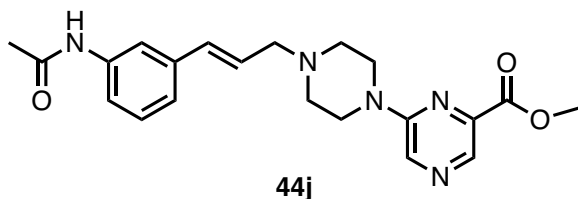
Yield: 53 %. **^{1}H-NMR** (400 MHz, CDCl$_3$): δ ppm 8.59 (s, 1H), 8.26 (s, 1H) 7.56 (m, 2H), 7.30 (m, 1H), 7.21 (m, 1H) ,6.53 (d, *J* = 15.6 Hz, 1H), 6.28 (dt, *J* = 15.6 Hz, 6.4 Hz ,1H), 4.01 (s, 3H), 3.82 (m, 4H), 3.64 (d, *J* = 6.4 Hz, 2H), 2.96 (m, 4H), 2.23 (s, 3H); **^{13}C-NMR** (100 MHz, CDCl$_3$): δ ppm 170.2, 165.2, 153.8, 143.5, 138.3, 137.4, 136.8, 131.6, 129.7, 128.2, 127.5, 124.6, 125.2, 124.8, 60.8, 52.5, 52.3, 43.9, 39.4

General procedure for the amide conversion 45 a-i.

Synthesis of (E)-6-(4-(3-(2-chlorophenyl) allyl) piperazin-1-yl) pyrazine-2-carboxamide 45a .

45a
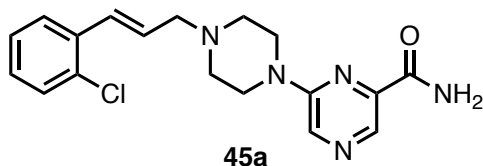
Compound **44a** (80.0 mg, 0.13 mmol) were dissolevd in a 7M solution of NH$_3$ in MeOH(1.7 mL, 7N) in a deidicated MW vials equipped with a stir bar, thencapped andinserted into the cavity of a Microwave system apparatus. The reaction mixture was heated at 170 W for 10 min (internal temperature 45°C). This procedure was repeated for three times. After cooling, the reaction mixture was diluted with DCM and the organic layer was washed three times with H$_2$O and then with brine. The organic phases were separated and dried with NaSO$_4$, filtered and evaporated under reduce pressure. The crude residue was purified with flash chromatography on silica gel (EtOAc 100% to EtOAc / MeOH 96:4) to afford compound **45a**. **Yield:** 42%. **^{1}H-NMR** (400 MHz, DMSO-d$_6$): δ ppm 8.44 (s, 1H), 8.32 (s, 1H), 8.02 (bs, 1H), 7.70 (d, *J* = 7.6 Hz, 1H), 7.59 (bs, 1H), 7.41 (d, *J* = 7.6 Hz, 1H), 7.28 (m ,2H), 6.83 (d, *J* = 16.0 Hz, 1H), 6.37 (dt, *J* = 16.0 Hz, 6.4 Hz, 1H), 3.67 (s, 4H), 3.19 (d, *J* = 6.4 Hz, 2H), 2.51 (t, *J* = 4.4 Hz , 4H) **^{13}C-NMR** (100 MHz, DMSO-d$_6$): δ ppm 163.4, 155.4, 146.4, 135.7, 135.2, 133.91, 133.3, 131.7, 129.9, 129.7, 128.7, 126.3, 125.6, 58.5, 52.2, 45.4. **MS (ES)** *m/z* 358 [M+H]$^+$, 380 [M+Na]$^+$.

Characterization of (E)-6-(4-(3-(4-chlorophenyl) allyl) piperazin-1-yl) pyrazine-2-carboxamide 45b.

45b
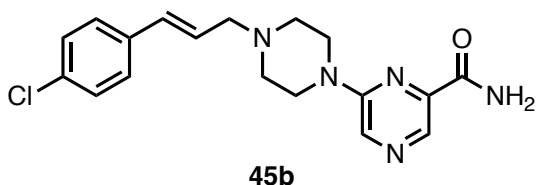
Yield: 14%. **^{1}H-NMR** (500 MHz, CDCl$_3$+ 2ggt CD$_3$OD): δ ppm 8.56 (s, 1H), 8.35 (s, 1H), 7.41 (m, 2H), 7.35 (m, 2H), 6.58 (d, *J* = 15.9 Hz, 1H), 6.32 (m, 1H), 3.71 (s, 4H), 3.25 (s, 2H), 2.68 (m, 4H); **^{13}C-NMR** (125 MHz, CDCl$_3$+ 2ggt CD$_3$OD): δ ppm 163.6, 154.8, 146.5, 135.7, 135.2, 134.6, 133.9, 132.6, 128.6, 127.4, 124.8, 58.4, 52.2, 44.8. **MS (ES)** *m/z* 358 [M+H]$^+$, 380 [M+Na]$^+$.

Characterization of (E)-6-(4-(3-(2-(trifluoromethyl) phenyl) allyl) piperazin-1-yl) pyrazine-2-carboxamide 45c.

45c
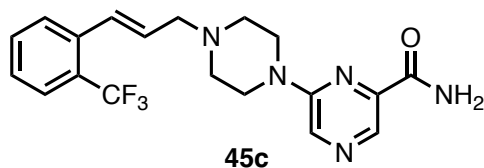
Yield: 25%. **¹H-NMR** (400 MHz, CD$_2$Cl$_2$): δ ppm 8.56 (s, 1H), 8.33 (s, 1H), 7.70 (d, *J* = 7.6 Hz, 1H), 7.64 (d, *J* = 8.0 Hz, 1H), 7.55 (m, 1H), 7.40 (m, 1H), 7.42 (d, *J* = 16.0 Hz, 1H), 6.35 (dt, *J* = 16.0 Hz, 6.4 Hz, 1H), 3.82 (s, 4H), 3.48 (s, 2H), 2.89 (s, 4H); **¹³C-NMR** (100 MHz, CD$_2$Cl$_2$): δ ppm 164.2, 155.0, 151.3, 136.0, 134.1, 133.5, 132.0, 129.8, 129.7, 127.7, 127.6, 127.5, 124.9, 61.9, 53.7, 45.2. **MS (ES)** *m/z*

Characterization of (E)-6-(4-(3-(2-(trifluoromethoxy) phenyl) allyl) piperazin-1-yl) pyrazine-2-carboxamide 45d.

45d
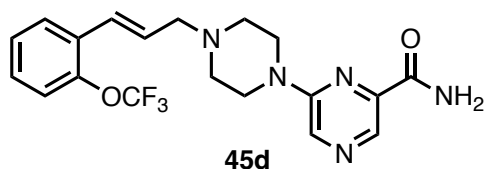
Yield: 70%. **¹H-NMR** (400 MHz, CD$_2$Cl$_2$): δ ppm 8.55 (s, 1H), 8.32 (s, 1 H), 7.63 (m, 2H), 7.45 (bs, 1H), 7.29 (s, 1H), 7.25 (s ,1H), 6.82 (d, *J* = 16.0 Hz, 1H), 6.35 (dt, *J* = 16 Hz, 6.4 Hz, 1H), 6.08 (bs, 1H), 3.66 (t, *J* = 4.4 Hz, 4H), 3.24 (d, *J* = 6.4 Hz, 2H), 2.63 (t, *J* = 4.4 Hz, 4H); **¹³C-NMR** (100 MHz, CD$_2$Cl$_2$): δ ppm 166.2, 153.1, 146.06, 140.8, 134.2, 131.4, 130.4, 129.9, 128.5, 127.1, 126.9, 125.5, 121.3, 60.6, 52.4, 44.4. **MS (ES)** *m/z*

Characterization of (E)-6-(4-(3-(3-chlorophenyl) allyl) piperazin-1-yl) pyrazine-2-carboxamide 45e.

45e
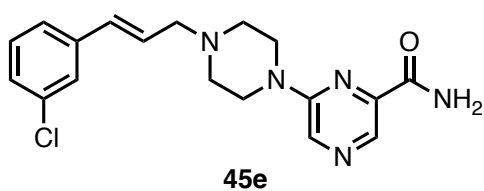
Yield: 37%. **¹H-NMR** (300 MHz, DMSO): δ ppm 8.45 (s, 1H), 8.32 (s, 1H), 8.04 (bs, 1H), 7.63 (bs, 1H), 7.53 (t, *J* = 1.8 Hz, 1H), 7.33 (m, 3H), 6.56 (d, *J* = 15.9 Hz, 1H) 6.43 (m, 1H), 3.67 (t, *J* = 4.5 Hz, 4H), 3.15 (d, *J* = 6.0 Hz, 2H), 2.51 (t, *J* = 4.5 Hz, 4H). **¹³C-NMR** (75 MHz, DMSO): 166.1, 153.4, 146.3, 139.8, 136.3, 133.9, 133.4, 132.6, 131.4, 129.6, 127.4, 126.5, 124.3, 59.6, 52.4, 44.7. **MS (ES)** *m/z* 358 [M+H]⁺, 380 [M+Na]⁺.

Characterization of (E)-6-(4-(3-(3-(dimethylcarbamoyl) phenyl) allyl) piperazin-1-yl) pyrazine-2-carboxamide 45f.
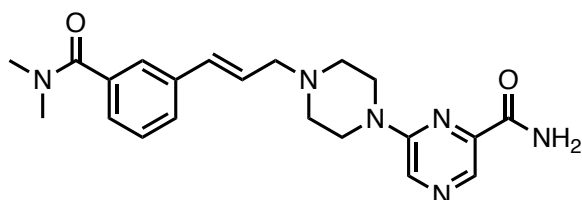
45f

Yield: 12% **¹H-NMR** (400 MHz, CD₃OD): δ ppm 8.41 (s, 1H), 8.37(s, 1H), 7.52 (d, *J* = 7.6 Hz, 1H), 7.46 (s, 1H), 7.40 (t, *J* = 7.6 Hz, 1H), 7.27 (d, *J* = 7.6 Hz, 1H), 6.65 (d, *J* = 16.0 Hz, 1H), 6.39 (dt , *J* = 16.0 Hz, 6.8 Hz, 1H), 3.75 (t, *J* = 4.4 Hz, 4H), 3.25 (d, *J* = 6. 8 Hz, 2H), 3.09 (s ,3H), 2.98 (s, 3H), 2.66 (t, *J* = 4.4 Hz, 4H); **¹³C-NMR** (100 MHz, CD₃OD): δ ppm 172.1, 167.3, 153.4, 137.2, 136.4, 133.6, 132.9, 130.2, 128.5, 127.3, 126.3, 125.6, 124.4, 60.2, 52.2, 38.5, 34.1, 31.6.

Characterization of (E)-6-(4-(3-(4-(ethylcarbamoyl) phenyl) allyl) piperazin-1-yl) pyrazine-2-carboxamide 45g.
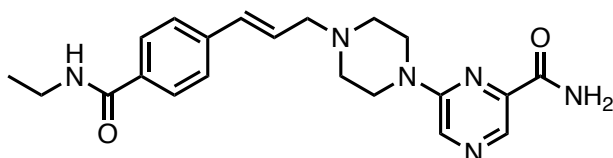
45g

**Yield:** 69% **¹H-NMR** (400 MHz, CD₃OD): δ ppm 8.43 (s, 1H), 8.39 (s, 1H), 7.76 (d, *J* = 8.4 Hz, 2 H), 7.50 (d, *J* = 8.4 Hz, 2H), 6.70 (d, *J* = 16.0 Hz, 1H), 6.44 (dt, *J* = 16.0 Hz, 6.8 Hz, 1H), 3.79 (t, *J* = 4.4 Hz, 4H), 3.39 (q, *J* = 7.2 Hz, 2H), 3.35 (d , *J* = 6.8 Hz, 2H), 2.76 (t, *J* = 4.4 Hz, 4H), 1.20 (t, *J* = 7.2 Hz, 3H); **¹³C-NMR** (100 MHz, CD₃OD): δ ppm 168.1, 167.3, 153.3, 141.6, 139.6, 133.7, 133.6, 133.5, 130.4, 127.2, 126.0, 59.9, 52.0, 43.4, 34.3, 13.4

Characterization of (E)-6-(4-(3-(4-(methylcarbamoyl) phenyl) allyl) piperazin-1-yl) pyrazine-2-carboxamide 45h.
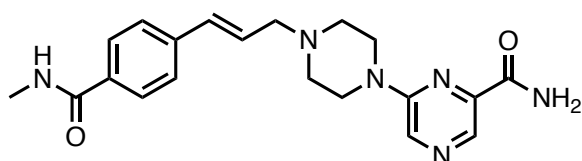
45h

Yield: 46% **¹H-NMR** (400 MHz, CD₃OD): δ ppm 8.41 (s, 1H), 8.36, (s, 1H), 7.75 (d, *J* = 8.4 Hz, 2H), 7.48 (d, *J* = 8.4 Hz, 2H), 6.65 (d, *J* = 16.0 Hz, 1H), 6.42 (dt, *J* = 16.0 Hz, 6.8 Hz, 1H), 3.73 (t, *J* = 4.4 Hz, 4H), 3.25 (d, *J* = 6.8 Hz, 2H), 2.89 (s, 3H), 2.65 (t, *J* = 4.4 Hz, 4H); **¹³C-NMR** (100 MHz, CD₃OD): δ ppm 168.8, 167.3, 153.4, 141.6, 139.9, 133.6, 133.0, 132.8, 130.2, 127.2, 127.1, 125.9, 60.2, 52.2, 43.7, 32.4.

Characterization of (E)-6-(4-(3-(3-(ethylcarbamoyl) phenyl) allyl) piperazin-1-yl) pyrazine-2-carboxamide 45i.
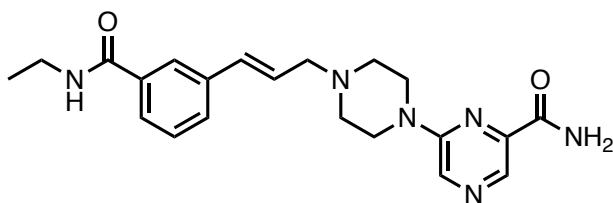
45i

Yield: 52% **¹H-NMR** (400 MHz, CD₂Cl₂): δ ppm 8.52 (s, 1H), 8.29 (s, 1H), 7.83 (s, 1H), 7,62(d, *J* = 7.6Hz, 1H), 7.50 (d, *J* = 7.6 Hz, 1H), 7.37 (t, *J* = 7.6 Hz, 1H), 6.77 (bs, 1H), 6.59 (d, *J* = 16 Hz, 1H), 6.33 (dt, *J* = 16 Hz, 6.4 Hz, 1H), 3.65 (t, *J* = 4.4 Hz, 4H), 3.45 (q, *J* = 7.2 Hz, 2H), 3.21 (d, *J* = 6.4 Hz, 2H), 2.61 (t, *J* = 4.4 Hz, 4H), 2.45 (bs, 2H), 1.22 (t, J = 7.2 Hz, 3H); **¹³C-NMR** (100 MHz, CD₂Cl₂): δ 167.2, 166.5, 153.1, 140.8, 137.2, 135.2, 134.0, 132.3, 131.3, 129.0, 128.7, 127.3, 125.8,124.7, 60.6, 52.4, 44.3, 34.8, 14.4.

Characterization of (E)-6-(4-(3-(3-acetamidophenyl)allyl)piperazin-1-yl)pyrazine-2-carboxamide 45j.
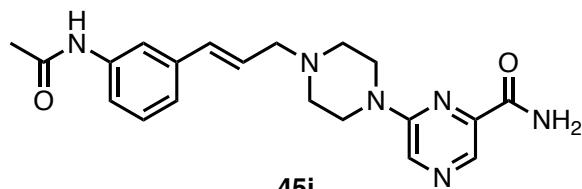

45j

Yield: 95% **¹H-NMR** (500 MHz, CDCl₃): δ 8.63 (s, 1H), 8.30 (s, 1H), 7.66 (s, 1H), 7.61 (s, 1H), 7.46 (bs, 1H), 7.25 (m, 1H), 7.23 (d, *J* = 7.9 Hz, 1H), 7.12 (d, *J* = 7.5 Hz, 1H), 6.51 (d, *J* = 15.9 Hz, 1H), 6.28 (m, 1H), 5.93 (bs, 1H), 3.64 (m, 4H), 3.20 (d, *J* = 6.7 Hz, 2H), 2.62 (m, 4H), 2.16 (s, 3H). **¹³C-NMR** (125 MHz, CDCl₃): δ167.1, 165.4, 153.4, 142.3, 138.8, 137.5, 134.5, 133.9, 130.3, 127.9, 127.7, 123.2, 119.9, 117.1, 58.9, 52.6, 45.8, 23.7.

Synthesis of the common intermediate 44.

Synthesis of methyl pyrazine-2-carboxylate 46.
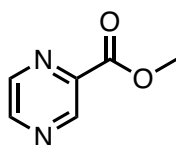
46

To a solution of pyrazinoic acid (2000.0 mg, 16.13 mmol) in MeOH (11.0 mL) under magnetic stirring, sulfuric acid (3.5 mL, 66.46 mmol) was added dropwise. The mixture was stirred at room temperature for 24 h. Then, the excess of acid was quenched with a saturated aqueous solution of NaHCO₃ until basic pH was reached, and the resulting mixture was concentrated *in vacuo*. The aqueous residue was extracted three times with DCM. The combined organic layers were washed with saturated NaCl solution, dried over Na₂SO₄, filtered and finally evaporated. The residue was purified by flash chromatography (PE/EtOAc 6:4) to afford the product **46** as a white solid. **Yield:** 54%. **¹H-NMR** (400 MHz, CDCl₃) δ ppm 9.22 (s, 1H), 8.69 (s, 1H), 8.63 (s, 1H), 3.95 (s, 3H). **¹³C-NMR** (100 MHz, CDCl₃) δ ppm 164.2, 147.6, 146.1, 144.2, 143.1, 53.0. **MS (ES)** *m/z* = 161.1 [M+Na]⁺, 139.1 [M+H]⁺.

Synthesis of 3-(methoxycarbonyl)pyrazine 1-oxide 46
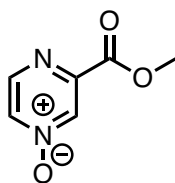
47

To a solution of compound **46** (500.0 mg, 3.62 mmol) in 1,2-dichloroethane (5.0 mL) under magnetic stirring, m-chloroperbenzoic acid (1620.0 mg, 7.24 mmol) was added. The suspension was gently warmed to 60 °C until a light-yellow solution was obtained and stirred for 16 h. Then, the solution was cooled to room temperature and diluted with DCM (15.0 mL). The precipitate was removed by filtration and washed with DCM. The joined organic layers were dried over K_2CO_3, filtered and evaporated. The solid residue was dissolved in DCM and the minimal amount of MeOH required and titrated with hexane several times. The desired compound **47** was then collected by filtration as a light-yellow solid. **Yield:** 85%. **^{1}H-NMR** (400 MHz, CDCl$_3$) δ ppm 8.68 (s, 1H), 8.50 (s, 1H), 8.17 (s, 1H), 3.97 (s, 3H). **^{13}C-NMR** (100 MHz, CDCl$_3$) δ ppm 162.6, 147.5, 147.3, 135.9, 135.8, 53.5. **MS (ES)** *m/z* = 155.0 [M+H]$^+$.

Synthesis of methyl 6-chloropyrazine-2-carboxylate 48.
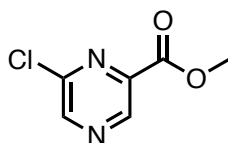
48

Compound **47** (120.0 mg, 0.78 mmol) was dissolved in SOCl$_2$ (850 µL) and the mixture was stirred at reflux for 7 h. Then, the mixture was cooled to room temperature and put in an ice bath. The excess of SOCl$_2$ was carefully quenched with pure water and neutralized with a 1M solution of K_2CO_3. The resulting aqueous layer was extracted three times with DCM. The organic layers were washed with saturated NaCl solution, dried over Na_2SO_4, filtered and finally evaporated. The residue was purified by flash chromatography (DCM/EtOAc 95:5) to afford compound **48**. **Yield:** 45%. **^{1}H-NMR** (400 MHz, DMSO-d$_6$) δ ppm 9.15 (s, 1H), 9.03 (s, 1H), 3.90 (s, 3H). **^{13}C-NMR** (100 MHz, CDCl$_3$) δ ppm 163.1, 149.1, 148.0, 143.5, 142.4, 53.3. **MS (ES)** *m/z* = 195.0 [M+Na]$^+$, 173.0 [M+H]$^+$

Synthesis of methyl 6-(piperazin-1-yl) pyrazine-2-carboxylate 43
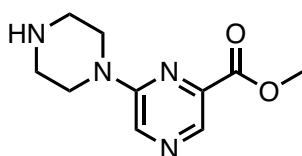
43

Methyl 6-chloropyrazine-2-carboxylate **48** (60.6 mg, 0.35 mmol,) was dissolved in 6 mL of DMF in a MW tube equipped with a stir bar. Then piperazine (30.2 mg, 0.35 mmol) and DIPEA (73µL, 0.42 mmol) were added and the tube inserted into the cavity of a Microwave system apparatus and heated at 170

W for 15 min (internal temperature 60°C,). After cooling, the reaction mixture was diluted with EtOAc and then washed several times with a basic solution of K_2CO_3 in H_2O. Then the organic layer was washed with brine, dried over Na_2SO_4, filtered and evaporated under reduce pressure. The crude residue was purified with flash chromatography on silica gel (DCM/ MeOH = 95:5) to give the corresponding products **43**. **Yield:** 54% **^{1}H-NMR** (400 MHz, CD_3OD): δ ppm 8.35 (s, 1 H), 8.34(s, 1 H), 3.91(s, 3 H), 3.65(t, *J*= 5.2 Hz, 4 H), 2.92(t, *J*= 5.2 Hz, 4 H); **^{13}C-NMR** (100 MHz, CD_3OD): δ ppm 165.3, 154.2, 140.1, 133.9, 132.3, 51.7, 44.6, 44.3.

Synthesis of N-(3-(hydroxymethyl)phenyl) acetamide.
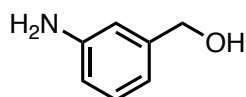
49j

To a solution of 3-Aminobenzyl alcohol (508.0 mg, 4.13 mmol) in dry THF (6.0 mL) cooled at 0˚ with an ice bath, acetic anhydride (500 µL, 5.10 mmol) was added dropwise and stirred at room temprature for 15 minutes. The reaction was quenched by the addition of NaOH 2.5M (2.0 mL), $NaHCO_3$(ss) (2.0 mL) and MeOH (5.0 mL). This solution was stirred at room temperature 15 minutes, then dissolved in EtOAc and washed with water for three times and then brine. The combined organic phases were seprated and driedover Na_2SO_4. Flash chromatography using EP/EtOAc 3:7 as eluent afford compound **49j. Yield** 57%.**^{1}H-NMR** (400 MHz, CD_3OD): δ ppm 7.53 (m, 1H), 7.44 (m,1H),7.27 (m, 1H), 7.08 (m,1H), 4.56 (s, 2H), 2.78 (t, *J* = 6.4 Hz, 1H), 2.15 (s, 3H); **^{13}C-NMR** (100 MHz, CD_3OD): δ ppm 170.2, 143.2, 138.8, 129.8, 121.3, 120.4, 120.10, 65.1, 23.8.

4.3.7   Indole *N*-alkylation

General Procedure for the N- alkylation.
In a MW vial 3-methyl-1*H*-indole was solubilized in EtOAc (0.50 mL). Then 1-propanephosphonic acid cyclic anhydride 50% in EtOAc (0.625 mL, 1.05 mmol) and the appropriate aldehyde/ketone were subsequentially added to the initial solution. The dedicated microwave vial was then capped and heated in a Biotage® Initiator $^+$, following one of these procedures:
PROCEDURE A: 3-methyl-1*H*-indole (1eqiuv.), ketone/aldehyde (3 eqiuv.), 20 minutes, 120 °C.
PROCEDURE B: 3-methyl-1*H*-indole (1 equiv.), ketone/aldehyde (3 equiv.), 20 minutes, 140 °C.
PROCEDURE C: 3-methyl-1*H*-indole (1 eqiuv.), ketone/aldehyde (5 equiv.), 1 hour, 160 °C**.**
The reaction was arrested by addition of TEA (0.500 mL, 3.57 mmol)

Synthesis of 1-(3,6-dihydro-2H-pyran-4-yl)-3-methylindole 50.
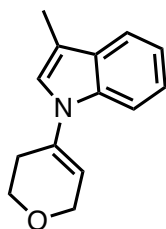
50

3-methyl-1*H*-indole (91.8 mg, 0.700 mmol) and tetrahydropyran-4-one (210 mg, 0.210mmol) were treated using the **General Procedure A,** but instead heating the reaction, this one was stirred at room temperature for 3 hours. Column chromatography (0-15% DCM in isohexane) was performed to yield the title product as a yellow solid (66 mg, 44% yield). **^{1}H-NMR** (400 MHz, Acetone-d_6) δ 7.56 (ddt, *J* =

14.4 Hz, 7.7 Hz, 1.0 Hz, 2H), 7.22 – 7.15 (m, 2H), 7.09 (ddd, J = 8.0 Hz, 7.0 Hz, 1.0 Hz, 1H), 5.92 (tt, J = 2.9 Hz, 1.5 Hz, 1H), 4.34 (q, J = 2.8 Hz, 2H), 3.95 (t, J = 5.4 Hz, 2H), 2.60 (ttd, J = 5.4 Hz, 2.7 Hz, 1.5 Hz, 2H), 2.30 (d, J = 1.2 Hz, 3H). **^{13}C-NMR** (100 MHz, Acetone-d_6) δ 135.67, 133.27, 129.73, 123.63, 121.92, 119.40, 118.84, 116.50, 111.46, 111.13, 64.33, 63.96, 8.71.

Tert-butyl 4-(3-methylindol-1-yl)-3,6-dihydro-2H-pyridine-1-carboxylate 51.
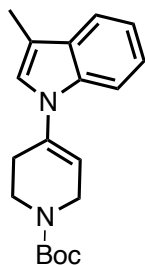
51

3-methyl-1H-indole (91.8 mg, 0.700 mmol) and tert-butyl 4-oxopiperidine-1-carboxylate (418 mg, 0.210 mmol) were treated using **General Procedure A,** but instead heating the reaction, this one was stirred at room temperature for 4 hours. Column chromatography (0-40% DCM in isohexane) was performed to yield the title product as a yellow oil (120 mg, 50% yield). **^{1}H-NMR** (400 MHz, Acetone-d_6) δ ppm 7.55 (ddt, J = 8.0 Hz, 1.7 Hz, 0.8 Hz, 2H), 7.14 (dddd, J = 33.8 Hz, 8.0 Hz, 7.0 Hz, 1.0 Hz, 3H), 5.91 (s, 1H), 4.17 (d, J = 3.0 Hz, 2H), 3.75 (t, J = 5.7 Hz, 2H), 2.63 (dddt, J = 7.0 Hz, 4.1 Hz, 2.6 Hz, 1.3 Hz, 2H), 2.31 (d, J = 1.1 Hz, 3H), 1.51 (s, 9H). **^{13}C-NMR** (100 MHz, Acetone-d_6) δ ppm 152.94, 136.64, 130.53, 124.82, 122.78, 120.24, 119.70, 112.34, 111.93, 79.87, 41.82, 34.70, 28.59, 24.44, 17.82, 17.80, 14.96, 8.17. **LCMS (ESI+)** m/z .313.1 [M+H]$^+$; (280 nm): t_R = 3.4 min, >95%.

Ethyl 4-(3-methyl-1H-indol-1-yl) cyclohex-3-ene-1-carboxylate 52.
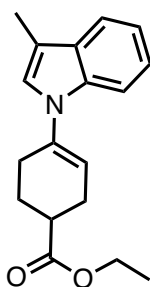
52

3-methyl-1H-indole (91.8 mg, 0.700 mmol) and *tert*-butyl ethyl 4-oxocyclohexanecarboxylate (357 mg, 0.210 mmol) were treated using **General Procedure A.** Column chromatography (0-40% DCM in isohexane) was performed to yield the title product as a yellow oil (79 mg, 40% yield). **^{1}H-NMR** (400 MHz, Acetone-d_6) δ ppm 7.55 – 7.41 (m, 2H), 7.16 – 7.09 (m, 2H), 7.05 (ddd, J = 8.0 Hz, 7.0 Hz, 1.1 Hz, 1H), 5.87 (dqd, J = 3.3 Hz, 1.9 Hz, 1.4 Hz, 1H), 4.26 – 4.04 (m, 2H), 2.78 – 2.71 (m, 1H), 2.58 – 2.50 (m, 3H), 2.28 (d, J = 1.1 Hz, 3H), 2.23 – 2.16 (m, 1H), 1.97 (dddd, J = 13.2 Hz, 10.7 Hz, 9.1 Hz, 6.0 Hz, 1H), 1.26 (t, J = 7.1 Hz, 3H).**^{13}C-NMR** (100 MHz, Acetone-d_6) δ ppm 174.32, 135.96, 135.51, 129.36, 124.18, 121.64, 119.06, 118.68, 117.83, 110.93, 59.93, 38.48, 27.48, 26.64, 25.33, 13.68, 8.68.**LCMS (ESI+)** m/z .284.3 [M+H]$^+$; (280 nm): t_R = 3.4 min, >95%

Bibliography

(1)   Garcia-Rubio, R.; de Oliveira, H. C.; Rivera, J.; Trevijano-Contador, N. The Fungal Cell Wall: Candida, Cryptococcus, and Aspergillus Species. *Frontiers in Microbiology* **2020**, *10* (January), 1–13. https://doi.org/10.3389/fmicb.2019.02993.

(2)   Bueno, D. J.; Silva, J. O. *Fungi: The Fungal Hypha*, Second Edi.; Elsevier, 2014; Vol. 2. https://doi.org/10.1016/B978-0-12-384730-0.00132-4.

(3)   Kibbler, C. C.; Barton, R.; Neil, A.; Gow, R.; Howell, S.; Maccallum, D. M.; Manuel, J. *Oxford Textbook of Medical Mycology*; 2018. https://doi.org/10.1093/med/9780198755388.001.0001.

(4)   Köhler, J. R.; Hube, B.; Puccia, R.; Casadevall, A.; Perfect, J. R. Fungi That Infect Humans. *The Fungal Kingdom* **2017**, No. 4, 813–843. https://doi.org/10.1128/9781555819583.ch39.

(5)   Pierce, C.; Vila, T.; Romo, J.; Montelongo-Jauregui, D.; Wall, G.; Ramasubramanian, A.; Lopez-Ribot, J. The Candida Albicans Biofilm Matrix: Composition, Structure and Function. *Journal of Fungi* **2017**, *3* (1), 14. https://doi.org/10.3390/jof3010014.

(6)   Rajendran, R.; Sherry, L.; Nile, C. J.; Sherriff, A.; Johnson, E. M.; Hanson, M. F.; Williams, C.; Munro, C. A.; Jones, B. J.; Ramage, G. Biofilm Formation Is a Risk Factor for Mortality in Patients with Candida Albicans Bloodstream Infection-Scotland, 2012-2013. *Clinical Microbiology and Infection* **2016**, *22* (1), 87–93. https://doi.org/10.1016/j.cmi.2015.09.018.

(7)   Nobile, C. J.; Johnson, A. D. Candida Albicans Biofilms and Human Disease. *Annual Review of Microbiology* **2015**, *69* (1), 71–92. https://doi.org/10.1146/annurev-micro-091014-104330.

(8)   Perović-Ottstadt, S.; Adell, T.; Chaidir, C.; Wiens, M.; Korzhev, M.; Gamulin, V.; Müller, I.; Müller, W. A (1→3)-β-d-glucan Recognition Protein from the Sponge Suberites Domuncula. *European journal of biochemistry / FEBS* **2004**, *271*, 1924–1937. https://doi.org/10.1111/j.1432-1033.2004.04102.x.

(9)   Casadevall, A. Fungi and the Rise of Mammals. *PLOS Pathogens* **2012**, *8* (8), 1–3. https://doi.org/10.1371/journal.ppat.1002808.

(10)   Kronstad, J. W.; Attarian, R.; Cadieux, B.; Choi, J.; D'Souza, C. A.; Griffiths, E. J.; Geddes, J. M. H.; Hu, G.; Jung, W. H.; Kretschmer, M.; Saikia, S.; Wang, J. Expanding Fungal Pathogenesis: Cryptococcus Breaks out of the Opportunistic Box. *Nature Reviews Microbiology* **2011**, *9* (3), 193–203. https://doi.org/10.1038/nrmicro2522.

(11)   Park, B. J.; Wannemuehler, K. A.; Marston, B. J.; Govender, N.; Pappas, P. G.; Chiller, T. M. Estimation of the Current Global Burden of Cryptococcal Meningitis among Persons Living with HIV/AIDS. *AIDS* **2009**, *23* (4), 525–530. https://doi.org/10.1097/QAD.0b013e328322ffac.

(12)   Nicola, A. M.; Robertson, E. J.; Albuquerque, P.; da Silveira Derengowski, L.; Casadevall, A.; Dromer, F. Nonlytic Exocytosis of Cryptococcus Neoformans from Macrophages Occurs *In Vivo* and Is Influenced by Phagosomal PH. *mBio* **2011**, *2* (4), e00167-11. https://doi.org/10.1128/mBio.00167-11.

(13)   Kainz, K.; Bauer, M. A.; Madeo, F.; Carmona-Gutierrez, D. Fungal Infections in Humans: The Silent Crisis. *Microbial cell (Graz, Austria)*. Shared Science Publishers OG June 1, 2020, pp 143–145. https://doi.org/10.15698/mic2020.06.718.

(14) Ibáñez-Martínez, E.; Ruiz-Gaitán, A.; Pemán-García, J. Update on the Diagnosis of Invasive Fungal Infection. *Revista espanola de quimioterapia : publicacion oficial de la Sociedad Espanola de Quimioterapia* **2017**, *30 Suppl 1*, 16–21.

(15) Pappas, P. G.; Lionakis, M. S.; Arendrup, M. C.; Ostrosky-Zeichner, L.; Kullberg, B. J. Invasive Candidiasis. *Nature Reviews Disease Primers* **2018**, *4* (May), 1–20. https://doi.org/10.1038/nrdp.2018.26.

(16) Yapar, N. Epidemiology and Risk Factors for Invasive Candidiasis. *Therapeutics and Clinical Risk Management* **2014**, *10* (1), 95. https://doi.org/10.2147/TCRM.S40160.

(17) Krcmery, V.; Barnes, A. J. Non-Albicans Candida Spp. Causing Fungaemia: Pathogenicity and Antifungal Resistance. *J Hosp Infect* **2002**, *50* (4), 243–260. https://doi.org/10.1053/jhin.2001.1151.

(18) Gonzalez-Lara, M. F.; Ostrosky-Zeichner, L. Invasive Candidiasis. *Semin Respir Crit Care Med* **2020**, *41* (01), 3–12.

(19) Limper, A. H.; Adenis, A.; Le, T.; Harrison, T. S. Fungal Infections in HIV/AIDS. *Lancet Infect Dis* **2017**, *17* (11), e334–e343. https://doi.org/10.1016/S1473-3099(17)30303-1.

(20) Azoulay, E.; Russell, L.; van de Louw, A.; Metaxa, V.; Bauer, P.; Povoa, P.; Montero, J. G.; Loeches, I. M.; Mehta, S.; Puxty, K.; Schellongowski, P.; Rello, J.; Mokart, D.; Lemiale, V.; Mirouse, A. Diagnosis of Severe Respiratory Infections in Immunocompromised Patients. *Intensive Care Medicine* **2020**, *46* (2), 298–314. https://doi.org/10.1007/s00134-019-05906-5.

(21) Cataldo, M. A.; Tetaj, N.; Selleri, M.; Marchioni, L.; Capone, A.; Caraffa, E.; Caro, A. di; Petrosillo, N. Incidence of Bacterial and Fungal Bloodstream Infections in COVID-19 Patients in Intensive Care: An Alarming "Collateral Effect." *Journal of Global Antimicrobial Resistance* **2020**, *23*, 290–291. https://doi.org/10.1016/j.jgar.2020.10.004.

(22) Rawson, T. M.; Moore, L. S. P.; Zhu, N.; Ranganathan, N.; Skolimowska, K.; Gilchrist, M.; Satta, G.; Cooke, G.; Holmes, A. Bacterial and Fungal Coinfection in Individuals With Coronavirus: A Rapid Review To Support COVID-19 Antimicrobial Prescribing. *Clinical infectious diseases : an official publication of the Infectious Diseases Society of America* **2020**, *71* (9), 2459–2468. https://doi.org/10.1093/cid/ciaa530.

(23) Song, G.; Liang, G.; Liu, W. Fungal Co-Infections Associated with Global COVID-19 Pandemic: A Clinical and Diagnostic Perspective from China. *Mycopathologia* **2020**, *185* (4), 599–606. https://doi.org/10.1007/s11046-020-00462-9.

(24) Garey, K. W.; Rege, M.; Pai, M. P.; Mingo, D. E.; Suda, K. J.; Turpin, R. S.; Bearden, D. T. Time to Initiation of Fluconazole Therapy Impacts Mortality in Patients with Candidemia: A Multi-Institutional Study. *Clinical Infectious Diseases* **2006**, *43* (1), 25–31. https://doi.org/10.1086/504810.

(25) Clancy, C. J.; Nguyen, M. H. Finding the "Missing 50%" of Invasive Candidiasis: How Nonculture Diagnostics Will Improve Understanding of Disease Spectrum and Transform Patient Care. *Clinical Infectious Diseases* **2013**, *56* (9), 1284–1292. https://doi.org/10.1093/cid/cit006.

(26) Roemer, T.; Krysan, D. J. Antifungal Drug Development: Challenges, Unmet Clinical Needs, and New Approaches. *Cold Spring Harb Perspect Med* **2014**, *4* (5). https://doi.org/10.1101/cshperspect.a019703.

(27) Roemer, T.; Krysan, D. J. Unmet Clinical Needs , and New Approaches. *Cold Spring Harb Perspect Med* **2014**, *4*, a019703.

(28)   Fernández-García, R.; de Pablo, E.; Ballesteros, M. P.; Serrano, D. R. Unmet Clinical Needs in the Treatment of Systemic Fungal Infections: The Role of Amphotericin B and Drug Targeting. *Int J Pharm* **2017**, *525* (1), 139–148. https://doi.org/10.1016/j.ijpharm.2017.04.013.

(29)   Posteraro, B.; Sanguinetti, M.; Fiori, B.; la Sorda, M.; Spanu, T.; Sanglard, D.; Fadda, G. Caspofungin Activity against Clinical Isolates of Azole Cross-Resistant Candida Glabrata Overexpressing Efflux Pump Genes. *Journal of Antimicrobial Chemotherapy* **2006**, *58* (2), 458–461. https://doi.org/10.1093/jac/dkl237.

(30)   Anderson, J. B. Evolution of Antifungal-Drug Resistance: Mechanisms and Pathogen Fitness. *Nature Reviews Microbiology* **2005**, *3* (7), 547–556. https://doi.org/10.1038/nrmicro1179.

(31)   Perlin, D. S.; Rautemaa-Richardson, R.; Alastruey-Izquierdo, A. The Global Problem of Antifungal Resistance: Prevalence, Mechanisms, and Management. *The Lancet Infectious Diseases* **2017**, *17* (12), e383–e392. https://doi.org/10.1016/S1473-3099(17)30316-X.

(32)   Cowen, L. E.; Sanglard, D.; Howard, S. J.; Rogers, P. D.; Perlin, D. S. Mechanisms of Antifungal Drug Resistance. *Cold Spring Harbor Perspectives in Medicine* **2015**, *5* (7), 1–22. https://doi.org/10.1101/cshperspect.a019752.

(33)   Albertson, G. D.; Niimi, M.; Cannon, R. D.; Jenkinson, H. F. Multiple Efflux Mechanisms Are Involved in Candida Albicans Fluconazole Resistance. *Antimicrob Agents Chemother* **1996**, *40* (12), 2835–2841.

(34)   van Daele, R.; Spriet, I.; Wauters, J.; Maertens, J.; Mercier, T.; van Hecke, S.; Brüggemann, R. Antifungal Drugs: What Brings the Future? *Medical Mycology* **2019**, *57* (Supplement_3), S328–S343. https://doi.org/10.1093/mmy/myz012.

(35)   Fuentefria, A. M.; Pippi, B.; Dalla Lana, D. F.; Donato, K. K.; de Andrade, S. F. Antifungals Discovery: An Insight into New Strategies to Combat Antifungal Resistance. *Letters in Applied Microbiology* **2018**, *66* (1), 2–13. https://doi.org/10.1111/lam.12820.

(36)   Dreassi, E.; Zizzari, A. T.; D'Arezzo, S.; Visca, P.; Botta, M. Analysis of Guazatine Mixture by LC and LC-MS and Antimycotic Activity Determination of Principal Components. *J Pharm Biomed Anal* **2007**, *43* (4), 1499–1506. https://doi.org/10.1016/j.jpba.2006.10.029.

(37)   G. Eldon Brown. Efficacy of Guazatine and Iminoctadine for Control of Postharvest Decays of Oranges. *Plant Disease* **1988**, *72* (10), 906–908.

(38)   Manetti, F.; Castagnolo, D.; Raffi, F.; Zizzari, A. T.; Rajamaki, S.; D'Arezzo, S.; Visca, P.; Cona, A.; Fracasso, M. E.; Doria, D.; Posteraro, B.; Sanguinetti, M.; Fadda, G.; Botta, M. Synthesis of New Linear Guanidines and Macrocyclic Amidinourea Derivatives Endowed with High Antifungal Activity against Candida Spp. and Aspergillus Spp. *Journal of Medicinal Chemistry* **2009**, *52* (23). https://doi.org/10.1021/jm900760k.

(39)   Castagnolo, D.; Raffi, F.; Giorgi, G.; Botta, M. Macrocyclization of Di-Boc-Guanidino-Alkylamines Related to Guazatine Components: Discovery and Synthesis of Innovative Macrocyclic Amidinoureas. *European Journal of Organic Chemistry* **2009**, *2009* (3), 334–337. https://doi.org/10.1002/ejoc.200801109.

(40)   Miel, H.; Rault, S. Conversion of N,N'-Bis(Tert-Butoxycarbonyl)Guanidines to N-(N'-Tert-Butoxycarbonylamidino)Ureas. *Tetrahedron Letters* **1998**, *39* (12), 1565–1568. https://doi.org/10.1016/S0040-4039(98)00025-2.

(41)   STEFANIA, S.; BRUNELLA, P.; MAURIZIO, S.; MAURIZIO, B.; GIORGIO, M.; FILOMENA, D. E. L.; JEAN-DENIS, D.; DAVIDE, D. NEW MACROCYCLIC AMIDINOUREA DERIVATIVES, METHODS OF PREPARATION AND USES THEREOF AS CHITINASE INHIBITORS, 2014.

(42)   MAURIZIO, B.; FRANCESCO, R.; PAOLO, V. LINEAR AND CYCLIC GUANIDINE DERIVATIVES, METHOD OF PREPARATION AND USES THEREOF, 2009.

(43)   Deodato, D.; Maccari, G.; de Luca, F.; Sanfilippo, S.; Casian, A.; Martini, R.; D'Arezzo, S.; Bonchi, C.; Bugli, F.; Posteraro, B.; Vandeputte, P.; Sanglard, D.; Docquier, J.-D. D.; Sanguinetti, M.; Visca, P.; Botta, M.; D'Arezzo, S.; Bonchi, C.; Bugli, F.; Posteraro, B.; Vandeputte, P.; Sanglard, D.; Docquier, J.-D. D.; Sanguinetti, M.; Visca, P.; Botta, M.; D'Arezzo, S.; Bonchi, C.; Bugli, F.; Posteraro, B.; Vandeputte, P.; Sanglard, D.; Docquier, J.-D. D.; Sanguinetti, M.; Visca, P.; Botta, M. Biological Characterization and in Vivo Assessment of the Activity of a New Synthetic Macrocyclic Antifungal Compound. *Journal of Medicinal Chemistry* **2016**, *59* (8), 3854–3866. https://doi.org/10.1021/acs.jmedchem.6b00018.

(44)   Sanguinetti, M.; Sanfilippo, S.; Castagnolo, D.; Sanglard, D.; Posteraro, B.; Donzellini, G.; Botta, M. Novel Macrocyclic Amidinoureas: Potent Non-Azole Antifungals Active against Wild-Type and Resistant Candida Species. *ACS Med Chem Lett* **2013**, *4* (9), 852–857. https://doi.org/10.1021/ml400187w.

(45)   Chouhan, G.; Alper, H. Synthesis of Ring-Fused Oxazolo- and Pyrazoloisoquinolinones by a One-Pot Pd-Catalyzed Carboxamidation and Aldol-Type Condensation Cascade Process. *The Journal of Organic Chemistry* **2009**, *74* (16), 6181–6189. https://doi.org/10.1021/jo9010574.

(46)   Ding, R.; He, Y.; Wang, X.; Xu, J.; Chen, Y.; Feng, M.; Qi, C. Treatment of Alcohols with Tosyl Chloride Does Not Always Lead to the Formation of Tosylates. *Molecules* **2011**, *16* (7), 5665–5673. https://doi.org/10.3390/molecules16075665.

(47)   Cordovilla, C.; Bartolomé, C.; Martínez-Ilarduya, J. M.; Espinet, P. The Stille Reaction, 38 Years Later. *ACS Catalysis* **2015**, *5* (5), 3040–3053. https://doi.org/10.1021/acscatal.5b00448.

(48)   Zamperini, C.; Maccari, G.; Deodato, D.; Pasero, C.; D'Agostino, I.; Orofino, F.; de Luca, F.; Dreassi, E.; Docquier, J. D.; Botta, M. Identification, Synthesis and Biological Activity of Alkyl-Guanidine Oligomers as Potent Antibacterial Agents. *Scientific Reports* **2017**, *7* (1), 8251. https://doi.org/10.1038/s41598-017-08749-6.

(49)   Pasero, C.; D'Agostino, I.; de Luca, F.; Zamperini, C.; Deodato, D.; Truglio, G. I.; Sannio, F.; del Prete, R.; Ferraro, T.; Visaggio, D.; Mancini, A.; Guglielmi, M. B.; Visca, P.; Docquier, J.-D.; Botta, M. Alkyl-Guanidine Compounds as Potent Broad-Spectrum Antibacterial Agents: Chemical Library Extension and Biological Characterization. *Journal of Medicinal Chemistry* **2018**, *61* (20), 9162–9176. https://doi.org/10.1021/acs.jmedchem.8b00619.

(50)   Gradillas, A.; Pérez-Castells, J. Macrocyclization by Ring-Closing Metathesis in the Total Synthesis of Natural Products: Reaction Conditions and Limitations. *Angew Chem Int Ed Engl* **2006**, *45* (37), 6086–6101. https://doi.org/10.1002/anie.200600641.

(51)   Nelson, D. J.; Manzini, S.; Urbina-Blanco, C. A.; Nolan, S. P. Key Processes in Ruthenium-Catalysed Olefin Metathesis. *Chemical Communications* **2014**, *50* (72), 10355–10375. https://doi.org/10.1039/c4cc02515f.

(52)   Manetti, F.; Cona, A.; Angeli, L.; Mugnaini, C.; Raffi, F.; Capone, C.; Dreassi, E.; Zizzari, A. T.; Tisi, A.; Federico, R.; Botta, M. Synthesis and Biological Evaluation of Guanidino Compounds Endowed with Subnanomolar Affinity as Competitive Inhibitors of Maize Polyamine Oxidase. *Journal of Medicinal Chemistry* **2009**, *52* (15), 4774–4785. https://doi.org/10.1021/jm900371z.

(53)   Posteraro, B.; Martucci, R.; la Sorda, M.; Fiori, B.; Sanglard, D.; de Carolis, E.; Florio, A. R.; Fadda, G.; Sanguinetti, M. Reliability of the Vitek 2 Yeast Susceptibility Test for Detection of in Vitro Resistance to Fluconazole and Voriconazole in Clinical Isolates of Candida Albicans and Candida Glabrata. *J Clin Microbiol* **2009**, *47* (6), 1927–1930. https://doi.org/10.1128/JCM.02070-08.

(54)   Pfaller, M. A.; Boyken, L. B.; Hollis, R. J.; Kroeger, J.; Messer, S. A.; Tendolkar, S.; Diekema, D. J. Validation of 24-Hour Fluconazole MIC Readings versus the CLSI 48-Hour Broth Microdilution Reference Method: Results from a Global Candida Antifungal Surveillance Program. *Journal of Clinical Microbiology* **2008**, *46* (11), 3585–3590. https://doi.org/10.1128/JCM.01391-08.

(55)   Barry, A. L.; Pfaller, M. A.; Brown, S. D.; Espinel-Ingroff, A.; Ghannoum, M. A.; Knapp, C.; Rennie, R. P.; Rex, J. H.; Rinaldi, M. G. Quality Control Limits for Broth Microdilution Susceptibility Tests of Ten Antifungal Agents. *Journal of Clinical Microbiology* **2000**, *38* (9), 3457–3459. https://doi.org/10.1128/JCM.38.9.3457-3459.2000.

(56)   Rex, J. H.; Barbara D. Alexander; Andes, D.; Arthington-Skaggs, B.; Brown, S. D.; Chaturvedi, V.; Ghannoum, M. A.; Espinel-Ingroff, A.; Knapp, C. C.; Ostrosky-Zeichner, L.; Pfaller, M. A.; Sheehan, D. J.; Walsh, T. J.; CLSI. *Reference Method for Broth Dilution Antifungal Susceptibility Testing of Yeasts; Third Informational Supplement*; 2005; Vol. Clinical a.

(57)   Pasero, C.; D'Agostino, I.; de Luca, F.; Zamperini, C.; Deodato, D.; Truglio, G. I.; Sannio, F.; del Prete, R.; Ferraro, T.; Visaggio, D.; Mancini, A.; Guglielmi, M. B.; Visca, P.; Docquier, J.-D.; Botta, M. Alkyl-Guanidine Compounds as Potent Broad-Spectrum Antibacterial Agents: Chemical Library Extension and Biological Characterization. *Journal of Medicinal Chemistry* **2018**, *61* (20), 9162–9176. https://doi.org/10.1021/acs.jmedchem.8b00619.

(58)   C, M. B.; E, O. M.; Marco, V.; H, C. J. Polyamines and Their Role in Virus Infection. *Microbiology and Molecular Biology Reviews* **2022**, *81* (4), e00029-17. https://doi.org/10.1128/MMBR.00029-17.

(59)   Casero, R. A.; Murray Stewart, T.; Pegg, A. E. Polyamine Metabolism and Cancer: Treatments, Challenges and Opportunities. *Nature Reviews Cancer* **2018**, *18* (11), 681–695. https://doi.org/10.1038/s41568-018-0050-3.

(60)   Fukuyama, T.; Jow, C.-K.; Cheung, M. 2- and 4-Nitrobenzenesulfonamides: Exceptionally Versatile Means for Preparation of Secondary Amines and Protection of Amines. *Tetrahedron Letters* **1995**, *36* (36), 6373–6374. https://doi.org/https://doi.org/10.1016/0040-4039(95)01316-A.

(61)   Fukuyama, T.; Cheung, M.; Jow, C.-K.; Hidai, Y.; Kan, T. 2,4-Dinitrobenzenesulfonamides: A Simple and Practical Method for the Preparation of a Variety of Secondary Amines and Diamines. *Tetrahedron Letters* **1997**, *38* (33), 5831–5834. https://doi.org/https://doi.org/10.1016/S0040-4039(97)01334-8.

(62)   Fukuyama, T.; Cheung, M.; Kan, T. N-Carboalkoxy-2-Nitrobenzenesulfonamides: A Practical Preparation of N-Boc-, N-Alloc-, and N-Cbz-Protected Primary Amines.

(63)   Borgini, M.; Orofino, F.; Truglio, G. I.; Balestri, L.; Botta, M. A Gram-Scale Synthesis of a Macrocyclic Amidinourea with Strong Antifungal Activity through a Fukuyama Tri-Protected Polyamine Intermediate. *ARKIVOC* **2019**, *2019* (4), 168–177. https://doi.org/10.24820/ark.5550190.p010.895.

(64)   Hughes, D. L.; Reamer, R. A.; Bergan, J. J.; Grabowski, E. J. J. A Mechanistic Study of the Mitsunobu Esterification Reaction. *J Am Chem Soc* **1988**, *110* (19), 6487–6491. https://doi.org/10.1021/ja00227a032.

(65)   Imagawa, H.; Tsuchihashi, T.; Singh, R. K.; Yamamoto, H.; Sugihara, T.; Nishizawa, M. Triethyl- (or Trimethyl-)Silyl Triflate-Catalyzed Reductive Cleavage of Triphenylmethyl (Trityl) Ethers with Triethylsilane. *Organic Letters* **2003**, *5* (2), 153–155. https://doi.org/10.1021/ol0271988.

(66)   Kan, T.; Fukuyama, T. Ns Strategies: A Highly Versatile Synthetic Method for Amines. *Chemical Communications* **2004**, No. 4, 353–359. https://doi.org/10.1039/B311203A.

(67) Orofino, F.; Truglio, G. I.; Fiorucci, D.; D'Agostino, I.; Borgini, M.; Poggialini, F.; Zamperini, C.; Dreassi, E.; Maccari, L.; Torelli, R.; Martini, C.; Bernabei, M.; Meis, J. F.; Khandelwal, N. K.; Prasad, R.; Sanguinetti, M.; Bugli, F.; Botta, M. In Vitro Characterization, ADME Analysis, and Histological and Toxicological Evaluation of BM1, a Macrocyclic Amidinourea Active against Azole-Resistant Candida Strains. *International Journal of Antimicrobial Agents* **2020**, *55* (3), 105865. https://doi.org/https://doi.org/10.1016/j.ijantimicag.2019.105865.

(68) Zhang, Y.; Huo, M.; Zhou, J.; Xie, S. PKSolver: An Add-in Program for Pharmacokinetic and Pharmacodynamic Data Analysis in Microsoft Excel. *Computer Methods and Programs in Biomedicine* **2010**, *99* (3), 306–314. https://doi.org/https://doi.org/10.1016/j.cmpb.2010.01.007.

(69) Lenardon, M. D.; Munro, C. A.; Gow, N. A. R. Chitin Synthesis and Fungal Pathogenesis. *Current Opinion in Microbiology* **2010**, *13* (4), 416–423. https://doi.org/https://doi.org/10.1016/j.mib.2010.05.002.

(70) Kumar, A.; Zhang, K. Y. J. *Human Chitinases: Structure, Function, and Inhibitor Discovery*; Springer Singapore, 2019; Vol. 1142. https://doi.org/10.1007/978-981-13-7318-3_11.

(71) Rinaudo, M. Chitin and Chitosan: Properties and Applications. *Progress in Polymer Science (Oxford)*. July 2006, pp 603–632. https://doi.org/10.1016/j.progpolymsci.2006.06.001.

(72) Merzendorfer, H. Insect Chitin Synthases: A Review. *Journal of Comparative Physiology B* **2006**, *176* (1), 1–15. https://doi.org/10.1007/s00360-005-0005-3.

(73) Ohno, T.; Armand, S.; Hata, T.; Nikaidou, N.; Henrissat, B.; Mitsutomi, M.; Watanabe, T. A Modular Family 19 Chitinase Found in the Prokaryotic Organism Streptomyces Griseus HUT 6037. *Journal of Bacteriology* **1996**, *178* (17), 5065–5070. https://doi.org/10.1128/jb.178.17.5065-5070.1996.

(74) Kzhyshkowska, J.; Mamidi, S.; Gratchev, A.; Kremmer, E.; Schmuttermaier, C.; Krusell, L.; Haus, G.; Utikal, J.; Schledzewski, K.; Scholtze, J.; Goerdt, S. Novel Stabilin-1 Interacting Chitinase-like Protein (SI-CLP) Is up-Regulated in Alternatively Activated Macrophages and Secreted via Lysosomal Pathway. *Blood* **2006**, *107* (8), 3221–3228. https://doi.org/10.1182/blood-2005-07-2843.

(75) Ohno, M.; Togashi, Y.; Tsuda, K.; Okawa, K.; Kamaya, M.; Sakaguchi, M.; Sugahara, Y.; Oyama, F. Quantification of Chitinase MRNA Levels in Human and Mouse Tissues by Real-Time PCR: Species-Specific Expression of Acidic Mammalian Chitinase in Stomach Tissues. *PLOS ONE* **2013**, *8* (6), e67399-.

(76) Boot, R. G.; Blommaart, E. F.; Swart, E.; Ghauharali-van der Vlugt, K.; Bijl, N.; Moe, C.; Place, A.; Aerts, J. M. Identification of a Novel Acidic Mammalian Chitinase Distinct from Chitotriosidase. *J Biol Chem* **2001**, *276* (9), 6770–6778. https://doi.org/10.1074/jbc.M009886200.

(77) Sutherland, T. E. Chitinase-like Proteins as Regulators of Innate Immunity and Tissue Repair: Helpful Lessons for Asthma? *Biochemical Society Transactions* **2018**, *46* (1), 141–151. https://doi.org/10.1042/BST20170108.

(78) Reese, T. A.; Liang, H.-E.; Tager, A. M.; Luster, A. D.; van Rooijen, N.; Voehringer, D.; Locksley, R. M. Chitin Induces Accumulation in Tissue of Innate Immune Cells Associated with Allergy. *Nature* **2007**, *447* (7140), 92–96. https://doi.org/10.1038/nature05746.

(79) Walker, J. A.; McKenzie, A. N. J. TH2 Cell Development and Function. *Nature Reviews Immunology* **2018**, *18* (2), 121–133. https://doi.org/10.1038/nri.2017.118.

(80) Zhu, Z.; Zheng, T.; Homer, R. J.; Kim, Y.-K. K.; Chen, N. Y.; Cohn, L.; Hamid, Q.; Elias, J. A. Acidic Mammalian Chitinase in Asthmatic Th2 Inflammation and IL-13 Pathway Activation. *Science (1979)* **2004**, *304* (5677), 1678–1682. https://doi.org/10.1126/science.1095336.

(81) Létuvé, S.; Kozhich, A.; Humbles, A.; Brewah, Y.; Dombret, M.-C.; Grandsaigne, M.; Adle, H.; Kolbeck, R.; Aubier, M.; Coyle, A. J.; Pretolani, M. Lung Chitinolytic Activity and Chitotriosidase Are Elevated in Chronic Obstructive Pulmonary Disease and Contribute to Lung Inflammation. *Am J Pathol* **2010**, *176* (2), 638–649. https://doi.org/10.2353/ajpath.2010.090455.

(82) Lee, C. G.; Herzog, E. L.; Ahangari, F.; Zhou, Y.; Gulati, M.; Lee, C.-M.; Peng, X.; Feghali-Bostwick, C.; Jimenez, S. A.; Varga, J.; Elias, J. A. Chitinase 1 Is a Biomarker for and Therapeutic Target in Scleroderma-Associated Interstitial Lung Disease That Augments TGF-B1 Signaling. *J Immunol* **2012**, *189* (5), 2635–2644. https://doi.org/10.4049/jimmunol.1201115.

(83) Hong, J. Y.; Kim, M.; Sol, I. S.; Kim, K. W.; Lee, C.-M.; Elias, J. A.; Sohn, M. H.; Lee, C. G. Chitotriosidase Inhibits Allergic Asthmatic Airways via Regulation of TGF-β Expression and Foxp3(+) Treg Cells. *Allergy* **2018**, *73* (8), 1686–1699. https://doi.org/10.1111/all.13426.

(84) Fitz, L. J.; Declercq, C.; Brooks, J.; Kuang en, W.; Bates, B.; Demers, D.; Winkler, A.; Nocka, K.; Jiao, A.; Greco, R. M.; Mason, L. E.; Fleming, M.; Quazi, A.; Wright, J.; Goldman, S.; Hubeau, C.; Williams, C. M. M. Acidic Mammalian Chitinase Is Not a Critical Target for Allergic Airway Disease. *American Journal of Respiratory Cell and Molecular Biology* **2012**, *46* (1), 71–79. https://doi.org/10.1165/rcmb.2011-0095OC.

(85) van Dyken, S. J.; Liang, H. E.; Naikawadi, R. P.; Woodruff, P. G.; Wolters, P. J.; Erle, D. J.; Locksley, R. M. Spontaneous Chitin Accumulation in Airways and Age-Related Fibrotic Lung Disease. *Cell* **2017**, *169* (3), 497-509.e13. https://doi.org/10.1016/j.cell.2017.03.044.

(86) Sakudaá, S.; Isogai, A.; Matsumoto, S.; Suzuki, A. *THE JOURNAL OF ANTIBIOTICS*; 1987.

(87) Sakuda, S.; Inoue, H.; Nagasawa, H. Novel Biological Activities of Allosamidins. *Molecules*. June 2013, pp 6952–6968. https://doi.org/10.3390/molecules18066952.

(88) Omura, S.; Arai, N.; Yamaguchi, Y.; Masuma, R.; Iwai, Y.; Namikoshi1, M.; Turberg, A.; Kolbl1, H.; Shiomi, K. *Argifin, a New Chitinase Inhibitor, Produced by Gliocladium Sp. FTD-0668 I. Taxonomy, Fermentation, and Biological Activities*; 2000; Vol. 53.

(89) Hirose, T.; Sunazuka, T.; Omura, S. Recent Development of Two Chitinase Inhibitors, Argifin and Argadin, Produced by Soil Microorganisms. *Proceedings of the Japan Academy Series B: Physical and Biological Sciences* **2010**, *86* (2), 85–102. https://doi.org/10.2183/pjab.86.85.

(90) Rao, F. v.; Houston, D. R.; Boot, R. G.; Aerts, J. M. F. G.; Hodkinson, M.; Adams, D. J.; Shiomi, K.; Ō̄mura, S.; van Aalten, D. M. F. Specificity and Affinity of Natural Product Cyclopentapeptide Inhibitors against A. Fumigatus, Human, and Bacterial Chitinases. *Chemistry & Biology* **2005**, *12* (1), 65–76. https://doi.org/10.1016/j.chembiol.2004.10.013.

(91) Schüttelkopf, A. W.; Andersen, O. A.; Rao, F. v; Allwood, M.; Lloyd, C.; Eggleston, I. M.; van Aalten, D. M. F. Screening-Based Discovery and Structural Dissection of a Novel Family 18 Chitinase Inhibitor*. *Journal of Biological Chemistry* **2006**, *281* (37), 27278–27285. https://doi.org/https://doi.org/10.1074/jbc.M604048200.

(92) Schüttelkopf, A. W.; Andersen, O. A.; Rao, F. v; Allwood, M.; Rush, C. L.; Eggleston, I. M.; van Aalten, D. M. F. Bisdionin C—A Rationally Designed, Submicromolar Inhibitor of Family 18 Chitinases. *ACS Medicinal Chemistry Letters* **2011**, *2* (6), 428–432. https://doi.org/10.1021/ml200008b.

(93)   Rao, F. v.; Andersen, O. A.; Vora, K. A.; DeMartino, J. A.; van Aalten, D. M. F. Methylxanthine Drugs Are Chitinase Inhibitors: Investigation of Inhibition and Binding Modes. *Chemistry and Biology* **2005**, *12* (9), 973–980. https://doi.org/10.1016/j.chembiol.2005.07.009.

(94)   Cole, D. C.; Olland, A. M.; Jacob, J.; Brooks, J.; Bursavich, M. G.; Czerwinski, R.; Declercq, C.; Johnson, M.; Joseph-Mccarthy, D.; Ellingboe, J. W.; Lin, L.; Nowak, P.; Presman, E.; Strand, J.; Tam, A.; Williams, C. M. M.; Yao, S.; Tsao, D. H. H.; Fitz, L. J. Identification and Characterization of Acidic Mammalian Chitinase Inhibitors. *Journal of Medicinal Chemistry* **2010**, *53* (16), 6122–6128. https://doi.org/10.1021/jm100533p.

(95)   Mazur, M.; Olczak, J.; Olejniczak, S.; Koralewski, R.; Czestkowski, W.; Jedrzejczak, A.; Golab, J.; Dzwonek, K.; Dymek, B.; Sklepkiewicz, P. L.; Zagozdzon, A.; Noonan, T.; Mahboubi, K.; Conway, B.; Sheeler, R.; Beckett, P.; Hungerford, W. M.; Podjarny, A.; Mitschler, A.; Cousido-Siah, A.; Fadel, F.; Golebiowski, A. Targeting Acidic Mammalian Chitinase Is Effective in Animal Model of Asthma. *Journal of Medicinal Chemistry* **2018**, *61* (3), 695–710. https://doi.org/10.1021/acs.jmedchem.7b01051.

(96)   Mazur, M.; Dymek, B.; Koralewski, R.; Sklepkiewicz, P.; Olejniczak, S.; Mazurkiewicz, M.; Piotrowicz, M.; Salamon, M.; Jędrzejczak, K.; Zagozdzon, A.; Czestkowski, W.; Matyszewski, K.; Borek, B.; Bartoszewicz, A.; Pluta, E.; Rymaszewska, A.; Mozga, W.; Stefaniak, F.; Dobrzański, P.; Dzwonek, K.; Golab, J.; Golebiowski, A.; Olczak, J. Development of Dual Chitinase Inhibitors as Potential New Treatment for Respiratory System Diseases. *Journal of Medicinal Chemistry* **2019**, *62* (15), 7126–7145. https://doi.org/10.1021/acs.jmedchem.9b00681.

(97)   Koralewski, R.; Dymek, B.; Mazur, M.; Sklepkiewicz, P.; Olejniczak, S.; Czestkowski, W.; Matyszewski, K.; Andryianau, G.; Niedziejko, P.; Kowalski, M.; Gruza, M.; Borek, B.; Jedrzejczak, K.; Bartoszewicz, A.; Pluta, E.; Rymaszewska, A.; Kania, M.; Rejczak, T.; Piasecka, S.; Mlacki, M.; Mazurkiewicz, M.; Piotrowicz, M.; Salamon, M.; Zagozdzon, A.; Napiorkowska-Gromadzka, A.; Bartlomiejczak, A.; Mozga, W.; Dobrzański, P.; Dzwonek, K.; Golab, J.; Nowotny, M.; Olczak, J.; Golebiowski, A. Discovery of OATD-01, a First-in-Class Chitinase Inhibitor as Potential New Therapeutics for Idiopathic Pulmonary Fibrosis. *Journal of Medicinal Chemistry* **2020**, *63* (24), 15527–15540. https://doi.org/10.1021/acs.jmedchem.0c01179.

(98)   Andryianau, G.; Kowalski, M.; Piotrowicz, M. C.; Rajkiewicz, A. A.; Dymek, B.; Sklepkiewicz, P. L.; Pluta, E.; Stefaniak, F.; Czestkowski, W.; Olejniczak, S.; Mazur, M.; Niedziejko, P.; Koralewski, R.; Matyszewski, K.; Gruza, M.; Zagozdzon, A.; Salamon, M.; Rymaszewska, A.; Welzer, M.; Dzwonek, K.; Golab, J.; Olczak, J.; Bartoszewicz, A.; Golebiowski, A. Benzoxazepine-Derived Selective, Orally Bioavailable Inhibitor of Human Acidic Mammalian Chitinase. *ACS Medicinal Chemistry Letters* **2020**, *11* (6), 1228–1235. https://doi.org/10.1021/acsmedchemlett.0c00092.

(99)   Jiang, X.; Kumar, A.; Motomura, Y.; Liu, T.; Zhou, Y.; Moro, K.; Zhang, K. Y. J.; Yang, Q. A Series of Compounds Bearing a Dipyrido-Pyrimidine Scaffold Acting as Novel Human and Insect Pest Chitinase Inhibitors. *Journal of Medicinal Chemistry* **2020**, *63* (3), 987–1001. https://doi.org/10.1021/acs.jmedchem.9b01154.

(100)   Maccari, G.; Deodato, D.; Fiorucci, D.; Orofino, F.; Truglio, G. I.; Pasero, C.; Martini, R.; de Luca, F.; Docquier, J.-D.; Botta, M. Design and Synthesis of a Novel Inhibitor of T. Viride Chitinase through an in Silico Target Fishing Protocol. *Bioorganic & Medicinal Chemistry Letters* **2017**, *27* (15), 3332–3336. https://doi.org/https://doi.org/10.1016/j.bmcl.2017.06.016.

(101) Huang, Q.-S.; Xie, X.-L.; Liang, G.; Gong, F.; Wang, Y.; Wei, X.-Q.; Wang, Q.; Ji, Z.-L.; Chen, Q.-X. The GH18 Family of Chitinases: Their Domain Architectures, Functions and Evolutions. *Glycobiology* **2012**, *22* (1), 23–34. https://doi.org/10.1093/glycob/cwr092.

(102) L, C. M.; M, H. W.; ADAM, G.; P, B. R.; MARZENA, M.; SYLWIA, O.; JACEK, O. SUBSTITUTED AMINO TRIAZOLES, AND METHODS USING SAME, 2015.

(103) Yamamoto, Y.; Shimizu, E.; Ban, K.; Wada, Y.; Mizusaki, T.; Yoshimura, M.; Takagi, Y.; Sawama, Y.; Sajiki, H. Facile Hydrogenative Deprotection of N-Benzyl Groups Using a Mixed Catalyst of Palladium and Niobic Acid-on-Carbon. *ACS Omega* **2020**, *5* (6), 2699–2709. https://doi.org/10.1021/acsomega.9b03226.

(104) Studer, M.; Blaser, H.-U. Influence of Catalyst Type, Solvent, Acid and Base on the Selectivity and Rate in the Catalytic Debenzylation of 4-Chloro-N,N-Dibenzyl Aniline with PdC and H2. *Journal of Molecular Catalysis A: Chemical* **1996**, *112* (3), 437–445. https://doi.org/https://doi.org/10.1016/1381-1169(96)00151-3.

(105) Sajiki, H. Selective Inhibition of Benzyl Ether Hydrogenolysis with Pd/C Due to the Presence of Ammonia, Pyridine or Ammonium Acetate. *Tetrahedron Letters* **1995**, *36* (20), 3465–3468. https://doi.org/10.1016/0040-4039(95)00527-J.

(106) Docquier, J.-D.; Lamotte-Brasseur, J.; Galleni, M.; Amicosante, G.; Frère, J.-M.; Rossolini, G. M. On Functional and Structural Heterogeneity of VIM-Type Metallo-β-Lactamases. *Journal of Antimicrobial Chemotherapy* **2003**, *51* (2), 257–266. https://doi.org/10.1093/jac/dkg067.

(107) Vedejs, E.; Marth, C. F. Mechanism of Wittig Reaction: Evidence against Betaine Intermediates. *J Am Chem Soc* **1990**, *112* (10), 3905–3909. https://doi.org/10.1021/ja00166a026.

(108) Byrne, P. A.; Gilheany, D. G. The Modern Interpretation of the Wittig Reaction Mechanism. *Chemical Society Reviews* **2013**, *42* (16), 6670–6696. https://doi.org/10.1039/C3CS60105F.

(109) Kim, E.; Park, S.; Chang, S. Silylative Reductive Amination of α,β-Unsaturated Aldehydes: A Convenient Synthetic Route to β-Silylated Secondary Amines. *Chemistry - A European Journal* **2018**, *24* (22), 5765–5769. https://doi.org/10.1002/chem.201800958.

(110) Park, C.-M.; Oie, T.; Petros, A. M.; Zhang, H.; Nimmer, P. M.; Henry, R. F.; Elmore, S. W. Design, Synthesis, and Computational Studies of Inhibitors of Bcl-XL. *J Am Chem Soc* **2006**, *128* (50), 16206–16212. https://doi.org/10.1021/ja0650347.

(111) Tondreau, A. M.; Darmon, J. M.; Wile, B. M.; Floyd, S. K.; Lobkovsky, E.; Chirik, P. J. Enantiopure Pyridine Bis(Oxazoline) "Pybox" and Bis(Oxazoline) "Box" Iron Dialkyl Complexes: Comparison to Bis(Imino)Pyridine Compounds and Application to Catalytic Hydrosilylation of Ketones. *Organometallics* **2009**, *28* (13), 3928–3940. https://doi.org/10.1021/om900224e.

(112) Ligiero, C. B. P.; Visentin, L. C.; Giacomini, R.; Filgueiras, C. A. L.; Miranda, P. C. M. L. 2,3,5,6-Tetra(Pyrazin-2-Yl)Pyrazine: A Novel Bis-Bidentate, Bis-Tridentate Chelator. *Tetrahedron Letters* **2009**, *50* (28), 4030–4032. https://doi.org/https://doi.org/10.1016/j.tetlet.2009.04.098.

(113) Scanio, M. J. C.; Shi, L.; Bunnelle, W. H.; Anderson, D. J.; Helfrich, R. J.; Malysz, J.; Thorin-Hagene, K. K.; van Handel, C. E.; Marsh, K. C.; Lee, C.-H.; Gopalakrishnan, M. Structure–Activity Studies of Diazabicyclo[3.3.0]Octane-Substituted Pyrazines and Pyridines as Potent A4β2 Nicotinic Acetylcholine Receptor Ligands. *Journal of Medicinal Chemistry* **2011**, *54* (21), 7678–7692. https://doi.org/10.1021/jm201045m.

(114) Gobbo, P.; Gunawardene, P.; Luo, W.; Workentin, M. S. Synthesis of a Toolbox of Clickable Rhodamine B Derivatives. *Synlett* **2015**, *26* (9), 1169–1174. https://doi.org/10.1055/s-0034-1380191.

(115) Abe, Y.; Kayakiri, H.; Satoh, S.; Inoue, T.; Sawada, Y.; Inamura, N.; Asano, M.; Hatori, C.; Sawai, H.; Oku, T.; Tanaka, H. A Novel Class of Orally Active Non-Peptide Bradykinin B2 Receptor Antagonists. 2. Overcoming the Species Difference between Guinea Pig and Man. *Journal of Medicinal Chemistry* **1998**, *41* (21), 4053–4061. https://doi.org/10.1021/jm980214f.

(116) Bonar-Law, R. P. Porphyrin Synthesis in Surfactant Solution: Multicomponent Assembly in Micelles. *The Journal of Organic Chemistry* **1996**, *61* (11), 3623–3634. https://doi.org/10.1021/jo9600161.

(117) Engen, K.; Vanga, S. R.; Lundbäck, T.; Agalo, F.; Konda, V.; Jensen, A. J.; Åqvist, J.; Gutiérrez-de-Terán, H.; Hallberg, M.; Larhed, M.; Rosenström, U. Synthesis, Evaluation and Proposed Binding Pose of Substituted Spiro-Oxindole Dihydroquinazolinones as IRAP Inhibitors. *ChemistryOpen* **2020**, *9* (3), 325–337. https://doi.org/10.1002/open.201900344.

(118) Diwakarla, S.; Nylander, E.; Grönbladh, A.; Vanga, S. R.; Khan, Y. S.; Gutiérrez-de-Terán, H.; Ng, L.; Pham, V.; Sävmarker, J.; Lundbäck, T.; Jenmalm-Jensen, A.; Andersson, H.; Engen, K.; Rosenström, U.; Larhed, M.; Åqvist, J.; Chai, S. Y.; Hallberg, M. Binding to and Inhibition of Insulin-Regulated Aminopeptidase by Macrocyclic Disulfides Enhances Spine Density. *Molecular Pharmacology* **2016**, *89* (4), 413. https://doi.org/10.1124/mol.115.102533.

(119) Svensson, F.; Engen, K.; Lundbäck, T.; Larhed, M.; Sköld, C. Virtual Screening for Transition State Analogue Inhibitors of IRAP Based on Quantum Mechanically Derived Reaction Coordinates. *Journal of Chemical Information and Modeling* **2015**, *55* (9), 1984–1993. https://doi.org/10.1021/acs.jcim.5b00359.

(120) Diwakarla, S.; Nylander, E.; Grönbladh, A.; Vanga, S. R.; Khan, Y. S.; Gutiérrez-de-Terán, H.; Sävmarker, J.; Ng, L.; Pham, V.; Lundbäck, T.; Jenmalm-Jensen, A.; Svensson, R.; Artursson, P.; Zelleroth, S.; Engen, K.; Rosenström, U.; Larhed, M.; Åqvist, J.; Chai, S. Y.; Hallberg, M. Aryl Sulfonamide Inhibitors of Insulin-Regulated Aminopeptidase Enhance Spine Density in Primary Hippocampal Neuron Cultures. *ACS Chemical Neuroscience* **2016**, *7* (10), 1383–1392. https://doi.org/10.1021/acschemneuro.6b00146.

(121) Kaushik, N. K.; Kaushik, N.; Attri, P.; Kumar, N.; Kim, C. H.; Verma, A. K.; Choi, E. H. Biomedical Importance of Indoles. *Molecules* **2013**, *18* (6), 6620–6662. https://doi.org/10.3390/molecules18066620.

(122) Geiger, H. A.; Wurst, M. G.; Daniels, R. N. DARK Classics in Chemical Neuroscience: Psilocybin. *ACS Chemical Neuroscience* **2018**, *9* (10), 2438–2447. https://doi.org/10.1021/acschemneuro.8b00186.

(123) Berger, M.; Gray, J. A.; Roth, B. L. The Expanded Biology of Serotonin. *Annual Review of Medicine* **2009**, *60* (1), 355–366. https://doi.org/10.1146/annurev.med.60.042307.110802.

(124) Gunata, M.; Parlakpinar, H.; Acet, H. A. Melatonin: A Review of Its Potential Functions and Effects on Neurological Diseases. *Revue Neurologique* **2020**, *176* (3), 148–165. https://doi.org/https://doi.org/10.1016/j.neurol.2019.07.025.

(125) Qin, H.-L.; Liu, J.; Fang, W.-Y.; Ravindar, L.; Rakesh, K. P. Indole-Based Derivatives as Potential Antibacterial Activity against Methicillin-Resistance Staphylococcus Aureus (MRSA). *European Journal of Medicinal Chemistry* **2020**, *194*, 112245. https://doi.org/https://doi.org/10.1016/j.ejmech.2020.112245.

(126) Sherer, C.; Snape, T. J. Heterocyclic Scaffolds as Promising Anticancer Agents against Tumours of the Central Nervous System: Exploring the Scope of Indole and Carbazole Derivatives. *European Journal of Medicinal Chemistry* **2015**, *97*, 552–560. https://doi.org/https://doi.org/10.1016/j.ejmech.2014.11.007.

(127) Zhang, M.-Z.; Chen, Q.; Yang, G.-F. A Review on Recent Developments of Indole-Containing Antiviral Agents. *European Journal of Medicinal Chemistry* **2015**, *89*, 421–441. https://doi.org/https://doi.org/10.1016/j.ejmech.2014.10.065.

(128) Chadha, N.; Silakari, O. Indoles as Therapeutics of Interest in Medicinal Chemistry: Bird's Eye View. *European Journal of Medicinal Chemistry* **2017**, *134*, 159–184. https://doi.org/10.1016/j.ejmech.2017.04.003.

(129) Humphrey, G. R.; Kuethe, J. T. Practical Methodologies for the Synthesis of Indoles. *Chemical Reviews* **2006**, *106* (7), 2875–2911. https://doi.org/10.1021/cr0505270.

(130) Baumann, M.; Baxendale, I. R.; Ley, S. v; Nikbin, N. An Overview of the Key Routes to the Best Selling 5-Membered Ring Heterocyclic Pharmaceuticals. *Beilstein journal of organic chemistry* **2011**, *7*, 442–495. https://doi.org/10.3762/bjoc.7.57.

(131) Vicente, R. Recent Advances in Indole Syntheses: New Routes for a Classic Target. *Organic & Biomolecular Chemistry* **2011**, *9* (19), 6469–6480. https://doi.org/10.1039/C1OB05750B.

(132) Karchava, A. v; Melkonyan, F. S.; Yurovskaya, M. A. New Strategies for the Synthesis of N-Alkylated Indoles (Review). *Chemistry of Heterocyclic Compounds* **2012**, *48* (3), 391–407. https://doi.org/10.1007/s10593-012-1006-2.

(133) Leblanc, B.; Charuel, C.; Ku, W.; Ogilvie, R. Acceptability of Low Levels of Genotoxic Impurities in New Drug Substances. *International Journal of Pharmaceutical Medicine* **2004**, *18* (4), 215–220. https://doi.org/10.2165/00124363-200418040-00003.

(134) Sobol, Z.; Engel, M. E.; Rubitski, E.; Ku, W. W.; Aubrecht, J.; Schiestl, R. H. Genotoxicity Profiles of Common Alkyl Halides and Esters with Alkylating Activity. *Mutation Research/Genetic Toxicology and Environmental Mutagenesis* **2007**, *633* (2), 80–94. https://doi.org/https://doi.org/10.1016/j.mrgentox.2007.05.004.

(135) Fletcher, S. The Mitsunobu Reaction in the 21st Century. *Organic Chemistry Frontiers* **2015**, *2* (6), 739–752. https://doi.org/10.1039/C5QO00016E.

(136) Clanton, N. A.; Spiller, T. E.; Ortiz, E.; Gao, Z.; Rodriguez-Poirier, J. M.; DelMonte, A. J.; Frantz, D. E. A Metal-Free Reductive N-Alkylation of Indoles with Aldehydes. *Organic Letters* **2021**, *23* (9), 3233–3236. https://doi.org/10.1021/acs.orglett.1c00179.

(137) Rüdiger Escher, P. B. Synthesis of N-(1-Carboxy-5-Aminopentyl)Dipeptides as Inhibitors of Angiotensin Converting Enzyme. *Angewandte Chemie International Edition in English* **1985**, *25* (3), 277–278.

(138) Wissmann, H.; Kleiner, H.-J. New Peptide Synthesis. *Angewandte Chemie International Edition in English* **1980**, *19* (2), 133–134. https://doi.org/https://doi.org/10.1002/anie.198001331.

(139) ANDREAS, M.; STEFAN, S.; SVEN, N. METHOD FOR PRODUCING NITRILES AND ISONITRILES BY USING DEHYDRATION REACTORS WITH PROPANEPHOSPHONIC ACID ANHYDRIDES, 2005.

(140) ANDREAS, M.; STEFAN, S.; CLAUDIUS, B. METHOD FOR THE PRODUCTION OF ALDEHYDES AND KETONES BY OXIDISING PRIMARY AND SECONDARY ALCOHOLS WITH ALKYLPHOSPHONIC ACID ANHYDRIDES, 2005.

(141) Fred Burkhart, Dr. M. H. Prof. Dr. H. K. Stereoselective Synthesis of a C-Glycosidic Analog of N-Glucoasparagine. *ANGEWANDTE CHEMIE* **1997**, *36* (11), 1191–1192.

(142) Crawforth, J. M.; Paoletti, M. A One-Pot Synthesis of Imidazo[1,5-a]Pyridines. *Tetrahedron Letters* **2009**, *50* (34), 4916–4918. https://doi.org/https://doi.org/10.1016/j.tetlet.2009.06.061.

(143) Zumpe, F. L.; Flüß, M.; Schmitz, K.; Lender, A. Propane Phosphonic Acid Anhydride: A New Promoter for the One-Pot Biginelli Synthesis of 3,4-Dihydropyrimidin-2(1H)-Ones. *Tetrahedron Letters* **2007**, *48*, 1421–1423.

(144) Desroses, M.; Wieckowski, K.; Stevens, M.; Odell, L. R. A Microwave-Assisted, Propylphosphonic Anhydride (T3P®) Mediated One-Pot Fischer Indole Synthesis. *Tetrahedron Letters* **2011**, *52* (34), 4417–4420. https://doi.org/https://doi.org/10.1016/j.tetlet.2011.06.053.

(145) Cruz, A. R.; Zolotukhin, M. G.; Morales, S. L.; Cardenas, J.; Cedillo, G.; Fomine, S.; Salmon, M.; Carreón-Castro, M. P. Use of 4-Piperidones in One-Pot Syntheses of Novel, High-Molecular-Weight Linear and Virtually 100%-Hyperbranched Polymers. *Chemical Communications* **2009**, No. 29, 4408–4410. https://doi.org/10.1039/B907042G.

Appendix:

SCIENTIFIC PRODUCTION:

Lorenzo J.I. Balestri, Ilaria D'Agostino, Enrico Rango, Chiara Vagaggini, Rosalba Marchitiello, Melinda Mariotti, Alexandru Casian, Davide Deodato, Giuseppina I. Truglio, Francesco Orofino, Maurizio Sanguinetti, Francesca Bugli, Lorenzo Botta, Elena Dreassi. *Focused Library of Phenyl-Fused Macrocyclic Amidinoureas as Antifungal Agents. **Molecular Diversity*** 2021. Manuscript Accepted. DOI 10.1007/s11030-022-10388-7

Matteo Borgini, Francesco Orofino, Giuseppina I. Truglio, Lorenzo J.I. Balestri, Maurizio Botta. A gram-scale synthesis of a macrocyclic amidinourea with strong antifungal activity through a Fukuyama tri-protected polyamine intermediate. **Arkivoc**, 2019;2019:168-177.
DOI https://doi.org/10.24820/ark.5550190.p010.895

SEMINAR AND CONGRESS PARTICIPATIONS:
- "**Variations on a theme-vinylogues Mukaiyama aldol reactions in the total synthesis of natural products.**"-Markus Kalesse. (October 2018).
- **"Applying concepts from nature for the design of greener and smarter catalyst."-**Jack L.Y.Chen (January 2019).
- **"11th International Workshop on Alkaptonuria (AKU)."** Annalisa Santucci (January 2019).
- "**From bench to bedside: Noscapine as chemotherapeutic agent-journey of two decades."-**Ramesh Chandra (February 2019).
- "**XII European Workshop in Drug Design."** (EWDD) **-**Maurizio Botta. (May 2019).
- "**Minicourse Protein Physics.**" -Paolo Carloni (June 2019).
- "**Complementary Skills."** (September 2019)
- **"Synthetic lethality as a new paradigm for the development of anticancer agents."**-Andrea Cavalli (November 2019).
- **"Biosensor for the future.**"-Simona Scarano, (November 2019).
- **"Merck Young Chemists' Symposium 2019.**"-SCI giovani. (November 2019).
- **"Realization and application of an innovative technological platform powered by QM/MM simulation for the development of photoactive molecules."** (December 2019)
- **"Exploiting suitable two-carbon nitrogen-containing electrophiles as alkylating agent and their application to the synthesis of valuable compounds."-**Giovanni Piersanti (January 2020).
- **"Computational Design of Light Driven Molecular Rotary Motors."-**Michael Filatov, (January 2020).
- **"MRSF-TDDFT: A New Method for Ground and Excited State Properties."** -Cheol Ho Choni (January 2020).
- **"8th MS J-Day "**(DSM-SCI) (July 2020).
- **" Italian Young Medicinal Chemistry Virtual Meeting."** (DCF-SCI). (July, 2020)
- **"Corso** Microimprendo**" - II EDIZIONE** (2020DU0032) (January 2021).
- **"8th European Workshop in Drug Synthesis." (**EWDS) (May 2021)
- **"European Chemical Biology Symposium.**"(ECBS) (May 2021)
- **"Antibiotics & Bacterial Resistance: Infinite war."** (July 2021)
- "**European School of Medicinal Chemistry."** (ESMEC) (July 2021)